Replication, Recombination and Chromosome Segregation in *Escherichia coli*

Martin A. White

Thesis presented for the degree of Doctor of Philosophy

Institute of Cell Biology

The University of Edinburgh

October 2009

Declaration

I hereby declare that this thesis was composed by me, and the research presented is my own, except where otherwise stated. This work has not been submitted for any other degree or professional qualification.

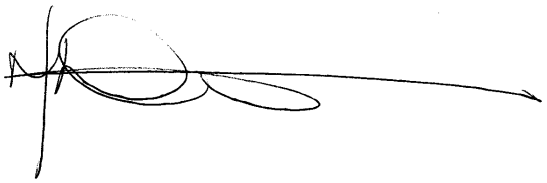

Martin White

2009

Acknowledgements

I would like to thank David Leach for encouraging me to forgo getting a proper job and instead take on the challenge of a PhD in his lab. It has been both a pleasure and a privilege to be a member of the Leach lab and I sincerely thank all colleagues past and present for making it so, with a particular mention going to out to the two Johns.

I would also like to thank Dave Sherratt for the gifts of plasmids pWX6, pLau43 and pLau44, Bénédicte Michel for the gift of plasmid pGB2, John Eykelenboom and Mark Strebel for allowing me to present their unpublished data, Elise Darmon for critical reading of the thesis, and the Medical Research Council for funding this work.

Thank yous aside, it was suggested to me that I should give a quote in my acknowledgements that sums up all that I have learned during the course of my PhD. I couldn't think of one, so here's a random one from my hero Bruce Lee:

"Empty your mind, be formless, shapeless – like water. Now you put water into a cup, it becomes the cup; you put water into a bottle, it becomes the bottle; you put it in a teapot, it becomes the teapot. Now water can flow, or it can crash. Be water, my friend." *Bruce Lee*

Mull over that!!

Abstract

SbcCD has been shown to cleave a DNA hairpin formed by a palindromic DNA sequence on the lagging strand template of the *E. coli* chromosome. This activity was exploited to create a unique system for inducing a single site-specific DNA double-strand break (DSB) once per replication cycle. First, this work shows that the SOS response induced by this DSB is only essential for viability following multiple cycles of cleavage and repair. Next, the SOS-inducible inhibitor of cell division SfiA is shown to be dispensable for survival, despite demonstrating that cleavage of the palindrome causes both an increase in cell size and a delay in nucleoid segregation. A model of the *E. coli* cell cycle is presented to reconcile the observation that growth under chronic DSB induced conditions has no effect on generation time despite causing an increase in cell size. This system of DSB induction was then coupled with fluorescence markers on both sides of the palindrome to visualise the consequence of the DSB *in vivo*. Cleavage of the DNA hairpin by SbcCD in a *recA*$^-$ mutant was used to selectively degrade the chromosome that replicated the palindrome on the lagging strand of replication, allowing two genetically identical sister chromosomes to be distinguished. This approach was used to show that chromosome segregation in *E. coli* is not random, but results in the segregation of lagging strand replicated DNA to mid-cell and leading strand replicated DNA to cell poles. Finally, this system for visualising the site of an inducible DSB was optimised for use in various other mutant backgrounds to allow the events of DSB repair to be dissected. This work provides a solid basis for further investigation into the relationship between replication, recombination and chromosome segregation in the model organism *E. coli*.

Abbreviations

ADP	Adenosine diphosphate
Amp	Ampicillin
Amp^R	Ampicillin resistance cassette
ANOVA	Analysis of Variance
Ara	Arabinose
ATC	Anhydrotetracycline
ATP	Adenosine Triphosphate
BrdU	5-Bromodeoxyuridine
CFP	Cyan Fluorescent Protein
Cm	Chloramphenicol
Cm^R	Chloramphenicol resistance cassette
$Conc^n$	Concentration
DAPI	4’,6-diamidino-2-phenylindole dihydrochloride
dsDNA	double-stranded DNA
DSB	DNA Double-Strand Break
DSE	DNA Double-Strand End
eCFP	enhanced Cyan Fluorescent Protein
eYFP	enhanced Yellow Fluorescent Protein
GFP	Green Fluorescent Protein
GFPmut3.1	Green Fluorescent Protein variant mut3.1
Gluc	Glucose
Gm	Gentamycin
Gm^R	Gentamycin resistance cassette
GTP	Guanosine Triphosphate
HJ	Holliday Junction
IPTG	Isopropyl-β-D-Thiogalactopyranoside
$I\text{-}SceI_{cs}$	I-SceI cleavage site
InDel	Insertion or Deletion
Km	Kanamycin
Km^R	Kanamycin resistance cassette

lacZχ-	Allele of *lacZ* with a Chi site mutated
L_{lag}	Lagging Strand Replicated Left Replichore
L_{lead}	Leading Strand Replicated Left Replichore
MCS	Multiple Cloning Site
OD_{600}	Optical Density at 600 nm
SD	Standard Deviation
SDM	Site-Directed Mutagenesis
SEM	Standard Error of the Mean
ssDNA	single-stranded DNA
UV-light	Ultraviolet light
pal	246 bp interrupted DNA palindrome
PCR	Polymerase Chain Reaction
PMGR	Plasmid Mediated Gene Replacement
PSF	Point Spread Function
Q1	1^{st} Quartile
Q3	3^{rd} Quartile
RFP	Red Fluorescent Protein
R_{lag}	Lagging Strand Replicated Right Replichore
R_{lead}	Leading Strand Replicated Right Replichore
SMC	Structural Maintenance of Chromosomes
SNP	Single Nucleotide Polymorphism
Spc	Spectinomycin
Spc^R	Spectinomycin resistance cassette
τ	Generation time
w/v	weight per unit volume
v/v	volume per unit volume

Table of Contents

Tables and Figures

Chapter 1

Introduction

1.1 Introduction

The maintenance of genomic stability is crucial for human health, as instability underlies many cancers and inherited human disorders such as Down's syndrome and Huntington's disease. Fundamental to the maintenance of genome stability are the cellular processes of DNA replication, repair by homologous recombination and chromosome segregation. Although the Gram negative bacterium *Escherichia coli* has proved to be an important model organism for the study of the highly conserved processes of DNA replication and homologous recombination, very little is currently known about how it segregates its chromosomes into daughter cells. This is despite recent evidence showing that the events of replication and repair occur within the context of a progressively segregating chromosome (Nielsen *et al.*, 2006a; Wang *et al.*, 2005). It is therefore not only important to study chromosome segregation as a mechanism of maintaining genomic stability itself, but also to better appreciate the convergence of the fields of the 'three Rs' – replication, recombination and repair (Hanawalt, 2007).

1.2 DNA Replication in *E. coli*

E. coli has a genome of ~4.6 Mbp of DNA located on a single, circular chromosome that replicates bidirectionally from the origin of replication. Although *E. coli* is a haploid organism, in fast growth conditions individual cells will often contain up to eight partially replicated chromosomes (Fossum *et al.*, 2007). To ensure the faithful transmission of the genome through generations, replication of this chromosome must be synchronously initiated on all sister chromosomes in a timely manner that is

appropriate for the growth conditions of the cell. Following initiation, the two replication forks must overcome a number of obstacles to ensure complete and faithful replication of the chromosome. Finally, the two replication forks must meet to allow the newly replicated sister chromosomes to segregate into each of the two daughter cells.

1.2.1 Replication Initiation

The *E. coli* chromosome contains a single origin of replication, known as *oriC*. *oriC* is a sequence of approximately 250 bp that is composed of three different types of repetitive element that are binding sites for the initiator protein DnaA (Mott and Berger, 2007). DnaA is a member of the AAA^+ ATPase family of proteins and has very high affinity for both ADP and ATP. While ADP-DnaA binds the repeats of *oriC* with low affinity throughout the cell cycle (Grimwade *et al.*, 2007), ATP-DnaA binds *oriC* with higher affinity and in a co-operative manner that results in oligomerization and the formation of a large protein complex (Simmons *et al.*, 2003). With the aid of negatively supercoiled DNA and DNA binding proteins (Fis, IHF and HU), the ATP-DnaA protein complex melts an AT rich region of *oriC* known as the DNA unwinding element, or DUE, and loads the replicative helicase DnaB onto what will become the lagging strand templates of the two replication forks (Chodavarapu *et al.*, 2008; Mott and Berger, 2007; Ryan *et al.*, 2002; Wold *et al.*, 1996). When not bound to DNA, DnaB is found in a complex with the helicase loader DnaC, which interestingly is a paralogue of DnaA (Koonin, 1992). Loading of DnaB to the ssDNA of *oriC* is facilitated by direct interactions between DnaA and DnaB (Seitz *et al.*, 2000) and possibly DnaA and DnaC (Mott *et al.*, 2008). Once the

replisome is successfully established, untimely re-initiation is prevented by three distinct mechanisms known as origin sequestration, DnaA titration and regulatory inactivation of DnaA (RIDA).

As well as being composed of DnaA binding sites, *oriC* contains 11 repeats of the sequence GATC. This sequence is found throughout the *E. coli* genome and the adenine of the sequence is methylated on both strands of the DNA by the action of Dam methyl-transferase (Lobner-Olesen *et al.*, 2005). Following replication however, the GATC sequences become transiently hemimethylated. SeqA protein binds these hemimethylated sequences with high affinity and blocks DnaA from initiating a new round of replication for approximately one third of the cell cycle (Bach *et al.*, 2003; Nievera *et al.*, 2006). This process is known as origin sequestration. Close to *oriC* lies a locus known as *datA*, which also binds DnaA with high affinity. It is believed that the function of this locus is to titrate the cellular concentration of DNA-free DnaA in order to prevent premature re-initiation from *oriC* (Nozaki *et al.*, 2009b). In addition to these two mechanisms, RIDA negatively regulates replication initiation by DnaA by directly stimulating ATP hydrolysis of ATP-DnaA in a reaction involving another DnaA paralogue known as Hda (Camara *et al.*, 2005; Kato and Katayama, 2001).

While the mechanism of replication initiation and the factors negatively regulating re-initiation are well understood, the factors that stimulate initiation in a cell cycle dependent manner are not. Whereas the cellular concentration of DnaA molecules does not vary substantially throughout the cell cycle (Sekimizu *et al.*, 1988), the various proportions of ADP-DnaA and ATP-DnaA do, with the level of ATP-DnaA peaking around the time of replication initiation (Kurokawa *et al.*, 1999).

It is therefore clear that regulation of the conversion of ADP-DnaA into ATP-DnaA is important for the temporal control of replication initiation. Interestingly, two new chromosome regions (called DnaA reactivating sequence, or DARS, 1 and 2) were recently identified that positively regulate replication initiation by directly promoting conversion of ADP-DnaA to ATP-DnaA by a nucleotide exchange mechanism (Fujimitsu *et al.*, 2009).

Although, the timing of replication initiation was once thought to be instigated by the cell reaching a critical cell mass (Donachie, 1968), it is now known that it is instead linked to the growth rate of the cell (Boye *et al.*, 1996; Wold *et al.*, 1994). How the cell measures its growth rate and links it with the process of replication initiation is still unknown. Interestingly, a GFP tagged DnaA was found to localise in a helical structure through the longitudinal axis of the cell, in a pattern similar to (but distinct from) the cytoskeletal protein MreB (Boeneman *et al.*, 2009). This localisation raises the possibility that an interaction with the membrane is responsible for linking replication initiation with growth rate. However, independently constructed DnaA-fluorescent protein fusions did not reveal such a localisation pattern (Nozaki *et al.*, 2009a) and it is currently unclear why there is a discrepancy between the two results. It has also been hypothesised that the rate of replication initiation might be regulated in response to DNA damage (Foti *et al.*, 2005), but despite *seqA* mutants (which have a hyper-initiation phenotype) being sensitive to UV-irradiation (Sutera and Lovett, 2006), replication initiation in wild-type cells was found not be altered in response to UV-irradiation (Rudolph *et al.*, 2007).

1.2.2 The *E. coli* Replisome

The *E. coli* genome encodes five different DNA polymerases. DNA polymerase I is primarily involved with filling gaps (nick translation) that arise during replication and DNA repair (Patel *et al.*, 2001), DNA polymerases II, IV, and V are DNA damage inducible (Iwasaki *et al.*, 1990; Schlacher and Goodman, 2007; Wagner *et al.*, 1999) and DNA polymerase III (Pol III) is the main polymerase responsible for chromosomal replication. Pol III functions in a multi-protein complex known as the Pol III holoenzyme, which is composed of three distinct functional units: the replicative polymerase Pol III, a processivity factor known as the β sliding clamp, and the γ/τ clamp loader (Johnson and O'Donnell, 2005). As well as loading the β sliding clamp, the γ/τ clamp loader is also required to couple the two DNA polymerases that are associated with leading and lagging strand DNA synthesis, to the replicative helicase of the replication fork. This occurs *via* direct interactions that the τ subunit of the clamp loader makes with both the Pol III core and the replicative helicase DnaB (Gao and McHenry, 2001a, b). Interestingly however, although only two polymerases are required at each replication fork, it has been proposed that the Pol III holoenzyme is actually composed of three replicative polymerases *in vivo* (McInerney *et al.*, 2007).

Also present at the replication fork, is the replicative helicase DnaB that unwinds the parental dsDNA and the primase DnaG. The PolIII holoezyme, DnaB, and DnaG together, form what is known as the replisome of the cell (Figure 1.1). The functional composition of DnaB is a homohexamer that encircles ssDNA, which in the replisome is the lagging strand template (Bailey *et al.*, 2007). Since DnaB only encircles one of the DNA strands, the parental dsDNA is unwound by steric

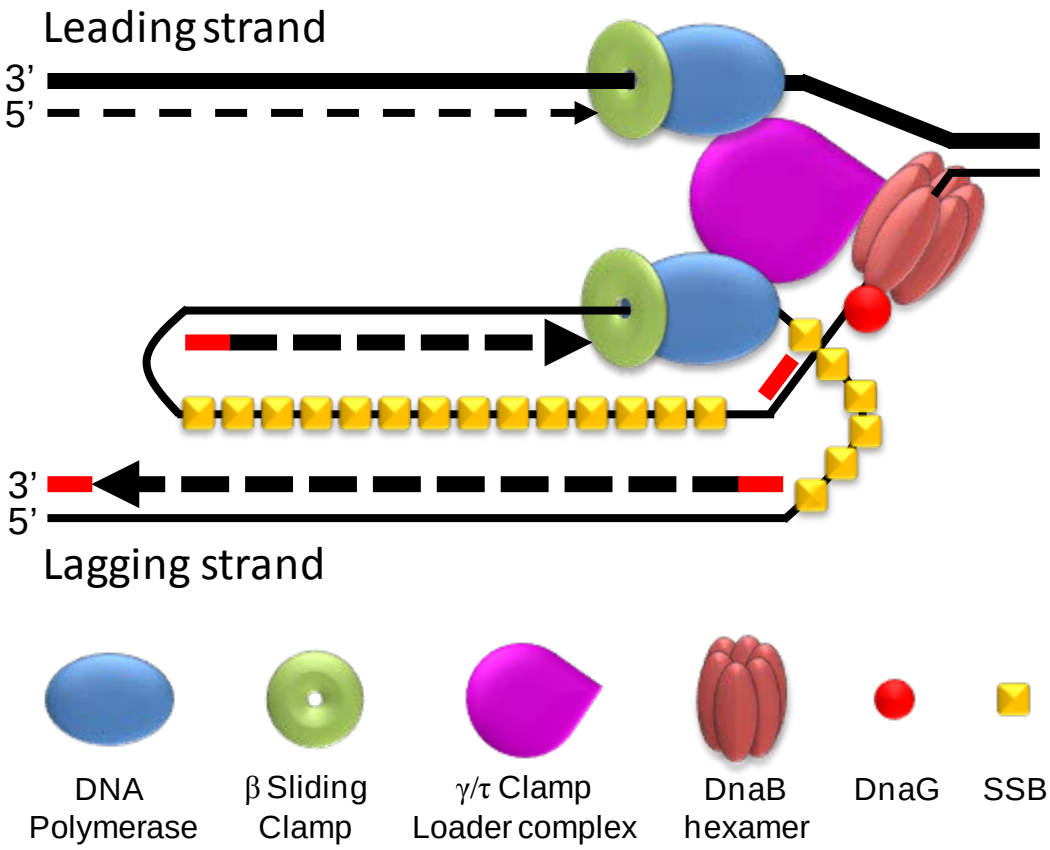

Figure 1.1 The *E. coli* replisome. For simplicity only two DNA polymerases are shown, although a third may be present. SSB is single-stranded DNA binding protein. Although only one is drawn, up to three DnaG monomers can interact with a single DnaB hexamer. Dashed lines indicated newly synthesised DNA. Red lines indicate RNA primers. Components are not shown to scale.

occlusion of the leading strand template as the helicase tracks along the DNA. As well as interacting with Pol III indirectly *via* the clamp loader, DnaB also interacts directly with the primase DnaG, with as many as three DnaG monomers binding a single DnaB hexamer (Bailey *et al.*, 2007; Corn and Berger, 2006; Mitkova *et al.*, 2003). DnaG is an RNA polymerase that is essential for priming DNA synthesis since DNA polymerases cannot initiate DNA synthesis *de novo*.

Due to the 5' to 3' polarity of DNA synthesis, one strand of each replication fork (the leading strand) is replicated continuously whereas the other (the lagging strand) is replicated discontinuously. The length of fragments (known as Okazaki fragments) synthesised on the lagging strand is determined by the rate at which DnaG deposits RNA primers. In *E. coli* DnaG interacts both weakly with DnaB and non-specifically with the ssDNA along which it tracks (Corn *et al.*, 2008), and deposits new RNA primers approximately once every 2 kb (McInerney *et al.*, 2007). Therefore, unlike the leading strand template, the lagging strand template contains stretches of ssDNA that becomes bound by single-stranded DNA binding (SSB) protein (Lecointe *et al.*, 2007; Witte *et al.*, 2003). Another consequence of the polarity of DNA synthesis is that the two polymerases of the replication fork will track along the DNA in opposite directions. In order to ensure that both polymerases track with the replicative helicase in the same direction in space, the lagging strand template becomes looped in what is known as the trombone model for replication (Alberts *et al.*, 1983), Figure 1.1. This loop grows and shrinks during each cycle of Okazaki fragment synthesis as revealed by single molecule experiments using individual bacteriophage T7 replisomes, but is believed to average about one Okazaki fragment (~2 Kb) in size (Hamdan *et al.*, 2009).

1.2.3 Impediments to Replication Fork Progression

As well as being equipped to replicate the chromosome, replication forks must also be prepared to overcome the numerous obstacles that they may encounter. For example, approximately 1% of logarithmic-phase *E. coli* cells were found to be induced for the SOS response (Pennington and Rosenberg, 2007). Approximately

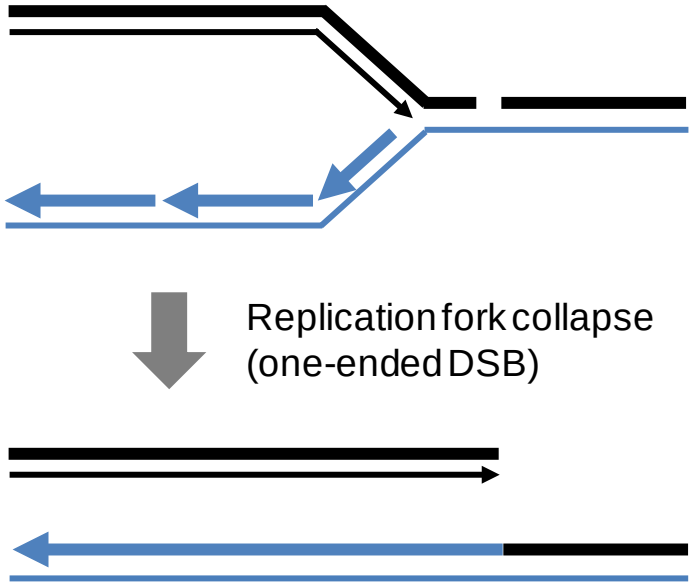

Figure 1.2 Replication fork collapse. Replication through a ssDNA lesion causes replication fork collapse, also known as a one-ended DNA double-strand break or a dsDNA end. The one-ended DNA double-strand break is processed by the RecBCD pathway of homologous recombination in order to re-establish the replication fork.

two thirds of this spontaneous SOS induction was dependent on RecB (indicating the presence of DNA double-strand breaks) and one third dependent on the RecF protein (indicating the presence of ssDNA gaps). Notably, the majority of spontaneous DNA double-strand breaks are believed to be caused by replication through a single-strand nick or gap (Kuzminov, 1995). This would lead to replication fork collapse (Figure 1.2), which would require the RecBCD pathway of homologous recombination to re-establish the replication fork (for details of this reaction see section 1.3).

ssDNA gaps and DNA double-strand breaks are not the only impediment to replication fork progression. The use of a temperature sensitive allele of the helicase loader DnaC showed that in the absence of induced DNA damage, 18% of cells

require the re-assembly of a replication fork per round of replication (Maisnier-Patin *et al.*, 2001). Other impediments to replication fork progression include collision with RNA polymerase and tightly bound protein-DNA complexes. Head on collisions of the replisome with RNA polymerase can result in replication fork arrest, whereas co-directional collision has little or no effect since the polymerase can use the mRNA transcript as a primer to continue DNA synthesis (Pomerantz and O'Donnell, 2008). Interestingly, it has been hypothesised that this difference in the fate of head-on and co-directional collisions caused a selective pressure that has resulted in a bias towards highly expressed genes being located on the leading strand template of the *E.coli* chromosome (Rocha, 2004; Rocha *et al.*, 2003). The fate of replisome collision with DNA-bound protein complexes is less clear. Both operator bound Tet and Lac repressor proteins (TetR and LacI) have been found to block replication *in vivo* (Payne *et al.*, 2006; Possoz *et al.*, 2006). Although replication resumes rapidly after relief of these blocks by addition of inducer to the growth medium, it is unclear whether or not re-start requires re-assembly of the replisome. This is because forks blocked by protein-DNA complexes have limited stability *in vitro* (McGlynn and Guy, 2008) but homologous recombination proteins are not required for re-start *in vivo* (Possoz *et al.*, 2006). It is therefore possible that *in vivo*, replication forks that encounter a protein block stall, but do not collapse.

Two major pathways are known for the re-establishment of replication following replication fork stalling. Either replication is directly re-started using the PriA or PriC proteins, or the fork is remodelled by a process known as replication fork reversal that involves many of the homologous recombination proteins (Heller and Marians, 2006; McGlynn and Lloyd, 2002; Michel *et al.*, 2004). Interestingly,

some of the proteins involved in these reactions may be targeted to the travelling replication fork by interactions with SSB (Lecointe *et al.*, 2007). Other potential blocks and DNA lesions may not prove to be an impediment to replication fork progression at all. The fate of a co-directional collision with RNA polymerase has already been discussed, but also the frequent re-cycling of the lagging strand polymerase during Okazaki fragment synthesis provides a mechanism of 'skipping over' lesions located on this DNA strand (Langston and O'Donnell, 2006).

1.2.4 Supercoiling, Catenation and Chromosome Segregation

During replication, unwinding of the parental DNA duplex results in an accumulation of positive supercoils ahead of the replication fork (Champoux, 2001). To prevent the torsional stress associated with positive supercoiling from inhibiting further unwinding of the DNA by DnaB (and thereby blocking replication fork progression), the DNA must be relaxed. In *E. coli* this is either achieved by the action of the type II topoisomerase DNA Gyrase (Nollmann *et al.*, 2007) or by diffusion of the positive supercoiling back into the newly replicated DNA. Diffusion of the positive supercoiling into newly replicated DNA causes the partially replicated sister chromosomes to become interwound. Interwinding of partially replicated sister chromosomes is known as pre-catenation, because following completion of chromosome replication, pre-catenation will cause the sister chromosomes to become physically linked **(**Figure 1.3), and this linkage is known as catenation (Peter *et al.*, 1998). In *E. coli*, chromosomes are decatenated by the action of topoisomerase IV (Zechiedrich and Cozzarelli, 1995; Zechiedrich *et al.*, 1997). The action of topoisomerase IV on catenanes has implicated this protein in the process of

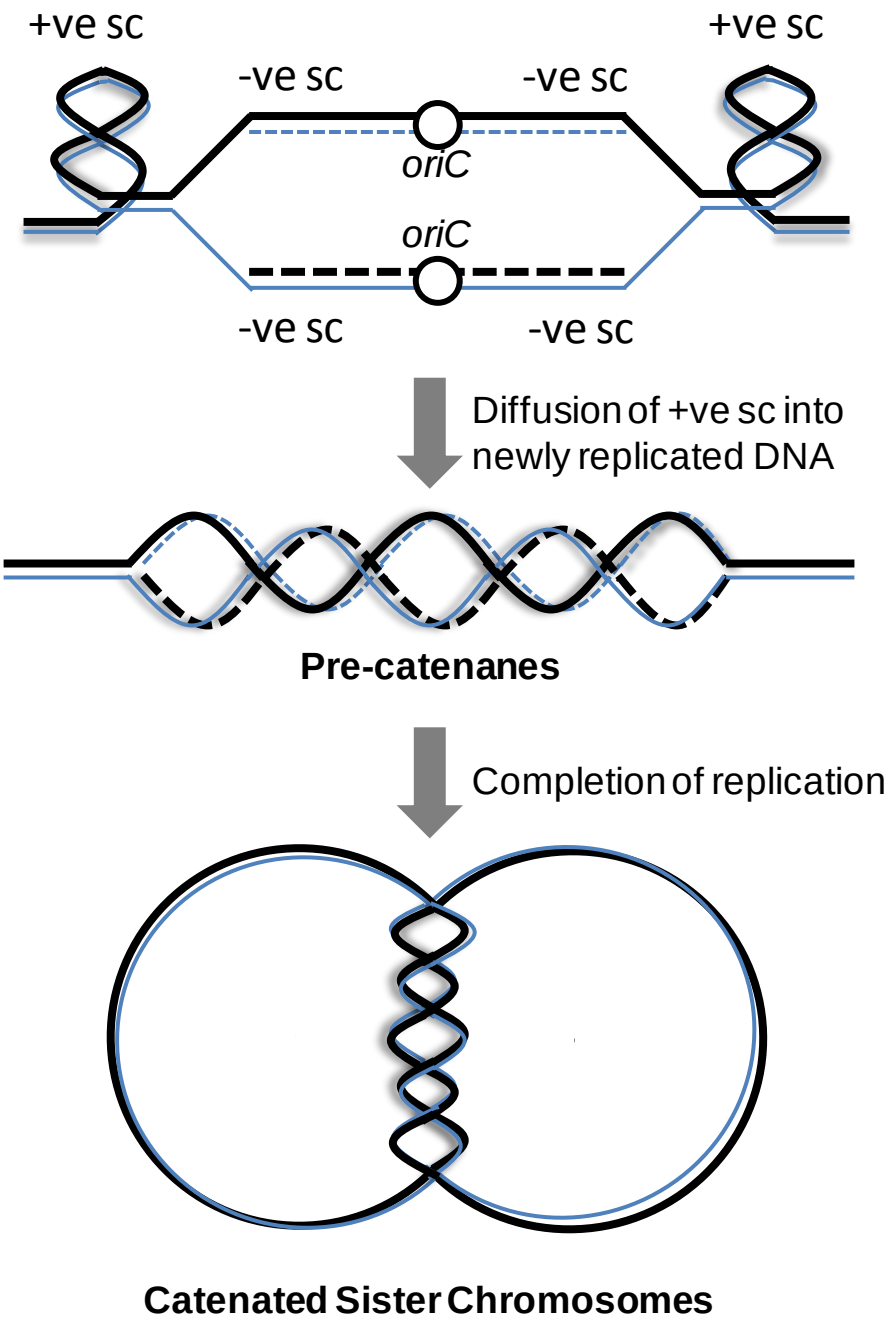

Figure 1.3 Positive supercoiling and catenation of sister chromosomes. Due to the helical nature of DNA, unwinding of the parental dsDNA during replication results in positive supercoiling (+ve sc) ahead of the replication fork and negative supercoiling (-ve sc) behind the fork. Diffusion of positive supercoiling back into the newly replicated DNA behind the fork results in interwound DNA (pre-catenanes). If pre-catenanes persist, then following completion of replication the two sister chromosomes will be physically linked (catenated). Dashed lines indicate newly replicated DNA.

chromosome segregation (Madabhushi and Marians, 2009; Wang *et al.*, 2008).

1.2.5 Replication Termination

In order to complete replication, the two replication forks that began diverging at *oriC* must converge. This occurs within a specific region of the *E. coli* chromosome known as the terminus. The terminus region of the *E. coli* chromosome is located diametrically opposite *oriC* and contains numerous sequences known as *Ter*. *Ter* are binding sites for the Tus protein, which when bound to *Ter* only allows replication to proceed in one direction (Kaplan and Bastia, 2009). The presence of *Ter* sites with opposite polarity on either side of the terminus region provides a 'replication fork trap' for the two migrating replisomes and ensures that they converge somewhere within this region (Duggin *et al.*, 2008). The exact point within the terminus where the two forks converge is unclear. Although physical evidence shows that convergence happens at the *Ter* sites (Duggin and Bell, 2009), mutational bias suggests that convergence of the replication forks happens somewhere near a sequence involved in the resolution of chromosome dimers, *dif* (Hendrickson and Lawrence, 2007). It is known however, that the location of the termination site is important, since engineered chromosome inversions that result in one replisome having to replicate more DNA that other renders the RecA, RecBC and FtsK proteins essential for viability (Esnault *et al.*, 2007; Lesterlin *et al.*, 2008).

Little is known mechanistically about what happens when the two forks converge, and whether or not the process is a simple matter of the two replisomes colliding or if a mechanism exists to control this reaction. An interaction between the helicase RecQ and Topoisomerase III (mediated by SSB) was recently shown to

aid the resolution of converging replication forks in *E. coli* through the use of an engineered plasmid containing an *oriC* and two *Ter* sites (Suski and Marians, 2008). Another study has shown that the convergence of replication forks outside of the terminus region (*e.g.* as can happen during DNA repair reactions) may pose a threat to genome stability if not resolved properly (Rudolph *et al.*, 2009).

1.3 DNA Double-Strand Break Repair in *E. coli*

DNA double-strand breaks (DSBs), defined as cleavage of both strands of the dsDNA helix, are genotoxic DNA lesions that can be generated by a number of sources. These include endogenous and exogenous DNA-damaging agents and aberrant replication events (Kowalczykowski, 2000). Importantly however, in organisms other than *E. coli*, DSBs are specifically induced by cells, *e.g.* during meiosis (Gerton and Hawley, 2005). Two different classes of DSB exist, and each has a slightly different consequence for repair. The two classes are known as one-ended and two-ended DSBs. One-ended DSBs are primarily caused by replication through a nicked DNA template, which results in replication fork collapse (Figure 1.2), whereas two-ended DSBs are what would be generated, for example, by a dsDNA endonuclease. If inaccurately repaired, DSBs can initiate chromosomal rearrangements as well as result in the deletion of essential genes and are associated with a wide variety of carcinomas in humans (Kastan and Bartek, 2004; Khanna and Jackson, 2001; Thompson and Schild, 2002). Consequently, in order to preserve genome stability and integrity, organisms have evolved a number of cellular processes for the efficient recognition and repair of DSBs.

Of these cellular processes, two distinct pathways have evolved for the repair of DSBs. One repair reaction involves ligating the two ends of the break back together and is known as non-homologous end-joining (NHEJ), for reviews see (Hasty, 2008; Lieber *et al.*, 2003; Yano *et al.*, 2009). NHEJ is believed to be the predominant method of DSB repair in vertebrate cells during G1 to early S phase (Rodrigue *et al.*, 2006) and interestingly, despite being long thought to have only evolved in eukaryotic cells, NHEJ pathways have been identified in some prokaryotic species (Della *et al.*, 2004; Pitcher *et al.*, 2007). Although NHEJ is an efficient method of sealing the dsDNA ends of a two-ended DSB, it is unable to repair one-ended DSBs. Furthermore, the ends of a DSB may be exposed to nucleases and become degraded, leading to the irreversible loss of DNA sequence prior to the ligation of the dsDNA ends.

A second pathway of DSB repair that is well conserved from prokaryotes to eukaryotes (Cromie *et al.*, 2001) involves the use of an intact copy of the DNA region containing the break, *e.g.* a sister chromatid, as a template for its faithful repair. This reaction is known as homologous recombination. The molecular mechanism of homologous recombination is most comprehensively understood in the model organism *E. coli* (which lacks a NHEJ pathway) and occurs in three stages known as pre-synapsis, synapsis, and post-synapsis (Figure 1.4).

1.3.1 Homologous Recombination: Presynapsis

The first stage of homologous recombination is known as pre-synapsis and involves the resection of a blunt, or nearly blunt, end of a DSB by the protein complex RecBCD to form a 3’ ssDNA overhang. The RecB and RecD subunits of the

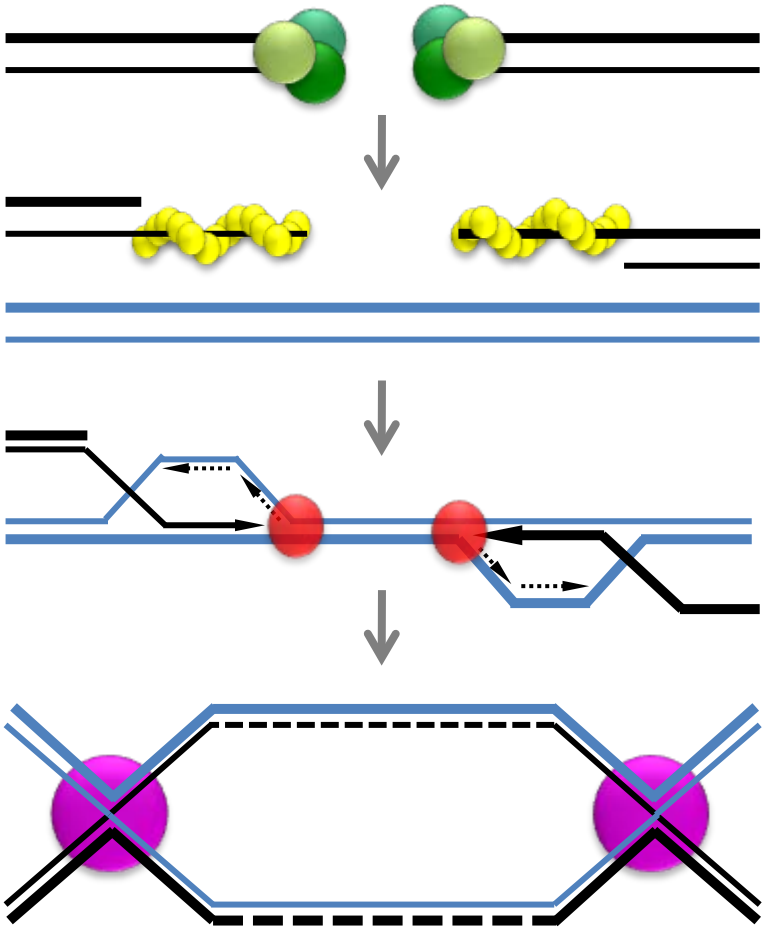

Figure 1.4 DNA double-strand break repair by homologous recombination in *E. coli*. RecBCD (green) binds to the ends of the DSB and resects the DNA to form a 3' ssDNA overhang onto which it loads the recombinase RecA (yellow). The RecA nucleoprotein filaments invade homologous sequences to form D-loops onto which PriA (red) loads the replicative helicase DnaB to establish replication forks. Replication fills in the gap caused by the DSB and the sister chromosomes, which are connected by a double Holliday junction, are resolved by RuvABC (purple).

complex both possess helicase activity and since RecB progresses in a 3' to 5' direction (Phillips *et al.*, 1997) and RecD progresses in a 5' to 3' direction (Dillingham *et al.*, 2003), the pair can translocate along a DNA duplex in the same

direction (one on either strand), unwinding the double-helix as they go (Singleton *et al.*, 2004). Concurrently, RecB uses its exonuclease activity to continually digest the strand of DNA it translocates on, while sporadically using its endonuclease activity to nick the strand on which RecD is located. This activity continues until the enzyme encounters a specific 8 bp sequence known as Chi (5'-GCTGGTGG) that is recognised by RecC. Chi sites are over-represented in the *E. coli* genome (Blattner *et al.*, 1997) and cause the RecBCD complex to pause before proceeding with nuclease activity that has both been attenuated and had its polarity switched (Spies *et al.*, 2007). Attenuation of the 3' to 5' exonuclease activity of RecB alongside activation of a weaker 5' to 3' exonuclease activity and continued helicase activity results in the formation of a 3' ssDNA overhang (Dillingham and Kowalczykowski, 2008).

As well as processing the ends of a DSB, RecBCD also actively loads RecA protein onto the 3' ssDNA overhang. This reaction is essential since RecA poorly competes with ssDNA binding protein (SSB) for the ssDNA, and is mediated through a direct interaction between the C-terminal domain of RecB and RecA in response to Chi recognition (Spies and Kowalczykowski, 2006). RecA polymerises on the 3' overhang to form a right-handed helical nucleoprotein filament in which the DNA is bound in a highly extended conformation (Chen *et al.*, 2008). As well as being essential for synapsis, this nucleoprotein filament also stimulates the SOS response of the cell (section 1.3.4).

1.3.2 Homologous Recombination: Homology Search and Synapsis

Synapsis involves the recognition of homologous DNA sequence by the RecA nucleoprotein filament followed by strand invasion to form heteroduplex DNA. RecA binds primarily to the sugar phosphate backbone of the ssDNA leaving bases exposed for recognition of homologous sequence (Bell, 2005; Chen *et al.*, 2008). Upon recognising sequence with sufficient homology, the nucleoprotein filament aligns the coated ssDNA alongside its homologous sequence and invades the DNA duplex (van der Heijden *et al.*, 2008). The invading ssDNA ejects its homologous strand on the DNA template and pairs with its complementary strand, to form a three stranded DNA structure known as a D- (displacement) loop (Figure 1.4). D-loops are recognised by PriA, which assembles a replication fork *via* its interactions with SSB (Cadman and McGlynn, 2004) and DnaC (Liu *et al.*, 1999).

Little is known about the process of homology search *in vivo* (Barzel and Kupiec, 2008). The major question that is yet to be addressed is whether homology search occurs by random diffusion of the RecA-nucleoprotein filament, or if it is in some way directed or facilitated. Although there is currently no evidence to suggest that homology search is an active process, it is difficult to comprehend how simple diffusion can facilitate the repair reaction within a physiologically relevant timescale when considering the low cellular concentration of the target (homologous sequence) and the high concentration of competitive non-homologous sequence (Minsky, 2003). This may not be an issue if the broken chromosome is already aligned with the preferred template for repair, *e.g.* a cohesed sister chromatid in the G2 cell cycle phase of eukaryotic cell growth (Kadyk and Hartwell, 1992; Unal *et al.*, 2007) or a sister chromosome during the period of post-replicative sister chromosome cohesion

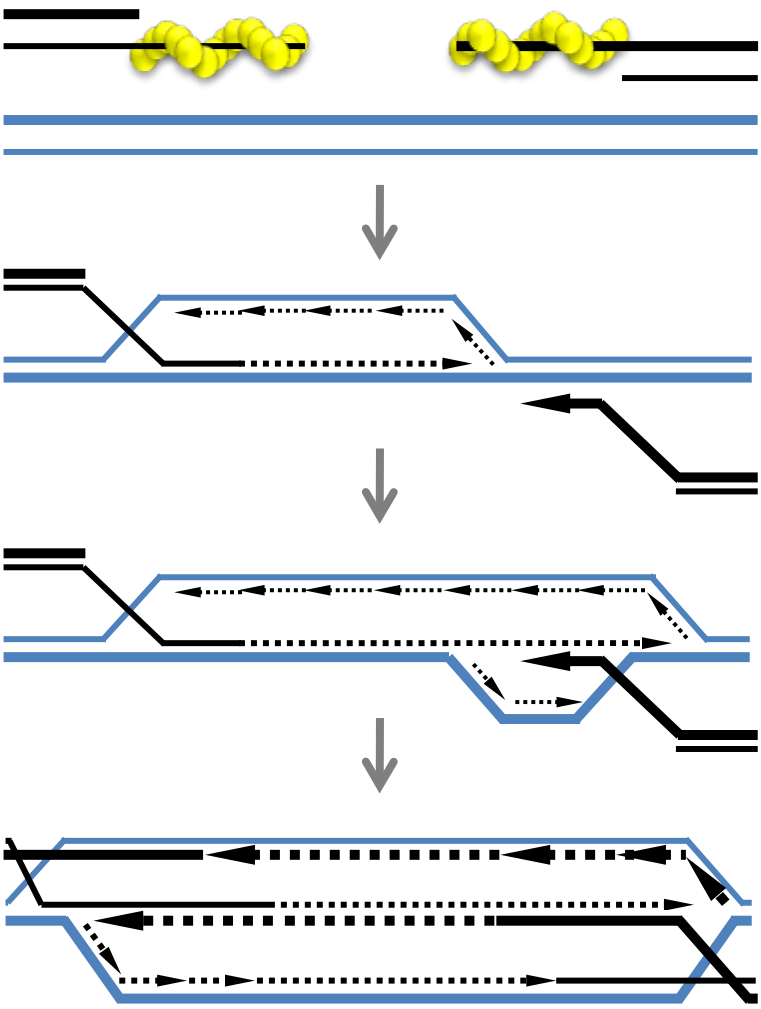

Figure 1.5 Un-coordinated DNA end invasion and divergent replication forks. If both DNA ends of a two-ended DSB are recombinogenic, then it possible for one RecA (yellow) coated DNA end to invade a homologous template (blue), and establish a replication fork before the other DNA end. This could result in the two RecA filaments establishing diverging replication forks rather than converging replication forks. In *E. coli* this would establish an origin independent round of chromosome replication.

in *E. coli* (Wang *et al.*, 2008). Importantly however, following this period of cohesion, sister chromosomes are segregated to opposite cell halves in *E. coli* (Nielsen *et al.*, 2006b; Wang *et al.*, 2006), complicating the search for homologous sequence.

Additionally, in nutrient rich growth media, each cell may possess up to eight partially replicated chromosomes (Morigen *et al.*, 2009). In order to successfully repair a two-ended DSB, each end must invade the same sister chromosome template in a manner that establishes two convergent replication forks (Figure 1.4). If synapsis of the two DNA ends were not co-ordinated then divergent replication forks could be established. This would effectively initiate an origin independent round of replication (Figure 1.5) creating an odd number of chromosomes within the cell. Invasion of different templates would also result in synthesis of an extra chromosome, but with two replication forks that would terminate on different chromosome templates. It is not currently known if *E. coli* has evolved a strategy to prevent these phenomena, or even if such events would have a negative effect on viability. Notably, the use of mutants that cause asynchronous replication initiation from *oriC* has revealed that *E. coli* cells can deal effectively with the presence of three nucleoids within a single cell (Bach and Skarstad, 2004).

1.3.3 Homologous Recombination: Post-synapsis

In order to complete the repair process, the joint molecule caused by synapsis has to be resolved. To achieve this, the three-strand heteroduplex of the D-loop is converted into a four-stranded structure, known as a Holliday junction (HJ), in a reaction that is potentially catalysed by the helicase RecG (Cromie *et al.*, 2001). HJs are the substrate for the protein complex RuvABC, which can extend the region of heteroduplex DNA by utilising the branch migration properties of RuvAB (Kaplan and O'Donnell, 2006). A dimer of RuvC, a HJ-specific endonuclease, can subsequently resolve the branched structure into two discrete duplexes by cleaving

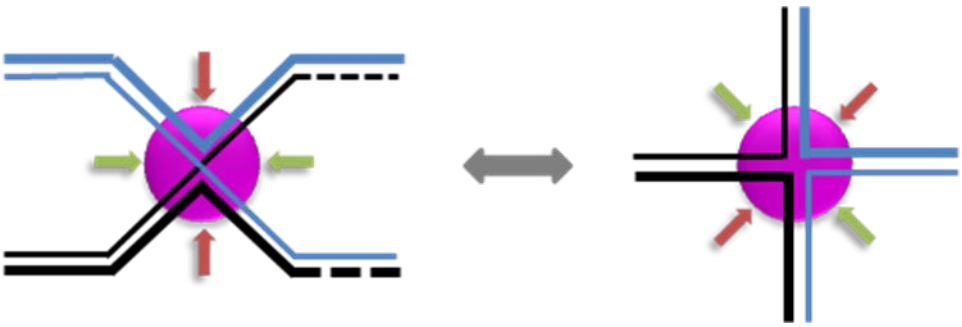

Figure 1.6 Different conformations of Holliday junctions. Conversion of a HJ from the conformation drawn in Figure 1.4 (left) to a square planar conformation (right). HJ resolution by RuvC occurs when HJs are in the square planar conformation. Arrows indicate the two possible orientations of RuvC cleavage.

opposite arms of the junction at certain preferred sequences (Eggleston and West, 2000). Cleavage of the HJ by RuvC occurs when the HJ is organised in the square planar conformation (Osman *et al.*, 2009), Figure 1.6. *In vivo* this substrate is formed by the binding of a tetramer of RuvA to the HJ (Rafferty *et al.*, 1996).

In the canonical DSB repair model of homologous recombination (Szostak *et al.*, 1983), the second end of a two-ended DSB is also recombinogenic and invades the template duplex, resulting in a double Holliday junction (Figure 1.4). However, although double Holliday junctions have been detected as recombination intermediates in *Saccharomyces cerevisiae* meiosis (Hunter and Kleckner, 2001), there is no physical evidence for their existence as DSB repair intermediates in *E. coli*, and indeed meiotic recombination has been shown to proceed via single HJs in *Schizosaccharomyces pombe* (Cromie *et al.*, 2006). Other models for DSB repair by homologous recombination that involve single Holliday junctions have also been proposed. These include break-induced replication (Kogoma, 1997) and synthesis-dependent strand annealing (Haber *et al.*, 2004).

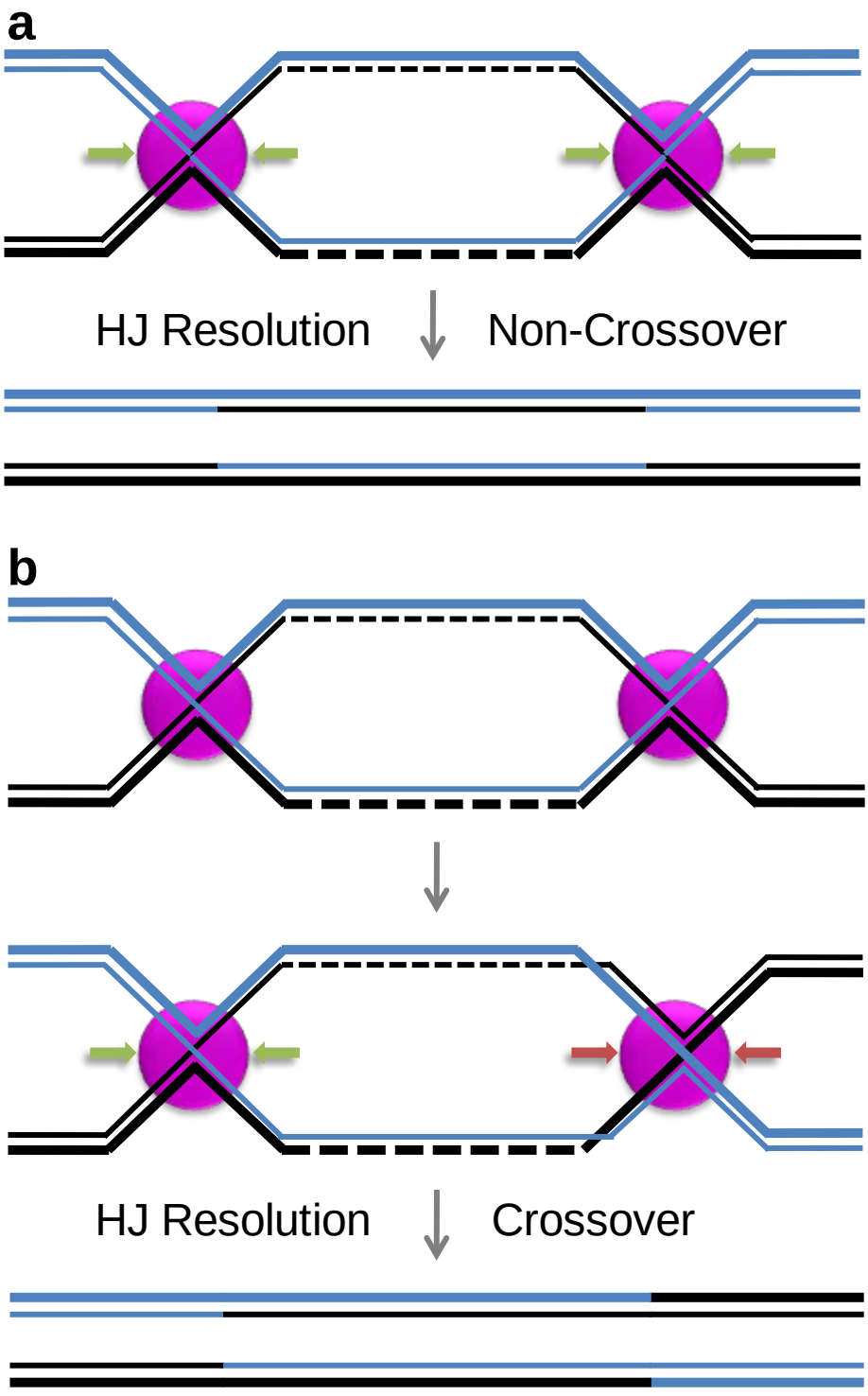

Figure 1.7 Holliday junction resolution and crossover formation. RuvC can resolve HJs in either of two orientations by cleaving either both 'Watson' (thick) or both 'Crick' (thin) strands of the four-way junction (Figure 1.6). When resolving a double HJ formed during DSB repair, (**a**) cleavage of both HJs in the same orientation will result in a non-crossover product, whereas (**b**) cleavage of the HJs in opposite orientations will result in a crossover product.

Depending on the orientation of HJ cleavage by RuvC at the two HJs, the outcome is either a crossover or a non crossover product (Figure 1.7). As a result of having a circular chromosome, a crossover event in *E. coli* results in the formation of a large chromosome dimer (Lesterlin *et al.*, 2004). Chromosome dimers consist of two physically linked sister chromosomes that must be resolved back into two independent circular chromosomes in order to permit segregation of the genome into the two daughter cells. In *E. coli*, resolution of chromosome dimers occurs by a site-specific recombination event that is mediated by the tyrosine recombinases XerC and XerD and occurs at a sequence known as *dif* (Blakely *et al.*, 1993; Blakely *et al.*, 2000) that is located close to the terminus of replication (Hendrickson and Lawrence, 2007). This recombination event requires a member of the division machinery (FtsK) to align the two *dif* sequences (Aussel *et al.*, 2002) and occurs only shortly before cell division (Kennedy *et al.*, 2008).

1.3.4 The SOS Response to DNA Damage

To improve their chances of survival, *E. coli* cells respond to the presence of DNA damage by inducing the transcription of a subset of approximately 40 genes (Courcelle *et al.*, 2001). This is known as the SOS response of the cell (Erill *et al.*, 2007; Kelley, 2006; Sutton *et al.*, 2000) and functions in contrast with the eukaryotic DNA damage response that tends to regulate proteins involved with survival by post-translational modifications rather than at the level of transcription regulation (Harper and Elledge, 2007). In the absence of DNA damage, the promoters of genes involved in the SOS response are repressed by the binding of the transcriptional repressor protein LexA (Brent and Ptashne, 1981) to a 20 bp consensus binding motif

known as the LexA box (Walker, 1984). *E. coli* uses the RecA-nucleoprotein filament (known as RecA*) as a sensor of DNA damage. As well as being essential for synapsis, RecA* acts as a coprotease that stimulates the auto-cleavage of LexA, which in turn derepresses the SOS regulon (Anderson and Kowalczykowski, 1998; Little *et al.*, 1980).

Examples of proteins that are under the control of the SOS regulon include the recombinase RecA, the inhibitor of cell division SfiA, the mutagenic polymerases Pol IV and Pol V, LexA itself, and a number of proteins of unknown function such as RecN (Courcelle *et al.*, 2001). Variation in the sequence of the LexA box at individual promoters results in a spectrum of affinities for LexA binding. This allows the response of individual components of the SOS regulon to DNA damage, to be fine tuned with regards to both the timing of induction and the extent of increased expression. For example, induction of RecN and LexA both peak at approximately 5 min post UV irradiation but show a 20-fold and 5-fold increase in transcription respectively. In contrast, transcription of the subunits of the mutagenic polymerase Pol V, UmuC and UmuD, does not peak until 40 min post UV irradiation (Courcelle *et al.*, 2001). Additionally, the SOS response is further fine-tuned by the post-translational regulation of certain proteins such as SfiA and UmuDC. SfiA is negatively regulated by the protease Lon (Mizusawa and Gottesman, 1983) such that only high levels of increased SfiA expression can result in cell division inhibition and the division process resumes as soon as possible following removal of the DNA damage signal. UmuDC on the other hand requires the presence of RecA* to not only induce transcription, but also to catalyse cleavage of the UmuD subunit into its active form and stimulate translesion synthesis itself by transferring a molecule of

ATP bound RecA to the active UmuDC complex (Jiang *et al.*, 2009; Schlacher *et al.*, 2006; Schlacher and Goodman, 2007). Regulation of Pol V at these three stages ensures that stress induced mutagenesis only occurs in cases of high levels of prolonged DNA damage.

1.3.5 Tools for Inducing DSBs in *E. coli*

A method for inducing DSBs is essential for the effective study of their consequences *in vivo*. Examples of methods for inducing DSBs in *E. coli* include exposure to UV-light (Rudolph *et al.*, 2008) and ionizing radiation (Harris *et al.*, 2009), and treatment with drugs such as bleomycin (Kosa *et al.*, 2004) and phleomycin (Beam *et al.*, 2002). While these treatments have been successfully used to investigate DSB repair in *E. coli*, the interpretation of results obtained from such studies are often complicated by the fact that they can induce not only DSBs but other types of DNA damage, such as ssDNA gaps. Therefore, although it is important to investigate the effects of DNA damaging agents that are applicable to human biology, for technical reasons it is often more desirable to be able to induce a specific lesion at a specific site in the chromosome.

With this in mind, the homing endonuclease I-SceI has been successfully exploited as a tool for inducing a site-specific DSB. I-SceI was originally isolated from the mitochondria of *S. cerevisiae* and found to induce a DSB at an 18 bp recognition sequence that shows moderate redundancy (Monteilhet *et al.*, 1990). Despite this redundancy, I-SceI has been successfully used to induce a unique DSB in organisms ranging from *E. coli* (Meddows *et al.*, 2004), to human and mouse cell lines (Moynahan *et al.*, 2001). The mode of action of I-SceI has been well

characterised and crystal structures showing intermediates in the cleavage reaction are available (Moure *et al.*, 2008). However, the problem with using a site-specific endonuclease to investigate DSB repair is that the cleavage site is present on all sister chromosomes. Therefore, induction of the endonuclease can result in cleavage of all sister chromosomes, preventing repair by homologous recombination. To resolve this problem, either the endonuclease has to be titrated (Meddows *et al.*, 2005; Meddows *et al.*, 2004) or a region of homology lacking the cleavage site must be provided on an episome, such as an F' plasmid (Pennington and Rosenberg, 2007). Recently however, a new tool has become available for inducing DSBs in *E. coli* that allows highly efficient induction of a site-specific DSB on only one of a pair of replicating sister chromosomes. This system involves the integration of a 246 bp interrupted DNA palindrome into the chromosome of a strain with an inducible SbcCD complex (Eykelenboom *et al.*, 2008).

1.3.6 Cleavage of a 246 bp DNA Palindrome by the Hairpin Endonuclease SbcCD

SbcCD is the *E. coli* homologue of the eukaryotic Mre11/Rad50 complex (Connelly and Leach, 2002). However, unlike Mre11/Rad50 which has well characterised roles in DNA replication (Tittel-Elmer *et al.*, 2009), DNA repair (Kinoshita *et al.*, 2009), meiosis (Borde, 2007) and telomere maintenance (Gao *et al.*, 2009); the exact role of SbcCD in *E. coli* biology remains a mystery. This is despite extensive biochemical analyses that have revealed both ATP-dependent exonuclease (Connelly *et al.*, 1997) and ATP-independent endonuclease activities (Connelly *et al.*, 1999). In common with each other, both Mre11/Rad50 and SbcCD have been shown to act on DNA

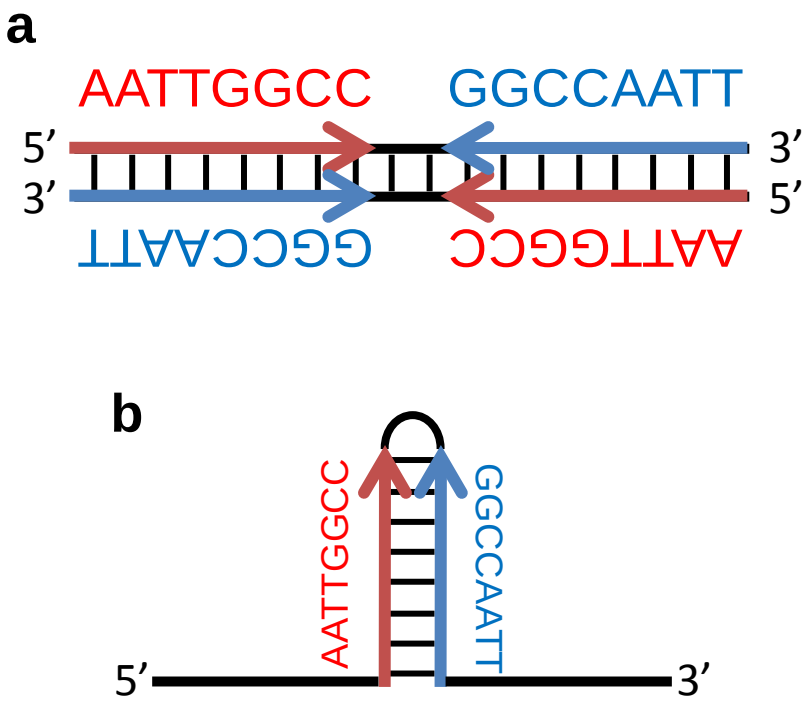

Figure 1.8 DNA palindromes and hairpins. Schematic representation of: **a**, a hypothetical 18 bp interrupted dsDNA palindrome. **b**, a DNA hairpin formed by an 18 bp interrupted ssDNA palindrome.

hairpins *in vitro* (Connelly *et al.*, 1998; Paull and Gellert, 1998) and palindromic DNA sequences *in vivo* (Cromie *et al.*, 2000; Farah *et al.*, 2005).

dsDNA palindromes are composed of identical 5’ to 3’ sequences on both strands of the dsDNA, and therefore have rotational symmetry (Figure 1.8a). Importantly, palindromes have the ability to form DNA hairpins when single stranded (Figure 1.8b). The palindrome used in this study is specifically a 246 bp interrupted DNA palindrome composed of two 111 bp palindrome arms separated by a 24 bp non-palindromic spacer. The presence of a spacer between the inverted repeats reduces its propensity for cruciform extrusion *in vitro* and can increase the

stability of the palindromic sequence *in vivo* (Kogo *et al.*, 2007). It was recently shown that, when this 246 bp sequence is integrated into the *lacZ* gene of the *E. coli* chromosome, SbcCD cleaves the palindrome on only one of a pair of replicating chromosomes, to form a two-ended DSB that is repaired by the RecBCD pathway of homologous recombination (Eykelenboom *et al.*, 2008). The fact that SbcCD only cleaves the palindrome on one of pair of replicating chromosomes is most likely due to the palindrome forming a DNA hairpin on the lagging strand template of replication, which due to its discontinuous nature of DNA synthesis results in stretches of ssDNA (Figure 1.9). In accordance with this hypothesis, the pattern of replication slippage of DNA palindromes in *E. coli* is consistent with hairpin formation on the lagging, but not on the leading strand template of replication (Pinder *et al.*, 1998).

Interestingly, the DSB formed by cleavage of the hairpin by SbcCD is repaired by RecBCD dependent homologous recombination, and this reaction also involves replication of the palindrome to repair the broken DNA. Although, genetic, physical, and cytological analyses show that SbcCD cleaves the palindrome approximately once per replication cycle (Eykelenboom *et al.*, 2008; White *et al.*, 2008), replicative repair either does not result in hairpin formation, or prevents SbcCD from accessing the new hairpin. If it did, then the cell would be caught in a destructive cycle of cleavage and repair, whereas the presence of SbcCD in a strain harbouring the 246 bp palindrome has no detectable effect on growth or viability (Eykelenboom *et al.*, 2008).

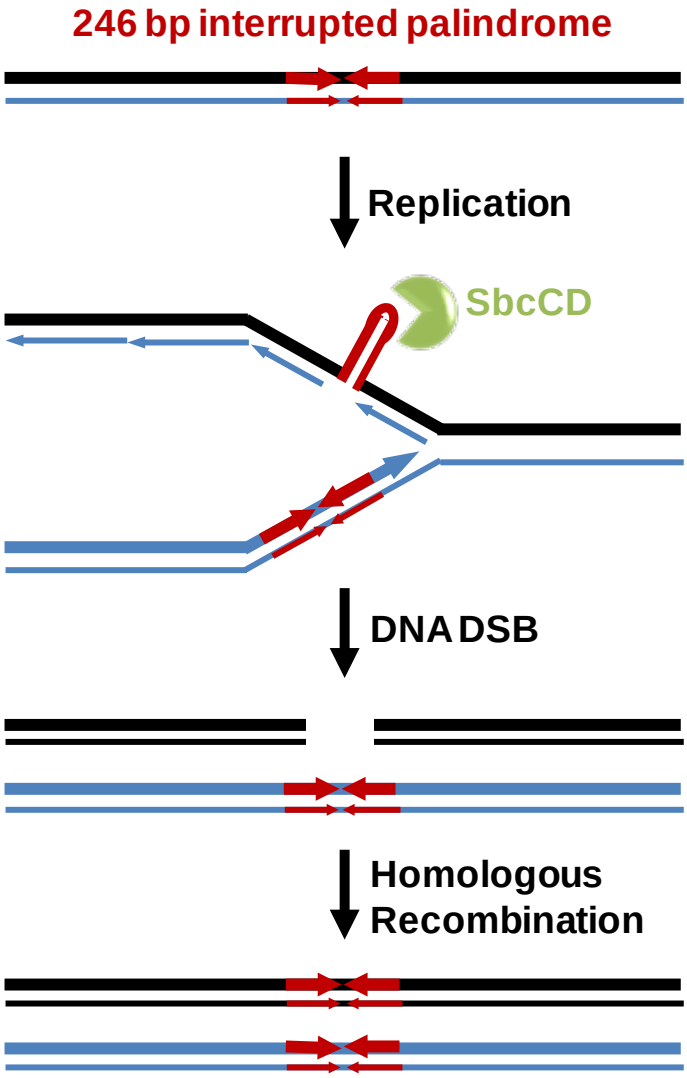

Figure 1.9 Replication dependent celavage of a 246 bp interrupted DNA palindrome in *E. coli*. A 246 bp interrupted palindrome forms a DNA hairpin on the lagging strand template of replication. This hairpin is a target for SbcCD, which cleaves to form a two-ended DSB. This DSB is then repaired by homologous recombination, restoring the original palindrome.

1.4 Chromosome Segregation in *E. coli*

The segregation of replicated DNA (sister chromosomes) to the two daughter cells during division is essential for the faithful transmission of the genome. It is therefore surprising that, despite being one of the most extensively studied model organisms, the mechanism by which *E. coli* carries out this fundamental aspect of cell biology is still unknown. In stark contrast, the basic nature of chromosome segregation in eukaryotic cells has been known for more than 50 years (Carlson, 1956; Inoue, 1981; Pickett-Heaps *et al.*, 1982; Rhoades and Vilkomerson, 1942). Much of this knowledge came from microscopy studies, and the tools available at the time were unable to detect any subcellular structures in prokaryotic cells. However, recent advancements in microscopy are now permitting in depth analyses of prokaryotic cell biology and have debunked the myth that prokaryotic cells are structureless bags of enzymes by revealing an array of cytoskeletal structures and internal localisations (Thanbichler and Shapiro, 2008). In particular, fluorescence microscopy is providing new insights into the mechanism of chromosome segregation in *E. coli*.

1.4.1 Eukaryotic Chromosome Segregation

In contrast to *E. coli*, eukaryotic cells have a cell-cycle with stringent checkpoints that control the transition between the different growth phases. The eukaryotic cell-cycle is divided into four phases known as G_1, S-phase, G_2 and mitosis. Collectively G_1, S-phase and G_2 are known as interphase. DNA is replicated during S-phase and segregated during mitosis, while G_1 and G_2 are growth phases that occur between DNA replication and segregation. Importantly, following replication, sister chromatids become bound by the protein complex cohesin, which ensures that the

sisters remain physically attached to each other until they separate during mitosis (Haering *et al.*, 2008; Peters *et al.*, 2008), and a strict checkpoint (known as the G_2 DNA damage checkpoint) exists in G_2 to ensure that the DNA is both fully replicated and undamaged before proceeding into mitosis. Interestingly, cohesin is essential for this checkpoint, and unlike its role in facilitating recombinational repair (Strom *et al.*, 2007; Unal *et al.*, 2007), its role in the G_2 DNA damage checkpoint is independent of its ability to facilitate cohesion of the sister chromatids (Watrin and Peters, 2009).

Mitosis itself is further divided into five discrete stages known as prophase, prometaphase, metaphase, anaphase and telophase. Mitosis begins in prophase with the dramatic condensation of chromosomes, in a reaction promoted by the protein complex condensin (Hudson *et al.*, 2009; St-Pierre *et al.*, 2009). Next, a bipolar array of microtubules, known as the mitotic spindle, is established following careful duplication and segregation of the centrosomes (microtubule organising centres, also known as the spindle pole bodies in yeast) (Bettencourt-Dias and Glover, 2007; Song *et al.*, 2008). Microtubules are composed of heterodimers of α-tubulin and β-tubulin arranged head to tail to form a tube (Nogales, 2000). During mitosis, microtubules extend from the centrosomes towards the chromosomes, where in prometaphase they attach to the centromeres of the chromosomes *via* a large protein complex, known as the kinetochore (DeLuca, 2007; Tanaka *et al.*, 2005). In order to segregate their chromosomes faithfully, each pair of sister chromatids must attach to two microtubules, one extending from each centrosome, and the attached chromosomes must align with one another. This is known as metaphase and correct alignment of the chromosomes and attachment to the microtubules must be fulfilled in order to

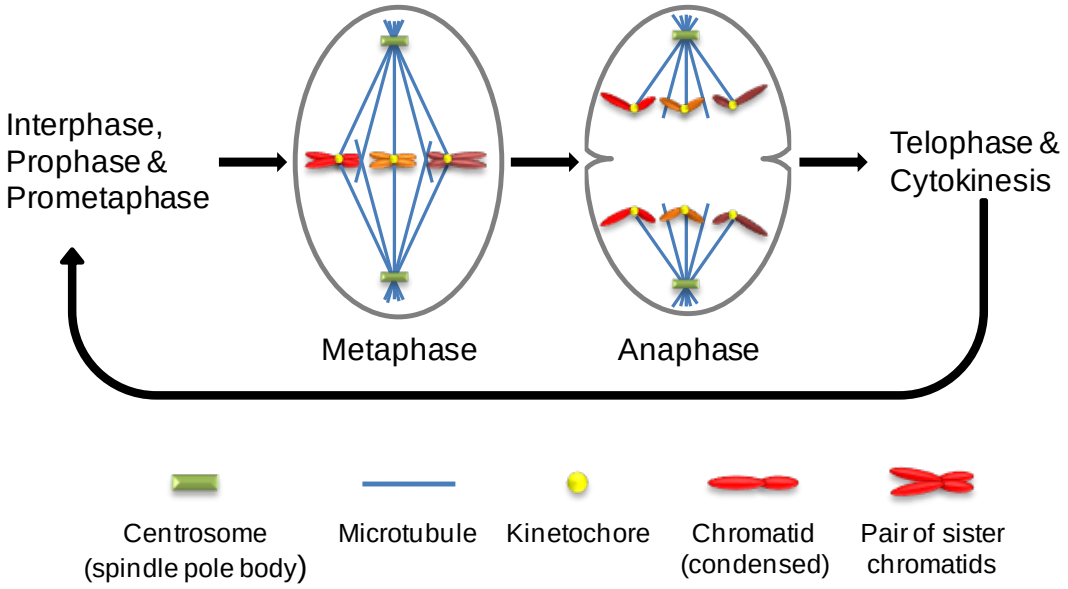

Figure 1.10 Chromosome segregation in eukaryotic cells. In interphase, chromosomes are replicated and the sister chromatids become cohesed. Mitosis begins in prophase with condensing of the chromatids and the formation of a bipolar array of microtubules emanating from a pair of centrosomes at opposite cell poles. Following this, the sister chromatids become attached to the mitotic spindles *via* centromere attached kinetochores before aligning at mid-cell during metaphase. During anaphase, the cohesion between the sister chromatids is removed and the attached microtubules depolymerise to move the sister chromatids to opposite cell poles in preparation for cell division (cytokinesis).

satisfy the spindle assembly checkpoint and proceed into segregation of the sister chromatids (Musacchio and Salmon, 2007).

Physical separation of the sister chromatids occurs during anaphase (Figure 1.10). First the cohesion between the sister chromatids is removed, by the protease Separase, which cleaves the cohesin subunit Scc1 (Hauf *et al.*, 2001; Sun *et al.*, 2009). Interestingly, very little is known about the forces that move the sister chromatids towards the centrosomes during anaphase. However, two models have been proposed. In the 'Pac-Man' model, kinetochores promote the depolymerisation

of the attached microtubules at their kinetochore attached (plus) end, whereas the 'poleward flux' model proposes that the microtubules depolymerise from their centrosome attached (minus) end. Both models permit the migration of the chromatids towards the centrosomes and there is evidence that both mechanisms not only exist, but work in tandem (Rogers *et al.*, 2004). Finally, the chromosomes decondense at telophase and the cells divide by cytokinesis.

1.4.2 Chromosome Segregation in *Caulobacter crescentus*

Like *E. coli*, *C. crescentus* is a Gram negative bacterium with a single, circular chromosome replicated bi-directionally from a single origin of replication. However, unlike *E. coli*, *C. crescentus* divides asymmetrically to produce both a motile daughter cell with a flagellum, known as a swarmer cell, and a sessile daughter cell, known as a stalked cell. Although only the stalked cells can divide, swarmer cells have the ability to differentiate into stalked cells by losing their flagellum and growing a stalk (Lawler and Brun, 2007). The interesting biology of *C. crescentus* has resulted in it becoming a well characterised model organism for the study of prokaryotic cell biology (Thanbichler and Shapiro, 2008) and recent advances have been made in understanding the mechanism by which *C. crescentus* segregates its chromosomes. By fluorescently labelling individual chromosomal loci, it has been shown that the genetic map of *C. crescentus* is recapitulated within the cells, with newly replicated origins of replication rapidly migrating to cell poles and the termini occupying mid-cell (Viollier *et al.*, 2004). The rapid migration of the replication origins was found to not be dependent on the replication origins themselves, but rather on a flanking sequence known as *parS* (Toro *et al.*, 2008).

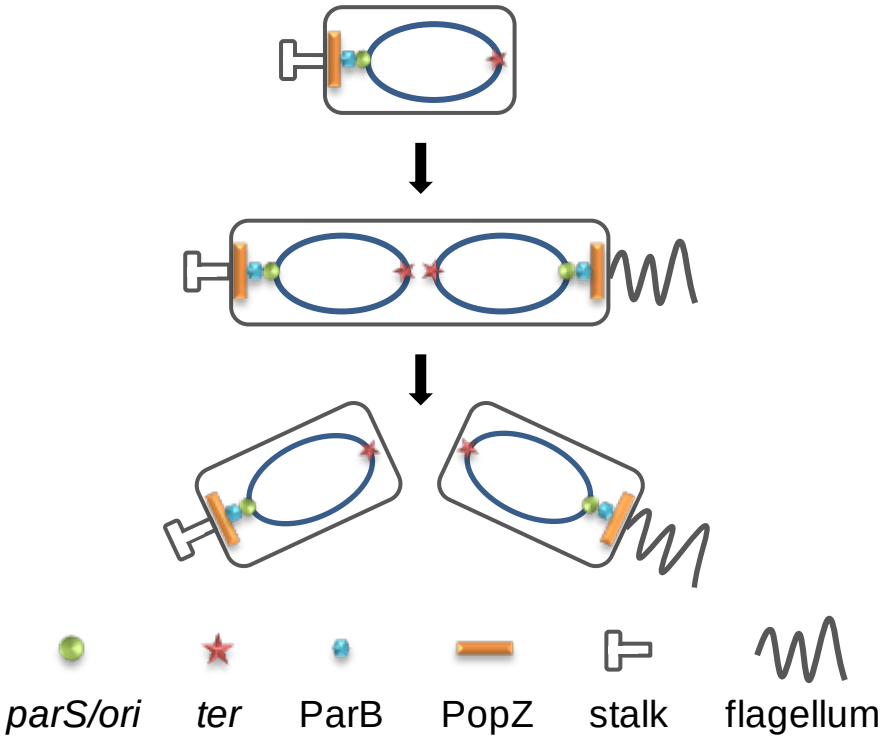

Figure 1.11 Chromosome segregation and cell division in *C. crescentus*. *C. crescentus* has a single, circular chromosome and differentiates during cell division to form a mobile, swarmer cell from a sessile stalked cell. For a swarmer cell to divide, it must shed its flagellum and grow a stalk. Although the cell divides asymmetrically, its sister chromosomes divide with bilateral symmetry such that its origins of replication (*ori*) are located at the cell poles and termini (*ter*) at mid-cell. This organisation is achieved by an interaction between *parS* bound ParB and the cell pole located protein PopZ.

parS is bound by the protein ParB, which in *C. crescentus* is essential for viability. It was recently shown by two independent groups that sister chromosomes are segregated in *C. crescentus* as a result of fixation of ParB-*parS* to the cell pole *via* an interaction with the cell pole localised protein PopZ (Bowman *et al.*, 2008; Ebersbach *et al.*, 2008a), Figure 1.11.

1.4.3 Chromosome Segregation in *Bacillus subtilis*

B. subtilis is a Gram positive bacterium that like *C. crescentus*, has become a model organism of choice for the study of prokaryotic cell biology (Thanbichler and Shapiro, 2008). During vegetative growth, *B. subtilis* divides symmetrically but under stress conditions, it differentiates to form a large mother cell and a small prespore. The prespore is later 'engulfed' by the mother cell to become an endospore (Piggot and Hilbert, 2004). More information is known about chromosome segregation during sporulation than vegetative growth. *B. subtilis* also contains a single, circular chromosome replicated bidirectionally from a single origin of replication (*oriC*).

During *B. subtilis* sporulation, as in *C. crescentus*, replicated *oriC* migrate rapidly to the cell poles in a process mediated by both a DNA binding protein and a cell pole localised protein. Here, the DNA binding protein is RacA and the cell pole localised protein is DivIVA (Ben-Yehuda *et al.*, 2003; Wu and Errington, 2003), Figure 1.12. It was recently shown that DivIVA locates to the cell poles by targeting negatively curved membranes (Lenarcic *et al.*, 2009). Interestingly, *B. subtilis* expresses a ParB homologue, known as SpoOJ, which also binds *parS* sites located close to *oriC*. Like *C. crescentus*, *parS* bound ParB protein plays an important role in chromosome segregation in *B. subtilis* (during sporulation) although it is not thought to be important for targeting *oriC* to the cell poles *per se*. Instead *parS* bound ParB recruits the SMC complex (also known as condensin), which organises the origin region and promotes chromosome segregation (Gruber and Errington, 2009; Sullivan *et al.*, 2009). SMC is related to the eukaryotic cohesin and condensin complexes as they all contain structural maintenance of chromosome (SMC)

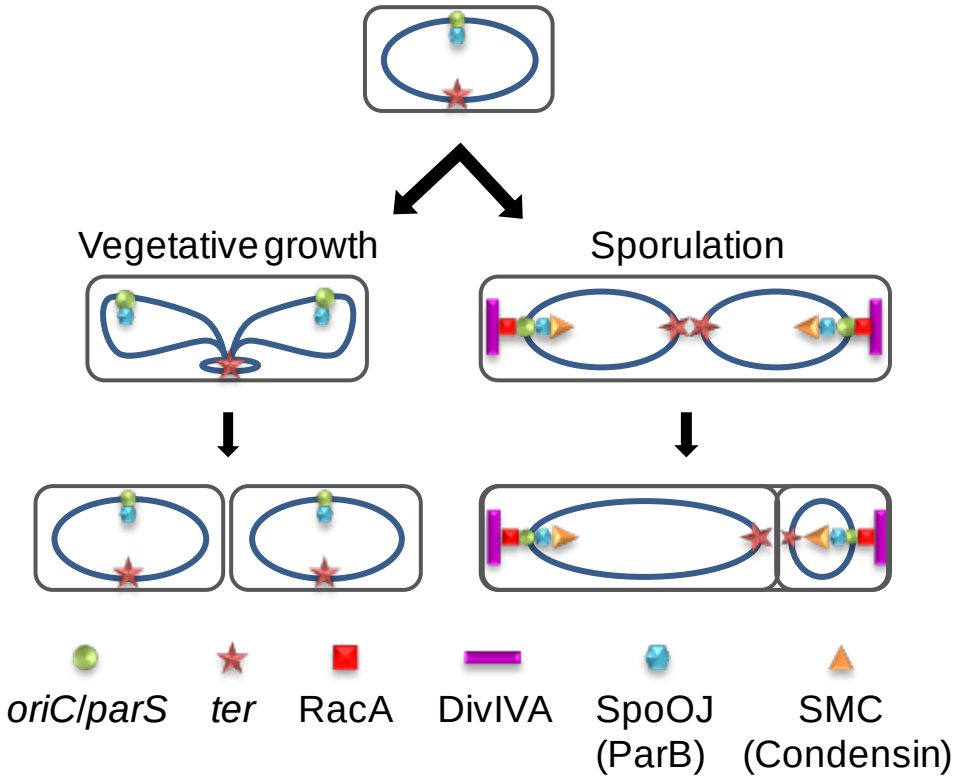

Figure 1.12 Chromosome segregation and cell division in *B. subtilis*. During vegetative growth, *B. subtilis* divides symmetrically with its origins of replication (*oriC*) located at the ¼ and ¾ positions of the cell. However, under stress conditions *B. subtilis* divides asymmetrically (sporulates), forming a large mother cell and small prespore. During sporulation the origins of replication become anchored to the cell poles *via* an interaction between DNA bound RacA and cell pole located DivIVA, and the chromosomes form what is known as an axial filament. This organisation requires an interaction between *parS* bound SpoOJ (ParB) protein and the SMC complex (condensin).

proteins. Chromosome segregation during vegetative growth is less well characterised, but is likely to occur by a different mechanism since replicated *oriC* in vegetative cells do not segregate to the cell poles but instead to the ¼ and ¾ positions of the cell (Berkmen and Grossman, 2006), Figure 1.12.

1.4.4 Chromosome Segregation in *E. coli*

Chromosome segregation in *E. coli* is less well characterised than in either *B. subtilis* or *C. crescentus*. Importantly, despite chromosomally encoded *parS* and ParB being highly conserved throughout the eubacteria kingdom, they are not found in *E. coli* (Livny *et al.*, 2007). *E. coli* does however express a functional analogue of the *B. subtilis* SMC complex (condensin) known as MukBEF. Interestingly, a MukB-GFP fusion localises to a region of the chromosome containing the origin of replication, where it was shown to promote normal chromosome segregation (Danilova *et al.*, 2007). The mechanism by which MukB localises to *oriC* and its precise function in promoting chromosome segregation still remain unclear, but may also involve DNA condensation (Cui *et al.*, 2008; Ohsumi *et al.*, 2001). Also, although the *E. coli* chromosome does not contain *parS* sites, a 25 bp sequence known as *migS* has been identified as having centromere-like properties. *migS* is located 211 kb from *oriC* (on the right replichore – clockwise on the genetic map) and migrates rapidly to opposite cell halves following replication (Fekete and Chattoraj, 2005; Yamaichi and Niki, 2004). However, insertion of *migS* in a plasmid containing *oriC* does not result in any specific localisation pattern of the plasmid (Yamaichi and Niki, 2004). It is therefore unlikely that *migS* mediates the tethering of DNA to the cell membrane in a mechanism analogous to *parS* in *C. crescentus*.

The pattern of chromosome segregation in *E. coli* (under slow growth conditions) has been described, and appears to be more similar to the pattern of chromosome segregation *B. subtilis* during vegetative growth than in either *C. crescentus* or sporulating *B. subtilis*. The region of the chromosome containing *oriC*

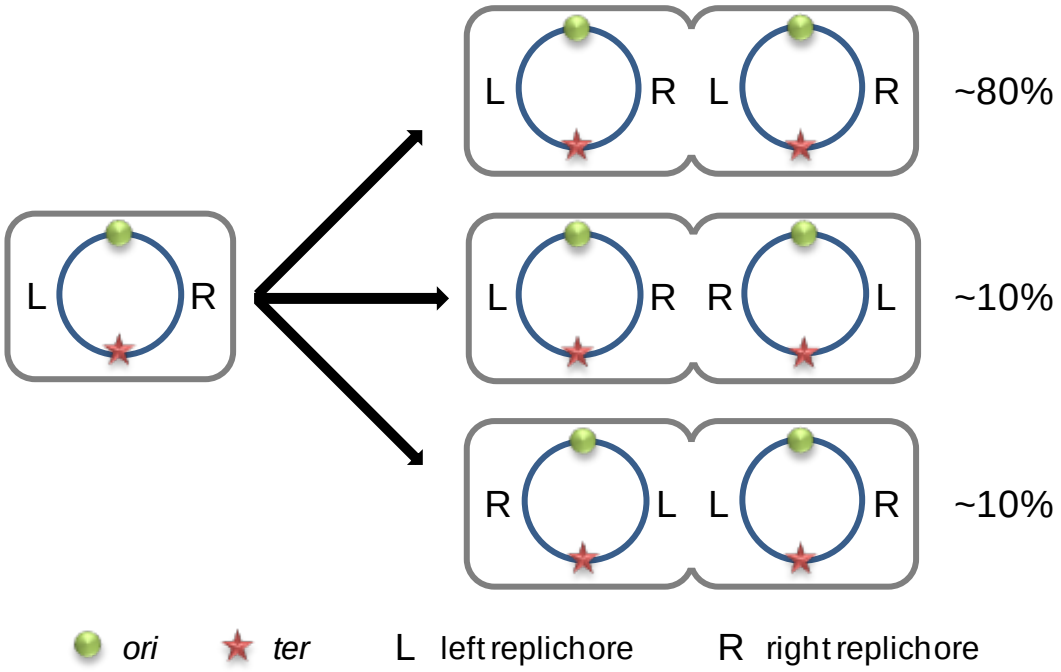

Figure 1.13 The pattern of chromosome segregation in *E. coli*. The genetic map of the *E. coli* chromosome is recapitulated within cells along their transverse axis. Following replication, the *oriC* region of the chromosome rapidly migrates to the ¼ and ¾ positions of the cell and the rest of the chromosome follows. The vast majority of cells (~80 %) segregate their sister chromosomes with translational symmetry.

migrates to the ¼ and ¾ positions of the cell and the genetic map is recapitulated on the transverse axis rather than the longitudinal axis (Niki *et al.*, 2000). Interestingly, the vast majority of cells show translational symmetry of the replicated chromosome (a left-right-left-right pattern of the 'left' and 'right' chromosome arms), with the rest showing mirror symmetry (Nielsen *et al.*, 2006b; Wang *et al.*, 2006), Figure 1.13. The reason why cells adopt different patterns of sister chromosome alignment is unclear but a recent study has shown that a block to replication fork progression can affect the relative proportions of the three segregation patterns in the population (Liu *et al.*., 2009).

Like *B. subtilis* and *C. crescentus*, chromosome segregation in *E. coli* is progressive (Nielsen *et al.*, 2006a; Wang *et al.*, 2005). Progressive segregation is however, preceded by a period of sister chromosome cohesion that is due, at least in part, to pre-catenation of the sister chromosomes (Bates and Kleckner, 2005; Wang *et al.*, 2008), see section 1.2.4. The mechanical force driving chromosome segregation is unknown. Indeed, it is still not clear that a mechanical force is necessary, but current data fail to be explained by either a model whereby sister chromosomes spontaneously partition (Jun and Mulder, 2006), or an alternative model of passive chromosome segregation, whereby replication origins attach to the cell membrane and segregation occurs as a result of elongation of the cell membrane, (Elmore *et al.*, 2005; Jacob *et al.*, 1963; Thanbichler and Shapiro, 2006). However, an integral membrane protein (SetB) has been identified as having a role in chromosome segregation, although it is not clear whether this effect is direct or indirect (Espeli *et al.*, 2003).

An attractive candidate for providing mechanical force for active chromosome segregation is the essential actin-like cytoskeletal protein MreB (Kruse *et al.*, 2005). A defect in chromosome segregation following MreB depletion has been reported, although the observation was contested (Karczmarek *et al.*, 2007; Kruse *et al.*, 2006). However, a more recent study has shown that MreB can regulate Topoisomerase IV (Madabhushi and Marians, 2009), suggesting that if MreB plays a role in chromosome segregation it is not as a force generator but as a regulator of the removal of precatenanes (Wang *et al.*, 2008). Interestingly, the integral membrane protein SetB was found to interact with MreB (Espeli *et al.*, 2003). Other models of active chromosome segregation involve indirect forces, such as transcription

(Dworkin and Losick, 2002; Kruse *et al.*, 2006) and DNA replication, although again there is conflicting evidence about this. For example, a model whereby replicated DNA is extruded from a stationary replisome is unlikely to function in *E. coli* as its two replisomes have been shown to be linked to each other neither physically or functionally (Breier *et al.*, 2005; Lemon and Grossman, 2000; Reyes-Lamothe *et al.*, 2008).

1.5 Cell Division in *E. coli*

E. coli cells do not differentiate during cell division but instead divides symmetrically to produce two indistinguishable daughter cells. Symmetric cell division requires the cell division machinery to be accurately placed at mid-cell. Also, the timing of cell division must be well synchronized with the growth rate of the cell in order to maintain cell size through the generations. However, there must also be a degree of flexibility in the regulation of cell division so that the cell can cope with various stresses such as a delay in chromosome segregation.

1.5.1 The Divisome

The process of cell division requires the formation of a large protein complex known as the divisome (Goehring and Beckwith, 2005). At the heart of the divisome is the tubulin-like protein FtsZ, which initiates cell division by polymerizing into a dynamic ring structure around the circumference of the cell (Michie and Lowe, 2006). This ring structure is known as the Z ring and serves as a landing pad for the rest of the divisome components. Along with FtsZ, the divisome is composed of at

least twelve other proteins: FtsA, FtsB, FtsEX, FtsI, FtsK, FtsL, FtsN, FtsQ, FtsW, ZipA, ZapA, and AmiC. Although the precise function of many of these proteins is unclear, their main roles in cell division appear to be recruiting and organising the divisome, stabilising the Z ring, connecting the Z ring to the cytoplasmic membrane, synthesising cell wall material, and hydrolysing peptidoglycan to separate the two daughter cells (Goehring *et al.*, 2006; Goehring *et al.*, 2007; Gonzalez and Beckwith, 2009; Weiss, 2004). Cell division is instigated by the Z ring producing a contractile force that drives invagination of the cell membranes. However, despite FtsZ being well characterised, the mechanism by which the Z ring produces a contractile force is still unknown (Allard and Cytrynbaum, 2009; Lan *et al.*, 2009).

1.5.2 Regulation of Cell Division

To maintain cell size, it is important that the process of cell division is co-ordinated within the cell cycle and regulated both temporally and spatially. There are two known mechanisms that negatively regulate Z ring assembly spatially and therefore aid selection of the division site. The first mechanism, known as nucleoid occlusion, acts to prevent the Z ring from assembling over unsegregated sister chromosomes (Yu and Margolin, 1999). Nucleoid occlusion is mediated by a nucleoid associated protein (SlmA) that binds FtsZ and prevents Z ring assembly (Bernhardt and de Boer, 2005). The second mechanism involves the proteins MinC, MinD and MinE, and prevents the Z ring from assembling at DNA-free regions at the cell poles (Lutkenhaus, 2002). MinC and MinD form a complex that inhibits the ‘scaffolding’ function of FtsZ by interacting with its C-terminal tail (Dajkovic *et al.*, 2008; Shen and Lutkenhaus, 2009). Interestingly, MinCD prevents Z ring formation at the cell

poles by oscillating between the two poles of the cell in 40 – 50 second intervals (Raskin and de Boer, 1999). This oscillation activity is stimulated by MinE (Rowland *et al.*, 2000) and causes the MinCD complex to be more concentrated at the cell poles than mid-cell (Thanbichler and Shapiro, 2008).

Despite much investigation into the factors regulating Z ring assembly spatially, the mechanism that triggers Z ring assembly under normal growth conditions is poorly understood, although it is known to not be directly affected by chromosome replication (Bernander and Nordstrom, 1990). However, a positive regulator of Z ring assembly (ZapB) has recently been identified in *E. coli* (Ebersbach *et al.*, 2008b) and work in *B. subtilis* has identified a metabolic sensor that determines cell size by inhibiting Z ring formation (Weart *et al.*, 2007). The most studied negative regulator of cell division is the SOS inducible protein SfiA (also known as SulA). SfiA inhibits Z ring assembly by preventing FtsZ from hydrolyzing GTP (Cordell *et al.*, 2003). Surprisingly, despite it being widely believed that the reason for inhibiting cell division during the SOS response is to give the cell enough time to repair its DNA and segregate its chromosomes prior to cell division, SfiA is not essential for survival of UV-irradiation (Gottesman *et al.*, 1981). This insensitivity may be due to the presence of some redundant pathway (such as nucleoid occlusion) or another SOS-inducible inhibitor of cell division (Hill *et al.*, 1997).

1.5.3 FtsK – a Protein that Links Recombination, Chromosome Segregation and Cell Division

The motor protein FtsK is a member of the divisome that is required to resolve chromosome dimers that result from crossover formation during the repair of DNA double-strand breaks (section 1.3). To resolve a chromosome dimer, the *E. coli* cell induces a site-specific recombination event at a sequence named *dif*, which is located in the terminus region of the *E. coli* chromosome (Bigot *et al.*, 2007). This site-specific recombination reaction requires the FtsK protein and two related tyrosine recombinases, XerC and XerD (Blakely *et al.*, 1993; Blakely *et al.*, 2000). The role of FtsK in dimer resolution is to align the two *dif* sequences on the chromosome dimer and stimulate the XerC/D recombination event.

FtsK is a DNA translocase that functions as a hexameric ring structure that encircles dsDNA (Massey *et al.*, 2006). It is loaded onto the chromosome at specific 8 bp sequences known as KOPS (FtsK Orientating Polar Sequences), which are skewed on the two halves of the chromosome as to ensure the orientation of FtsK towards *dif* (Bigot *et al.*, 2005; Lowe *et al.*, 2008). Upon alignment of *dif*, FtsK stimulates the site-specific recombination event *via* a direct interaction with XerD (Aussel *et al.*, 2002; Yates *et al.*, 2006). The timing of XerCD recombination at *dif* is believed to be restricted to shortly before cell division as a result of the interaction between FtsK and the divisome (Kennedy *et al.*, 2008). Although FtsK has been shown to locate at the septum (Wang *et al.*, 2005) and interact with many divisome proteins *via* its N-terminus, its actual role in cell division is unclear but it possibly plays a role in stabilizing the divisome (Grenga *et al.*, 2008).

1.6 Scope of this Thesis

This thesis concentrates on the study of an inducible, replication dependent site-specific DSB in the chromosome of *E. coli* that is caused by cleavage of a DNA hairpin by the hairpin endonuclease SbcCD. The DNA hairpin is formed by a 246 bp interrupted DNA palindrome on the lagging, but not the leading, strand template of replication. As a result, cleavage occurs on only one of a pair of sister chromosome, once per replication cycle and the DSB can be efficiently repaired by RecBCD homologous recombination (Eykelenboom *et al.*, 2008). In Chapter 3, the effect of this DSB on growth, cell division, and nucleoid segregation is investigated using both genetic and cell biology approaches. In order to make a more detailed investigation into the effect of this DSB on chromosome segregation, the palindrome was labelled with fluorescent markers on either side, allowing the location of the two ends of the DSB within the cell to be identified and distinguished. Chapter 4 discusses the construction, characterisation and optimisation of this system. In Chapter 5, by investigating chromosome segregation following DNA hairpin cleavage by SbcCD in a *recA*$^-$ mutant, this system of fluorescently labelling the ends of the DSB was not used to investigate chromosome segregation in the context of DSB repair, but rather utilised as a tool for distinguishing leading, and lagging strand replicated DNA (White *et al.*, 2008). Finally, Chapter 6 describes how this system was further modified to make it suitable to use this system to investigate chromosome segregation in the context of DNA repair.

Chapter 2

Materials and Methods

2.1 Materials

2.1.1 Media, Antibiotics and Inducers

Liquid growth media were stored at room temperature except during experiments when they were pre-warmed to the desired temperature. M9-minimal medium was filter sterilised prior to use, whereas all other liquid growth media were autoclaved. To obtain solid media, agar was added to liquid media prior to autoclaving except for M9-minimal agar where 2 % agar-distilled water was first autoclaved, melted, and allowed to cool prior to the addition of salts and sugar. Melted agar was stored at 55 °C and allowed to cool prior to the addition of antibiotics and inducers (when required). Recipes for growth media are shown in Table 2.1 and details of antibiotics and inducers used in this study can be found in Table 2.2.

2.1.2 Enzymes

All restriction enzymes were purchased from New England Biolabs (NEB). GoTaq® and *Pfu* DNA polymerase were purchased from Promega. All enzymes were used according to the manufacturer's guidelines.

2.1.3 Buffers and Solutions

All buffers and solutions were stored at room temperature. Unless stated otherwise, chemicals were dissolved in double distilled, sterile water (Milli-Q®).

Media	Composition
L Broth	1 % Bacto-tryptone, 0.5 % yeast extract, 1 % NaCl; pH adjusted to 7.5 with NaOH
LB Agar	1 % Bacto-tryptone, 0.5 % yeast extract, 1 % NaCl, 1.5 % Bacto-agar; pH adjusted to 7.5 with NaOH
LC Agar	1 % tryptone, 0.5 % yeast extract, 0.5 % NaCl, 1 % Difco-agar; pH adjusted to 7.2 with NaOH
LC Top Agar	1 % tryptone, 0.5 % yeast extract, 0.5 % NaCl, 0.7 % Difco-agar; pH adjusted to 7.2 with NaOH
M9 Salts (4x)	28 g Na_2HPO_4, 12 g KH_2PO_4, 2 g NaCl, 4 g NH_4Cl; made up to 1 L with double-distilled sterile water
M9-Minimal Media	1 x M9 salts, 0.2 % glycerol, 1 mM $MgSO_4$, 5µM $CaCl_2$
M9-Minimal Agar	1 x M9 salts, 0.2 % glycerol, 1 mM $MgSO_4$, 5µM $CaCl_2$, 1.5 % Bacto-agar
Phage Buffer	7 g Na_2HPO_4, 5 g NaCl, 3 g KH_2PO_4, 1 mM $MgSO_4$, 1 mM $CaCl_2$, and 1 % gelatine; made up to 1 L with double-distilled sterile water

Table 2.1 Bacteria growth media. Concentrations indicated as percentages are weight/volume (w/v).

EDTA (pH 8)

0.5 M stock solutions were adjusted to pH 8.0 using 10 M NaOH and filter sterilised.

TAE Buffer (50x)

2 M Tris base, 0.05 M EDTA (pH 8) and 57.1 ml glacial acetic acid made up to 1 L with distilled water and filter sterilised. TAE was used at a working concentration of 1x.

Antibiotic/ Inducer	Abbrev	Solvent	Stock Conc^n	Final* Conc^n
Ampicillin	Amp	H_2O	100 mg ml^{-1}	100 μg ml^{-1}
Cephalexin	Ceph	H_2O	10 mg ml^{-1}	10 μg ml^{-1}
Chloramphenicol	Cm	100 % ethanol	50 mg ml^{-1}	50 μg ml^{-1}
Gentamycin	Gm	H_2O	10 mg ml^{-1}	10 μg ml^{-1}
Kanamycin	Km	H_2O	50 mg ml^{-1}	50 μg ml^{-1}
Spectinomycin	Spc	H_2O	25 mg ml^{-1}	50 μg ml^{-1}
Anhydrotetracycline	ATC	50 % ethanol	100 μg ml^{-1}	100 ng ml^{-1}
Isoproply-β-D-Thiogalactopyranoside	IPTG	H_2O	1 M	0.5 mM

*Unless otherwise stated; Abbrev is abbreviation and Conc^n is concentration.

Table 2.2 Antibiotics and inducers. Stock solutions of the antibiotics and inducers listed above were stored at -20 °C.

2.2 Molecular Biology Methods

2.2.1 Plasmid Purification

To isolate plasmid DNA, the *E. coli* strain harbouring the desired plasmid was first grown overnight with appropriate selection in L broth at either 37 °C, or 30 °C (if the plasmid was temperature sensitive). Plasmids were extracted from these cells using a QIAprep® Spin Miniprep Kit (Qiagen) according to the manufacturer's guidelines. Following Qiagen's recommendations, low copy number plasmids (pTOF24 and its derivatives) were isolated from 5 ml of overnight culture as opposed to 1 ml of

culture for high copy number plasmids. Plasmid DNA was stored in double distilled sterile water at -20 °C.

2.2.2 Genomic DNA Extraction

2.2.2.1 Boiled Cell Method

For the majority of polymerase chain reaction (PCR) applications, boiling cells produced genomic DNA of adequate quality to act as a template. Cells were boiled by suspending a single colony in 30 µl of sterile water and heating to 99.9 °C for 10 min before centrifuging for 3 min in a microcentrifuge. 2 µl of the resulting supernatant was used as a template for a 25 µl PCR reaction.

2.2.2.2 Kit Method

When the DNA amplified by PCR was needed for cloning, the genomic DNA used as a template was isolated using a Wizard® Genomic DNA purification kit (Promega) according to the manufacturer's instructions. This genomic DNA was eluted in double distilled, sterile water and stored at -20 °C.

2.2.3 Polymerase Chain Reaction

2.2.3.1 Standard PCR

PCR reactions were carried out in a thermo-cycler. GoTaq® Flexi DNA polymerase, (Promega) was used for all reactions unless the PCR product was required for cloning, in which case a high-fidelity polymerase with proof-reading activity (*Pfu* DNA polymerase, Promega) was used. PCR reactions were carried out according to

manufacturer's guidelines. The melting temperatures of primers were calculated by the manufacturer of the oligonucleotides (MWG).

2.2.3.2 Site-Directed Mutagenesis

Site-directed mutagenesis (SDM) is a PCR based technique for the *in vitro* introduction of point mutations and small insertions/deletions into a plasmid. Methylated template plasmid DNA was first isolated from the *dam*$^{+}$ *hsdR*$^{-}$ *E. coli* strain XL1-blue and then the entire plasmid was amplified by PCR using *Pfu* DNA polymerase and primers containing the desired mutation(s). Following thermal cycling, 1 µl of the restriction enzyme DpnI was directly added to the PCR mixture, which was then incubated for 4 h at 37 °C. This step resulted specifically in the restriction of the original plasmid since DpnI only cleaves methylated DNA and *in vitro* replicated DNA is unmethylated. Next, the nicked circular PCR products were introduced into XL1-blue by $CaCl_2$ transformation, where it could be ligated and amplified. Finally, plasmids were extracted from the transformants and sequenced for the desired mutations. Mutagenic primers were designed and reaction conditions calculated by following guidelines outlined in the QuickChange® Site-Directed Mutagenesis Kit manual (Stratagene).

2.2.3.3 Cross-over PCR

Cross-over PCR is a technique for the precise hybridisation of DNA molecules without the use of DNA ligase (Horton *et al*., 1989) that was used for the construction of homology arms for plasmid mediate gene replacement (PMGR) vectors (see section 2.3.3). First, the two individual homology arms were created by PCR amplification of the *E. coli* chromosome using *Pfu* DNA polymerase and purified using a QIAquick® PCR Purification Kit (Qiagen) by following the

manufacturer's instructions. Importantly, two of the primers (the reverse primer of the 1st homology arm and the forward primer of the 2nd homology arm) were designed to have 20-30 bp of homology to one another. After purification, these two PCR products were used as a template for a second round of PCR amplification using the forward primer of the first homology arm and the reverse primer of the second homology arm. After denaturation and annealing, the two initial PCR products hybridise at their complementary overhangs, allowing the fused fragment to be amplified using the (restriction site tagged) external primers.

2.2.4 Cloning

Purified DNA was digested with restriction endonucleases according to the manufacturer's guidelines. When cloning into a single restriction site, the linearised vector may re-ligate with itself. To reduce the background of re-ligated vector in such reactions, 5' phosphates were removed from the ends of the linearised plasmids by the addition of calf intestinal phosphatase (NEB, 1 µl), followed by a 30 min incubation at 37 °C. Digested and dephosphorylated DNA was purified prior to ligation using a QIAquick® PCR Purification Kit (Qiagen) following the manufacturer's instructions and stored at -20 °C if necessary. When required, digested DNA was run on an agarose gel (see section 2.2.6) and the desired fragment isolated by gel extraction using a QIAquick Gel Extraction Kit (Qiagen) prior to ligation. Ligations were carried out using a Quick Ligation™ Kit (New England Biolabs) with an approximate insert to vector ratio of 3:1. 3 µl of the ligation mix was used to transform the *recA*$^-$ *dam*$^+$ *hsdR*$^-$ *E. coli* strain XL1-blue in order to store and propagate the cloned plasmid.

2.2.5 BigDye DNA Sequencing

PCR products were purified using a QIAquick® PCR Purification Kit (Qiagen) prior to carrying out the sequencing reaction using a BigDye® Terminator v3.1 Cycle-Sequencing Kit (Applied Biosystems) according to the manufacturer's instructions. Samples were run on an ABI PRISM 3100-Avant Genetic Analyzer by The Gene Pool, University of Edinburgh (https://www.wiki.ed.ac.uk/display/GenePool/Home).

2.2.6 Agarose Gel Electrophoresis

DNA fragments acquired from PCR reactions and restriction digests were separated by size using 1 % agarose in TAE (w/v) gels that were ran in TAE (1x) buffer. In order to visualise the DNA, the nucleic acid stain SafeView (NBS Biologicals) was added directly to the agarose gel and buffer according to the manufacturer's guidelines. Gels were ran between 80 and 130 volts for up to 1 hour and viewed under a UV lamp (UVIdoc, by UVItec). DNA ladders (1 kb or 100 bp DNA ladder, NEB) were used to estimate the size of DNA.

2.2.7 Illumina Solexa Sequencing

Solexa sequencing is a next-generation sequencing technology that provides a rapid and cost effective method for the sequencing of entire genomes. Samples were sequenced using an Illumina Solexa 1G platform and aligned with the published sequence for the *E. coli* K12 strain MG1655 (GenBank: U00096) by The Gene Pool, University of Edinburgh (https://www.wiki.ed.ac.uk/display/GenePool/Home). To reduce the probability of obtaining false-positives, a high stringency threshold was used to identify single nucleotide polymorphisms (SNPs). For a SNP to be deemed

real the sequence had to be covered by at least ten reads and at least 90 % of high quality bases had to differ from the sequence onto which it was aligned. Insertions and deletions (InDels) were identified using the alignment software SOAP, which was only established to identify InDels of up to 3 bp. Only InDels that had been identified by at least three independent reads were deemed to be real.

2.3 Microbiology Methods

2.3.1 Storage of Bacteria

E. coli strains were stored at -80 °C in 40 % glycerol (v/v) by mixing equal volumes of (stationary phase) liquid cell culture and 80 % glycerol. Bacteria were stored in the short-term (up to 2 weeks) at 4 °C on inverted agar plates sealed with Parafilm®.

2.3.2 $CaCl_2$ Transformation

A culture of the strain to be transformed was first grown at 37 °C in L broth with agitation to an optical density at 600 nm (OD_{600}) of ~ 0.5 (mid-exponential phase of growth) before spinning down 1 ml aliquots in a bench top centrifuge for 1 min. The supernatant was then discarded and the cells gently re-suspended in 500 µl of fresh, ice-cold 0.1 M $CaCl_2$ and then left on ice for 30 min. This cell suspension was then spun down for 30 seconds and re-suspended in 100 µl of 0.1 M $CaCl_2$ prior to the addition of DNA (~10 ng of plasmid DNA or ~25 ng of ligation mix). Following this, the cells were left on ice for a further 30 min and then heat-shocked at 37 °C for 5 min before briefly placing back on ice. Next, 400 µl of L broth was added to the

cell suspension that was then incubated for 1 h at 37 °C (or 30 °C for 2 h if the plasmid was temperature sensitive) in order to give the transformed cells time to express the selection marker. Finally 200 µl of the cell suspension was plated onto selective media and incubated overnight at the appropriate temperature.

2.3.3 Plasmid Mediated Gene Replacement

Genetic engineering has been greatly advanced by the advent of 'recombineering'. Recombineering is a homologous recombination approach to making precise alterations to chromosomal DNA. Briefly, this involves flanking the desired alteration (deletion, insertion *etc*.) with DNA that is homologous to the locus that is to be modified. Following transformation with this cassette, two independent recombination events at the flanking homology will result in the original chromosomal locus being replaced with the desired alteration. These cassettes are typically made by a crossover PCR reaction (see section 2.2.3.3). However, since linear DNA is rapidly degraded in *E. coli*, it is not possible to simply transform cells with the resulting PCR fragment. Two alternative approaches are used to circumvent this problem. Either bacteriophage proteins can be used to inhibit degradation of the linear construct and promote homologous recombination (Sharan *et al*., 2009) or the construct can be cloned into a plasmid vector.

Plasmid mediated gene replacement (PMGR) is a method of recombineering in *E. coli* that utilises plasmids based on the gene replacement vectors of Link and collaborators (Link *et al*., 1997). The plasmid used in this study, pTOF24 (Merlin *et al*., 2002), is one such plasmid and contains the following important features: a temperature sensitive replication protein (encoded by $repA^{ts}$) that is functional at 30

°C but not at 42 °C, a positive selection marker (*cat*) encoding chloramphenicol resistance, a negative selection marker (*sacB*) encoding Levansucrase (an enzyme that makes *E. coli* sensitive to the sugar sucrose) and a unique cloning site (PstI/SalI) (Fig. 2.1a). PMGR vectors were created by fusing together two DNA sequences, each containing ~ 400 bp of homology to the *E. coli* chromosome, by crossover PCR (see section 2.2.3.3). Primers for this reaction were designed to flank the fused DNA sequence with PstI and SalI restriction sites, allowing subsequent cloning into pTOF24. Importantly, although deletion vectors were designed to create an in-frame mutation to limit any potential downstream effects, the insertion vectors used in this study did not necessarily result in an in-frame alteration to the chromosome.

To manipulate the *E. coli* chromosome, the strain of interest was first transformed with the PMGR vector by selecting for chloramphenicol resistance at the permissive temperature (30 °C). Transformants were then streaked out onto fresh chloramphenicol plates and incubated at the restrictive temperature (42 °C). As the plasmid cannot replicate at 42 °C, only strains that have integrated the plasmid into their chromosome will survive at 42 °C in the presence of chloramphenicol. This integration into the chromosome can occur by homologous recombination at either one of the two homology arms in the plasmid. Integrants, which were identified as large colonies on chloramphenicol plates at 42 °C, were then purified by streaking onto fresh chloramphenicol plates and incubated at 42 °C.

Next, excision of the integrated plasmid from the chromosome was permitted by inoculating L broth with a single colony and allowing the culture to grow overnight at 30 °C (without selection for the plasmid). Presence of the plasmid was then selected against, by plating a dilution of the overnight culture (typically 100 µl

of a 10^{-5} dilution) onto LB agar plates supplemented with 5 % sucrose. Since Levansucrase is not 100 % effective as a negative selection marker, colonies from the sucrose plates were subsequently screened for chloramphenicol sensitivity to ensure that the plasmid had been lost.

As with integration, resolution of the plasmid out of the chromosome can occur by homologous recombination at either of the two homology arms. When the second recombination event occurred within the same homology arm that was used for the integration event, the chromosome was not altered. However, when different homology arms were used for the integration and excision event, then a precise insertion/deletion event occurred (see Figure 2.1b). This type of alteration to the chromosome is termed markerless because it results in the loss of the selection marker (*cat*) that was used to select for the integration event. As a result, it is possible to use this technique to make multiple, sequential modifications to the chromosome without running out of suitable selection markers. Finally, these alterations were first screened for by PCR and then confirmed by either sequencing (in the case of inserting Chi-arrays using pDL3181 and pDL3192), microscopy (for insertion of either operator array), or testing ultraviolet light sensitivity (for recombination mutants).

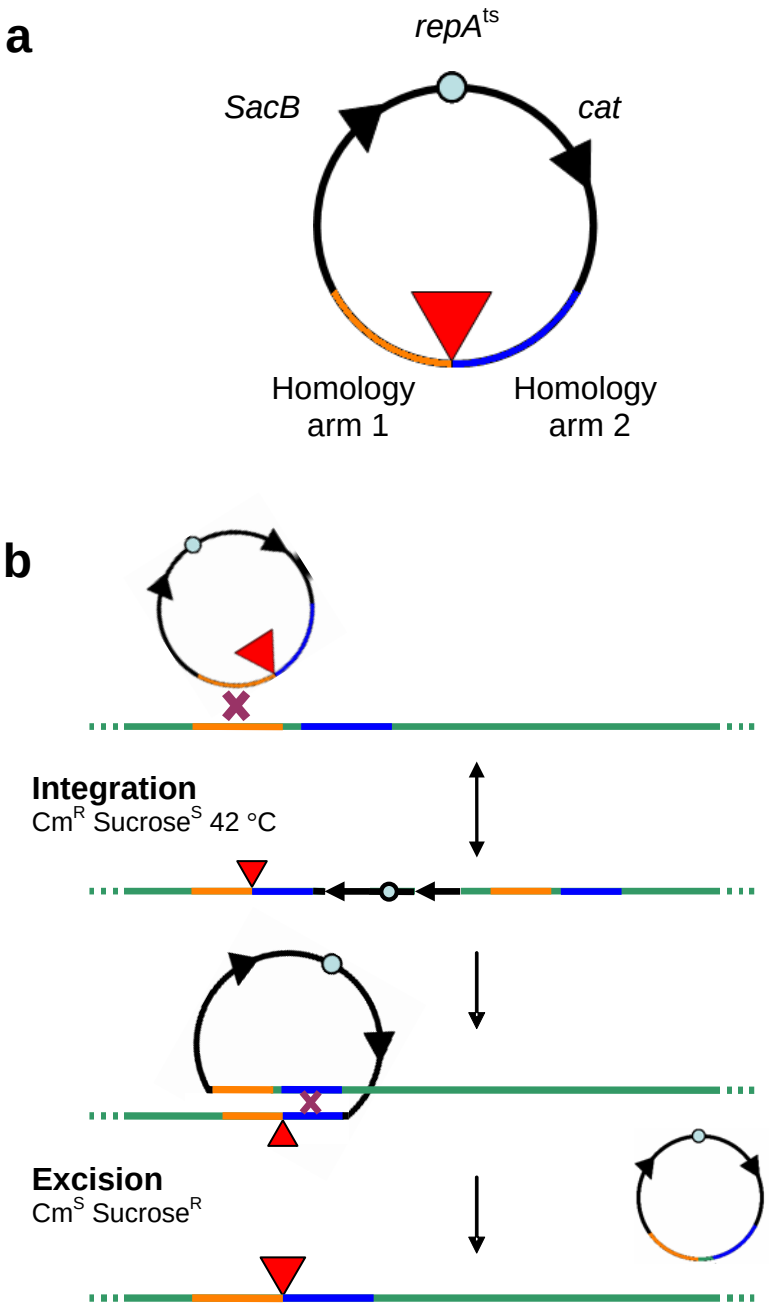

Figure 2.1 Plasmid mediated gene replacement. **a**, Schematic representation of a temperature sensitive PMGR vector, *cat* encodes chloramphenicol resistance and *sacB* an enzyme (Levansucrase) that makes cells sensitive to sucrose. The red triangle indicates a DNA sequence to be integrated into the chromosome. **b**, Cartoon of the main stages involved in PMGR. Integration of the vector is selected for by growth at 42 °C on chloramphenicol plates. Excision of the vector is selected for by growth on sucrose supplemented media and checked by screening for chloramphenicol sensitivity. Colonies with the desired chromosomal alteration are typically screened for by PCR. A recombination event is indicated by a purple cross.

2.3.4 P1 Transduction

P1 is a generalised transducing phage that can be used to transfer chromosomal DNA from one *E. coli* strain to another. This technique takes advantage of an infrequent aberrant event in the P1 lytic growth cycle, when the phage packages host *E. coli* chromosomal DNA (~ 100 kb) into the phage head (Thierauf *et al*., 2009). When such phage particles infect a new host cell, the packaged chromosomal DNA can replace the homologous chromosomal region of the new host by RecA dependent homologous recombination. Since this event is infrequent, the gene or mutation to be transferred must by linked to a genetic marker (such as an antibiotic resistance) in order to select for the desired transductants.

2.3.4.1 Preparing a P1 Lysate

A culture of the *E. coli* strain carrying the gene or mutation of interest was grown to mid-exponential growth phase (OD_{600} of ~ 0.5) at 37°C in L broth supplemented with 2.5 mM $CaCl_2$. 200 µl of this culture was then mixed with 100 µl of a range of P1 lysate (that had been grown on the wild-type *E. coli* K12 strain MG1655) dilutions. 10^{-4}, 10^{-5} and 10^{-6} in phage buffer was typically used as well as phage buffer only as a cell only control. This was then incubated for 30 minutes at 37 °C with gentle agitation to allow for phage adsorption. 2.5 ml of molten LC top agar supplemented with 5 mM $CaCl_2$ was then added to the cell-phage mix and then poured onto an LC agar plate containing 5 mM $CaCl_2$ and incubated upright at 37 °C overnight. Next, phages were then harvested from the plate that gave confluent lysis by removing the top agar and adding it to 5 ml of phage buffer. This mixture was then vortexed with 100 µl of chloroform to kill any *E. coli* cells present and then left

at 4 °C for 30 min. Finally, following centrifugation (5,000 rpm for 10 minutes at room temperature), the supernatant was transferred to a fresh bottle containing 100 µl of chloroform and stored at 4 °C in the dark.

2.3.4.2 P1 Transduction

A culture of the *E. coli* strain to be transduced was grown overnight in L broth supplemented with 2.5 mM $CaCl_2$ at 37 °C with shaking prior to centrifuging 1 ml aliquots in a bench top centrifuge for 1 min. Supernatant was discarded and the cells re-suspended in 100 µl of L broth containing 2.5 mM $CaCl_2$. This was then mixed with 100 µl of either a range of dilutions of the desired P1 lysate, typically neat or 10^{-1} in phage buffer along with phage buffer only as a cell only control, and incubated at 37 °C with gentle agitation for 20 min. Next, 800 µl of L broth supplemented with 2 mM sodium citrate was then added to the culture to prevent further infection by the phage and the cells incubated at 37 °C with gentle agitation for a further 1 hour to allow time for the selection marker to be expressed. Finally, 200 µl of this culture was plated onto selective media and incubated at 37 °C overnight. Successful transductants were then purified from residual phage by streaking onto fresh selective LB agar plates twice, sequentially. Transductants were tested phenotypically to ensure the successful co-transduction of the desired mutation with the selection marker.

2.3.5 Phenotypic Tests

2.3.5.1 Ultraviolet Light Sensitivity

In order to test the sensitivity of recombination mutants (*recA*$^-$ and Δ*recB*) to ultraviolet (UV) light, cultures of the potential mutants and their respective (recombination proficient) parental strains were grown overnight in 5 ml L broth (37 °C with agitation). Serial dilutions of these cultures were then spotted onto LB agar plates in duplicate before exposing one of the plates to 1 J/m^2 of UV-light using a UV Stratalinker™ 1800 (Stratagene). Both plates were then incubated at 37 °C overnight in the dark, and the relative UV-light sensitivities of the parent strains and the recombination mutants were compared the next day.

2.3.5.2 Microscopy

Successful integrations of the operator arrays (*tetO* and *lacO*) were tested by microscopy, following transformation with a plasmid that expressed TetR-YFP and LacI-CFP (pWX6 or pDL3196). Transformants were grown overnight in M9-minimal medium supplemented with 0.2 % glucose and 100 ng ml^{-1} ATC (see section 4.5) and sampled for microscopy as described in section 2.4. In the presence of the operator arrays, the fluorescent repressors bind to the array of their DNA binding (operator) sites (TetR-YFP binds *tetO* and LacI-CFP binds *lacO*). Operator bound TetR-YFP appears as a yellow fluorescent focus and LacI-CFP as a cyan fluorescent focus. Expression of TetR-YFP and LacI-CFP proteins in cells lacking the operator arrays rarely results in the appearance of fluorescent foci (see section 4.9) that may represent protein aggregate structures.

2.4. Microscopy Methods

2.4.1 Image Acquisition

Unless otherwise stated, live cells were mounted onto a bed of 1 % agarose in H_2O (w/v) for viewing under the microscope. Images were acquired using a Zeiss Axiovert 200 fluorescence microscope equipped with a Photometrics cool-SNAP charge-coupled device camera, a MS2000 XY piezo z stage and the acquisition software MetaMorph 6.3r2. All brightfield images were acquired using phase contrast. Images were typically acquired at a resolution of 129 nm per pixel. Notably, this resolution is higher than the optical resolution of light, which for standard widefield fluorescence microscopy is approximately $\lambda/2$ or 200 nm. Strains were cultured in M9-minimal media for fluorescence microscopy for the dual purpose of improving the imaging by reducing the background fluorescence and simplifying analyses by reducing the number of chromosomes within the cells (see section 3.3.4).

2.4.2 Deconvolution

Fluorescence images were acquired at multiple z-sections (typically ± 800 nm, 9 images at an interval of 200 nm) and then subject to three-dimensional adaptive point-spread function (blind) deconvolution using the software Autodeblur and Autovisualise v9.3. Deconvolution is a computational technique for reassigning out of focus light to its point of origin based on the mathematical modelling of the out of focus light as a point spread function (PSF). Although it is possible to calculate the PSF for a specific microscope set up using sub-resolution fluorescent microsphere of

known diameter (*e.g.* PS-Speck™ microscope point source kit available from Invitrogen), it is a difficult and time consuming process. Adaptive blind deconvolution does not rely on the PSF being known, but instead derives the underlying PSF for the z-stack using a method based on maximum likelihood estimation and constrained iteration. Deconvolution was used to reduce noise and improve resolution of the fluorescence images post-acquisition. All fluorescence images were deconvolved prior to analysis.

2.4.3 Time-lapse Microscopy

The Zeiss Axiovert 200 fluorescence microscope was encased within an incubator (Solent Scientific) that allowed the temperature to be set and stably maintained (± 2 °C) within a range of 32 °C to 42 °C. Incubation of microscopy slides at 37 °C resulted in the desiccation of the solid growth media on which the cells were mounted. As well as potentially causing desiccation of the cells, this phenomenon also resulted in a major drifting of the cells, mainly in the z axis but also in the x and y axes, from the field of view causing difficulties for long term imaging. To create a more stable platform for imaging, a sealable chamber was created by the adhesion of a CoverWell™ imaging chamber gasket (Invitrogen) to a glass slide. This chamber was then filled with molten growth media that was allowed to set under a glass coverslip for flatness. Next, a sample of cell culture was spotted onto the growth media and the chamber covered by a glass coverslip. Finally, the edges of the coverslip were coated with silicon grease to help seal the chamber.

2.4.4 Cell Length Measurements

Cell lengths were measured using the 'fiber length' measurement of the image analysis software MetaMorph v6.3r2. This calculates length using the formula:

$$\textbf{Fibre Length} = \tfrac{1}{4}[P + \sqrt{(P^2 - 16A)}]$$

Where P is the perimeter of the object (cell)

A is the area of the object (cell)

This method of calculating cell length was deemed appropriate since it takes into account any curvature of the cell as opposed to the 'length' measurement of MetaMorph v6.3r2 that only measures the length of the longest chord of the object (cell).

2.4.5 Centroid Analysis

To measure the distance between pairs of YFP and CFP foci (section 4.9.2), MetaMorph v6.3r2 was used to identify the x and y coordinates of the centroids of the YFP and CFP foci on their respective maximum projection images. Centroid analysis is a method of identifying the point that represents the centre of the mass of an object, which in this case was either a YFP or a CFP fluorescent focus. As such, the accuracy of this technique is limited by the resolution at which the images were acquired rather than the resolution of light. The method of identifying centroids used here was weighted for the fluorescence intensity of the pixels of the object ('intensity center' measurement of MetaMorph). The x and y co-ordinates of neighbouring YFP and CFP foci was then used to triangulate the distance between the two. Importantly,

this calculation does not take into account the distance between the foci in the z plane.

2.5 Statistical Analyses

Statistical analyses were performed using the software Minitab 15.

2.6 *E. coli* Strains

Strains that were used in this study are listed in Table 2.3. XL1-Blue was used for all cloning procedures and the propagation of plasmid DNA, whereas derivatives of MG1655 were used for experiments.

2.7 Plasmids

Plasmids used in this study are listed in Table 2.4. The *E. coli* strain XL1-Blue was used for all cloning procedures and the propagation of plasmid DNA.

2.8 Oligonucleotides

Oligonucleotides were manufactured by MWG Biotech where they were synthesised, HPSF purified and lyophilized. 100 mM stock solutions were made by dissolving in sterile water and stored at -20 °C. Working solutions were made up to 5 mM in sterile water and stored at -20 °C. Primers were designed using the internet-based tool Primer3 (http://frodo.wi.mit.edu/cgi-bin/primer3/primer3_www.cgi). Oligonucleotides used in this study are shown in Table 2.5.

Strain	Genotype	Plasmid	Source or Construction
XL1-Blue	*recA1*, *endA1*, *gyrA96*, *thi-1*, *hsdR17*, *supE44*, *relA1*, *lac*, [F' *proAB*, *lacI*^{q}, *lacZ*ΔM15, Tn*10*]		Stratagene
DB1318	*recD1014 hsdR2 zgq202*::Tn*10* *recA*::Cm^{R}		(Wertman *et al*., 1986)
DS984	*recF lacI*^{q} *lacZ*ΔM15 *xerCY17*::Cm^{R}		(Colloms *et al*., 1996)
GR47	*lexA3 dif*Δ*6*::Km^{R}		(Recchia *et al*., 1999)
N1642	*lexA3 malE*::Tn*10*		(Lloyd *et al.*, 1987)
MG1655	F^{-} λ^{-} *ilvG*$^{-}$ *rfb-50 rph-1*		(Blattner *et al*., 1997)
BW27784	MG1655 *lacI*^{q} *rrnB3* Δ*lacZ4787 hsdR514* Δ(*araBAD*)*567* Δ(*rhaBAD*)*568* Δ(*araFGH*) Φ (ΔP_{araE} P_{CP18}-*araE*)		(Khlebnikov *et al.*, 2001)
DL1777	MG1655 *lacI*^{q} *lacZ*χ^{-}		(Eykelenboom *et al*., 2008)
DL1780	BW27784 ΔP_{sbcDC} P_{BAD}-*sbcDC*		(Eykelenboom *et al*., 2008)
DL2006	DL1780 *lacZ*::pal *cynX*::Gm^{R}		(Eykelenboom *et al*., 2008)
DL2075	DL2006 *recA*::Cm^{R}		(Eykelenboom *et al*., 2008)
DL2237	DL2006 *xerCY17*::Cm^{R}		DL2006 x P1[DS984], John Eykelenboom
DL2241	DL2006 *dif*Δ*6*::Km^{R}		DL2006 x P1[GR47], John Eykelenboom
DL2283	MG1655 *araB*::P_{BAD}-Km^{R}		PMGR using pDL1625
DL2520	BW27784 *araB*::P_{BAD}-Km^{R}		BW27784 x P1[DL2283]
DL2573	DL1780 *lacZ*$^{+}$ *cynX*::Gm^{R}		(Eykelenboom *et al*., 2008)

DL2605	DL2573 *recA*::Cm^R		(Eykelenboom *et al*., 2008)
DL2829	DL2573 *lexA3 malE*::Tn*10*		DL2573 x P1[N1642], John Eykelenboom
DL2830	DL2006 *lexA3 malE*::Tn*10*		DL2006 x P1[N1642], John Eykelenboom
DL2875	DL1777 *cynX*::[(240x*tetO*)::Gm^R]		PMGR using pDL1709
DL2877	DL1780 *lacI*^{q} *lacZ*χ^- *lacZ*$^+$ *cynX*::[(240x*tetO*)::Gm^R]		DL1780 x P1[DL2875]
DL2879	DL2520 *lacI*^{q} *lacZ*χ^- *lacZ*$^+$ *cynX*::[(240x*tetO*)::Gm^R]		DL2520 x P1[DL2875]
DL2894	DL2879 *araB*::P$_{BAD}$-*I-SceI*		PMGR using pDL2655
DL3072	DL2894 *lacZ*::I-SceI$_{cs}$ *mhpC*::[(240x*lacO*)::Km^R]		PMGR using pDL2521, pDL2542
DL3073	DL3072 Δ*lacI*		PMGR using pDL3036
DL3276	BW27784 ΔP$_{sbcDC}$ P$_{BAD}$-*sbcDC lacZ*::pal *cynX*::[(240x*tetO*)::Gm^R] *mhpC*::[(240x*lacO*)::Km^R] Δ*lacI lacZ*χ^- *mhpA*::χχχ *lacZY*::χχχ		DL2877 PMGR using: pDL2774, pDL2542, pDL3036 pDL3181, pDL3192
DL3277	BW27784 ΔP$_{sbcDC}$ P$_{BAD}$-*sbcDC lacZ*$^+$ *cynX*::[(240x*tetO*)::Gm^R] *mhpC*::[(240xlacO)::Km^R] Δ*lacI lacZ*χ^- *mhpA*::χχχ *lacZY*::χχχ		DL2877 PMGR using: pDL2542, pDL3036, pDL3181, pDL3192
DL3278	BW27784 *araB*::P$_{BAD}$-*I-SceI lacZ*::I-SceI$_{cs}$ *cynX*::[(240x*tetO*)::Gm^R] *mhpC*::[(240x*lacO*)::Km^R] Δ*lacI lacZ*χ^- *mhpA*::χχχ *lacZY*::χχχ		DL2894 PMGR using: pDL2521, pDL2542, pDL3036, pDL3181, pDL3192
DL3279	BW27784 *araB*::P$_{BAD}$- *I-SceI lacZ*$^+$ *cynX*::[(240x*tetO*)::Gm^R] *mhpC*::[(240x*lacO*)::Km^R] Δ*lacI lacZ*χ^- *mhpA*::χχχ *lacZY*::χχχ		DL2894 PMGR using: pDL2542, pDL3036, pDL3181, pDL3192
DL3283	DL3276	+ pDL3196	
DL3284	DL3277	+ pDL3196	

DL3285	DL3278	+ pDL3196	
DL3286	DL3279	+ pDL3196	
DL3339	DL3276 *recA*::Cm^R		DL3276 x P1[DB1318]
DL3340	DL3277 *recA*::Cm^R		DL3277 x P1[DB1318]
DL3341	DL3278 *recA*::Cm^R		DL3278 x P1[DB1318]
DL3342	DL3279 *recA*::Cm^R		DL3279 x P1[DB1318]
DL3343	DL3339	+ pDL3196	
DL3344	DL3340	+ pDL3196	
DL3345	DL3341	+ pDL3196	
DL3346	DL3342	+ pDL3196	
DL3543	DL3276 Δ*recB*		PMGR using pDL2698
DL3544	DL3277 Δ*recB*		PMGR using pDL2698
DL3726	DL3543	+ pDL3718	
DL3727	DL3544	+ pDL3718	
DL4069	DL3276 *ykgC*::P_{mw1}-*lacI-cerulean,tetR-eyfp*		PMGR using pDL4068
DL4070	DL3277 *ykgC*::P_{mw1}-*lacI- cerulean,tetR-eyfp*		PMGR using pDL4068
DL4072	DL3278 *ykgC*:: P_{mw1}-*lacI-cerulean,tetR-eyfp*		PMGR using pDL4068
DL4073	DL3279 *ykgC*:: P_{mw1}-*lacI-cerulean,tetR-eyfp*		PMGR using pDL4068
DL4096	DL4069 Δ*recB*		PMGR using pDL2698
DL4097	DL4070 Δ*recB*		PMGR using pDL2698
DL4110	DL2573 Δ*sfiA*		PMGR using pDL1573

DL4111	DL2006 Δ*sfiA*		PMGR using pDL1573
DL4162	DL3277	+ pDL4161	

Table 2.3 *E. coli* Strains. *lacZ*χ- is an allele of *lacZ* with a Chi site removed. χχχ indicates an array of three Chi sites. *lacZY* is the intergenic region between *lacZ* and *lacY*.

Plasmid	Brief Description	Source or Construction
pCBA-*Sce*I	*I-SceI*; Amp^R, pMB1 ori	(Tremblay *et al*., 2000)
pGB2	Spc^R, pSC101 ori	(Churchward *et al.*, 1984)
pLau43	(240 x *lacO*)::Gm^R; Amp^R, pMB1 ori	(Lau *et al*., 2003)
pLau44	(240 x *tetO*)::Km^R; Amp^R, pMB1 ori	(Lau *et al*., 2003)
pRSETBmCherry	*mCherry*; Amp^R, pMB1 ori	(Shaner *et al.*, 2004)
pTOF24	*repA*^{TS} *sacB* Cm^R Km^R; used for PMGR, pSC101 ori	(Merlin *et al*., 2002)
pDL1573	pTOF24 derivative for making a precise deletion of *sfiA*; Cm^R, pSC101 ori	Julie Blyth
pDL1625	pTOF24 derivative for placing any specific gene under the control of P_{BAD} and integrating into the *araB* gene; Cm^R, pSC101 ori	(White *et al*., 2008)
pDL1709	pTOF24 derivative for integrating an array of 240 *tetO* sites into the *cynX* gene; Cm^R, Gm^R, pSC101 ori	(White *et al*., 2008)
pDL2521	pTOF24 derivative for integrating an I-$SceI_{cs}$ into the *lacZ* gene; Cm^R, pSC101 ori	(Eykelenboom *et al*., 2008)
pDL2542	pTOF24 derivative for integrating an array of 240 *lacO* sites into the *mhpC* gene; Cm^R, Km^R, pSC101 ori	(White *et al*., 2008)
pDL2655	pTOF24 derivative for integrating P_{BAD}-*I-SceI* into the *araB* gene; Cm^R, pSC101 ori	This study (section 4.3.2)

pDL2698	pTOF24 derivative for making a precise deletion of *recB*; Cm^R, pSC101 ori	Ewa Okely
pDL2774	pTOF24 derivative for integrating a 246bp palindrome into the *lacZ* gene; Cm^R, pSC101 ori	(Eykelenboom *et al*., 2008)
pDL2802	pTOF24 derivative for integrating any gene of interest into the *ykgC* gene; Cm^R, pSC101 ori	Ewa Okely
pDL3036	pTOF24 derivative for making a precise deletion of *lacI*; Cm^R, pSC101 ori	This study (section 4.5.2)
pDL3181	pTOF24 derivative for integrating an array of 3 Chi sites into the *mhpA* gene; Cm^R, pSC101 ori	This study (section 4.6)
pDL3192	pTOF24 derivative for integrating an array of 3 Chi sites in the intergenic region between *lacZ* and *lacY*; Cm^R, pSC101 ori	This study (section 4.6)
pWX6	*lacI-ecfp* and *tetR-eyfp* under a weak constitutive promoter (P_{ftsKi}); Amp^R, pMB1 ori	(Wang *et al.*, 2005)
pDL3194	*lacI-ecfp* under a weak constitutive promoter (P_{ftsKi}); Amp^R, pMB1 ori	This study (section 4.4.3)
pDL3195	*lacI-cerulean* under a weak constitutive promoter (P_{ftsKi}); Amp^R, pMB1 ori	This study (section 4.4.3)
pDL3196	*lacI-cerulean* and *tetR-eyfp* under a weak constitutive promoter (P_{ftsKi}); Amp^R, pMB1 ori	This study (section 4.4.3)
pDL3718	P_{ftsKi}-*lacI-cerulean,tetR-eyfp* cloned into MCS of pGB2; Spc^R, pSC101 ori	This study (section 6.1)

pDL4003	-10 region of P_{ftsKi} in pDL3718 mutated from **GG**TAAT to **TA**TAAT; Spc^R, pSC101 ori	This study (section 6.2)
pDL4004	-35 region of P_{ftsKi} in pDL3718 mutated from TTG**T**CA to TTG**A**CA; Spc^R, pSC101 ori	This study (section 6.2)
pDL4005	-35 region of P_{ftsKi} in pDL4003 mutated from TTG**T**CA to TTG**A**CA; Spc^R, pSC101 ori	This study (section 6.2)
pDL4068	pTOF24 derivative for integrating P_{mw1}-*lacI-cerulean,tetR-eyfp* into the *ykgC* gene; Cm^R, pSC101 ori	This study (section 6.3)
pDL4161	P_{ftsKi}-*lacI-cerulean,tetR-mcherry*; Amp^R, pMB1 ori	This study (section 4.10)

Table 2.4 Plasmids. All plasmids derived from pTOF24 are Cm^R, temperature sensitive (*repA*^{TS}) and carry the negative selection marker *sacB*. Amp is ampicillin, Cm is chloramphenicol, Gm is gentamycin, Km is kanamycin and Spc is spectinomycin.

Name	Sequence	Summary of Use
PMGR vector constructions and testing chromosome modifications		
DelI_Isc_testF	ACG GGT AGC AAA ACA GAT CG	Screen for presence of I-SceI$_{cs}$ in *lacZ*. Tested by in vitro cleavage of PCR product
DelI_Isc_testR	GAG GGG ACG ACG ACA GTA TC	
Ex-test_F	TTA TGC TTC CGG CTC GTA TG	Screen for presence of palindrome in *lacZ*
Ex-test_R	GGC GAT TAA GTT GGG TAA CG	
FP_NotI_F	AAA AAG CGG CCG CGC AGC GCG TAT TAT CGA AC	To amplify P$_{mw1}$-*lacI-cerulean,tetR-eyfp* from pDL4005 and clone into pDL2802
FP_NotI_R	AAA AAG CGG CCG CCT TCT CTC ATC CGC CAA AAC	
I-Sce1_F	AAA AAC **C**AT G**G**A AAA CAT CAA AAA AAA CCA GGT AAT GAA	Cloning of *I-SceI* into pDL1625
I-Sce 1_R	AAA AAG CGG CCG CTT ATT TCA GGA AAG TTT CGG AGG AG	
LacI_delta_F1	AAA AAC TGC AGG ACC ATT GAA CAG GCA GCG G	Crossover PCR to make pDL3036. Successful deletion of *lacI* was screened for using LacI_delta_F1 and LacI_delta_R2
LacI_delta_R1	**CAC GCT GGT TTG GCC AAT CAG CAA** CGA CTG	
LacI_delta_F2	**TTG CTG ATT GGC CAA ACC AGC GTG** GAC CGC TTG C	
LacI_delta_R2	AAA AAG TCG ACG CTG GCG AAA GGG GGA TGT GCT	

LacO-CF1	AAA AAG CTA GCT TTA ATG ACT GCG GAC AAG G	Crossover PCR to generate homology arms for pDL2542
LacO-CR1	**CTC GAG AAG GAT CCA ATC TAG A**C ATC AGC TTC AGG TTT TCG	
LacO-CF2	**TCT AGA TTG GAT CCT TCT CGA G**GC GAT CAC CTG GAA AAC TTC	
LacO-CR2	AAA AAC TGC AGT TAT GTG CTG AAT GGC GTA AG	
LacZY_Chi_F1	AAA AAC TGC AGA TTA GGG CCG CAA GAA AAC T	Crossover PCR to make pDL3192. Successful integration was tested by sequencing using LacZY_Chi_F1 and LacZY_Chi_R2
LacZY_Chi_R1	**CGA TGC TGA GCT GGT GGA CAC GCG CTG** GCT GGT GGT TAT TTT TGA CAC CAG ACC AAC TG	
LacZY_Chi_F2	**CAG CGC GTG TCC ACC AGC TCA GCA TCG** ACC ACC AGC ATT TCG CGT AAG GAA ATC CA	
LacZY_Chi_R2	AAA AAG TCG ACC ACC GGC GTT AAA ACA AAA G	
MhpA_Chi_F1	AAA AAC TGC AGA ATT CAA CAG CCA GGA AAC G	Crossover PCR to make pDL3181. Successful integration was tested by sequencing using primers MhpA_Chi_F1 and MhpA_Chi_R2
MhpA_Chi_R1	**CGC CAT GTG ACC ACC AGC GAG TCT GCG C**CC ACC AGC GCG CAA GCT GTT AAG CAA AG	
MhpA_Chi_F2	**GCG CAG ACT CGC TGG TGG TCA CAT GGC G**GC TGG TGG AAA TTC AAA GCG ACG TAC CG	

MhpA_Chi_R2	AAA AAG TCG ACG CCG TAA CGC CTT TAT TCA G	
ParaB-fwd	AAA AAC TGC AGA TTT TGC GCT TCA GCC ATA C	To test for integration of *araB*::P_{BAD}-*I-SceI* using pDL2655
CaraB-rev	AAA AAG TCG ACC GGT TGC AGG GTT TTC TCT A	
PBAD.F_test	GCA CGG CGT CAC ACT TTG	Screen for P_{BAD}::*sbcDC*
SbcD.R_test	TCA GGT TTT CCA CGC TCT CT	
recB-KO-F1	AAA AAC TGC AGT ACA AGG CGT TTT TCC CAA C	
recB-KO-R1	**ATC CAT CAG GGC GCG CAA AGG ATC** TAG TGT CTC G	Crossover PCR to make pDL2698. Successful deletion of *recB* was screened for using recB-KO-F1 and recB-KO-R2
recB-KO-F2	**GAT CCT TTG CGC GCC CTG ATG GAT** GAG ATG TTT G	
recB-KO-R2	AAA AAG TCG ACC AAT GGC ATG ATT CAC TTC G	
SfiA1-fwd	AAA AAC TGC AGC GCC ATA GAC TTT CAT CAA CC	
SfiA1-rev	TAA ATT TA**C TTA ATG ATA CAA ATT AGA GTG AAT TCT AGA TGA AGT GTA CAT AAT CAA TCC AGC**	Crossover PCR to generate homology arms used for the construction of pDL1573
SfiA2-fwd	CTC ACA GGG **GCT GGA TTG ATT ATG TAC ACT TCA TCT AGA ATT CAC TCT AAT TTG TAT CAT TAA G**	

SfiA2-rev	TTT TTG CTA GCC AGC CCA GTT TAG CAC CAG T	
SfiAKOtest_F	CAA CGG TCA GGC TGT AAC TG	Screen for deletion of *sfiA*
SfiAKOtest_R	ACC CCT GGC GAT GTA AAG TC	
TetO-CF1	AAA AAG CTA GCA AAT ATC TGC CGA CCA AAC C	Crossover PCR to generate homology arms for pDL1709
TetO-CR1	**CTC GAG AAG GAT CCA ATC TAG A**TT TAA TCA CCG AAG GCA TCA C	
TetO-CF2	**TCT AGA TTG GAT CCT TCT CGA G**TA TCA AAC ACT CGC CTG GTG	
TetO-CR2	AAA AAC TGC AGC CCA GAC CTA ACC CAC ACA C	
YkgC-F1	AAA AAC TGC AGG CAT CAA CAA ACG GCT AAG G	Crossover PCR to generate homology arms for pDL2802
YkgC-R1	**AAT GCG GTG CGG CCG CAA ATC TGT** GTG CTG CTG TGC	
YkgC-F2	**ACA GAT TTG CGG CCGCAC CGC ATT** GTA CGT GAT GAG	
YkgC-R2	AAA AAG TCG ACT GTT CTG GCG TCT GAT TTT G	
pDL3196 Construction and Sequencing		
eCFP_S72A_sdmF	GGG GCG TGC AGT GCT TC**G C**CC GCT ACC CCG ACC	Introduce the S72A mutation into eCFP by SDM
eCFP_S72A_sdmR	GGT CGG GGT AGC GG**G C**GA AGC ACT GCA CGC CCC	

eCFP_Y145AH148D_F	GCT GGA GTA CAA C**GC** CAT CAG C**G**A CAA CGT CTA TAT CAC CG	Introduce the Y145A and H148D mutations into eCFP by SDM
eCFP_Y145AH148D_R	CGG TGA TAT AGA CGT TGT **C**GC TGA TG**G C**GT TGT ACT CCA GC	
pWX6_CFPseqF	GCT TGC TGC AAC TCT CTC AG	Sequencing *cfp* in:
pWX6_CFPseqR	CGA TTC CGA CCT CAT TAA GC	- pDL3196
pWX6_CFPseqR3	CTT CTC TCA TCC GCC AAA AC	- pDL3194 and pDL3195

pDL3718 Construction

pGB2F	AAA AAG TCG ACG GTG ATG TCG GCG ATA TAG G	Amplify P_{ftsKi}-*lacI-cerulean,tetR-eyfp* from pDL3196 for cloning into pGB2
pGB2R	ACG GCG TTT CAC TTC TGA GT	

pDL4005 Construction

Minus10_F	GCG AAC AGG GGC ACA AC**T A**TA ATC GTG AAG TGC TGG	Mutate the -10 region of P_{ftsKi} from **GG**TAAT to **TA**TAAT
Minus10_R	CCA GCA CTT CAC GAT TA**T A**GT TGT GCC CCT GTT CGC	
Minus35_F	GGA AGC GCA GGG GAT TG**A** CAG CGA ACA GGG GCA C	Mutate the -35 region of P_{ftsKi} from TTG**T**CA to TTG**A**CA
Minus35_R	GTG CCC CTG TTC GCT G**T**C AAT CCC CTG CGC TTC C	

pMW2seqF	GAA CTG GAT CCG TTG TTC G	To screen for successful SDM of P_{ftsKi} on pDL3718
pMW2seqR	TGT AAT TCA GCT CCG CCA TC	
pDL4161 Construction		
TetR-mCherryA_F1	TCT AGC AGG AGG AAT TCA CCA	Crossover PCR to create a *tetR-mCherry* fusion
TetR-mCherryA_R1	**CGA GG**A TGT CAG ACC CAC TT	
TetR-mCherryA_F2	**CCT CG**A GTT GGT GAG CAA GGG CGA GGA G	
TetR-mCherryA_R2	AAA AAT CTA GAT TAC TTG TAC AGC TCG TCC ATG C	

Table 2.5 Oligonucleotides. Restriction sites for cloning into plasmids are underlined; sequences used for the crossover reaction or the site-directed mutagenesis are emboldened.

Chapter 3

The Effect of a Single Induced DNA Double-Strand Break on the Cell Cycle of *Escherichia coli*

3.1 Introduction

It was recently shown that SbcCD creates a DNA double-strand break (DSB) at a 246 bp interrupted palindrome in the chromosome of *E. coli* (Eykelenboom *et al*., 2008). Importantly, SbcCD does not target the DNA sequence of the palindrome for cleavage, but instead recognises a DNA hairpin (Connelly *et al*., 1998) that is formed by the palindrome during replication. This DNA hairpin forms on the lagging, but not the leading strand template of replication (Pinder *et al*., 1998) due to the polar nature of DNA synthesis which results in stretches of ssDNA on the lagging strand template (McInerney *et al*., 2007). As a result, SbcCD will only cleave one of a pair of replicating sister chromosomes. Not only does this observation have significant implications for the study of genome instability at palindromic DNA sequences, but it also provides us with a unique tool for the study of DSB repair by homologous recombination in *E. coli*.

The induction of a single DSB at a defined locus can be achieved by placing the *E. coli sbcDC* operon under the control of the arabinose inducible promoter P_{BAD} in a strain that harbours a 246 bp interrupted palindrome in the *lacZ* gene (DL2006). This system has two main advantages over other methods of inducing a single chromosomal DSB such as the use of the homing endonuclease I-SceI with a unique restriction site (Meddows *et al.*, 2004). Firstly, although SbcCD cleaves the palindrome to form a bone fide DSB with high efficiency, an intact sister chromosome will always be available to repair from and second, once the DSB has been repaired, the chromosome will not be cleaved again until the next round of replication. This gives the opportunity to culture cells in conditions where they are continually challenged with a DSB every round of replication allowing us to

compare and contrast the differences between acute and chronic exposure to a DSB. This chapter describes the effect of DSB induction on the growth and cell cycle of *E. coli*.

3.2 RecA and the Induction of the SOS Response

3.2.1 Introduction

The repair of a DSB caused by the cleavage of a DNA hairpin by SbcCD has been shown to proceed *via* the RecBCD pathway of repair, with a requirement for RecA, RecBCD, RuvABC, RecG and PriA demonstrated genetically (Eykelenboom *et al*., 2008). Additionally, a mutant of LexA (LexA3) that is not cleaved in the presence of a RecA filament (Little *et al*., 1980) was used to show that induction of the SOS response is essential for the survival of cells harbouring the palindrome and expressing SbcCD (John Eykelenboom, unpublished). Interestingly, although the SOS response of *E. coli* has been shown to result in the induction of at least 31 genes (Courcelle *et al.*, 2001), the viability of the *lexA3* strain can be fully rescued by constitutively over-expressing RecA (John Eykelenboom, unpublished). This requirement for extra RecA is however puzzling, because in order to have catalysed autocleavage of LexA (and hence stimulate the SOS response) RecA must have nucleated onto at least one of the two ends of the DSB, which in itself should be sufficient for repair.

This inconsistency could be explained by differences in the requirements for both SOS induction and successful homology recognition and DNA duplex invasion by the RecA nucleoprotein filament. Such differences have been recorded. For example it has been shown that the ATPase activity of RecA is important for strand

invasion (Cox *et al*., 2008) but is not required for induction of the SOS response (Gruenig *et al.*, 2008). Alternatively, there may be sufficient levels of RecA in the absence of SOS response induction in order to repair a single DSB and the phenotype observed in the *lexA3* strain is a consequence of chronic DSB induction.

3.2.2 Acute vs. Chronic DSB Induction

In an attempt to determine whether SOS-response induced levels of RecA is necessary for the repair of a single DSB, a comparison was made between cultures exposed to a short burst of DSB induction and those that had a DSB chronically induced overnight. Strains with the P_{BAD}-*sbcDC* inducible system and the 246 bp palindrome integrated into *lacZ* (DL2006, DL2075, and DL2830) were first grown to an optical density at 600 nm (OD_{600}) of 0.5 (mid-exponential phase of growth) in L broth. These cultures were then split into two and diluted to an OD_{600} of 0.2 in L broth supplemented with either 0.2 % arabinose (SbcCD induced) or 0.5 % glucose (SbcCD repressed). Following 30 min of growth, the cultures were sampled and serial dilutions plated onto LB agar plates supplemented with either 0.2 % arabinose or 0.5 % glucose.

Figure 3.1 shows that despite a 100-fold decrease in the viability of the *lexA3* mutant (DL2830) on an LB-arabinose agar plate (where cells are faced with chronic DSB induction), no detrimental effect of the *lexA3* mutation was observed following 30 min of SbcCD induction. It should be noted that 30 min of SbcCD induction is enough to cause a 100- to 1000-fold reduction in the viability of a *recA*$^-$ strain carrying the palindrome (DL2075) suggesting that >99 % of cells had suffered a DSB. This result indicates that induction of the SOS response is not essential for the

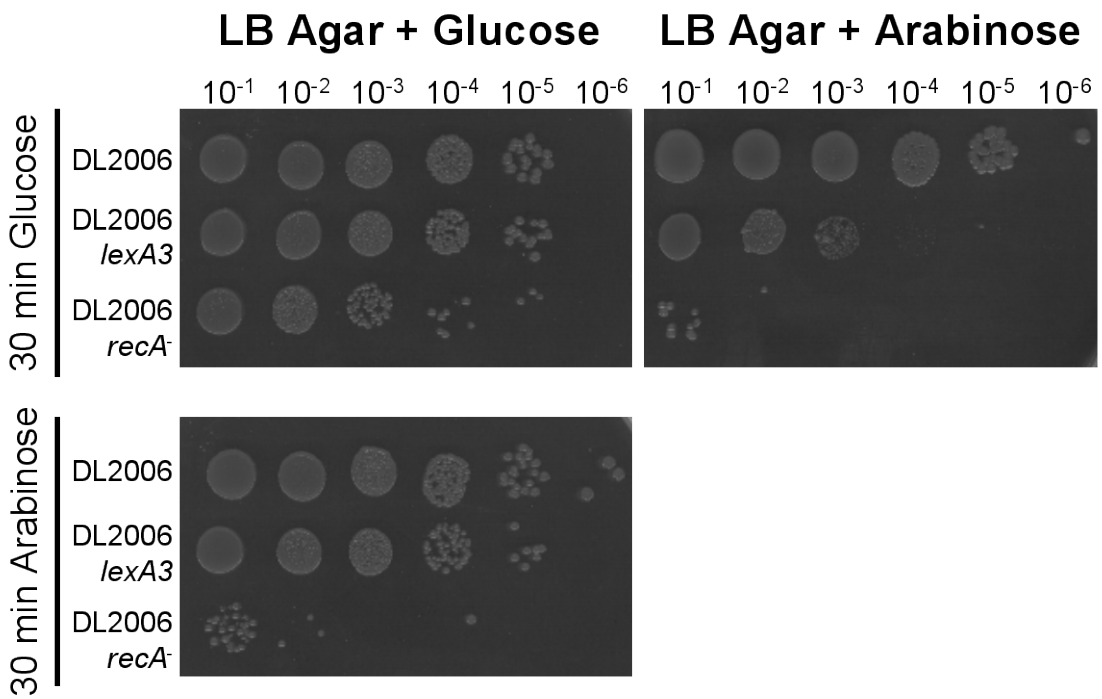

Figure 3.1 Viability of a *lexA3* mutant following cleavage of the palindrome by SbcCD. Cultures of DL2006 (P_{BAD}-*sbcDC lacZ*::pal) and its *lexA3* and *recA*$^-$ derivatives (DL2830 and DL2075 respectively) were grown for 30 min in either SbcCD repressed (0.5 % glucose) or SbcCD induced (0.2 % arabinose) conditions. Serial dilutions of these cultures were then spotted onto LB agar plates supplemented with either 0.5 % glucose or 0.2 % arabinose and grown overnight at 37 °C.

repair of a single DSB caused by cleavage of the palindrome by SbcCD.

Upon binding a (near) blunt dsDNA end (DSE), RecBCD degrades both strands of the DNA duplex until it encounters an octameric sequence known as Chi were it switches its exonuclease activity to preferably degrade in a 5' to 3' direction. This results in a 3' ssDNA overhang onto which RecBCD actively loads RecA. How far this activity extends *in vivo* is unknown and therefore so is the number of RecA molecules that are loaded onto each DSE in order to for recombination to occur successfully. However, it has been shown *in vitro* that only 80 bp is active in synapsis in a region of homology as large as 1 kb (van der Heijden *et al*., 2008) a value that corresponds to 25 – 30 RecA monomers (3 bp of ssDNA are bound by a single monomer of RecA in the presence of ATP (Zaitsev and Kowalczykowski, 1999). Considering that RecA is estimated to be present at a basal level of 800 to 1,200 molecules per cell during mid-log phase of growth in L broth (Karu and Belk, 1982), rising to an upper estimate of 100,000 molecules per cell following mitomycin C treatment (Stohl *et al*., 2003), there should be enough RecA in the absence of SOS induction to repair multiple DSBs. It is therefore unclear why and at which stage of growth the increase of RecA expression is necessary for cellular viability.

3.3 The SOS Response and Inhibition of Cell Division

3.3.1 Introduction

Even though induction of the SOS response is not necessarily essential for cellular viability following cleavage of the palindrome by SbcCD (section 3.2), this induced DSB is sufficient to induce transcription of *gfp* from the SOS reporter P_{sfiA}-*gfpmut3.1*, located on a low copy number plasmid (pGB150, Garry Blakely unpublished). SfiA is an inhibitor of cell division that acts by inhibiting polymerisation of the tubulin-like protein FtsZ (Trusca *et al*., 1998) that is responsible for formation of the septal ring (Errington *et al*., 2003) by preventing it from hydrolysing GTP (Cordell *et al.*, 2003). Although this evidence for increased expression from P_{sfiA} comes from the use of a plasmid, it is likely that *sfiA* is also being induced from the chromosome.

It is noteworthy however, that SfiA has a half-life much shorter than GFP (1.2 min (Mizusawa and Gottesman, 1983) compared to an estimated 24 h for GFPmut3.1 in *E. coli* (Franke *et al.*, 2007)) due in part to its post-translational regulation by the protease Lon (Gur and Sauer, 2008). This level of increased *sfiA* expression therefore may not result in inhibition of cell division if it is not high enough to enable SfiA to swamp Lon and effectively inhibit FtsZ. Evidence that this may be the case comes from the fact that induction of this DSB has no detectable effect on the growth rate (as indicated by OD_{600}) or the number of viable cells in the population (John Eykelenboom, unpublished), Figure 3.2. This result is contrary to that expected if the cells were filamenting, which would be indicated by a reduction in the number of viable cells per unit of optical density.

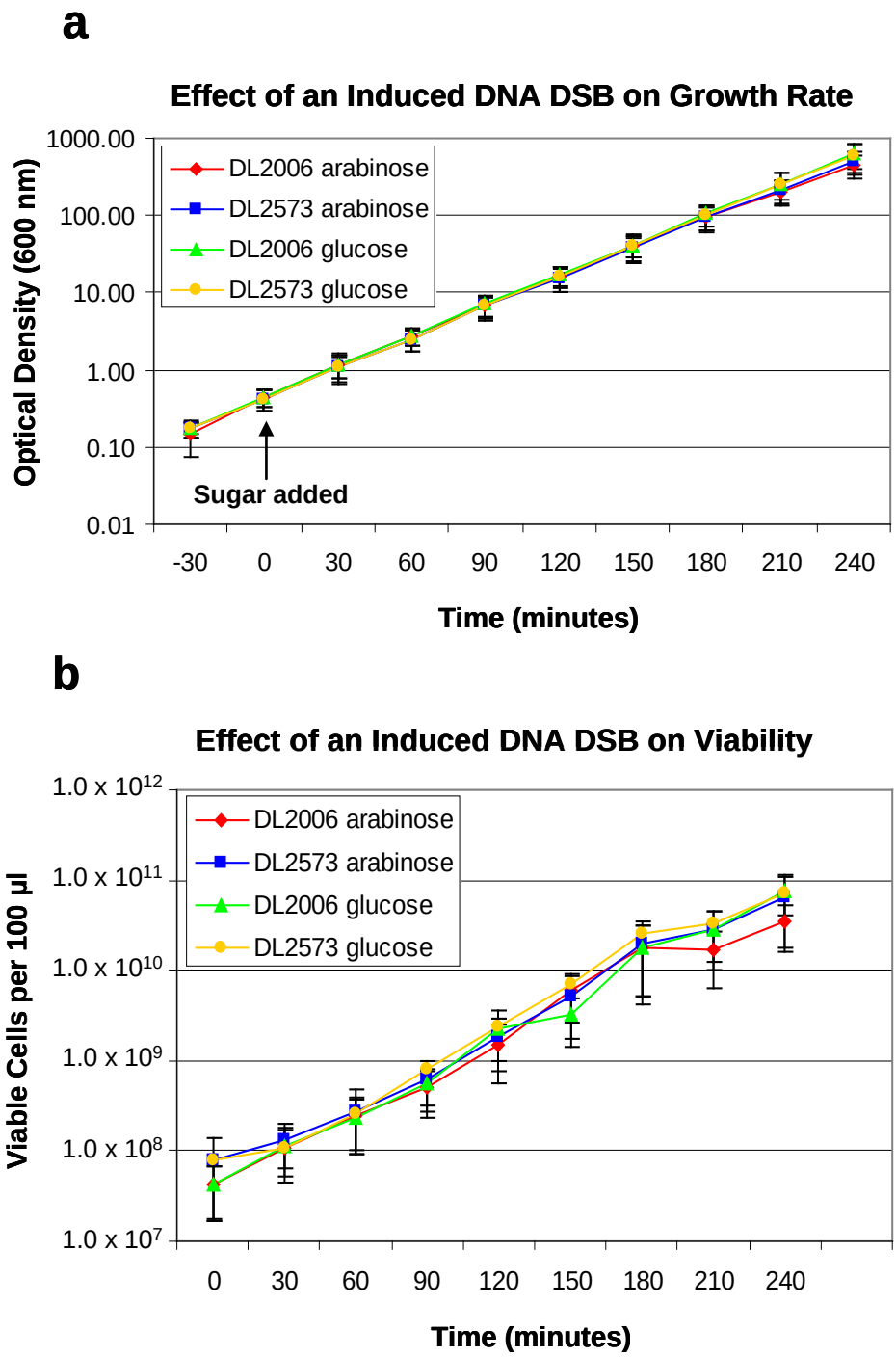

Figure 3.2 Effect of a single induced DSB on growth rate and cellular viability. Experiments were carried out in triplicate; error bars show the standard error of the mean. **a**, Growth curve of P_{BAD}-*sbcDC* strains either harbouring the palindrome in *lacZ* (DL2006) or not (DL2573). Cultures were maintained in exponential growth phase by diluting prior to OD_{600} reaching 1.0. **b**, Following measurement of the OD_{600}, cultures were sampled and plated on LB agar supplemented with glucose (SbcCD repressed). Colonies were counted the following day. These experiments were carried out by John Eykelenboom (unpublished).

3.3.2 Cellular Morphology Following an Induced DSB

Microscopy was used to gain direct evidence as to whether or not cell division was inhibited in response to cleavage of the palindrome by SbcCD. To do this, P_{BAD}-*sbcDC* strains either harbouring the palindrome in *lacZ* (DL2006) or not (DL2573) were grown to an OD_{600} of 0.5 in L broth at 37 °C in the absence of any added sugar, prior to splitting the culture into two and diluting to an OD_{600} of 0.2 in fresh L broth supplemented with either 0.5 % glucose (SbcCD repressed) or 0.2 % arabinose (SbcCD induced). Cells were sampled after 60 minutes of further growth and brightfield images gathered using the microscope at a resolution of 0.129 μm per pixel. In agreement with the growth curves (Figure 3.2) initial results from the microscopy experiments showed that cell division was not dramatically inhibited following the induced DSB, with long filamentous cells being rare and not unique to DSB induced conditions (see Figure 3.3 for representative images).

In order to ascertain whether or not there was a mild elongation of cells in the DSB induced conditions (DL2006, arabinose), cell lengths were measured using the 'fiber length' measurement of the image analysis software MetaMorph v6.3r2. Approximately 300 cells were measured for each strain/condition and this experiment repeated four times. The mean lengths from each independent experiment were used for statistical analysis. Results from this analysis showed that there was a mild, but reproducible inhibition of cell division in cells grown under DSB induced conditions as cells harbouring the palindrome (DL2006) were on average 1.11x longer than cells without (DL2573) following SbcCD induction, Figures 3.4 and Table 3.1. A 2-sample t-test shows that this difference is significant to 99 % confidence ($p = 0.006$). No reproducible difference was seen between these

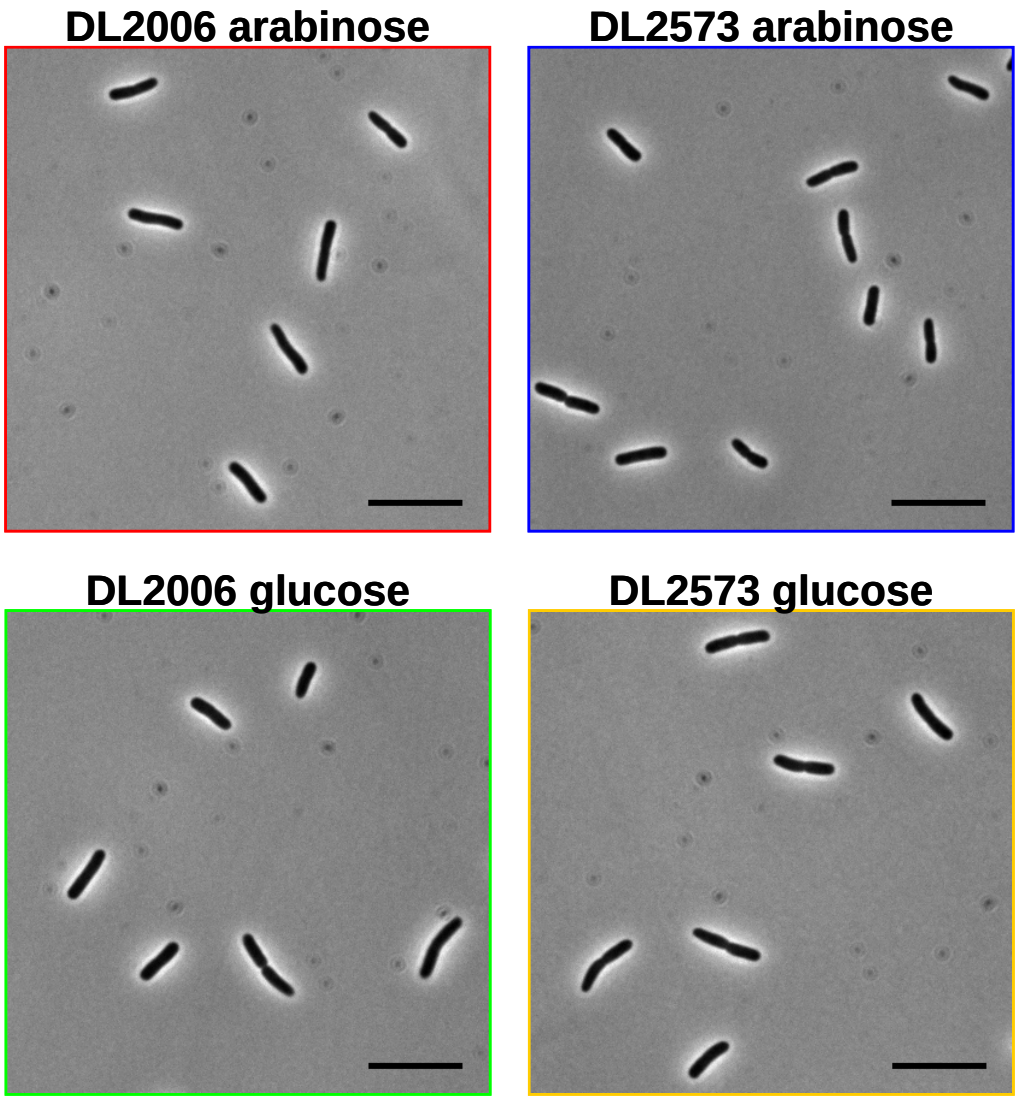

Figure 3.3 Morphology of cells following an induced DSB. Microscopy images of arabinose inducible SbcCD strains with either the palindrome integrated in *lacZ* (DL2006) or not (DL2573), following 1 h of growth in LB media supplemented with either 0.2 % arabinose (SbcCD induced) or 0.5 % glucose (SbcCD repressed); calibration bar shows 10 μm.

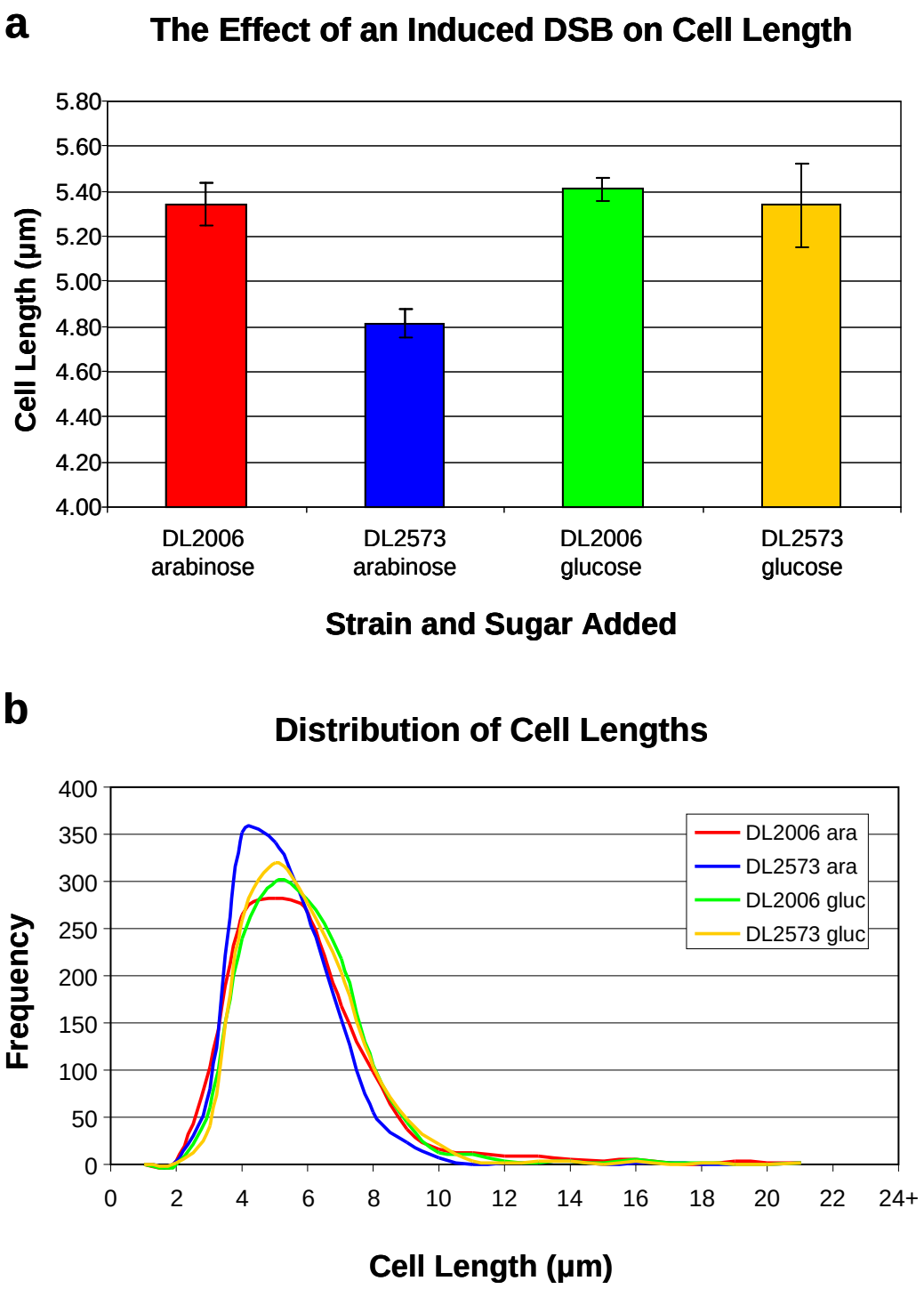

Figure 3.4 Effect of an induced DSB on cell length. **a**, Mean cell lengths of P_{BAD}-*sbcDC* strains with either the palindrome integrated in *lacZ* (DL2006) or not (DL2573) following 1 h of growth in LB media supplemented with either 0.2 % arabinose (SbcCD induced) or 0.5 % glucose (SbcCD repressed). *n* = 4, error bars are standard error of the mean. **b**, Distribution of cell lengths in the population cumulative over 4 experiments, *n* = 1200. Cultures grown in the presence of arabinose are labelled as ara and glucose as gluc.

Strain	Sugar	*n*	Mean (μm)	SEM	SD	Min (μm)	Median (μm)	Max (μm)
DL2006	Ara	4	5.345	0.0952	0.1904	5.105	5.379	5.516
DL2573	Ara	4	4.816	0.0640	0.1281	4.635	4.855	4.921
DL2006	Glu	4	5.410	0.0488	0.0975	5.316	5.402	5.521
DL2573	Glu	4	5.338	0.1860	0.3720	4.990	5.336	5.693

Table 3.1 Descriptive statistics of cell lengths. Mean cell lengths of P_{BAD}-*sbcDC* strains either harbouring the palindrome (DL2006) or not (DL2573) following 1 h of growth in LB media supplemented with either 0.2 % arabinose (SbcCD induced) or 0.5 % glucose (SbcCD repressed). SEM is standard error of the mean, SD is standard deviation, Ara is arabinose and Glu is glucose.

two strains when they were grown in SbcCD repressed conditions (glucose), as shown by a 2-sample t-test ($p = 0.734$). Additionally, a small effect of the sugar on cell length was found when comparing the *lacZ*$^+$ strain DL2573 grown in the presence of arabinose and glucose ($p = 0.077$, 2-sample t-test), a result that could be attributed to differences in the metabolism of these sugars. Importantly, both DL2006 and DL2573 are Δ*araFGH* and cannot metabolise arabinose, while they can metabolise glucose. The Δ*araFGH* mutation was introduced in order to keep the level of inducer (arabinose) constant; however it may exacerbate any differences in the growth rate of these cells in glucose or arabinose. An alternative explanation is that the cell length difference is not (or only partially) caused by differences in the metabolism of the sugars, but is rather a result of SbcCD induction. It is unclear however, how induction of a protein complex shown to possess both ssDNA

endonuclease and dsDNA exonuclease activity (Connelly *et al*., 1999; Connelly *et al*., 1998) could mediate a decrease in cell length.

Following this study, cell lengths have been measured in both *sbcDC*$^{+}$ and Δ*sbcDC* cells either harbouring or not the 246 bp palindrome in the *lacZ* gene (Elise Darmon, unpublished). Results of this experiment has confirmed that cells are longer when grown under DSB induced conditions and that this increase in cell length is specific to SbcCD^{+} cells containing the palindrome since no difference was observed between the average cell length of SbcCD^{+} and SbcCD^{-} cells lacking the palindromic sequence. These data are in accordance with the detectable level of SOS response induction in these cells as measure by John Eykelenboom (unpublished) using the reporter plasmid pGB150 (see section 3.3.1) and imply that the difference observed between DL2573 cultures grown in arabinose and glucose was not caused by differences in the expression of SbcCD.

Since similar cell length measurements were obtained for the four independent experiments, the data from each experiment were combined and frequency curves drawn (Figure 3.4b). This graph shows that the increase in cell length observed in DSB induced conditions (DL2006, arabinose) is small and appears to arise from a shift in the majority of the population towards being longer as opposed to the appearance of a sub-population of filamentous cells. This is in agreement with the distribution of GFP intensity in strains harbouring pGB150, which showed that the SOS response was induced across the whole population.

3.3.3 Nucleoid Morphology Following an Induced DSB

It is conceivable that induction of the DSB may interfere with chromosome segregation. In order to repair the DSB by homologous recombination, the broken sister chromosome must physically pair with an intact sister chromosome. Segregation of sister chromosomes has been shown to be progressive in *E. coli* cells cultured in slow growth conditions (Nielsen *et al.*, 2006a; Wang *et al.*, 2006), following a short period of post-replicative sister chromosome cohesion (Wang *et al*., 2008). The same may or may not be true for cells cultured in rich medium (*e.g.* L broth as used in the previous experiments) where cells are larger and carry more chromosomes in order to compensate for the increase in growth rate. Recent evidence suggests that sister chromosomes may be cohesed for longer (as much as an entire cell cycle) in cells cultured in fast growth conditions (Fossum *et al*., 2007).

If SbcCD cleaves the hairpin following this post-replicative cohesion, then repair would require the pairing of two previously segregated sister chromosomes. This pairing and the following stages of repair may impede the segregation of chromosomes, resulting in cell division being delayed by nucleoid occlusion, a phenomenon that in *E. coli* depends on the SlmA protein which interacts with chromosomal DNA in a non-specific manner (Bernhardt and de Boer, 2005). Nucleoid occlusion has however, only been identified in cells lacking a functional Min system of FtsZ regulation (Yu and Margolin, 1999), and so rather than working in addition to any effect of the induction of SfiA during the SOS response, nucleoid occlusion is thought to act as a failsafe mechanism for cell division regulation (Thanbichler and Shapiro, 2008).

In addition to the delay in chromosome segregation caused by repair of the initial break, if the outcome of Holliday junction resolution by RuvABC is the formation of a crossover product (Cromie *et al*., 2001), then the resulting dimeric chromosome would require resolution by the tyrosine recombinases XerC and XerD at the sequence *dif* (Blakely *et al.*, 1993; Blakely *et al.*, 2000). This site specific recombination event requires the motor FtsK (Lowe *et al.*, 2008) in order to align the two *dif* sequences and stimulate the recombination event (Aussel *et al*., 2002). Interestingly, FtsK is also a member of the divisome complex and essential for recruitment of FtsQ, FtsL, and FtsI to the septal ring (Chen and Beckwith, 2001). Since *dif* recombination occurs only shortly before cell division (Kennedy *et al*., 2008) it is possible that chromosome dimer resolution will result in some delay in cell division. There is however currently no evidence to show this.

A genetic requirement for XerCD and *dif* in the survival of SbcCD mediated palindrome cleavage has been demonstrated (John Eykelenboom, unpublished). However, unlike experiments carried out using a phage lambda harbouring the 246 bp palindrome (Cromie *et al*., 2000), there is no bias towards crossover formation when SbcCD cleaves the palindrome integrated into the chromosome. This is indicated by the fact that *xerC*¯ (DL2237) and Δ*dif* (DL2241) mutants do not show a marked decrease in viability following SbcCD mediated palindrome cleavage but rather gives a small colony phenotype in chronic DSB induced conditions (John Eykelenboom, unpublished). This data is consistent with an undefined proportion of repair events resulting in the formation of a dimeric chromosome.

As a means of testing the effect of the induced DSB on chromosome segregation, nucleoid morphology was visualised by staining the DNA with 4’,6-

diamidino-2-phenylindole dihydrochloride (DAPI). As for the previously reported cell length measurements (section 3.3.2), P_{BAD}-*sbcDC* strains either harbouring the palindrome in *lacZ* (DL2006) or not (DL2573) were grown to an OD_{600} of 0.5 in L broth at 37 °C in the absence of any added sugar prior to splitting the culture into two and diluting to an OD_{600} of 0.2 in fresh L broth supplemented with either 0.5 % glucose (SbcCD repressed) or 0.2 % arabinose (SbcCD induced). However, following the 60 minutes of growth in SbcCD induced/repressed conditions, 400 μg ml^{-} chloramphenicol was added to the growth medium and the cells cultured for a further 15 min (37 °C). Since DL2006 an DL2573 are not chloramphenicol resistant strains, this treatment resulted in condensation of the nucleoid (Zimmerman, 2002). Chloramphenicol treatment was then followed by an additional 15 min of growth at 37 °C in the presence of 1 μg ml^{-} DAPI prior to sampling for microscopy. Cells were imaged at a resolution of 0.129 μm per pixel and multiple *z*-sections (± 800 nm, 9 images at an interval of 200 nm) of the DAPI signal were captured. The stack of *z*-planes was deconvolved using the software Autodeblur and Autovisualize v9.32 and subsequently combined to give a maximum projection image using MetaMorph 6.3r2. Representative images are shown in Figure 3.5.

Although the imaged cells were likely to possess 4 to 8 origins of replication, most (>99 %) contained only 1 or 2 segregated nucleoids (Figure 3.5). This can be explained by the inhibition of translation resulting from chloramphenicol treatment causing the contraction of linked chromosomes (van Helvoort *et al.*, 1996). Induction of SbcCD in a strain harbouring the palindrome did not result in either the appearance of anucleate cells or an increase in the number of distinct nucleoids per

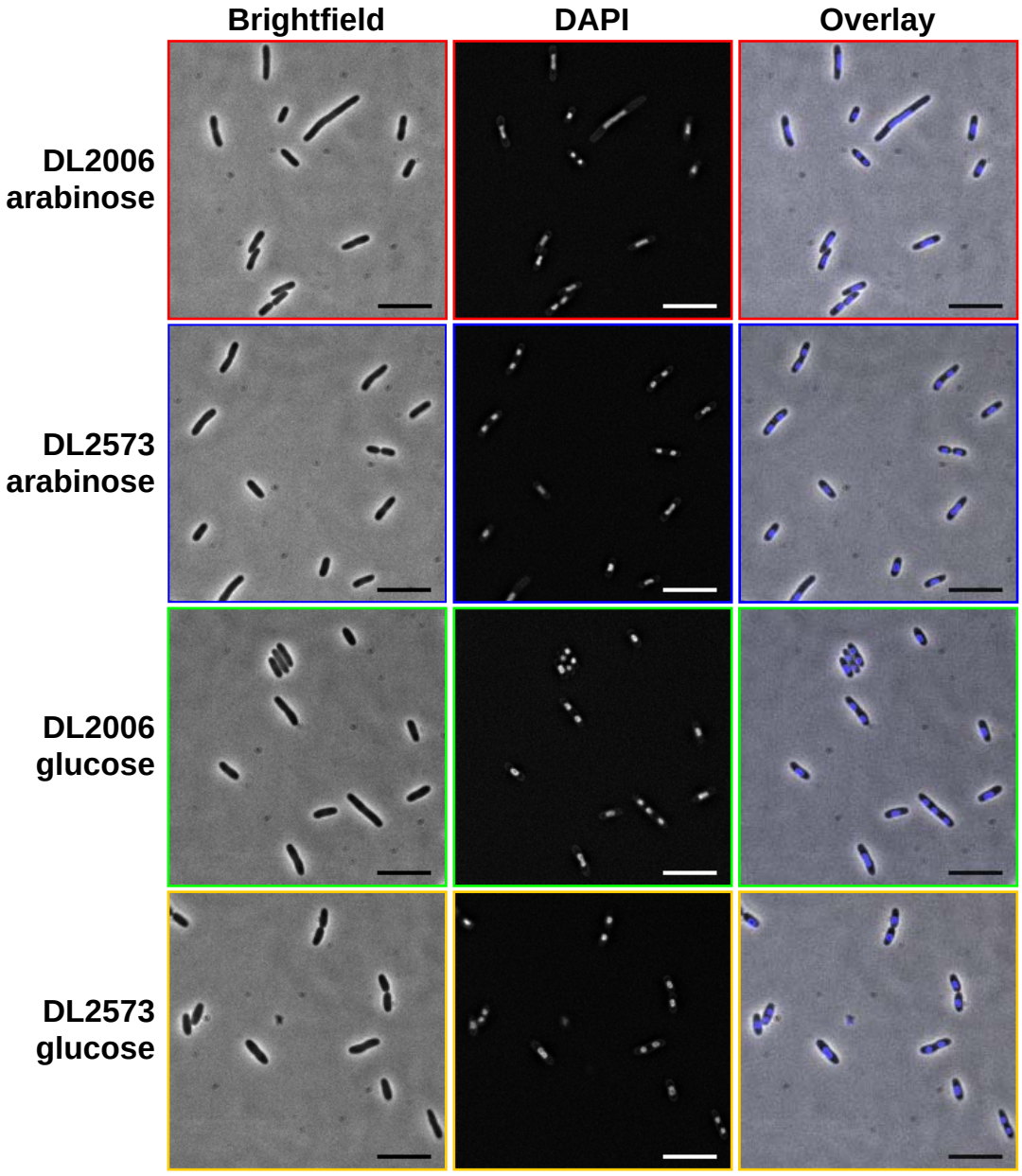

Figure 3.5 Morphology of nucleoids following an induced DSB. Microscopy pictures of arabinose inducible SbcCD strains either harbouring the palindrome in *lacZ* (DL2006) or not (DL2573). Following 1 h of growth in LB media supplemented with either 0.2 % arabinose (SbcCD induced) or 0.5% glucose (SbcCD repressed), nucleoids were condensed by chloramphenicol treatment prior to staining with DAPI. DAPI images are maximum projections of deconvolved images. DAPI signal in the overlay image is pseudo-coloured blue; calibration bar shows 10 μm.

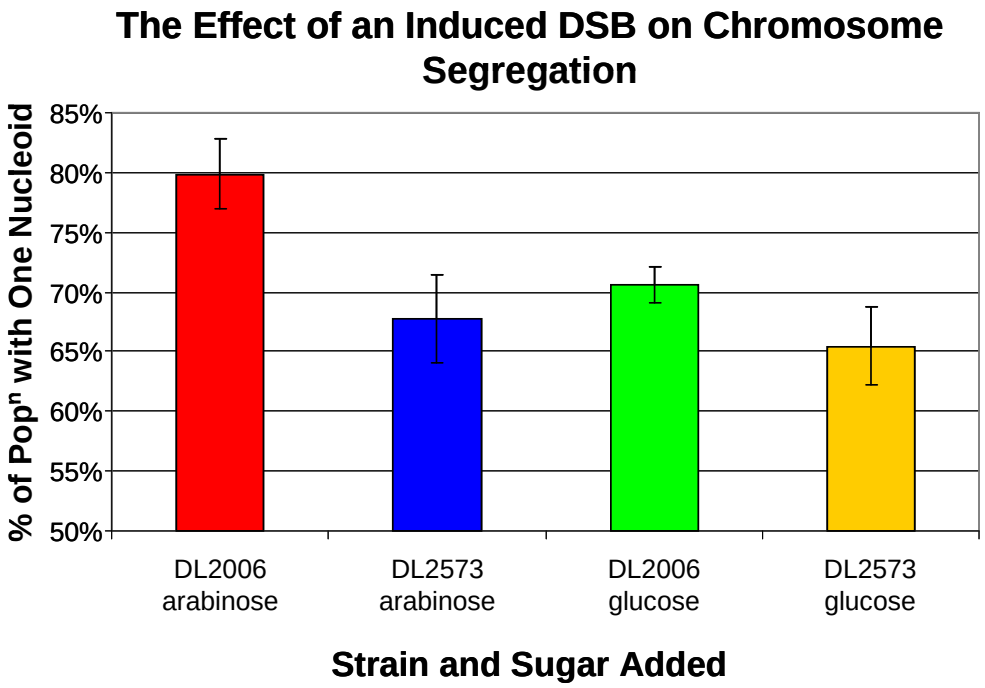

Figure 3.6 The effect of an induced DSB on chromosome segregation. The percentage of P_{BAD}-sbcDC cells either harbouring the palindrome in lacZ (DL2006) or not (DL2573) with a single discreet nucleoid following 1 h of exponential growth in either SbcCD induced (arabinose) or SbcCD repressed (glucose) conditions. Shown is the mean value obtained from three independent experiments, error bars show standard error of the mean. ANOVA, p = 0.036.

cell, with less than 1 % of cells containing more than two visible nucleoids whether or not SbcCD was induced or the palindrome was present (analysis of approximately 750 cells for each strain/condition, total from three independent experiments). The number of discreet nucleoids per cell was counted and consistent with a delay in nucleoid segregation, a higher proportion of cells harbouring the palindrome in *lacZ* had a single nucleoid following SbcCD induction when compared to the three controls (Figure 3.6). Analysis of variance (ANOVA) was carried out on the values obtained for the three independent experiments and showed that the increased number of cells with a single nucleoid in cells where a DSB had been induced was statistically significant (p = 0.036). It is possible that this observation either

represents a delay in chromosome segregation caused directly by homologous recombination or by chromosome dimer formation.

3.3.4 Effect of Cell Division Inhibition on Generation Time and Cell Mass

Although chronic DSB induction was shown to cause an increase in the average cell length of population (Figure 3.4), no effect was observed on the generation time of the culture (Figure 3.2b). This result could simply be explained by the increase in cell length being small and the error in viability measurements being large. Alternatively, this result could be explained by the dynamics of the *E. coli* cell cycle. In slow growth conditions, the *E. coli* cell cycle has three well defined periods (Haeusser and Levin, 2008). These are known as the B period (or G1), which is the interval between the previous cell division and replication initiation, the C period (or S-phase) when the chromosome is replicated, and the D period (or G2) which consists of the time interval between replication termination and cytokinesis.

In fast growth conditions the C period is longer than the time it takes for cells to double in mass (C is approximately 40 min and the generation time is less than 30 min). In order to prevent the replication of the chromosome from becoming a rate-limiting step, cells forgo their B period and establish overlapping C and D periods by inheriting partially replicated chromosome(s). Although the mechanism of replication initiation determination is not fully understood, it has been shown to be tightly coupled to growth rate (Boye *et al*., 1996), which in a culture of exponentially growing cells is constant (see Figure 3.2). Less well understood is what triggers FtsZ

to form the septal ring, however it is known that it is regulated in a manner that prevents it from forming over non-segregated nucleoids.

By taking into account these factors, a simple model was generated in order to predict what effect chronic inhibition of cell division would have on the average generation time (τ) of the population (Figure 3.7). This model is based on three assumptions. The first is that growth in chronic DSB induced conditions results in a delay in either the C or D period (or both), that is constant between successive generations. There is currently no direct evidence to support or refute this assumption. The second assumption is that replication initiation is not affected by DSB induction and there are a number of reasons as to why this is likely to be the case. For example, it has been shown that the rate of replication initiation is based on the growth rate of the population (Wold *et al*., 1994) as opposed to the cell mass (Cooper, 2006) and it has been demonstrated that chronic DSB induction has no effect on growth rate using this SbcCD inducible system (Figure 3.2a). Furthermore, whereas induction of the SOS response has the potential to increase the D period, for example by induction of SfiA, and possibly the C period by increased expression of Pol IV (Uchida *et al.*, 2008), there is currently no evidence that it plays a role in regulating replication initiation. In fact, it has been demonstrated that replication initiation in wild-type *E. coli* cells remains constant after exposure to high levels of UV-light (Rudolph *et al*., 2007). The final assumption is that cells divide symmetrically in half.

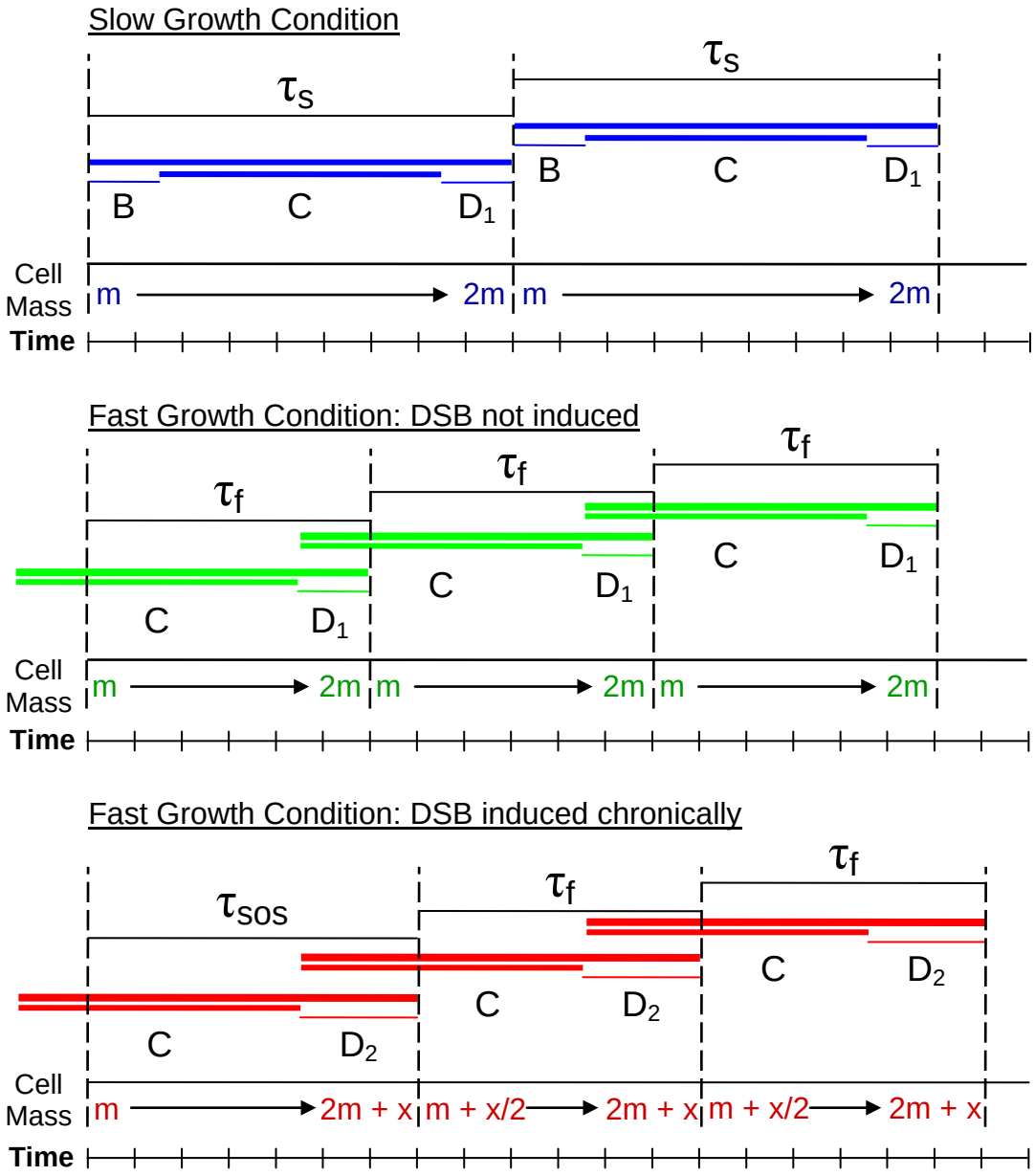

Figure 3.7 Modelling the effect of cell division inhibition on generation time. The *E. coli* cell cycle consists of three growth periods known as B, C, and D. In chronic DSB induced conditions, even though D (or C, or C & D) is constantly lengthened (*e.g.* by the SOS response), the generation time (τ) is only predicted to increase in the initial generation. This is a direct consequence of keeping replication initiation constant. Assuming the delay in D is constant with successive generations; τ will immediately return and be maintained at the level observed prior to SOS induction. Since growth rate is exponential (and constant), cells are predicted to maintain the 'extra' mass gained in the initial generation.

This model predicts that although the initial extension of the D period (or C, or D and C periods) will cause an increase in the average generation time and cell mass, the population will equilibrate with respect to both. This is because by keeping the timing of replication initiation constant, the second generation will inherit a larger amount of replicated chromosome than is normally observed at this growth rate. As a result, in the absence of any further delay in cell division, this second generation would have a τ shortened by the same length of time as τ was increased in the preceding generation. Therefore, with a constant delay in cell division (as assumed here for growth in chronic DSB induced conditions), τ instantly returns to that observed prior to (or in the absence of) induction of the SOS response. Since the generation time of the culture is only extended in one generation, the overall impact on the number of viable cells in the culture should be minimal. This could explain why no effect on viability or colony size has been detected. Finally, since growth rate is exponential rather than linear, cells should maintain the additional mass gained in the initial generation rather than equilibrate to the average cell mass detected in the absence of the SOS response. This could explain why an increase in cell length was detected even after 60 min of DSB induction.

3.3.5 Time-lapse Microscopy of Cells Grown under Chronic DSB Induced Conditions

In order to test the hypothesis that cell mass should equilibrate under chronic DSB conditions (section 3.3.4), time-lapse microscopy was used to follow single cells through multiple generations. Cultures of arabinose inducible SbcCD strains either harbouring the palindrome (DL2006) or not (DL2573) were first grown to exponential growth phase (OD_{600} of 0.2) in L broth. Samples were then taken and spotted onto a pad of LB agar supplemented with either 0.5 % glucose (SbcCD repressed) or 0.2 % arabinose (SbcCD induced) that was subsequently sealed with a coverslip (section 2.4.3). These cells were then allowed to grow under the microscope at 37 °C with phase contrast images acquired at a resolution of 0.129 μm per pixel every 30 s for a maximum of 3 h. Representative time-lapse sequences are shown in Figure 3.8.

Strikingly, cell growth on the slides under the microscope did not mimic the growth pattern observed in liquid medium. Cells appeared to be stressed even in the absence of SbcCD induced palindrome cleavage, as many grew larger than cells observed both in samples of liquid culture and at the initial time point of the time-lapse. This effect was independent of both the induction of SbcCD and the presence of the palindrome. However, induction of SbcCD in the strain harbouring the palindrome (DL2006, arabinose) resulted in a more extreme phenotype with many large filaments being observed, presumably due to the added SOS response induction resulting from cleavage of the palindrome.

The presumed stress leading to filamentous cells in the absence of the induced DSB is likely to be caused in main by growth in the sealed microscopy chamber rather than exposure to the halogen light used to capture the brightfield

images. This is because a similar filament phenotype was observed when slides were left at 37 °C in a dark incubator and imaged only after 2 h of growth (Figure 3.9). Interestingly, this phenotype was not observed when the cells were grown on M9-minimal agar (data not shown).

Although these experiments may not be directly comparable with the results obtained in liquid growth medium, a number of conclusions can be drawn. First, as expected from the viability data, cells can (and do) divide during growth under chronic DSB induced conditions. Second, although asymmetric cell division does occur, symmetric cell division predominates; an assumption on which the prediction of equilibration of cell mass was based (section 3.3.4). Unfortunately, under these conditions, cell mass is extremely heterogeneous within the population making it almost impossible to calculate a reproducible population mean. An alternative method for testing the effect of the SbcCD induced DSB on cell mass would be to calculate the mean cell length for the population of cells grown in L broth at various time points, following induction of SbcCD in a strain that harbours the palindrome in *lacZ* (DL2006). However, although this would make it possible to ascertain whether (and to what extent) mean cell length changes in the population over time, it would not allow generation time to be measured directly (as is possible using time-lapse microscopy).

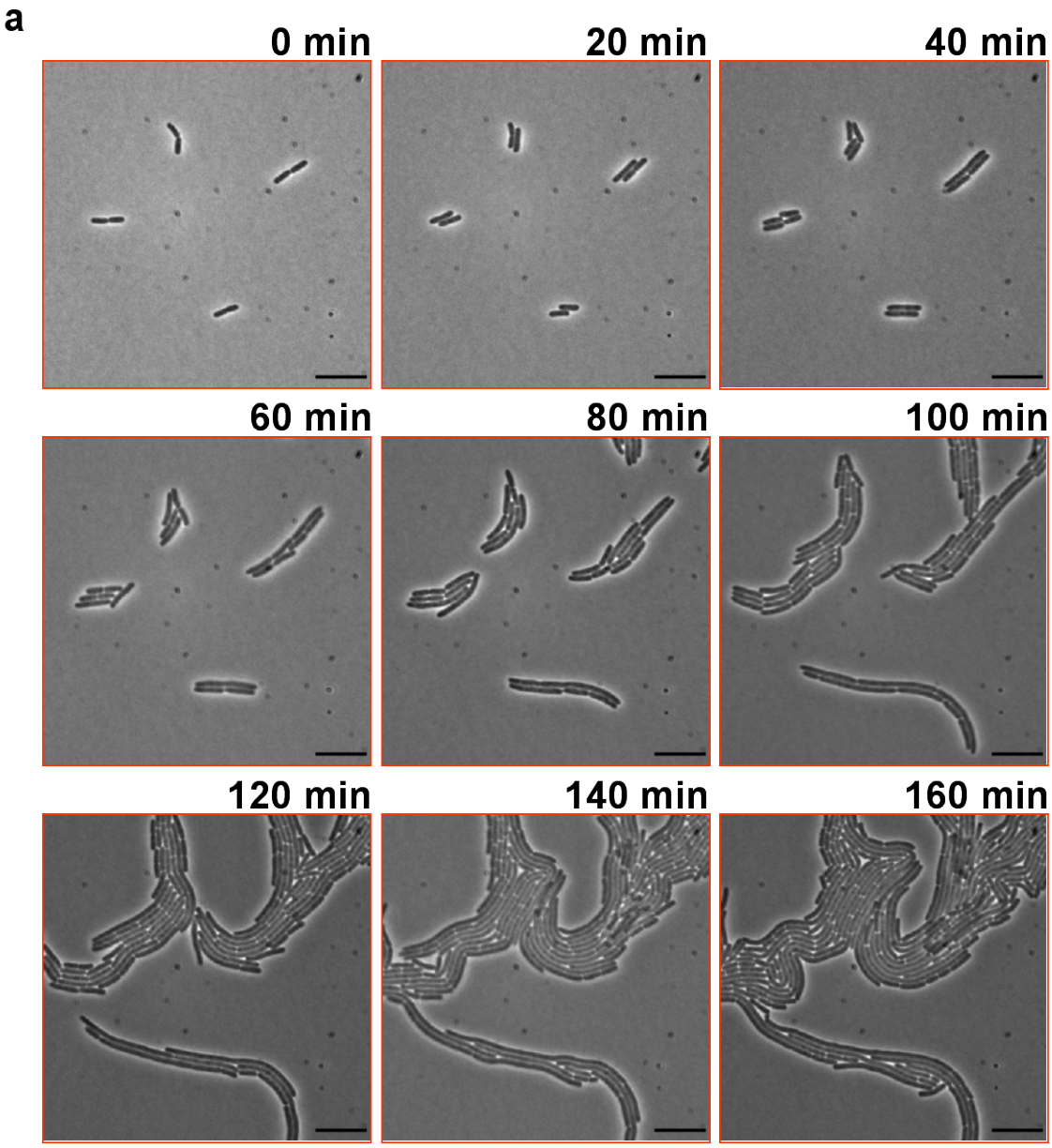
a
0 min
20 min
40 min
60 min
80 min
100 min
120 min
140 min
160 min

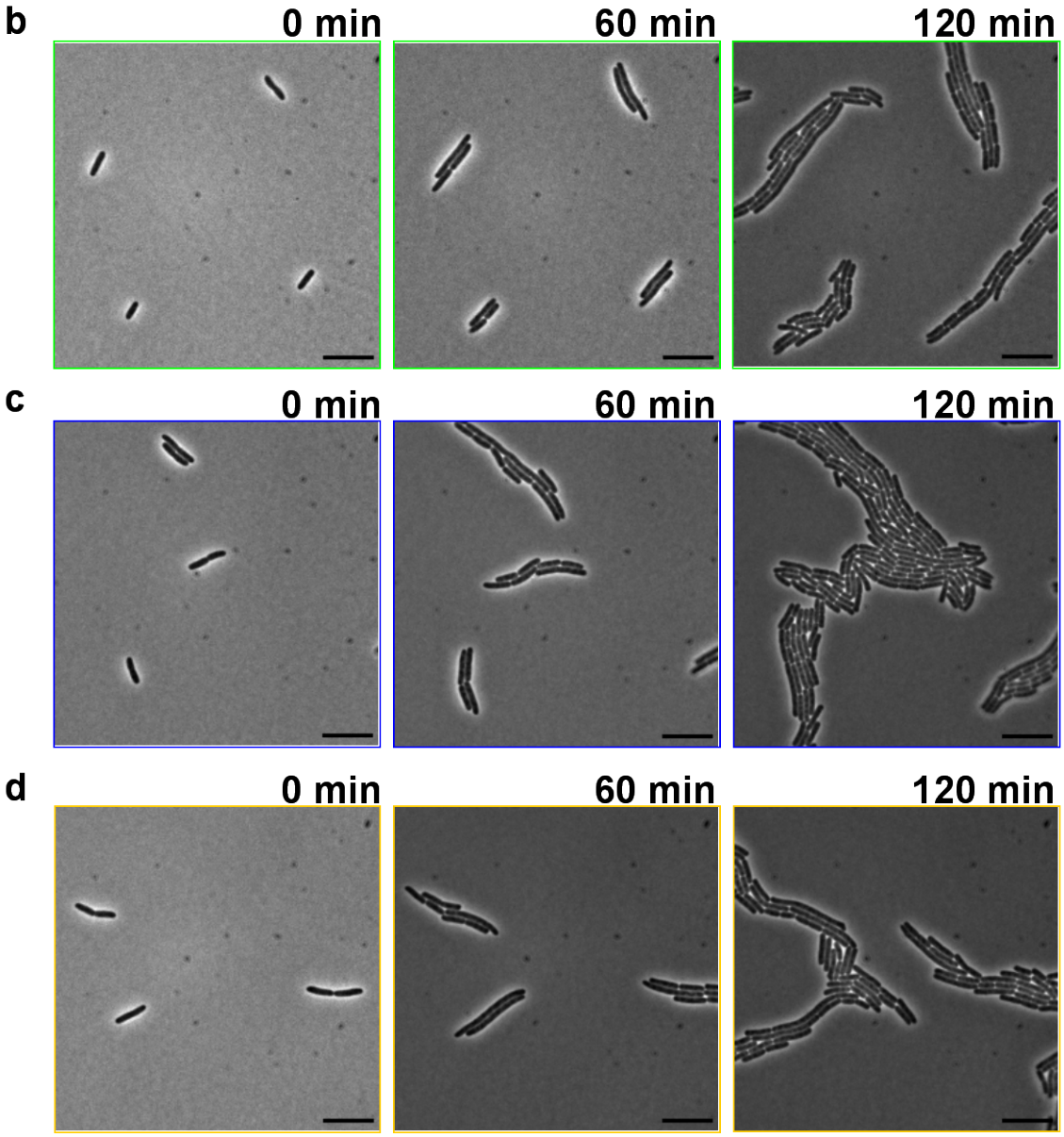

Figure 3.8 Time-lapse microscopy of cell growth under chronic DSB induced conditions. Cultures of arabinose inducible SbcCD strains either harbouring the palindrome in *lacZ* (DL2006) or not (DL2573) were grown at 37 °C on LB agar supplemented with either 0.5 % glucose (SbcCD repressed) or 0.2 % arabinose (SbcCD induced). Brightfield images were acquired every 30 s; calibration bar shows 10 µm. **a**, DL2006 LB agar + arabinose. **b**, DL2006 LB agar + glucose. **c**, DL2573 LB agar + arabinose. **d**, DL2573 LB agar + glucose.

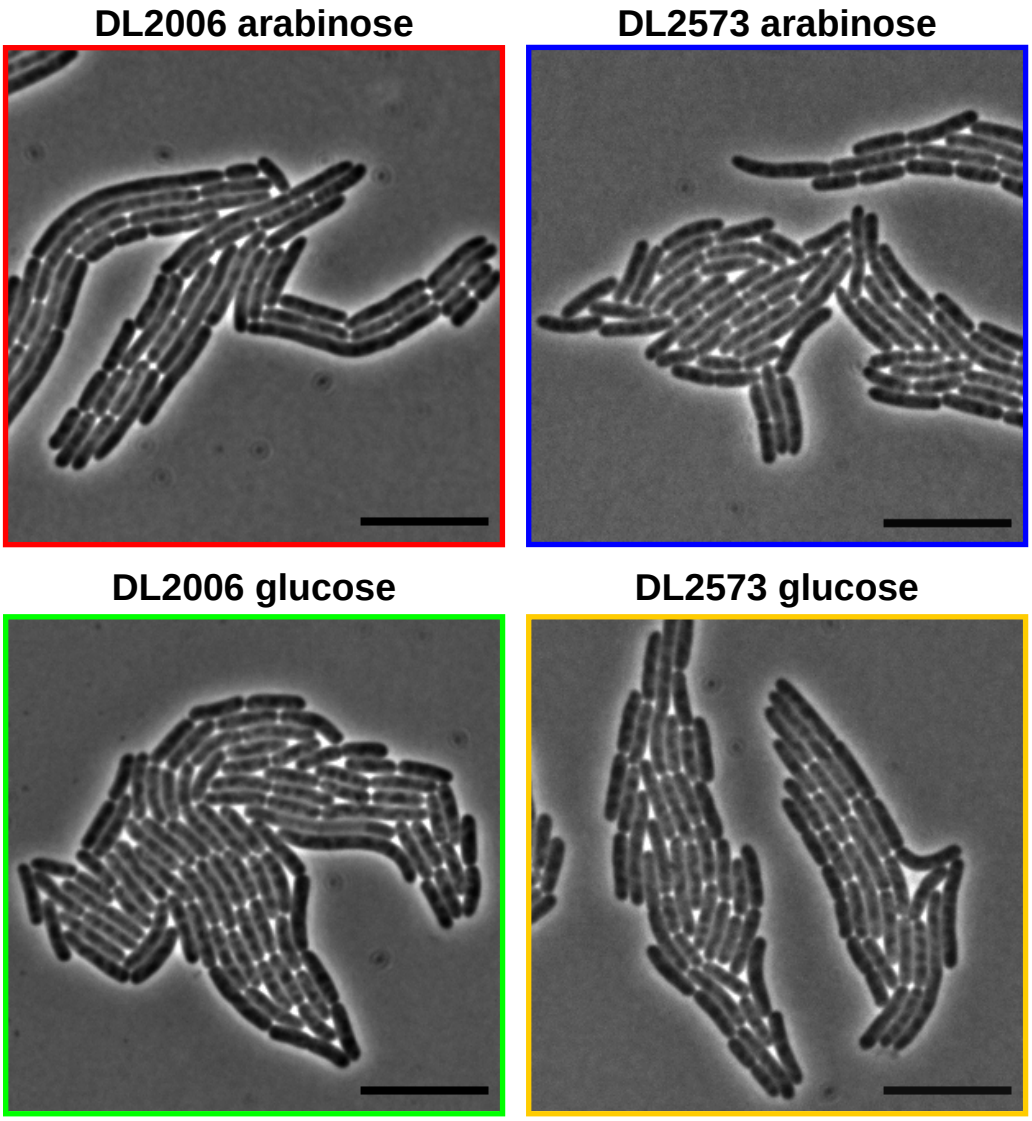

Figure 3.9 Microcolony formation in a sealed chamber under chronic DSB induced conditions. Samples of arabinose inducible SbcCD strains either harbouring the palindrome in *lacZ* (DL2006) or not (DL2573) were grown in a dark incubator for 2 h at 37 °C on LB agar supplemented with either 0.5 % glucose (SbcCD repressed) or 0.2 % arabinose (SbcCD induced), within sealed chambers used also for the time-lapse microscopy. Calibration bar shows 10 μm.

3.4 SfiA is not Essential for Viability in Chronic DSB Induced Conditions

3.4.1 Δ*sfiA* Constructions

Although cleavage of a DNA palindrome by SbcCD was shown to inhibit cell division (section 3.3.2), it was not known what was responsible for this DSB induced delay in cell division and whether or not it was essential for viability. Since the SOS response had also been shown to be induced during growth in these DSB induced conditions, it was hypothesised that the SOS response inducible inhibitor of cell division, SfiA may have a role in this reaction. To test this, Δ*sfiA* derivatives of P_{BAD}-*sbcDC* strains either harbouring the palindrome in the *lacZ* gene (DL2006) or not (DL2573) were constructed by PMGR under SbcCD repressed conditions (0.5 % glucose) using the plasmid pDL1573. This resulted in the arabinose inducible SbcCD strains DL4111 (*lacZ*::pal) and DL4110 (*lacZ*$^+$).

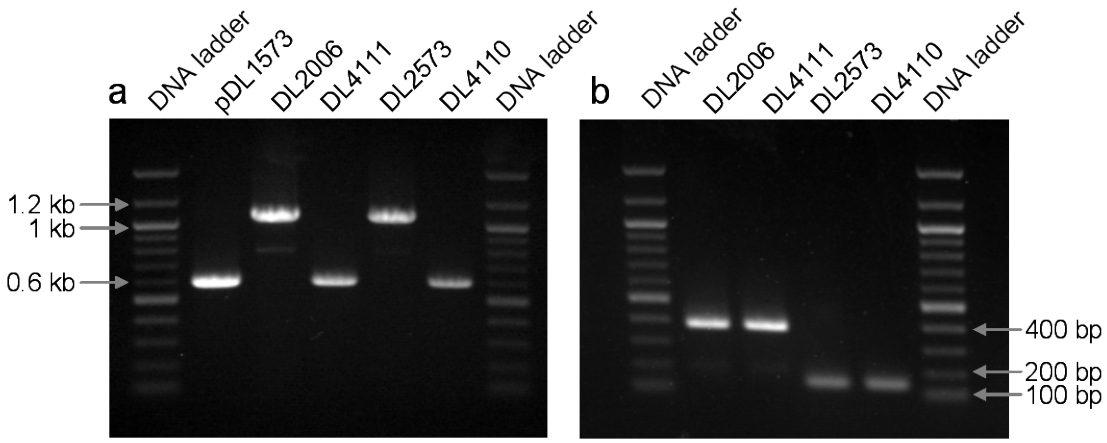

Figure 3.10 Confirmation of the *sfiA* deletion and presence of the palindrome by PCR. Strains DL4111 and DL4110 were screened by PCR for **a**) successful deletion of the *sfiA* gene (deletion product 598 bp; wild-type product 1066 bp) and **b**) presence of the 246 bp palindrome in *lacZ* (394 bp fragment if palindrome is present, 148 bp fragment if *lacZ*$^+$). DNA ladder is 100 bp DNA ladder (New England BioLabs).

Plasmid pDL1573 was constructed by cloning a crossover PCR product created by amplification of the *E. coli* chromosome using primer pairs SfiA1-fwd/rev and SfiA2-fwd/rev into the PstI/SalI restriction sites of the plasmid pTOF24 (Julie Blyth). PMGR using pDL1573 results in a 468 bp deletion of the *sfiA* gene. Successful deletion of *sfiA* and the presence of the palindrome were screened by PCR using primer pairs SfiAKOtest_F/R and ExtestF/R respectively (Figure 3.10).

3.4.2 Genetics of Δ*sfiA* Strains Following a Chronically Induced DSB

Cultures of P_{BAD}-*sbcDC* strains harbouring the palindrome (DL2006) or not (DL2573), and their *lexA3* (DL2830 and DL2829) and Δ*sfiA* derivatives (DL4111 and DL4110) were grown overnight in SbcCD repressed conditions (L broth supplemented with 0.5 % glucose). Serial dilutions of these stationary phase cultures were spotted onto three LB agar plates supplemented with 0.5 % glucose (SbcCD repressed condition) and one supplemented with 0.2 % arabinose (SbcCD induced condition). Two of the glucose plates were exposed to UV-light (1 J/m^2 and 1.5 J/m^2) whereas the third and the arabinose plate were not. The results (Figure 3.11) confirmed both the sensitivity of the *lexA3* strains to UV-light and chronic exposure to SbcCD mediated palindrome cleavage. In contrast, the Δ*sfiA* mutants were sensitive to neither.

sfiA mutants were originally isolated in a screen for suppression of the UV-light sensitivity of a *lon*$^-$ strain (Johnson and Greenberg, 1975) and following this, the resistance of *sfiA*$^-$ strains to UV-light was reported (Gottesman *et al*., 1981). Since Lon is a protease that inactivates SfiA, these results suggest that while SfiA is

not required for survival following UV-light induced DNA damage, its regulation is; as death ensues if SfiA is allowed to accumulate. These data show that alongside UV-light irradiation, SfiA is not essential for viability during chronic exposure to a DSB. A requirement for SfiA regulation (*i.e.* the viability of a *lon* mutant in response to cleavage of the palindrome by SbcCD) has yet to be determined.

The viability of Δ*sfiA* mutants in conditions of chronic DSB induction was also tested in slow growth conditions by plating serial dilutions of stationary phase cultures grown under SbcCD repressed conditions in M9-minimal (0.2 % glucose) media onto M9-minimal (0.2 % glycerol) agar plates supplemented with either 0.2 % glucose or 0.2 % arabinose (Figure 3.12). These plates were incubated at 37 °C for two consecutive days to compensate for the reduced growth rate. The results showed that while induction of SbcCD had no effect on the viability of the recombination proficient strain harbouring the palindrome (DL2006, arabinose), the *recA*$^{-}$ mutant was dead (DL 2075, arabinose) confirming that SbcCD also cleaves the palindrome when cells are grown under slow growth conditions. A cleavable LexA protein is also required for efficient survival of chronic DSB induction in minimal growth medium, although the reduction in viability observed in a *lexA3* mutant (DL2830) is approximately an order of magnitude less than the reduction observed in rich media (Figures 3.12). This result could be explained by an increased length of time between successive DSBs in minimal medium (due to the addition of a B period in the cell cycle) resulting in less demand on the cellular concentration of RecA. Finally, SfiA is dispensable for survival of chronic DSB induction in cells grown in minimal as well as in rich growth media.

The observation that SfiA is not essential for survival lends the possibility of

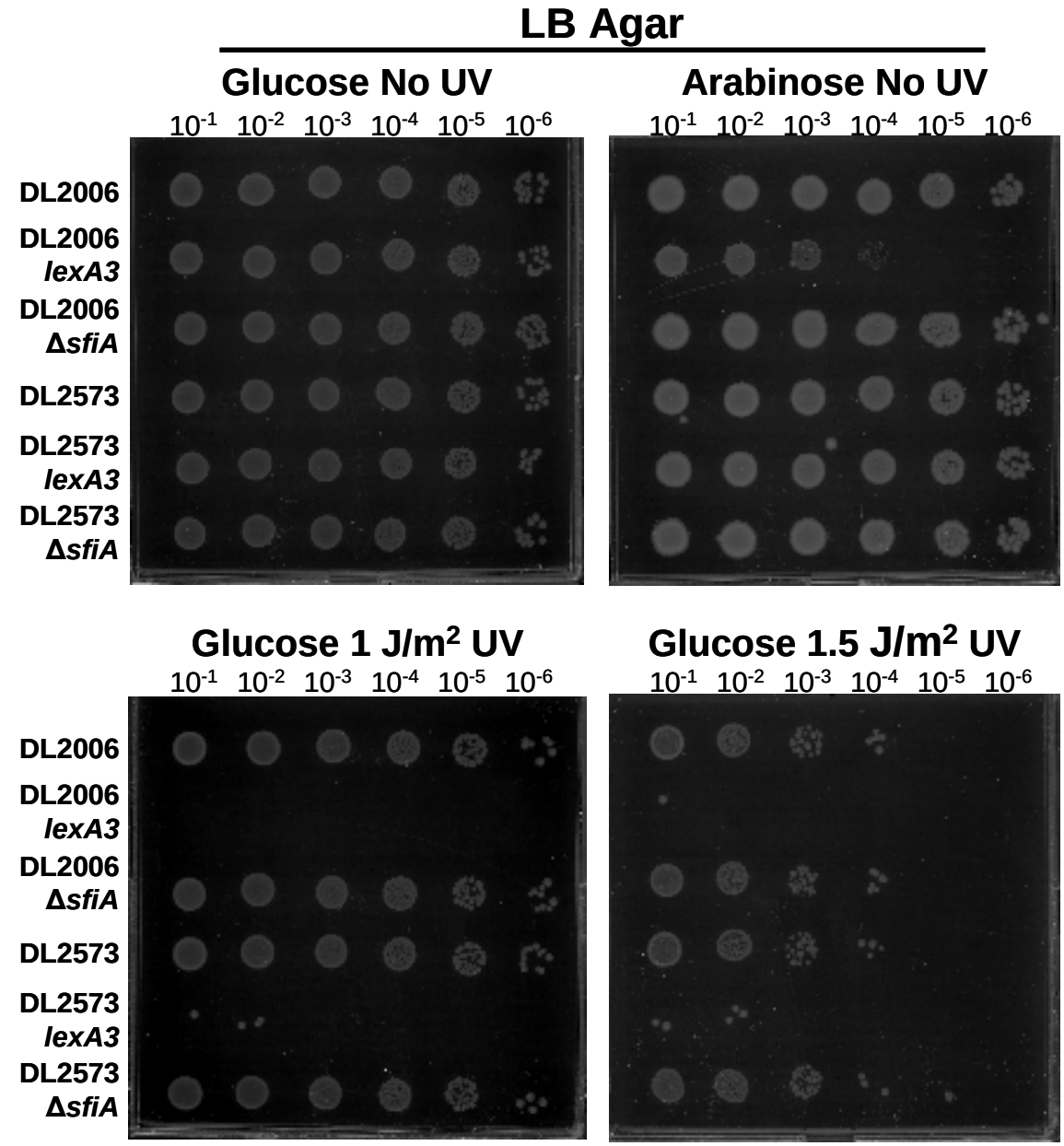

Figure 3.11 Viability of Δ*sfiA* mutants following DNA damage in nutrient rich growth medium. Ten-fold serial dilutions of stationary phase cultures of arabinose inducible SbcCD strains either harbouring the palindrome in *lacZ* (DL2006) or not (DL2573) along with their *lexA3* and Δ*sfiA* derivatives (DL2829, DL2830, DL4110, and DL4111) were plated onto LB agar plates supplemented with either 0.5 % glucose (SbcCD repressed) or 0.2 % arabinose (SbcCD induced) and exposed or not to UV-light.

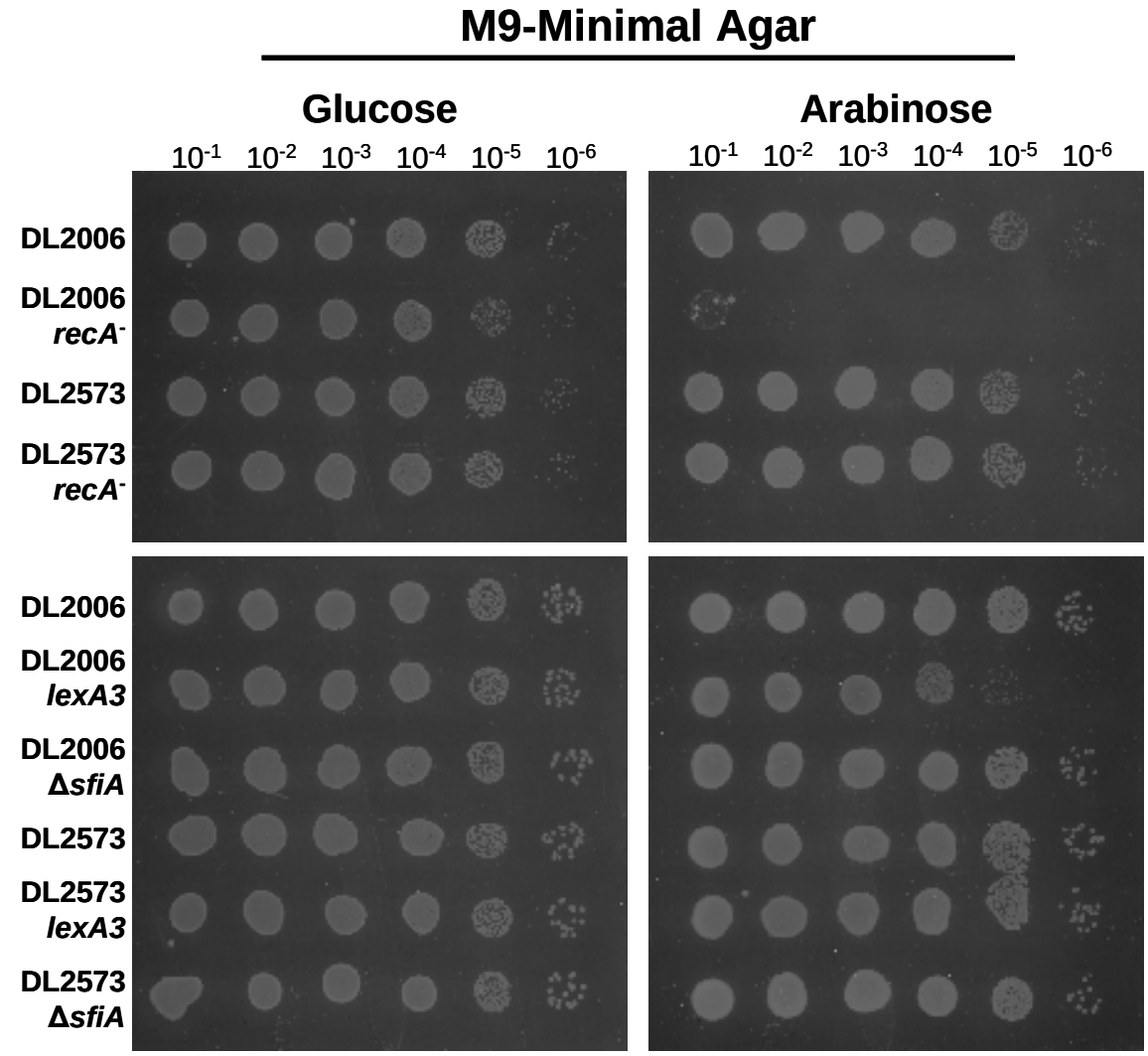

Figure 3.12 Viability of Δ*sfiA* mutants following DNA damage in minimal growth medium. Ten-fold dilutions of overnight cultures of arabinose inducible SbcCD strains either harbouring the palindrome in *lacZ* (DL2006) or not (DL2573), alongside their *recA*$^-$, *lexA3* and Δ*sfiA* derivatives (DL2075, DL2605, DL2829, DL2830, DL4110, and DL4111), were plated onto M9-minimal agar plates supplemented with either 0.5 % glucose (SbcCD repressed) or 0.2 % arabinose (SbcCD induced) and left to grow for 2 days at 37 °C.

testing the SfiA dependence of the observed increase in cell length caused by DSB induction (Figure 3.4). Following this study, Δ*sfiA* derivatives of a *sbcDC*$^{+}$ strain either harbouring the palindrome or not in the *lacZ* gene has been constructed and cell lengths measured (Elise Darmon, unpublished). This showed a significant SfiA dependence on the increase in cell length caused by SbcCD cleavage of the palindrome, alongside either a SfiA independent or redundant pathway of cell division inhibition. Interestingly, a SfiA independent mechanism of cell division inhibition has been identified and shown to be both *lexA* dependent and require DNA damage for its induction (Hill *et al*., 1997). Although this pathway may be contributing to the observed increase in cell mass, the observation that the viability of a *lexA3* mutant can be fully rescued by over-expressing RecA suggests that this pathway is unlikely to be essential for survival following cleavage of the palindrome by SbcCD.

3.4.3 Nucleoid Morphology of Δ*sfiA* Strains Following an Induced DSB

DAPI staining was used to study the nucleoid morphology of Δ*sfiA* mutants containing the arabinose inducible SbcCD construct and either harbouring the palindrome (DL4111) or not (DL4110). Cells were cultured in LB medium at 37 °C for 30 minutes in the absence of any added sugar prior to splitting the culture into two and growing for a further 60 min in either SbcCD induced (LB supplemented with 0.2 % arabinose) or SbcCD repressed (LB supplemented with 0.5 % glucose) conditions. Cultures were then grown for 15 min at 37 °C in the presence of 400 μg ml^{-} chloramphenicol in order to condense the nucleoids, which were subsequently

stained using DAPI (1 μg ml^{-}, 15 min of growth at 37 °C) prior to sampling for microscopy. Cells were imaged at a resolution of 0.129 μm per pixel and multiple *z*-sections (± 800 nm, 9 images at a 200 nm interval) of the DAPI signal were captured. The stack of *z*-planes were deconvolved using the software Autodeblur and Autovisualize v9.32 and the deconvolved *z*-stack combined to give a maximum projection image using MetaMorph 6.3r2. Representative images are shown in Figure 3.13.

The phenotype of the Δ*sfiA* strains was essentially indistinguishable from the *sfiA*$^{+}$ parental strains (DL2006 and DL2573, see Figure 3.5) with no striking difference observed between growth in DSB induced conditions (DL4111, arabinose) and the three controls. No anucleate cells were identified and less than 1 % of cells in all populations tested had more than 2 distinctly segregated nucleoids (300 cells total from 3 independent experiments). Additionally, cells were allowed to form micro-colonies by spotting mid-exponential phase cultures (grown in L broth) onto LB agar supplemented with either 0.5 % glucose or 0.2 % arabinose. These cells were then sealed within a chamber (see section 2.4.3) and allowed to grow in a dark incubator for 2 h at 37 °C. Remarkably, although Δ*sfiA* cells were less elongated (Figure 3.14) than the *sfiA*$^{+}$ parental strains (Figure 3.9) in the absence of the induced DSB many long filaments were still observed in the DSB induced condition (DL4111, arabinose).

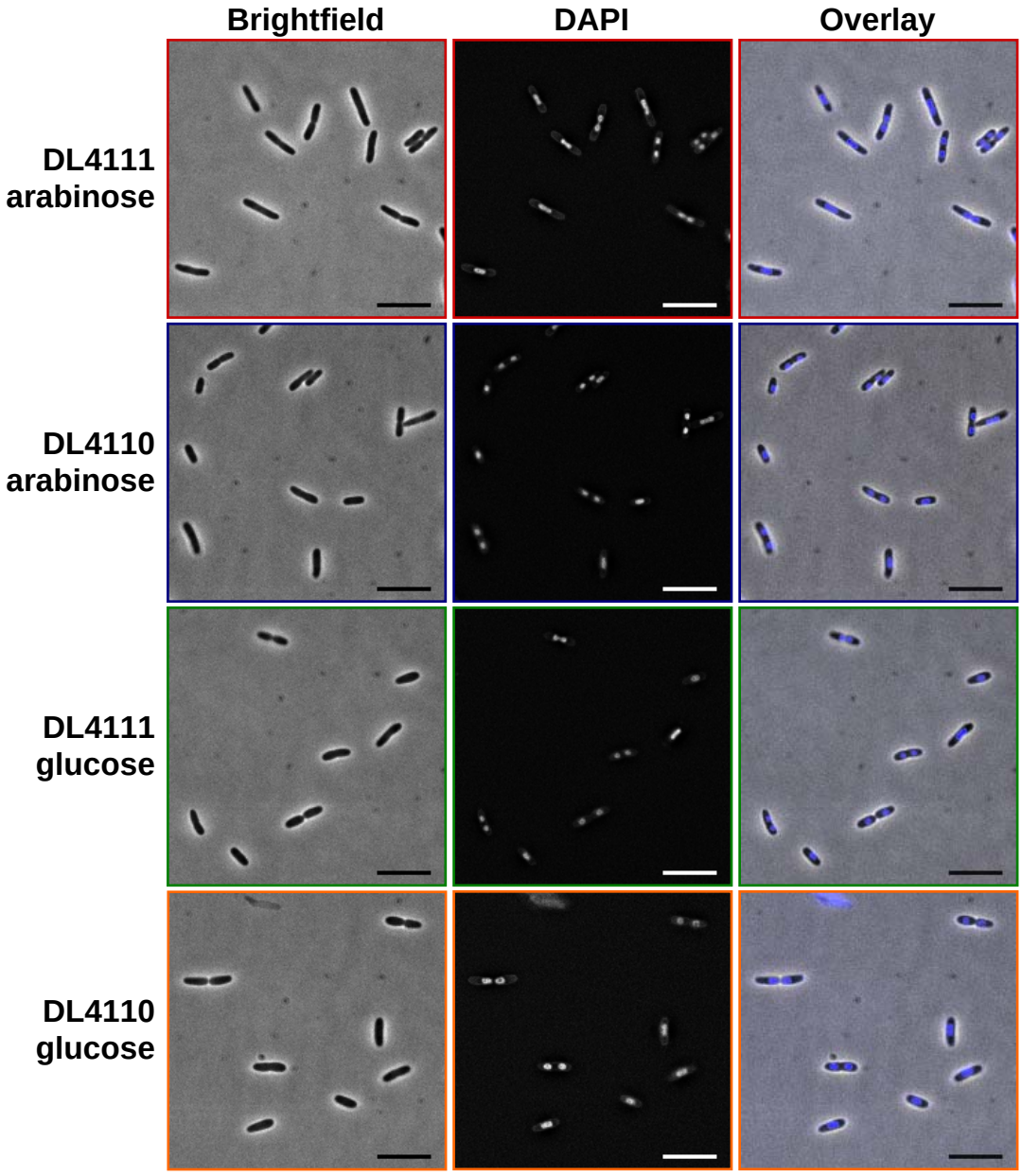

Figure 3.13 Morphology of nucleoids in Δ*sfiA* strains following an induced DSB. Microscopy images of Δ*sfiA* strains either harbouring the palindrome in *lacZ* (DL4110) or not (DL4111). Following 1 h of growth in either SbcCD induced (0.2 % arabinose) or SbcCD repressed (0.5 % glucose) conditions, nucleoids were condensed by chloramphenicol treatment prior to staining with DAPI. DAPI images are maximum projections of deconvolved images. DAPI signal in the overlay image is pseudo-coloured blue; calibration bar shows 10 μm.

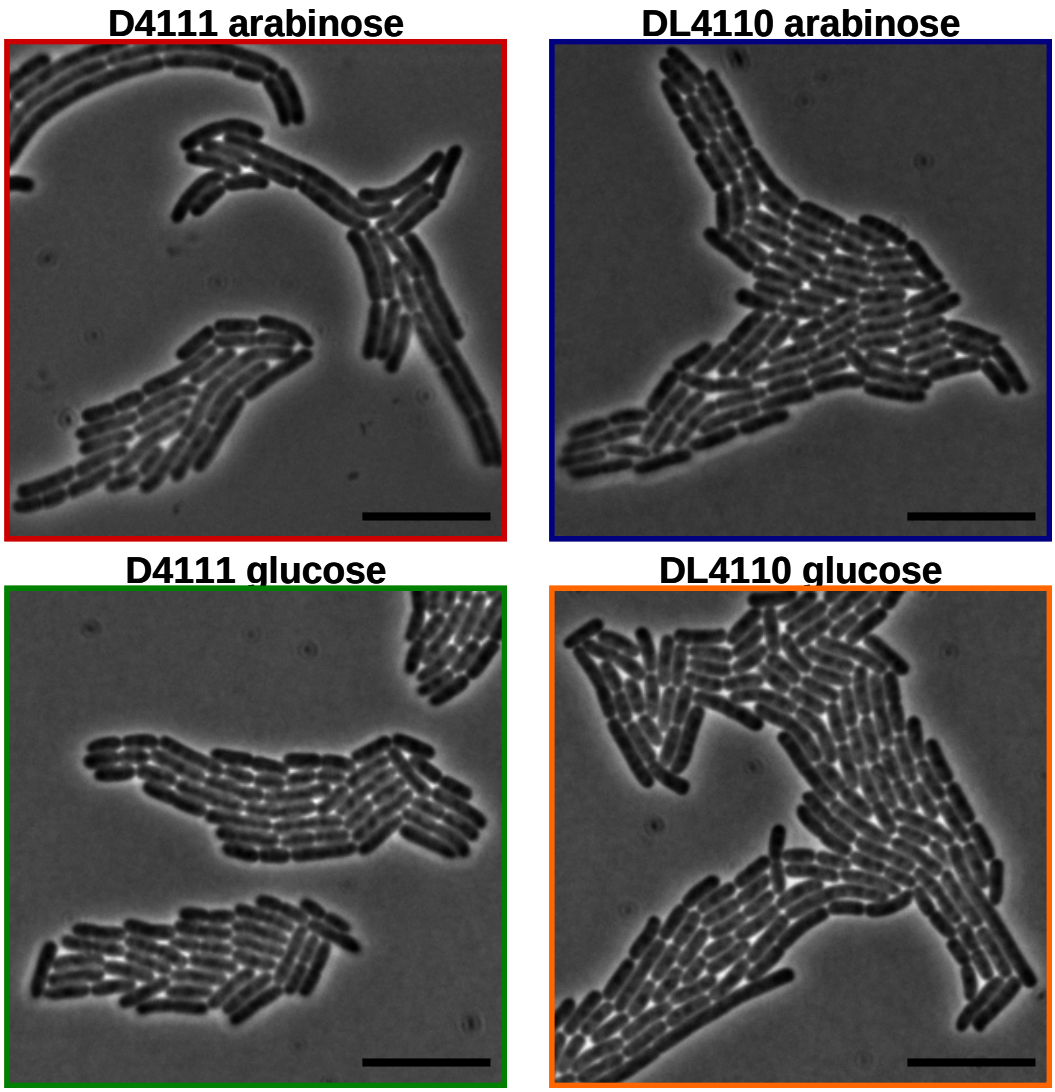

Figure 3.14 Microcolony formation of Δ*sfiA* strains within a sealed chamber. P_{BAD}-*sbcDC* Δ*sfiA* cells either harbouring the palindrome (DL4111) or not (DL41110) were grown in a dark incubator for 2 h at 37 °C on LB agar supplemented with either 0.5 % glucose (SbcCD repressed) or 0.2 % arabinose (SbcCD induced). The cells were grown within a sealed chamber as used for time-lapse microscopy. Calibration bar shows 10 μm.

3.5 Conclusions

It has been reported previously that induction of the hairpin endonuclease SbcCD results in the cleavage of a 246 bp DNA palindrome located on one of a pair of replicating sister chromosomes in *E. coli* (Eykelenboom *et al*., 2008). More recently it has been shown that this method of inducing a single chromosomal DSB results in the induction of the SOS response and that this induction is essential for maintaining cellular viability by increasing the amount of RecA molecules in the cell (John Eykelenboom, unpublished). Although the reason behind this requirement of extra RecA remains unclear, this study has shown that SOS induced levels of RecA is only essential after a number of generations of growth during which the DSB has been induced and is less critical under slow growth conditions. These data suggest that *E. coli* is able to repair a single chromosomal DSB without the need for inducing the SOS response.

This study has shown that induction of the SOS response caused by cleavage of the palindrome by SbcCD has a relatively mild effect on cellular morphology as compared to alternative methods of inducing DSBs such as UV-light (Rudolph *et al*., 2007) and the homing endonuclease I-SceI (Meddows *et al*., 2005). Cell lengths were measured and found to be on average 11 % longer in DSB induced conditions. Although the result from this study was slightly complicated by an effect of sugar (or SbcCD induction) on cellular length, further work comparing *sbcDC*$^{+}$ and Δ*sbcDC* strains grown using the same carbon source has confirmed that this increase in average cell length is only observed in strains that harbour the palindrome in *lacZ* and are expressing SbcCD (Elise Darmon, unpublished). This suggests that cell division is inhibited in chronic DSB induced conditions. Recent work has shown

that this inhibition of cell division is mainly caused by the SOS inducible inhibitor of cell division, SfiA (Elise Darmon, unpublished).

The effect of chronically inhibiting cell division was modelled using knowledge of regulation of the *E. coli* cell cycle. As a result it was hypothesised that following an initial increase in generation time, and hence cell mass, the subsequent generation time should return to normal. This could explain why chronic DSB induction was not found to have a discernable impact on generation time as measured by the change in number of colony forming units over time (John Eykelenboom, unpublished). The model also predicts that cell mass should equilibrate at a size determined by the initial delay in generation time. Although an increase in cell length had been demonstrated, cells were only sampled at a single time point of growth in SOS-response induced conditions. To test the hypothesis that this increase in average cell length is maintained through subsequent cell divisions, time-lapse microscopy was used to follow the growth of individual cells through multiple generations. Unfortunately these results were complicated by differences in the morphology of cells when grown in the conditions used for the time-lapse microscopy.

The observation that the viability of strains unable to induce the SOS response could be rescued by over-expressing RecA suggested that induction of the cell division inhibitor SfiA was not essential for survival following induction of the DSB. This hypothesis was tested by making a precise deletion of the *sfiA* gene and confirmed to be the case in both slow and fast growth conditions. DAPI staining of cell nucleoids showed that induction of the DSB did not result in the formation of anucleate cells in both *sfiA*$^{+}$ and Δ*sfiA* backgrounds. This suggests that cells can still

segregate their nucleoids and that cell division in the absence of SfiA induction does not occur prematurely. However, chromosome segregation is delayed to some extent following cleavage of the palindrome by SbcCD as revealed by an increase in the proportion of cells with a single discreet nucleoid. This delay may be caused directly by the action of homologous recombination, or indirectly by the formation of dimeric chromosomes. This opens up the possibility of investigating chromosome segregation in mutants defective for either Holliday junction resolution (a comparison of *ruv*$^-$ and *recG*$^-$ strains, both of which are inviable following SbcCD cleavage of the palindrome) or chromosome dimer resolution (*xerCD*$^-$ or Δ*dif*).

Chapter 4

The ‘Superconstruct’: A System for Visualising the Cellular Location of DNA Flanking an Induced DNA Double-Strand Break

4.1 Introduction

It was shown by microscopy in Chapter three, that an induced chromosomal DNA double-strand break (DSB) caused a delay in both the processes of cell division and chromosome segregation in *E. coli*. This investigation into the effect of cleavage of a 246 bp interrupted DNA palindrome by SbcCD on the cell cycle of *E. coli* was furthered by the development of a chromosomal construct (termed the superconstruct) that would allow a single DSB to be induced, and for the DNA ends of that break to be visualised using fluorescence microscopy (Figure 4.1). Furthermore, this system can distinguish the two ends of the break, allowing potential differences in their fates to be investigated. As such, this construct provides a means for investigating the effect that a single DSB has on the localisation of DNA within a cell during all stages of repair. This chapter discusses the construction, characterisation and optimisation of this system.

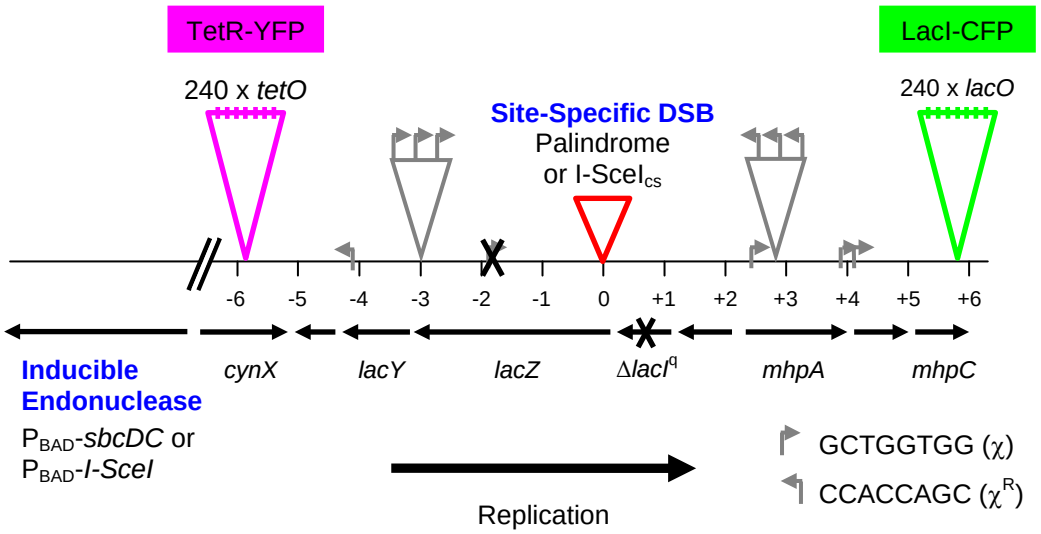

Figure 4.1 The 'Superconstruct': a system for visualising the ends of an induced chromosomal DNA double-strand break
An array of *tetO* and *lacO* sites integrated either side of a site-specific target for an arabinose inducible endonuclease are visualised upon the binding of TetR-YFP and LacI-CFP respectively. These fluorescent repressor proteins are expressed from a weak constitutive promoter on a plasmid (pDL3196). To limit competitive binding with LacI-CFP, the endogenous copy of *lacI* was deleted. To prevent a bias in the degradation of the two broken DNA ends by RecBCD, the only active Chi site between the break site and the operator arrays was removed and an array of three Chi sites inserted either side of the DSB site. These Chi arrays were designed to prevent the degradation of the two operator arrays by RecBCD prior to loading of RecA. Two strain backgrounds were constructed. One with an inducible SbcCD construct and a 246 bp palindrome in the *lacZ* gene and another with an inducible I-SceI construct and a unique I-SceI cleavage site (I-SceI$_{cs}$) in the *lacZ* gene. Figure adapted from (White *et al.*, 2008).

4.2 Using SbcCD to Induce a DSB at a Palindrome in *lacZ*

4.2.1 Introduction

In order to follow the dynamics of homologous recombination *in vivo*, a system for inducing a DSB at a defined locus was required. For this purpose the inducible SbcCD/palindrome system developed by John Eykelenboom and collaborators (Eykelenboom *et al*., 2008) was decided upon. This system involves the insertion of a 246 bp interrupted palindrome into the *lacZ* gene of an *E. coli* strain that has had the endogenous promoter of the *sbcDC* operon replaced with the arabinose inducible promoter P_{BAD}. Expression from this promoter is both negatively regulated by the repressor AraC and positively regulated by the global activator CRP; the combination of which results in a system that can be both rapidly switched on or off and makes >1000-fold repression possible when cells are grown in the presence of glucose (Guzman *et al*., 1995). In order to circumvent the problem of 'all or nothing' expression from this promoter (Siegele and Hu, 1997), all experimental strains using this system have the arabinose transporter *araE* placed under a constitutive promoter (derivatives of strain BW27784 (Khlebnikov *et al*., 2001)) thus giving homogenous expression from P_{BAD} in the population.

The major advantage of using this system for inducing a DSB is that although SbcCD cleaves the palindrome with high efficiency to create a bone fide two-ended DSB, it does so at only one of a pair of replicating sister chromosomes. This is because rather than targeting the DNA sequence of the palindrome, SbcCD recognises a DNA hairpin (Connelly *et al*., 1998) that is formed by the palindrome on the lagging, but not the leading strand template of replication (Pinder *et al*., 1998).

The ability to cleave one of a pair of sister chromosomes is of particular importance in *E. coli* because all DSBs are repaired by homologous recombination, a reaction that requires the presence of an intact homologous sequence to act as a template.

4.2.2 Constructing DL1780 *lacZ*$^+$

Although a derivative of BW27784 with the *sbcDC* operon placed under control of P_{BAD} was available (DL1780), this strain was *lacZ*$^-$ due to a deletion introduced during the construction of BW27784. DL1780 therefore lacked the necessary homology for integration of the palindrome into *lacZ*. Also, all available *lacZ*$^+$ derivates of DL1780 had a gentamycin resistance cassette integrated at a locus (*cynX*) that was to be used for integration of the *tetO* array (see section 4.4) and were therefore unsuitable for this study.

To make strain DL1780 *lacZ*$^+$, the *tetO* array (which is associated with a gentamycin resistance cassette) was first integrated into the *cynX* locus of strain DL1777 by PMGR using plasmid pDL1709. DL1777 is a derivative of the sequenced *E. coli* K12 strain MG1655 (*lacZ*$^+$) that had been made *lacI*^{q} and had a Chi site located in *lacZ* removed (*lacZ*χ-) by PMGR (Eykelenboom *et al*., 2008). The resulting strain (DL2875) contained both the *tetO* array at *cynX* and all the necessary homology required for subsequent integration of the rest of the superconstruct (Figure 4.1) associated with a gentamycin resistance marker. This strain was then used to make a P1 lysate in order to transduce *cynX*::[(240x*tetO*)::Gm^R] along with the *lacZ* region of DL2875 into strain DL1780 by selecting for gentamycin resistant transductants. The resulting strain (DL2877) was screened for the transfer of *cynX*::[(240x*tetO*)::Gm^R] by microscopy following

transformation with plasmid pWX6 (visible as a YFP fluorescent focus as a result of TetR-YFP binding to the *lacO* array). Successful co-transduction of *lacZ* (located 5.8 kb from *cynX*) was screened by PCR using primers ExtestF and ExtestR. This allowed subsequent integration of the 246 bp palindrome into the *lacZ* gene by PMGR using plasmid pDL2774.

4.3 Using I-SceI to Induce a DSB at a Unique Cleavage Site in *lacZ*

4.3.1 Introduction

Despite its usefulness for investigating DNA repair by homologous recombination in *E. coli*, the arabinose inducible SbcCD/palindrome system of creating a DSB had a potential drawback for this particular study. One of the central aims of this investigation was to follow the fate of the two broken DNA ends as they interacted with their sister chromosome during the process of homologous recombination. In order to do this, prior to DNA cleavage, the two sister chromosomes would have to have segregated at least to the extent where they were resolvable by light microscopy. It was postulated that this may not be the case when SbcCD cleaves the palindrome because the target for cleavage (a DNA hairpin) forms during replication and the endonuclease (SbcC-GFP) co-localises with the replisomes of the cell (Darmon *et al*., 2007). It is therefore possible that cleavage of the DNA hairpin by SbcCD occurs during post-replication cohesion of the sister chromosomes (Wang *et al*., 2008) in the majority of cells.

Therefore in order to complement work using the SbcCD/palindrome method of inducing a DSB, it was deemed prudent to construct strains that had a system of

inducing a single DSB in a replication independent manner. For this purpose, the homing endonuclease I-SceI was decided upon. Strains were then constructed that harboured the superconstruct (Figure 4.1) but were wild-type for the *sbcDC* operon and had the homing endonuclease I-SceI gene integrated into the chromosome under control of the arabinose inducible promoter (P_{BAD}) along with a unique cleavage site integrated in place of the palindrome in *lacZ* (strain DL3278).

I-SceI is a homing endonuclease originally isolated from an intron native to the mitochrondrial genome of *S. cerevisiae*. It has a 18 bp recognition sequence that despite having been shown to have some redundancy (Monteilhet *et al*., 1990), is large enough to make it a useful tool for inducing a single DSB at a defined locus in genomes as large and complex as human and mice (Moynahan *et al.*, 2001). Despite this, I-SceI does have its limitations as a tool for studying DSB repair in *E. coli*. Since *E. coli* is a haploid organism, any recognition site integrated into the chromosome will be present on all sister chromosomes. Therefore, unlike the case of SbcCD induced cleavage of a palindrome, induction of I-SceI has the potential to result in the cleavage of all chromosomes thereby preventing repair by homologous recombination.

4.3.2 Construction of an I-SceI Inducible Strain

Plasmid pDL1625 (White *et al*., 2008) was utilised in order to integrate an arabinose inducible I-SceI cassette into the chromosome. This plasmid allows for any gene of interest to be placed under the control of the arabinose inducible promoter P_{BAD} and subsequently integrated into the *araBAD* operon of *E. coli* by PMGR. To accomplish this, *I-SceI* was first amplified by PCR using pCBA-SceI (Tremblay *et*

al., 2000) as a template and primers (I-SceI_F and I-SceI_R) designed to flank the gene with NcoI and NotI restriction sites. This *I-SceI* fragment was subsequently cloned into pDL1625 using NcoI and NotI restriction enzymes, resulting in the replacement of a kanamycin resistance cassette that is present between the two homology arms of pDL1625. This plasmid (pDL2655) was sequenced to ensure that no mutations were introduced during the cloning of *I-SceI*.

To allow the quantity of I-SceI to be titrated within individual cells, it was desirable to integrate pDL2655 into the BW27784 strain background (see section 4.2.1). This was not directly possible however, since BW27784 lacked the homology necessary for PMGR as a result of a deletion of the *araBAD* operon. To overcome this, pDL1625 was first integrated into MG1655, a sequenced strain of *E. coli* K12 that possessed the necessary homology (*araBAD*$^+$) for PMGR. P1 lysate was then harvested from this strain (DL2283) and used to transduce the appropriate *araBAD* homology into BW27784 by selecting for kanamycin resistance. This strain (DL2520) was screened by PCR for the presence of the necessary homology using primers ParaB-fwd and CaraB-rev. After DL2520 was made *lacZ*$^+$ (see section 4.3.3) P_{BAD}-*I-SceI* was integrated into the chromosome by PMGR using pDL2655 to give strain DL2894. Successful integration of P_{BAD}-*I-SceI* was confirmed by PCR using primers ParaB-fwd and CaraB-rev.

4.3.3 Constructing DL2520 *lacZ*$^+$ and Integration of a Unique I-SceI Cleavage Site

It was necessary to make DL2520 *lacZ*$^+$ in order to integrate a unique I-SceI cleavage site ($I\text{-}SceI_{cs}$) by PMGR into the same locus (*lacZ*) as the palindrome is integrated in

strain DL3276. To do this, the same approach utilised to make DL1780 *lacZ*$^+$ (as outlined in section 4.2.2) was used again. Briefly, P1 lysate harvested from strain DL2875 was used to transduce *cynX*::[(240x*tetO*)::Gm^R] and *lacZ* (*lacZ*χ-) into DL2520 by selecting for gentamycin resistance. The resulting strain (DL2879) was screened for *cynX*::[(240x*tetO*)::Gm^R] by fluorescence microscopy following transformation with plasmid pWX6, and for *lacZ*$^+$ by PCR using primers ExtestF and ExtestR. By making DL2879 *lacZ*$^+$, a unique I-SceI$_{cs}$ could be introduced at the exact locus used for integration of the palindrome by PMGR using plasmid pDL2521 (Eykelenboom *et al*., 2008). Integration of the I-SceI$_{cs}$ was screened by PCR amplification of the *lacZ* region using primer pair DelI_Isc_testF/R followed by in vitro digestion using I-SceI (NEB).

4.4 The Use of Operator Arrays to Label the Ends of a DSB

4.4.1 Introduction

To visualise the co-ordination of DNA ends following a break *in vivo* by fluorescence microscopy, two arrays each consisting of 240 operator sites flanking an antibiotic resistance cassette, were integrated into the *E. coli* chromosome either side of *lacZ* by PMGR using plasmids pDL1709 and pDL2542. pDL1709 was used to integrate an array of *tetO* associated with a gentamycin resistance cassette into the *cynX* locus, which is located 5.8 kb origin proximal to the location of the DNA palindrome (or I-SceI$_{cs}$). pDL2542 was used to integrate an array of *lacO* associated with a kanamycin resistance cassette into the *mhpC* locus of the *E. coli* chromosome. Although originally designed to be at a similar distance from the palindrome (or I-

SceI$_{cs}$) as the *tetO* array (5.6 kb downstream), deletion of *lacI* (see section 4.5.1) resulted in the *lacO* array being located approximately 800 bp closer (4.8 kb origin distal to the *lacZ* locus).

The operator sites are recognition sequences for DNA binding repressor proteins, of which fluorescently labelled derivatives (TetR-eYFP and LacI-Cerulean) have been cloned into a high copy number plasmid (pDL3196, see section 4.4.3 for details of construction). These fluorescent repressors allow the cellular location of the operator arrays to be identified indirectly as either YFP or CFP fluorescent foci when viewed under a fluorescence microscope with appropriate filter sets. The operator arrays used in this project were derived from plasmids pLau43 and pLau44 developed by Ivy Lau and collaborators (Lau *et al*., 2003). Plasmids pDL1709 and pDL2542 were cloned prior the start of this project by Emily Wilson and Manuel Lopez-Vernaza respectively.

4.4.2 Construction of Plasmids pDL1709 and pDL2542

Plasmid pDL1709 was created in order to integrate an array of *tetO* sites into the *cynX* gene of the *E. coli* chromosome. To accomplish this, two homology arms flanking a multiple cloning site (MCS) were created by crossover PCR using the primer pairs TetO-CF1/TetO-CR1 and TetO-CF2/TetO-CR2 and cloned into the PstI and NheI restriction sites of the plasmid pTOF24. Following this, the array of *tetO* sites was digested out of pLau44 using XbaI and BamHI restriction enzymes and cloned into the previously formed plasmid using the XbaI and BamHI restriction sites present in the MCS.

Plasmid pDL2542 was created in a similar manner in order to integrate an array of *lacO* sites into the *mhpC* gene. The homology arms were created by crossover PCR using primer pairs LacO-CF1/LacO-CR1 and LacO-CF2/LacO-CR2 and cloned into the PstI and NheI restriction sites of the plasmid pTOF24. The array of *lacO* sites was digested out of pLau43 using XbaI and BamH1 restriction enzymes and cloned into the previously formed plasmid using the XbaI and BamHI restriction sites present in the MCS.

4.4.3 Converting enhanced CFP to Cerulean

Originally the two operator arrays were visualised using TetR-eYFP and LacI-eCFP fusion proteins expressed from a weak constitutive promoter (P_{ftsKi}) on a plasmid (pWX6, (Wang *et al.*, 2005)). However, in order to improve the imaging of the *lacO* array, the enhanced Cyan Fluorescent Protein (eCFP) fused to LacI was converted to a brighter variant of CFP known as Cerulean (Rizzo *et al.*, 2004). Mutations S72A, Y145A, and H148D were introduced into enhanced-CFP by site-directed mutagenesis (SDM). Initially *tetR-eyfp* was cloned out of pWX6 using XbaI (pDL3194) to prevent the primers from binding to the *eyfp* gene. Subsequently, two sequential rounds of SDM were carried out first using primers eCFP_S72A_sdmF/ eCFP_S72A_sdmR and then primers eCFP_Y145AH148D_F/ eCFP_Y145AH148D_R, to create plasmid pDL3195. Finally, *tetR-eyfp* was cloned back in to the XbaI restriction site of pDL3195 to make pDL3196. Using this variant produced CFP foci that were approximately nine-fold brighter than those previously obtained with the LacI-eCFP fusion and greatly improved both the quality and reproducibility of CFP imaging in this study.

4.5 Operator Arrays and Replication Stalling

4.5.1 Introduction

One drawback of using a fluorescent repressor-operator system to visualise DNA loci in *E. coli* is that it has the potential to disrupt DNA replication. This is caused by the operator bound repressors acting as an efficient block to replication fork progression (Possoz *et al.*, 2006). In order to prevent this, the affinity of repressor binding can be reduced by the addition of their cognate inducers to the growth medium (Anhydrotetracycline (ATC) for TetR-YFP and IPTG for LacI-CFP; (Lau *et al.*, 2003). However, this subsequently results in a reduction in the ability of the fluorescent repressors to form a focus. A balance must therefore be reached between having enough inducer present as not to perturb the cell cycle, while not having so much that you can no longer effectively visualise the tagged locus.

4.5.2 Deleting *lacI*

In order to prevent competitive binding with LacI-CFP, the endogenous non-fluorescent copy of *lacI* was deleted from the chromosome by PMGR using the plasmid pDL3036. As a consequence of this, imaging of the *lacO* array resulting from binding of LacI-CFP was much improved while problems with DNA replication through the operator array were negated, even in the absence of the inducer IPTG (see section 4.5.3). Prior to deletion of *lacI*, strains expressing LacI-CFP from pWX6 were inviable in the absence of IPTG and suffered from plasmid instability at low IPTG concentrations (<0.5 mM). To construct pDL3036, two homology arms were amplified from the chromosome of MG1655 using primer pairs LacI_delta_F1/ LacI_delta_R1 and LacI_delta_F2/ LacI_delta_R2 and then fused by

cross-over PCR using primers LacI_delta_F1 and LacI_delta_R2. The resulting PCR fragment was subsequently cloned into the PstI and SalI restriction sites of pTOF24.

Representative images of a *lacI*$^{+}$ strain (DL3072) and its Δ*lacI* derivative (DL3073) both expressing TetR-eYFP and LacI-eCFP from plasmid pWX6 are shown in Figure 4.2. Cultures were grown to mid-exponential phase of growth (OD_{600} of 0.5) in M9-minimal medium (0.2 % glucose) supplemented with 100 ng ml^{-1} ATC and either 0, 0.1, or 0.5 mM of IPTG. Strain DL3073 harbouring pWX6 was inviable in the absence of IPTG. Cells were imaged at a resolution of 0.129 μm per pixel and multiple *z*-sections (± 800 nm, 9 images at a 200 nm interval) of both CFP and YFP signals were taken. Exposure times for CFP and YFP image capture were 1000 ms and 500 ms respectively. The stacks of *z*-planes were deconvolved using the software Autodeblur and Autovisualize v9.32 and subsequently combined to give a maximum projection image using MetaMorph 6.3r2. Images shown were pseudocoloured using MetaMorph 6.3r2.

.

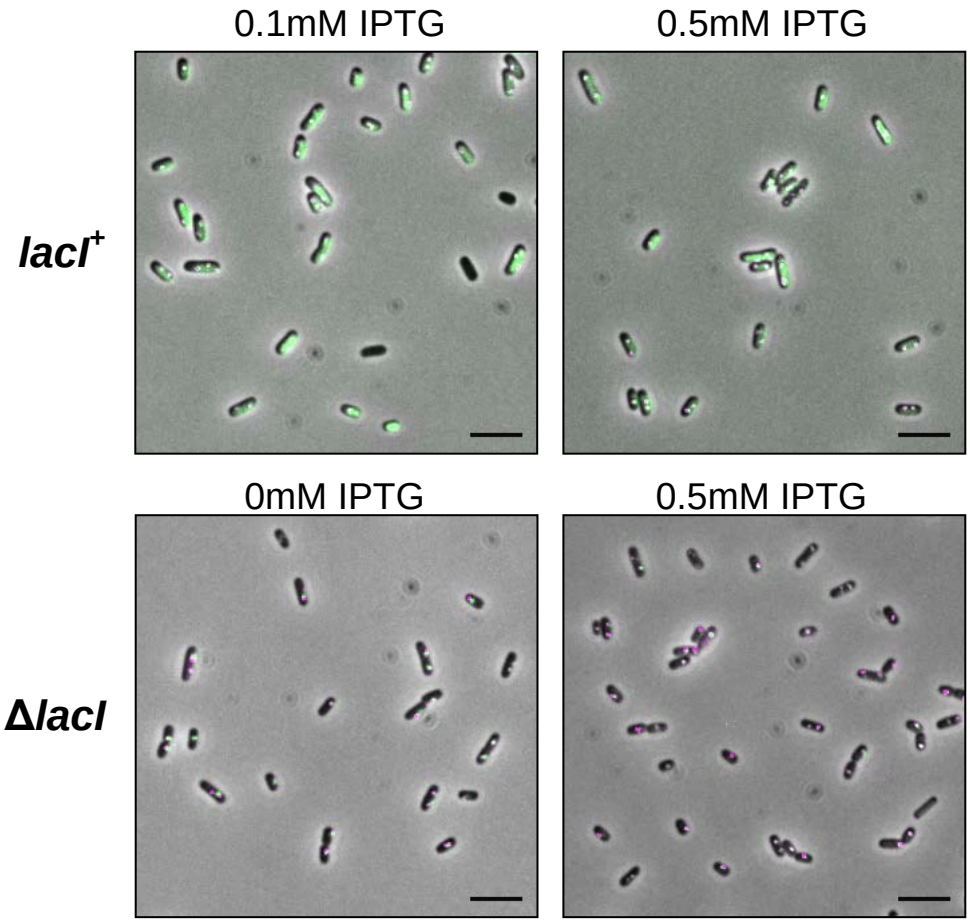

Figure 4.2 Effect of *lacI* deletion on imaging LacI-CFP. Cultures of a *lacI*$^{+}$ strain (DL3072) and its Δ*lacI* derivative (DL3073), both expressing the fluorescent repressors from pWX6, were grown overnight in minimal medium supplemented with 0.2 % glucose, 100 ng ml^{-1} ATC and IPTG as indicated. CFP signal is pseudocoloured green and YFP magenta, overlapping signal appears white; calibration bar shows 5 μm.

4.5.3 Using Inducers to Prevent Replication Blockage

A combination of growth curves, viability tests and microscopy was used to ascertain whether or not the presence of the fluorescent repressors was perturbing DNA replication. Strains possessing both operator arrays and either expressing fluorescent repressors (DL3285) or not (DL3278) from a plasmid (pDL3196) was grown overnight in M9-minimal medium (0.2 % glucose) supplemented with 100 ng ml^{-1} ATC and 0.5 mM IPTG. Ampicillin was added only to the medium used to culture strain DL3285 in order to select for maintenance of plasmid pDL3196. The following day, these stationary phase cultures were diluted in 37 °C in M9-minimal medium (0.2 % glucose) supplemented with various combinations of inducers (and ampicillin for DL3285) and grown for 6 h at 37 °C. The optical density of these cultures at 600 nm (OD_{600}) was measured every 30 min and serial dilutions spotted onto LB agar plates supplemented with 100 ng ml^{-1} ATC and 0.5 mM IPTG every 2 h. Finally, after 6 h of growth the cultures were sampled for viewing on the microscope. Cells were imaged at a resolution of 0.129 μm per pixel and multiple *z*-sections (± 800 nm, 9 images at a 200 nm interval) of both CFP and YFP signals were captured. The stacks of *z*-planes were deconvolved using the software Autodeblur and Autovisualize v9.32 and subsequently combined to give a maximum projection image using MetaMorph 6.3r2.

The results showed that over the 6 hours of growth, expression of LacI-Cerulean and TetR-eYFP had no effect on the optical density of the cultures even in the absence of inducers (Figure 4.3a). However, despite having an almost identical OD_{600}, cultures of DL3285 grown in the absence of the inducer ATC had markedly fewer viable cells than either cultures of DL3278 or DL3285 grown in the presence

a

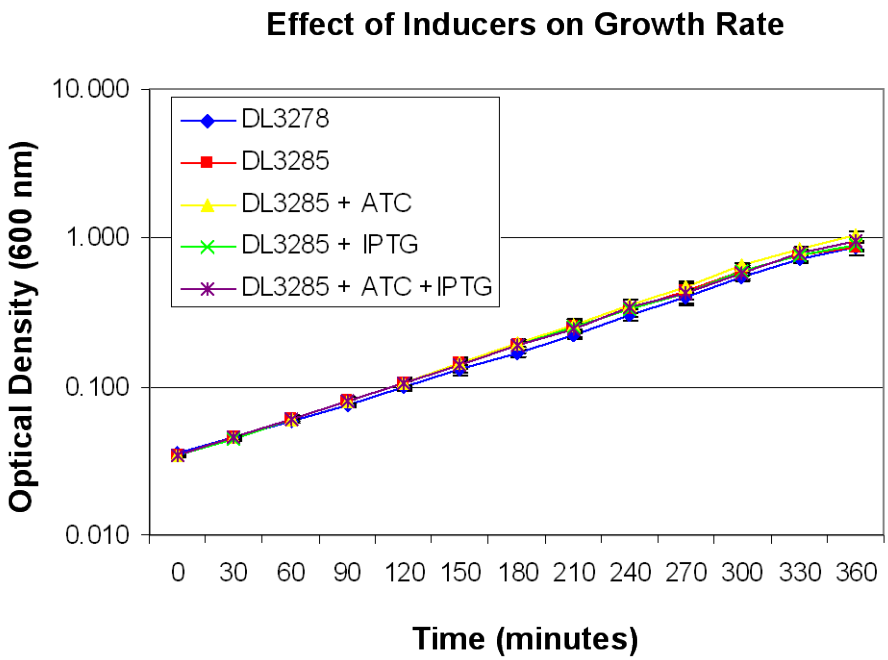
Effect of Inducers on Growth Rate
Optical Density (600 nm)
10.000
1.000
0.100
0.010
DL3278
DL3285
DL3285 + ATC
DL3285 + IPTG
DL3285 + ATC + IPTG
0 30 60 90 120 150 180 210 240 270 300 330 360
Time (minutes)

b

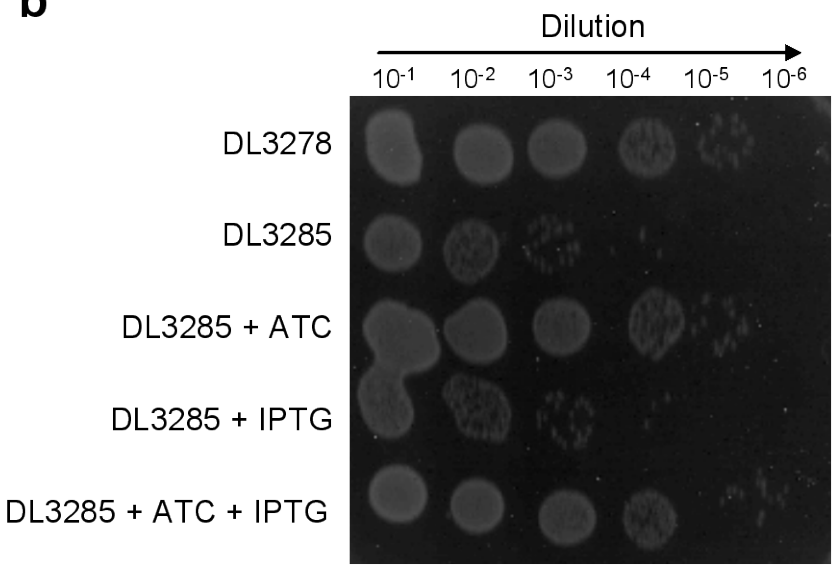
Dilution
10-1 10-2 10-3 10-4 10-5 10-6
DL3278
DL3285
DL3285 + ATC
DL3285 + IPTG
DL3285 + ATC + IPTG

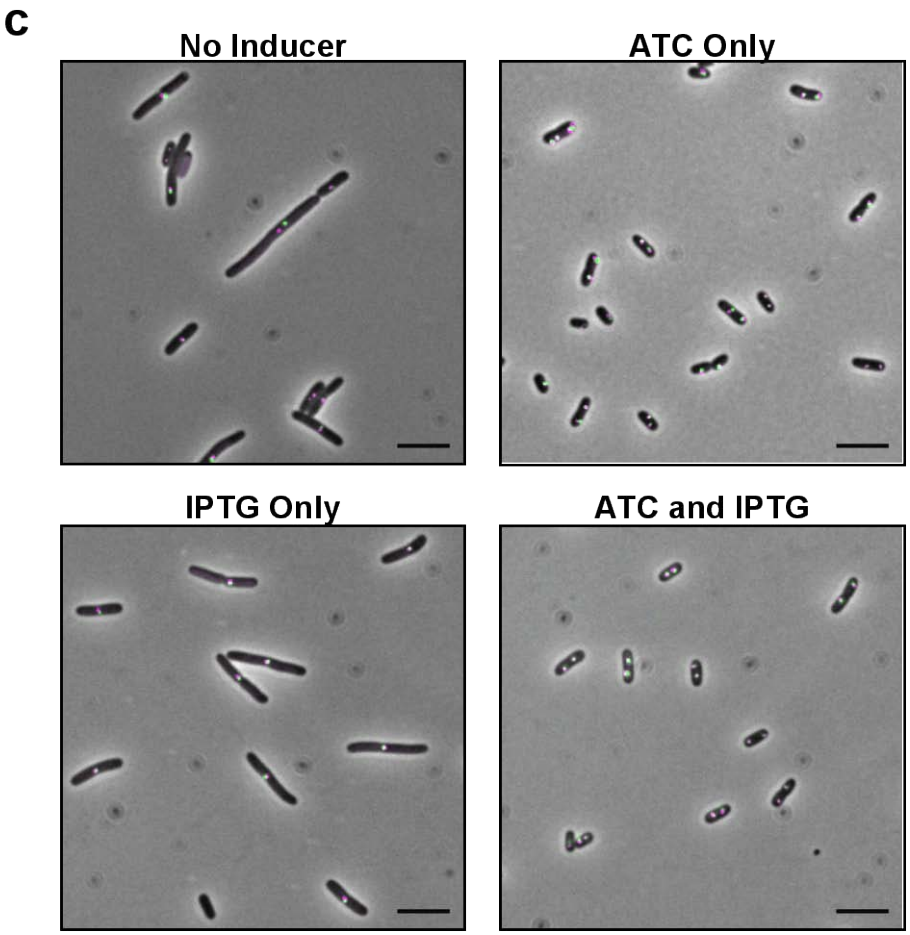

Figure 4.3 Effect of inducers on cells harbouring the operator arrays. **a**, Cells grown in minimal medium supplemented with 0.2 % glucose, and 100 ng ml^{-1} ATC and 0.5 mM IPTG as indicated, were sampled every 30 min and the OD_{600} measured. Although both strain DL3278 and DL3285 harbour a *tetO* and a *lacO* array, only DL3285 expresses TetR-eYFP and LacI-Cerulean. *n* = 3 and error bars are standard error of the mean. **b**, Cells were sampled after 360 min of growth and serial dilutions of culture spotted on LB agar plates supplemented with glucose, 100 ng ml^{-1} ATC and 0.5 mM IPTG. **c**, Representative images of strain DL3285 cultured with or without the inducers ATC and/or IPTG. Shown are maximum projection images of deconvolved CFP and YFP *z*-stacks overlaid with the brightfield image; CFP is pseudocoloured green and YFP magenta. Overlapping CFP and YFP signals appears white. Calibration bar shows 5 μm.

of ATC. This observation was most dramatic after 6 h of growth (Figure 4.3b). The observation that the optical density of the culture continued to increase while the number of colony forming units decreased suggested that the cells were filamenting, a hypothesis that was confirmed by the microscopy. Cultures lacking ATC had cells that were visibly longer than the same strain cultured in the presence of ATC. Additionally, the vast majority of these cells (>95 %) contained only a single visible twin CFP/YFP spot located at mid-cell (Figure 4.3c). This is in agreement with replication being blocked at the origin proximal (*tetO*) operator array as a result of impediment by *tetO* bound TetR-eYFP.

Although a requirement for ATC was apparent, the data suggested that IPTG was not. This was not the case with the *lacI*$^{+}$ strain DL3072 from which DL3278 was derived (section 4.5.2). To test for any subtle requirement for IPTG, cultures of DL3278 and DL3285 were grown overnight in M9-minimal medium (0.2% glucose) supplemented with or without 100 ng ml^{-1} ATC and/or 0.5 mM IPTG. These cultures were then diluted in fresh (37 °C) media and allowed to grow at 37 °C for 3 h (until OD_{600} was ~0.2) after which they were sampled for microscopy. Brightfield images were acquired at a resolution of 0.129 μm per pixel and cell lengths were measured using the 'fiber length' measurement of image analysis software MetaMorph v6.3r2. 300 cells were measured for each growth condition and the experiment repeated three times. The mean cell lengths from each independent experiment were used for statistical analyses.

The result showed no difference in the mean cell length of strains cultured in the presence or absence of IPTG, whether or not they were expressing LacI-CFP (Figure 4.4a). It also confirmed that there was no detectable difference in the

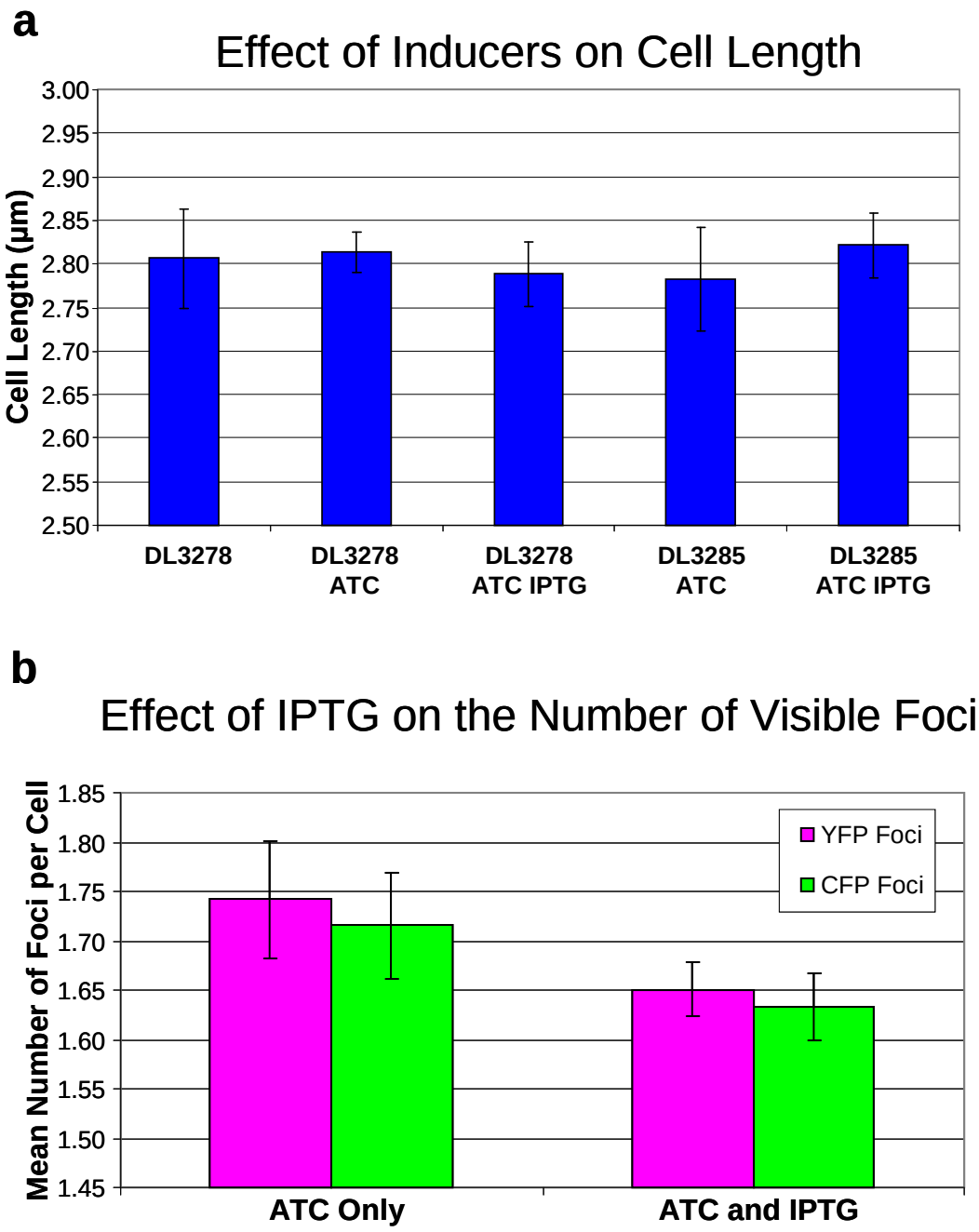

Figure 4.4 The effect of ATC and IPTG on cell growth. Cells were sampled for microscopy following growth in M9-minimal (glucose) medium supplemented with or without 100 ng ml^{-1} ATC and/or 0.5 mM IPTG. **a**, The mean cells lengths of the strains in the different conditions were calculated and shown not to be significantly different from one another (ANOVA, p = 0.967). Error bars are standard error of the mean, *n* = 3. **b**, The mean number of visible YFP and CFP foci per cell was calculated. Although slightly fewer foci were observed in the presence of IPTG, this difference was not significant (2 sample t-tests, for the number of YFP foci p = 0.248 and for the number of CFP foci p = 0.336).

morphology of cells expressing TetR-eYFP (DL3285) in the presence of 100 ng ml^{-1} ATC compared to an isogenic strain not expressing TetR-eYFP (DL3278). Analysis of Variance (ANOVA) showed there to be no statistical significance between the population means of the strains grown in the different conditions ($p = 0.967$, $n = 3$).

For strain DL3285, CFP and YFP images were taken along with the brightfield images used to measure cell lengths. Multiple z-sections (± 800 nm, 9 images at a 200 nm interval) of CFP and YFP images were acquired at a resolution of 0.129 μm per pixel. The stacks of *z*-planes were deconvolved using the software Autodeblur and Autovisualize v9.32 and subsequently combined to give a maximum projection image using MetaMorph 6.3r2. As well as measuring cell length, the number of visible YFP and CFP foci in each cell was counted. Although on average, cells had fewer YFP and CFP foci when cultured in the presence of 0.5 mM IPTG (Figure 4.4b), 2 sample t-tests showed that these differences were not significant ($p = 0.248$ for the mean number of YFP foci per cell and $p = 0.336$ for the mean number of CFP foci per cell). This result shows that the presence of IPTG in the growth medium has no detectable effect on the replication and segregation of the *lacO* array in cells expressing LacI-CFP.

Similar experiments were carried for strains DL3276, DL3277, and DL3279 and their derivatives expressing TetR-eYFP and LacI-Cerulean (DL3283, DL3284 and DL3286 respectively). However, since no effect on growth rate was observed for DL3285 in the absence of ATC, OD_{600} was not measured for cultures of these strains and viability only checked after 6 h of exponential growth. As for DL3285, only ATC (not IPTG) was required to prevent detectable blockage of replication at the operator arrays by the fluorescent repressors. Various concentrations of ATC

were tested for their effect on viability and this concentration was found to be in excess of that which is required. Although cells could be cultured in concentrations of ATC as low as 20 ng ml^{-1} this excess of ATC had no detectable effect on the imaging of TetR-eYFP.

4.6 The Use of Chi to Limit RecBCD Degradation of the Operator Arrays

In order not to bias degradation of one end of the induced DSB by RecBCD, the only active Chi site between the break site and the operator arrays (located in *lacZ*) was removed (see section 4.2.2). However, the lack of any active Chi sites between the break site (the 246 bp palindrome or I-SceI_{cs} in the *lacZ* gene) and either operator array opened up the possibility that they could be degraded by the exonuclease activity of RecBCD, thereby preventing the dynamics of homologous recombination from being studied. To this end, an array of three Chi sites was integrated by PMGR on both sides of the palindrome, into the intergenic region between *lacZ* and *lacY* and into the *mhpC* gene, using plasmids pDL3192 and pDL3181 respectively.

These arrays of three tandem Chi sites, each separated by a short 10 bp spacer, were chosen for their ability to act as a single, high-efficiency Chi site *in vitro* (Spies *et al*., 2003) and were engineered in the correct orientation as to stimulate RecBCD as it proceeds from the two DNA ends formed by cleavage of *lacZ*. Although the two Chi arrays are located a similar distance from their neighbouring operator array (~2.6 kb), due to the deletion of *lacI*, they are not equidistant from the break site (*lacZ*) with the origin proximal Chi site being 3 kb and the origin distal Chi site being 2.4 kb from the break site. Although these Chi

sites are located at a physiologically relevant distance from one another (Chi sequences are located on average every 5 kb in the *E. coli* genome (Malone *et al*., 1978)) they are not skewed in the manner that endogenous Chi sequences are typically found. The distribution of Chi in the *E. coli* chromosome is biased such that RecBCD is more likely to encounter an active Chi on the origin proximal arm of a DSB before an active Chi sites than the origin distal arm (Blattner *et al*., 1997; Kuzminov, 1995). This will not be the case in a DSB induced in *lacZ* in these strains.

To clone plasmids pDL3181 and pDL3192, the homology arms and array of Chi sites required for PMGR were fused by crossover PCR. Primer pairs MhpA_Chi_F1/ MhpA_Chi_R1 and MhpA_Chi_F2/ MhpA_Chi_R2 were used to create the homology arms for plasmid pDL3181 and primer pairs LacZY_Chi_F1/ LacZY_Chi_R1 and LacZY_Chi_F2/ LacZY_Chi_R2 were used to create the homology arms for plasmid pDL3192. These homology arms were cloned into the PstI and SalI restriction sites of plasmid pTOF24. Successful integration of the Chi arrays by PMGR was screened for by DNA sequencing.

4.7 Illumina Solexa Sequencing of Strain DL3276

Strain DL3276 which harbours all the chromosomal modifications of the superconstruct (Figure 4.1) was sequenced using Illumina Solexa technology alongside its parental strain BW27784. Both sequences were aligned against the *E. coli* K12 sequenced strain MG1655. The purpose of this sequencing was to detect any mutations that potentially arose during the process of strain construction, as well as to confirm the presence of all the precise alterations made by PMGR. The

usefulness of this approach was however limited by both the sequencing method and the bioinformatics analysis that at the time was only established for identifying single nucleotide polymorphisms (SNPs) and insertions/deletions (InDels) of up to and including three base pairs. The reason that this method (paired end reads) can only identify short insertions and deletions is because it sequences the DNA in only short stretches (known as 'reads') of approximately 40 to 50 bp. Other high throughput sequencing methods that utilise longer reads are available (*e.g.* Roche 454, average read length of ~400 bp); however these again may not have been able to pick up the large insertions and deletions created in this strain.

Sequence analysis (Table 4.1) showed that DL3276 possessed 19 individual SNPs and no small insertions or deletions when aligned against MG1655. Fifteen of the identified SNPs were also found in strain BW27784. The four SNPs identified in DL3276 and not BW27784, were known mutations that were introduced during the construction process (inherited from strain DL1777 (Eykelenboom *et al*., 2008)). Two of the SNPs were introduced in order to remove the Chi site present in *lacZ* that would stimulate recombination following cleavage of the palindrome or the I-SceI$_{cs}$ (see section 4.2.2). The others two SNPs are both the *lacI*^{q} mutation and L8 mutation of *lacZ*. *lacI*^{q} is a mutation in the promoter of *lacI* that reduces leaky expression of the *lac* operon by increasing expression of the repressor protein LacI (Muller-Hill *et al*., 1968). However, DL3276 (and all other strains harbouring the superconstruct) is Δ*lacI* making expression from the promoter P$_{lac}$ constitutive. The L8 mutation is a guanine to adenine transition in the binding site of the global activator CRP, the result of which is a reduction in the maximal expression from P$_{lac}$ (Malan and McClure, 1984).

Reference Position	Gene	Reference Base	Total High Quality Bases	Base With Highest Count	Additional Info
363298	*lacZ*	G	47	A	*Chi* K.O.[1, 3]
363301	*lacZ*	G	50	A	*Chi* K.O.[1, 3]
365633	*lacZ-lacI*	C	45	T	*lacZ* L8 [1]
366797	*lacI-mhpR*	G	56	A	$lacI^{q}$ [1]
502653	*ybaL-fsR*	C	48	T	[2]
547694	*ylbE*	A	46	G	[2, 3]
704236	*nagE*	T	34	C	[2, 4]
1335418	*acnA*	A	19	G	[2, 4]
1650355	*intQ*	T	22	C	[2, 4]
2842032	*hycG*	G	48	T	[2, 3]
3108443	*pheV*	C	16	A	[2]
3957957	*ppiC-yifO*	C	53	T	[2]
4091793	*rhaD*	C	30	T	[2, 4]
4159271	*fabR*	G	59	T	[2, 4]
4162146	*btuB*	C	60	G	[2, 4]
4472857	*yjgJ-yjgK*	A	62	G	[2]
4583503	*hsdR*	G	38	A	*hsdR514* [2, 4]
4600532	*yjjP*	C	55	T	[2, 4]
4614692	*yjjI*	G	65	T	[2, 4]

[1]Originated in strain DL1777; [2]Originated in strain BW27784; [3]synonymous mutation; [4]non-synonymous mutation

Table 4.1 Sequence alignment of the DL3276 and MG1655 genomes. Solexa sequencing revealed 19 SNPs that are present in DL3276 but not MG1655. The total number of high quality bases shows the number of reads that identified the SNPs.

4.8 Titration of Endonuclease

Induction of I-SceI in an *E. coli* strain containing an I-SceI$_{cs}$ can result in cell death, even if the strain is recombination proficient and therefore able to repair DSBs. This could be due either to I-SceI having cleaved all of the chromosomes in the cell, making homologous recombination impossible, or the occurrence of continual cycles of DNA cleavage and repair that prevents the cell from exiting the SOS response and dividing. It is therefore desirable to reduce the induced level of I-SceI to a concentration where DSBs are formed, but repaired efficiently. This can be tested for by lowering the concentration of inducer added to the growth medium to a level at which a recombination proficient strain can survive the DSB but a recombination deficient strain (*e.g.* a *recA*$^-$ mutant) cannot.

recA$^-$ derivatives of P$_{BAD}$-*sbcDC* 'superconstruct' strains DL3283 (*lacZ*::pal) and DL3284 (*lacZ*$^+$), and P$_{BAD}$-*I-SceI* 'superconstruct' strains DL3285 (*lacZ*::I-SceI$_{cs}$) and DL3286 (*lacZ*$^+$) were made by P1 transduction (*recA*::Cm^R) and confirmed as being UV-light sensitive. Cultures of DL3283, DL3284, DL3285, and DL3286 along with their *recA*$^-$ derivatives (DL3343, DL3344, DL3345, and DL3346 respectively) were grown overnight in M9-minimal media supplemented with 0.2 % glucose (inducible SbcCD/I-SceI repressed), ampicillin and 100 ng ml^{-1} ATC. Serial dilutions of these cultures were then made and spotted (10 μl) onto M9-minimal agar plates supplemented with ampicillin, ATC, and either 0.2 % glucose (SbcCD/I-SceI repressed) or a range of arabinose concentrations (SbcCD/I-SceI induced).

The results showed that the inviability of the *recA*$^-$ mutant that is associated with induction of SbcCD in a strain harbouring the palindrome in the *lacZ* gene, was not particularly sensitive to the concentration of arabinose used to induce SbcCD

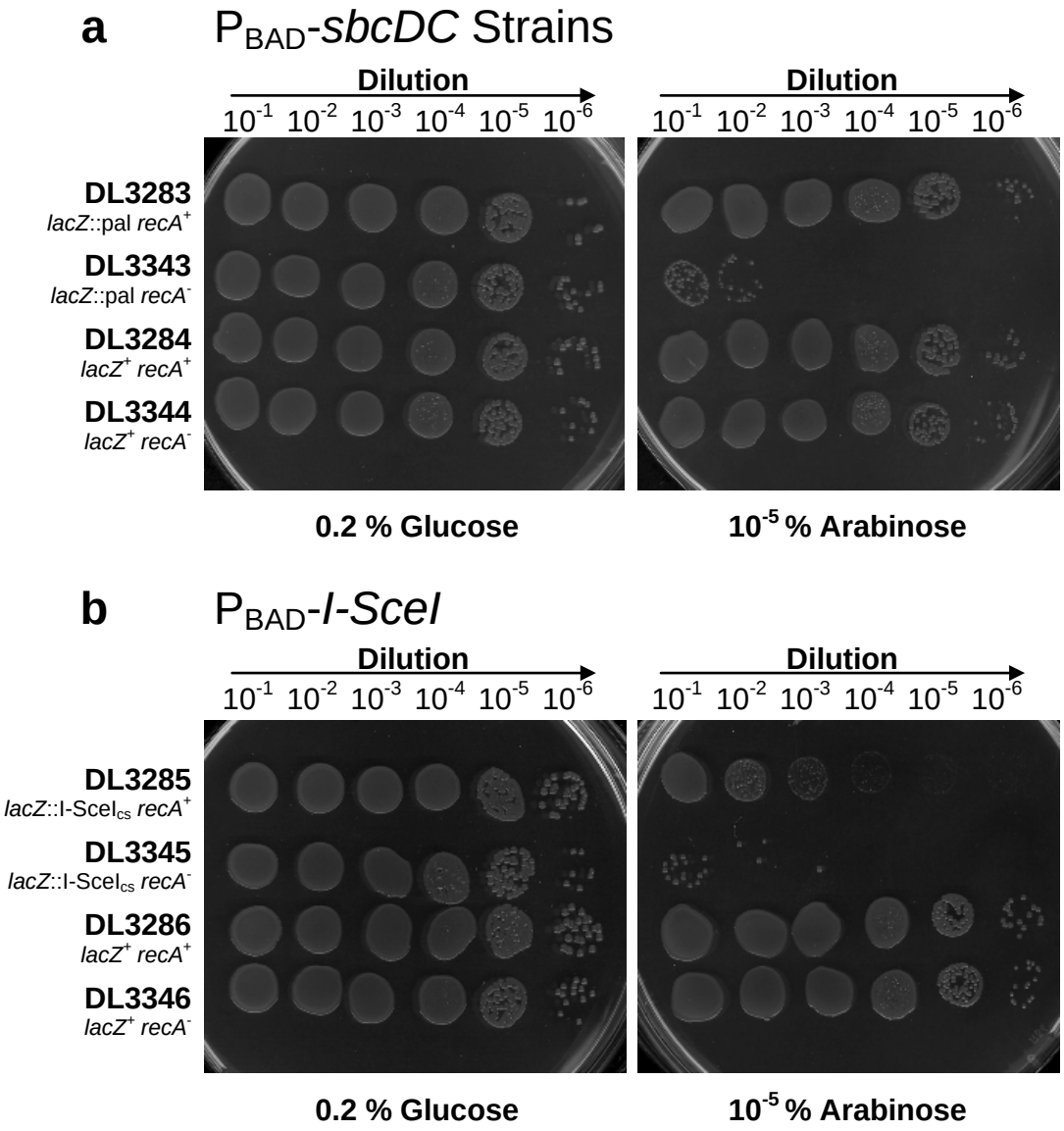

Figure 4.5 DSB induction at low inducer concentrations. Serial dilutions of cultures grown to stationary phase in M9-minimal media supplemented with 0.2 % glucose (inducible SbcCD/I-SceI repressed) were spotted onto M9-minimal agar plates supplemented with either glucose (SbcCD/I-SceI repressed) or arabinose (SbcCD/I-SceI induced). **a**, Viabilities of P$_{BAD}$-*sbcDC* 'superconstruct' strains DL3283 and DL3284 and their *recA*$^-$ derivatives DL3343 and DL3344**.** **b**, Viabilities of P$_{BAD}$-*I-SceI* 'superconstruct' strains DL3285 and DL3286 and their *recA*$^-$ derivatives DL3345 and DL3346.

expression (Figure 4.5a). A strong death phenotype of the *recA*$^-$ strain containing the palindrome (D3343) was observed even at very low arabinose concentrations and no concentration of arabinose was identified that caused either a reduction in the viability of the recombination proficient strain (DL3283), or an intermittent death phenotype in the *recA*$^-$ mutant. However, a minimum concentration of 10^{-6} % arabinose was required to induce death in strain DL3343 (data not shown).

These results differ to that observed for the P_{BAD}-*I-SceI* strains (Figure 4.5b). At high concentrations of arabinose (0.2 %), the viability of recombination proficient strain harbouring the I-SceI_{cs} in the *lacZ* gene (DL3285) was severely reduced (approximately 10^5-fold, Figure 4.6). A minimum concentration of 10^{-5} % arabinose was required to observe a reproducible death phenotype in the *recA*$^-$ strain DL3345. However, this concentration of inducer was also high enough to cause a death phenotype in the recombination proficient parental strain (DL3285). Unlike DL3345 however, this death phenotype did not manifest itself as a clear difference in the highest dilution of the culture in which survivor colonies can be seen. For DL3285, viable cells can still be identified at a dilution factor of 10^{-6}. These survivor colonies are however, very small and clearly different from the colonies formed when the same dilution of the culture is spotted onto a minimal agar plate supplemented with 0.2 % glucose. This suggests that I-SceI may not be killing DL3285 outright but rather hindering its ability to form colonies.

If this hypothesis is true then this phenotype should only be observed when DL3285 is grown in chronic I-SceI induced DSB conditions. To test the effect of transient I-SceI induction, cultures of DL3283, DL3284, DL3285, and DL3286 along with their *recA*$^-$ derivatives DL3343, DL3344, DL3345, and DL3346 were grown to

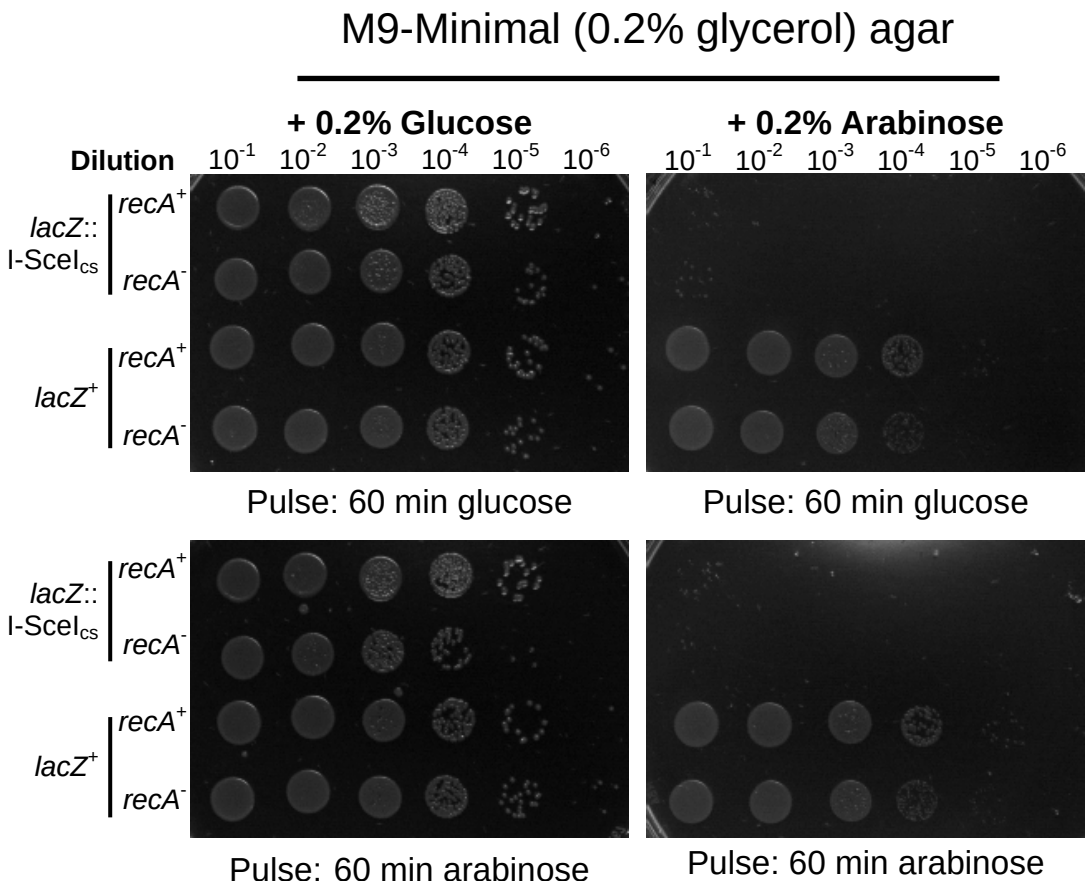

Figure 4.6 Acute vs. chronic I-SceI induction in slow growth conditions. Cultures of the P_{BAD}-*I-SceI* strains DL3285 (*lacZ*::I-SceI$_{cs}$), DL3286 (*lacZ*$^+$), DL3345 (*lacZ*::I-SceI$_{cs}$ *recA*$^-$), and DL3346 (lacZ$^+$ *recA*$^-$) were grown for 60 min in M9-minimal media supplemented with either 0.2% glucose (I-SceI repressed) or 10^{-5} % arabinose (I-SceI induced). Serial dilutions of these cultures were then spotted onto M9-minimal agar plates supplemented with either 0.2% glucose or 0.2 % arabinose.

an OD_{600} of 0.8 in M9-minimal medium supplemented with 0.2 % glucose (I-SceI repressed). Cultures were then split and diluted to an OD_{600} of 0.4 in fresh M9-minimal medium supplemented with either 0.2 % glucose or various concentrations of arabinose (I-SceI induced). After 1 h growth at 37 °C, these cultures were sampled and serial dilutions spotted onto M9-minimal agar plates supplemented with either 0.2 % glucose (I-SceI repressed) or 0.2 % arabinose (I-SceI induced). These plates were left to grow for 2 days at 37 °C and the results are shown in Figure 4.6.

Strains lacking the I-$SceI_{cs}$ in *lacZ* (DL3286 and DL3346) showed no decrease in viability whether I-SceI was induced transiently or chronically confirming that there are no endogenous I-$SceI_{cs}$ in the chromosome. However, both the *recA*$^+$ and *recA*$^-$ strains harbouring the I-$SceI_{cs}$ in *lacZ* (DL3285 and DL3345 respectively) were unable to form colonies on M9-minimal agar plates supplemented with 0.2 % arabinose. In contrast to growth on arabinose supplemented plates, transient I-SceI expression (60 min) did not adversely affect the viability of the *recA*$^+$ strain DL3285, despite causing the death of approximately 90 % of cells (10-fold decrease in viability) in the culture of the *recA*$^-$ derivative strain DL3345. Interestingly, this result was not affected by the concentration of arabinose used to express I-SceI transiently, since similar results were observed for arabinose concentrations ranging from 10^{-5} % to 0.2 % (data not shown).

The fact that a recombination proficient strain can survive in conditions where a recombination mutant cannot suggests that in slow growth conditions, *E. coli* can survive cleavage of the *lacZ* locus by I-SceI as long as it is given time to recover. This is similar to what has been shown for an I-SceI induced DSB in fast growth conditions (Meddows *et al.*, 2004).

4.9 Visualising the Location of the Superconstruct in Cells

4.9.1 Fluorescent Foci Indicate the Location of the *tetO* and *lacO* Arrays

The DNA sequences *tetO* and *lacO* act as binding sites for the proteins TetR and LacI respectively. Therefore, if an array of these operator sites is present in the chromosome it will result in the local concentration of its DNA binding protein. If its DNA binding protein has been fused to a derivative of GFP (*e.g.* TetR-YFP and LacI-CFP) then the location of this local concentration of protein within a cell can be identified with the use of a fluorescence microscope as a fluorescent focus. The cellular location of the superconstruct can therefore be visualised a twin YFP/CFP spot when the array of *tetO* sites (located in *cynX*) is bound by TetR-eYFP and the array of *lacO* sites (located in *mhpC*) is bound by LacI-Cerulean.

To ensure that the YFP and CFP foci did indeed represent the location of the superconstruct and were not artefacts of microscopy, a strain harbouring the *tetO* and *lacO* array and expressing TetR-eYFP and LacI-Cerulean (DL3283) was compared to an isogenic strain harbouring the two operator arrays but not expressing TetR-eYFP or LacI-Cerulean (DL3276) and a strain lacking operator arrays but expressing TetR-eYFP and LacI-Cerulean (DL2006 + pDL3196). The three strains were grown overnight in M9-minimal medium supplemented with 0.2 % glucose (SbcCD repressed) and 100 ng ml^{-1} of ATC prior to sampling for microscopy. Cells were imaged at a resolution of 0.129 μm per pixel and multiple *z*-sections (± 800 nm, 9 images at a 200 nm interval) of both CFP and YFP signals were captured. Post-acquisition, the stacks of *z*-planes were deconvolved using the software Autodeblur

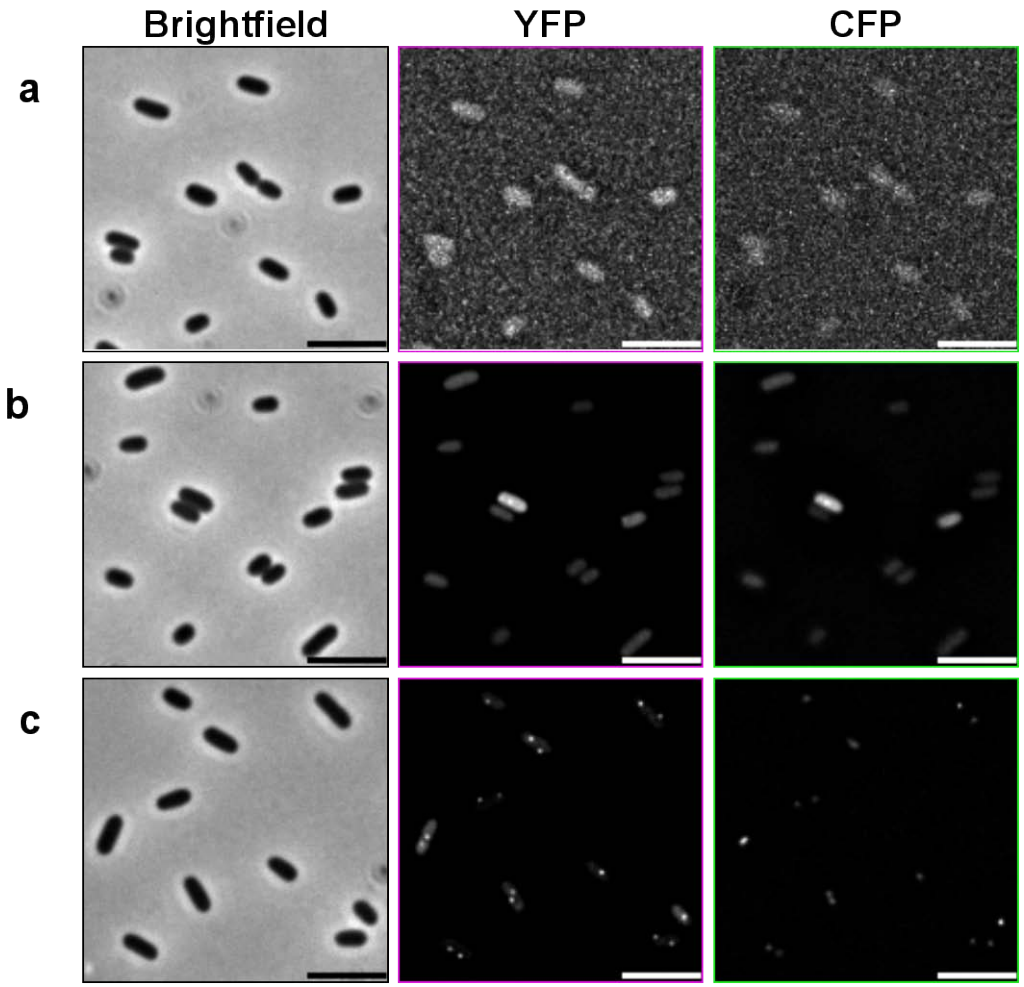

Figure 4.7 Identifying *tetO* and *lacO* with TetR-eYFP and LacI-Cerulean. YFP and CFP fluorescence emitted from stationary phase cultures of *E. coli* cells **a**, harbouring the *tetO* and *lacO* array but not expressing TetR-eYFP or LacI-Cerulean (DL3276); **b**, lacking the *tetO* and *lacO* arrays but expressing TetR-eYFP and LacI-Cerulean (DL2006 + pDL3196); **c**, harbouring the *tetO* and *lacO* arrays and expressing TetR-eYFP and LacI-Cerulean (DL3283). Images were acquired at a resolution of 0.129 μm per pixel; calibration bar shows 5 μm.

and Autovisualize v9.32 and subsequently combined to give a maximum projection image using MetaMorph 6.3r2. Representative images are shown in Figure 4.7. The results confirmed that bright YFP and CFP fluorescent foci are only detectable in cells that harbour both a *tetO* and *lacO* array and express TetR-eYFP and LacI-Cerulean. YFP and CFP fluorescent foci therefore provide an indirect method of observing the cellular positioning of the *tetO* and *lacO* arrays.

4.9.2 Proximity of the *tetO* and *lacO* Arrays

Surprisingly, despite there being only 10.6 kb of intervening DNA sequence between the two operator arrays, their bound TetR-eYFP and LacI-Cerulean proteins tend not to entirely co-localise as is clearly shown by high resolution (63.5 nm per pixel) images of a mid-exponential growth phase culture of strain DL3283 (Figure 4.8). It is possible that this is an artefact of microscopy because the YFP and CFP images are acquired sequentially and so the location of the *tetO* and *lacO* arrays may simply have moved slightly between image acquisitions. Alternatively, it is also possible that the two operator arrays are separated within cells to an extent that their locations can be resolved.

It was therefore sought out to quantify the distance between the *tetO* and *lacO* array in cells and to test whether or not this distance was affected by either SbcCD expression, the presence of a 246 bp interrupted DNA palindrome, or both (*i.e.* induction of a DSB in the intervening DNA). P_{BAD}-*sbcDC* strains expressing TetR-eYFP and LacI-Cerulean and harbouring a *tetO* and *lacO* array flanking the *lacZ* gene into which either a 246 bp palindrome was integrated (DL3283) or not (DL3284), were first grown at 37 °C to an OD_{600} of 1.0 in M9-minimal medium

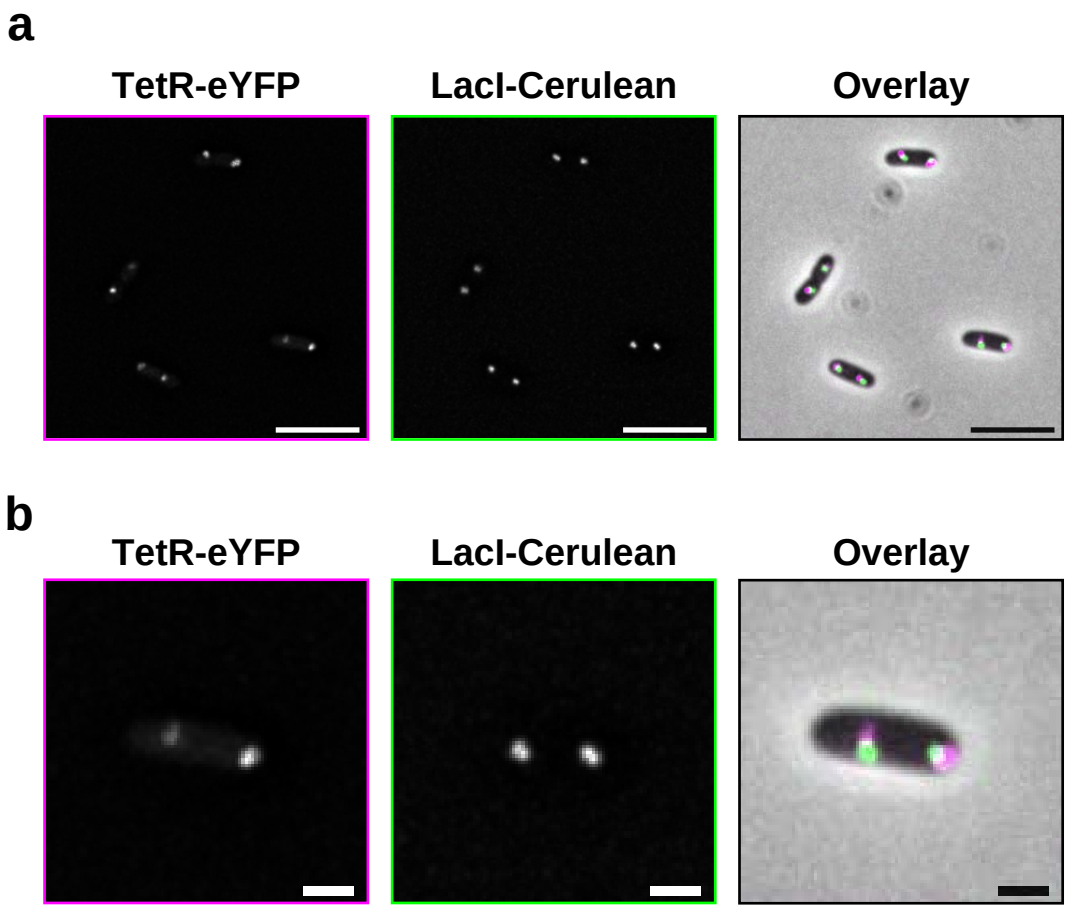

Figure 4.8 High resolution imaging of the superconstruct in cells. Representative image of a strain harbouring the supersconstruct and expressing TetR-eYFP and LacI-Cerulean from pDL3196 (DL3283). Cells were cultured in M9-minimal media supplemented with 0.2 % glucose (SbcCD repressed) and 100 ng ml^{-1} ATC. Images were acquired at a resolution of 64.5 nm per pixel; CFP is pseudocoloured green and YFP magenta, overlapping signal appears white. **a**, calibration bar shows 5 µm. **b**, increased magnification of a cell shown in **a**; calibration bar shows 1 µm.

supplemented with 100 ng ml^{-1} ATC and 0.2 % glucose (SbcCD repressed). These cultures were then diluted to an OD_{600} of 0.2 in M9-minimal medium supplemented with 100 ng ml^{-1} ATC and either 0.2 % glucose (SbcCD repressed) or 0.001 % arabinose (SbcCD induced), and left to grow for 1 h at 37 °C prior to sampling for microscopy.

Cells were imaged at a resolution of 0.129 μm per pixel and multiple *z*-sections (± 800 nm, 9 images at a 200 nm interval) of both CFP and YFP signals were captured. Post-acquisition, the stacks of *z*-planes were deconvolved using the software Autodeblur and Autovisualize v9.32 and subsequently combined to give a maximum projection image using MetaMorph 6.3r2. The intensity center measurement of MetaMorph was used to identify the co-ordinates of the centroids of the YFP and CFP foci (section 2.4.5) in order to calculate the distance between the two. 250 YFP and CFP foci were counted for each of the four samples, representing at least 100 individual cells.

The results showed the median distance between the centroids of neighbouring YFP and CFP was approximately 210 nm (Figure 4.9). No significant difference was found between the median distance of neighbouring YFP and CFP foci in strains DL3283 (*lacZ*::pal) and DL3284 ($lacZ^+$) whether or not SbcCD was induced (Kruskal-Wallis test, $p = 0.073$). The data for the four samples were negatively skewed, with more foci located >500 nm apart observed in the DSB induced condition (DL3283 $SbcCD^+$) than the three controls (Figure 4.9a). This accounts for the large difference in the calculated means of the four samples (Figure 4.9b).

a

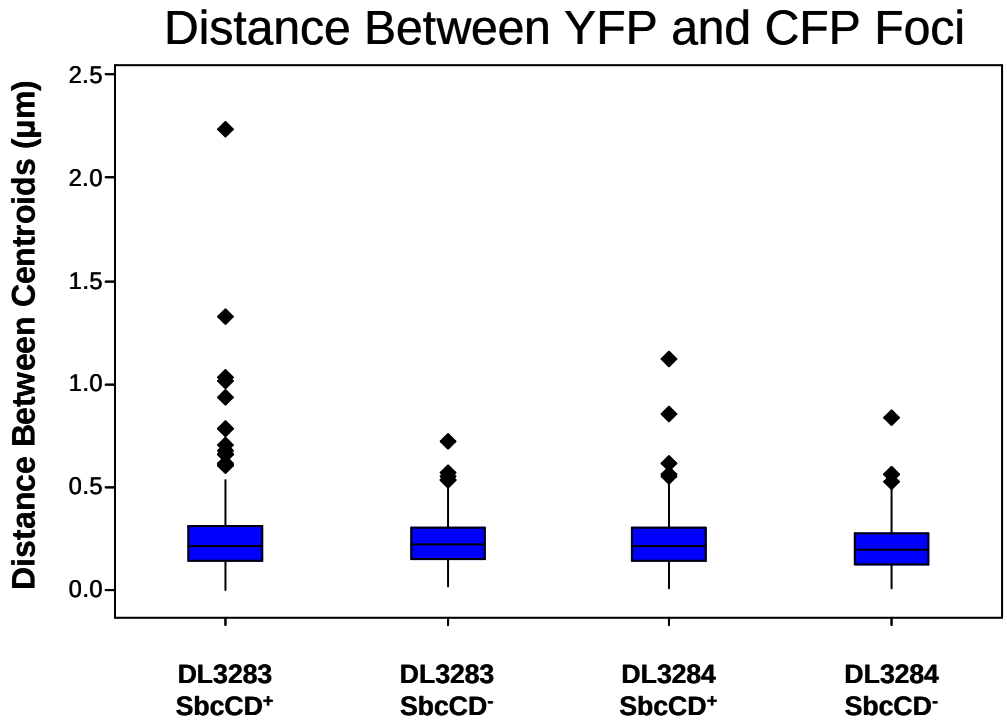

b

Strain	*n*	Mean (nm)	Median (nm)	Q1 (nm)	Q3 (nm)	SD
DL3283 SbcCD$^+$	250	262	216	142	314	216
DL3283 SbcCD$^-$	250	237	225	155	302	115
DL3284 SbcCD$^+$	250	236	212	138	302	139
DL3284 SbcCD$^-$	250	214	199	123	280	116

Q1 and Q3 are the first and third quartiles respectively

Figure 4.9 Distance between *tetO* and *lacO* arrays. P_{BAD}-*sbcDC* strains expressing TetR-eYFP and LacI-Cerulean and harbouring a *tetO* array in *cynX*, a *lacO* array in *mhpC* and either a 246 bp palindrome in *lacZ* (DL3283) or not (DL3284) were cultured in M9-minimal media supplemented with either 0.2 % glucose (SbcCD$^-$) or 0.001 % arabinose (SbcCD$^+$). Cells were imaged at a resolution of 129 nm per pixel and the distance between the centroids of YFP and CFP foci measured. **a**, distribution of distances between neighbouring YFP and CFP foci. **b**, descriptive statistics of the distribution of distances between neighbouring YFP and CFP foci.

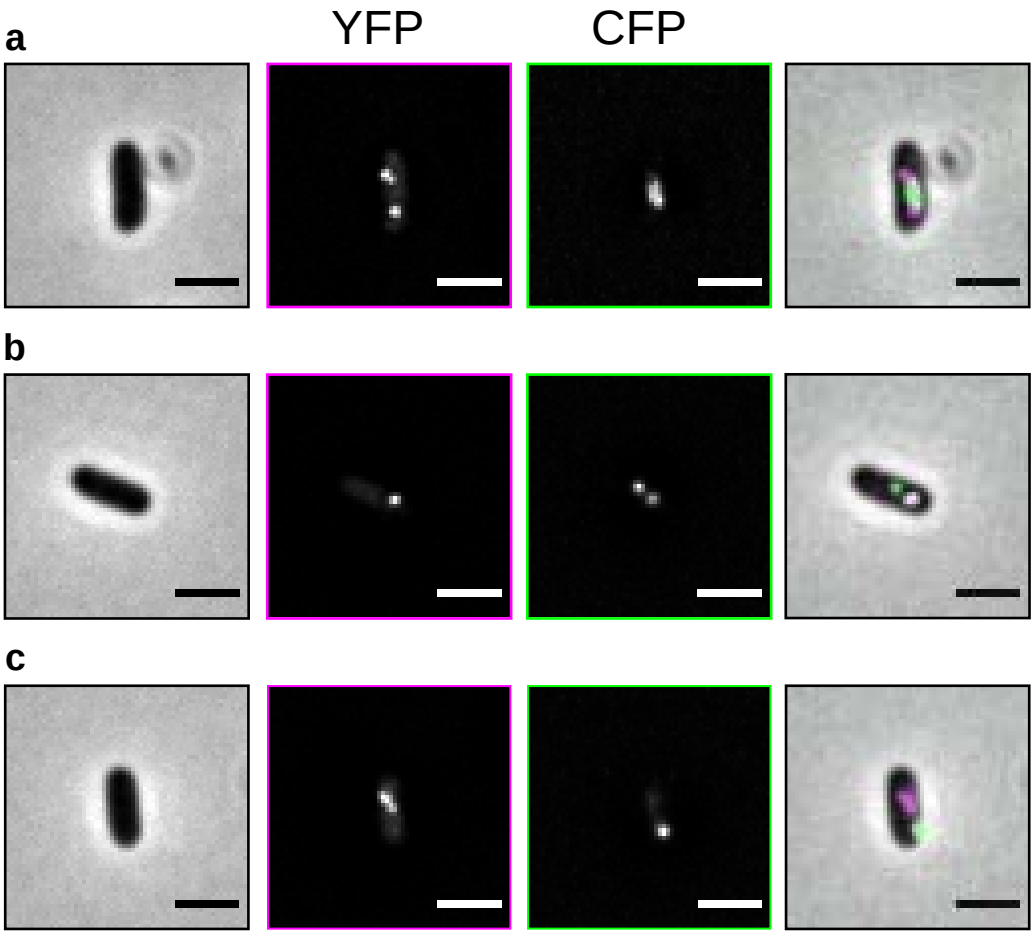

Figure 4.10 Cells with distant *tetO* and *lacO* arrays. P_{BAD}-*sbcDC* strain DL3283 which harbours an array of *tetO* sites in *cynX*, an array of *lacO* sites in *mhpC* and a 246 bp palindrome in *lacZ* was grown in M9-minimal medium supplemented with 0.001 % arabinose ($SbcCD^{+}$). The majority of cells with > 500 nm between neighbouring YFP and CFP foci appeared to be in the process of segregating the *lacO* array (**a**). However, some cells had an isolated YFP (or CFP) focus as well as an overlapping twin YFP/CFP spot (**b**), whereas others showed no co-localisation between their YFP and CFP foci at all (**c**). YFP is pseudocoloured magenta and CFP green, overlapping YFP and CFP foci appear white; calibration bar shows 2 μm.

The majority of cells with >500 nm between YFP and CFP centroids had two YFP foci flanking a large CFP focus (Figure 4.10a). These may represent cells in the process of segregating a recently replicated (origin distal) *lacO* array and were found in all of the four samples. The calculated distance between these centroids may therefore be larger than the real distance because the CFP focus was treated as a single object when it may in fact represent two overlapping CFP foci. Examples of other cell types with foci located > 500 nm apart are shown in Figure 4.10.

4.10 Construction of a Functional TetR-mCherry Fusion Protein

As well as providing a tool for investigating the fate of dsDNA ends following an induced DSB, the superconstruct could be used to investigate the dynamics of repair proteins at the site of a DSB. This could be achieved by expressing fluorescent fusions of the repair proteins as well as TetR-eYFP and LacI-Cerulean. In order to clearly distinguish the protein of interest and the two operator arrays the three proteins must be fused to different fluorescent proteins with limited, or preferably no, overlapping excitation and emission spectra (Shaner *et al.*, 2005). Therefore, if the two operator arrays are to be identified using TetR-eYFP and LacI-Cerulean fluorescent fusion proteins, the protein of interest would have to be fused to a derivative of red fluorescent protein (RFP). However, this is less than ideal because many proteins of interest have already been successfully fused to either GFP or YFP, *e.g.* SbcC-GFP (Darmon *et al.*, 2007), RecA-GFP (Renzette *et al.*, 2005), GFP-PriA (Lecointe *et al.*, 2007) and SSB-YFP (Reyes-Lamothe *et al.*, 2008).

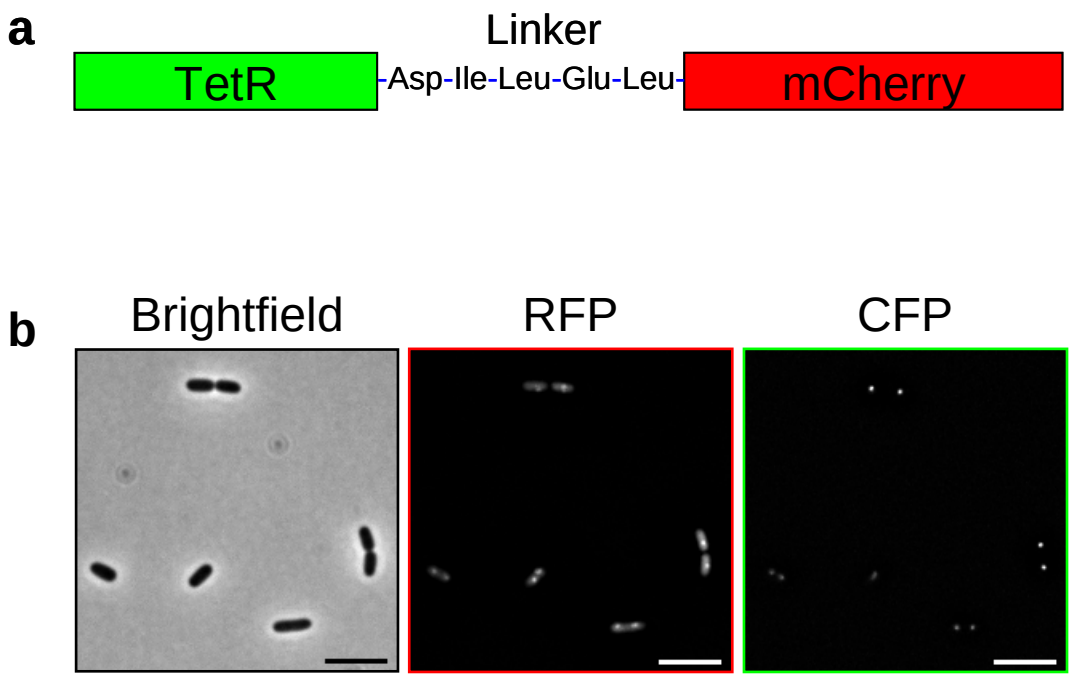

Figure 4.11 TetR-mCherry. *tetR* was fused in-frame to the red fluorescent protein derivative *mcherry* along with a 5 residue linker (**a**) and cloned into plasmid pDL3195 resulting in the operon P_{ftsKi}-*lacI-cerulean,tetR-mcherry*. **b**, representative images of a strain harbouring a *tetO* and *lacO* array and expressing LacI-Cerulean and TetR-mCherry (DL4162). Shown are maximum projections of deconvolved (for RFP and CFP only) z stacks. Images were acquired at a resolution of 0.129 µm per pixel, calibration bars show 5 µm.

It was therefore desirable to fuse TetR to an RFP protein in order to allow the two operator arrays to be identified by TetR-RFP and LacI-CFP in a cell that expresses either a YFP or GFP fusion to the protein of interest. As with GFPs, a variety of RFP derivatives are available (Shaner *et al.*, 2008). For the TetR-RFP fusion, the RFP derivative mCherry (Shaner *et al.*, 2004) was decided upon due to its brightness, photostability and availability. To create a TetR-mCherry fusion, *tetR* was first amplified by PCR from plasmid pDL3196 using primers TetR-mCherryA_F1 and

TetR-mCherryA_R1. Next, *mcherry* was amplified by PCR from plasmid pRSETB-mCherry using primers TetR-mCherryA_F2 and TetR-mCherry_R2. Finally, the two PCR products were fused by crossover PCR using primers TetR-mCherryA_F1 and TetR-mCherryA_R2 resulting in *mcherry* being fused in-frame to *tetR* along with a 15 bp spacer. Translation of this 15 bp spacer sequence results in a five amino acid linker (D-I-L-E-L) between TetR and mCherry, Figure 4.11a. This is the same linker sequence that was previously used by Ivy Lau and collaborators to create the TetR-eYFP fusion used elsewhere in this study (Lau *et al.*, 2003). The *tetR-mCherry* PCR fragment was then digested with XbaI and cloned into the XbaI restriction site of pDL3195, resulting in plasmid pDL4161 with the operon P_{ftsKi}-*lacI-cerulean,tetR-mcherry*. In order to test whether or not TetR-mCherry was functional, strain DL3277 which harbours the superconstruct was transformed with pDL4161 to give strain DL4162.

DL4162 was grown to an OD_{600} of ~ 0.2 in M9-minimal medium supplemented with 0.2 % glucose (SbcCD repressed) and 20 ng ml^{-1} of ATC prior to sampling for microscopy. 20 ng ml^{-1} of ATC was the minimum concentration of ATC that was tested and found to prevent replication blockage at the *tetO* array located in the *cynX* gene of cells expressing TetR-eYFP (see section 4.5.3). Images were acquired at a resolution of 0.129 μm per pixel and multiple *z*-sections (± 800 nm, 9 images at a 200 nm interval) of both RFP and CFP signals were captured. RFP images were acquired using an exposure time of 700 ms and CFP images with an exposure time of 500 ms. The stacks of *z*-planes were deconvolved using the software Autodeblur and Autovisualize v9.32 and subsequently combined to give a

maximum projection image using MetaMorph 6.3r2. Representative images are shown in Figure 4.11b.

Although a higher level of cellular background fluorescence was observed when imaging TetR-mCherry as compared to TetR-eYFP clear foci were obtainable (Figure 4.10). RFP foci were not observed in a strain that harboured the *tetO* array in *cynX* but did not express TetR-mCherry (DL3277) or in a strain that expressed TetR-mCherry from pDL4161 but lacked a *tetO* array (DL2006), data not shown. Although this fusion protein should provide a useful tool for the study of protein dynamics at the site of a DSB, it could potentially be improved by altering the linker or by fusing TetR to a brighter, more photostable RFP such as TagRFP-T (Shaner *et al.*, 2008)

4.11 Conclusions

A construct was designed and built into the chromosome of *E. coli* that would allow the dynamics of DNA double-strand break repair to be investigated both *in vivo* and in real time by combining a method of inducing a site-specific DSB, with a system for visualising the two dsDNA ends of that break. To visualise the two ends of the DSB independently by fluorescence microscopy, an array of *tetO* sites was integrated upstream and an array of *lacO* sites integrated downstream of a unique cleavage site in the *lacZ* gene of a strain with an arabinose inducible endonuclease. The array of *tetO* sites can be visualised by fluorescence microscopy upon the binding of a TetR-YFP fusion protein and the array of *lacO* sites upon the binding of a LacI-CFP fusion protein.

In order to improve imaging of the *lacO* array in this study, the CFP fused to LacI was mutated to a bright CFP variant (Cerulean) and the endogenous *lacI* gene deleted to prevent competitive binding. Binding of the fluorescent repressor proteins was shown not to disrupt DNA replication when cells were cultured in the presence of 100 ng ml^{-1} ATC. Finally, to prevent the operator arrays from being resected by RecBCD following cleavage of *lacZ* by the inducible endonuclease, an array of three Chi sites was integrated on both sides of *lacZ* between the cleavage site and the operator array.

Two complementary systems of inducing a site-specific DSB in the *lacZ* gene were established for this study. The first system required the integration of a 246 bp DNA palindrome in the *lacZ* gene of a strain that had the *sbcDC* operon placed under the control of the arabinose inducible promoter P_{BAD}. SbcCD cleaves a DNA hairpin formed by the palindrome on the lagging strand template during replication (Eykelenboom *et al*., 2008). The second system involved creating a chromosomal I-SceI construct under the control of the arabinose inducible promoter P_{BAD} as well as insertion of a unique I-SceI cleavage site in the *lacZ* gene. Both systems were checked genetically by comparing the sensitivities of recombination proficient and recombination deficient (*recA*$^-$) stains to induction of the DSB and concluded to be functional.

Since *E. coli* is a haploid organism, an integrated unique I-$SceI_{cs}$ will be present on all sister chromosomes, raising the possibility that all chromosomes will be cleaved following I-SceI induction and making repair by homologous recombination impossible. In an attempt to promote the survival of a recombination proficient strain harbouring a unique I-$SceI_{cs}$ following I-SceI induction, the

concentration of inducer (arabinose) was titrated to the lowest level where significant death of a recombination deficient (*recA*$^-$) was still detectable in minimal growth medium (10^{-5} % arabinose). However, this concentration of inducer was still high enough to cause a substantial defect in the colony formation ability of the recombination proficient strain when grown in chronic I-SceI DSB induced conditions. In contrast, 60 min of growth in I-SceI induced conditions had no detectable effect on the viability of the recombination proficient strain in minimal growth medium while causing at least an approximate 10-fold reduction in the viability of a *recA*$^-$ strain. Therefore, unless cleavage of the chromosome by I-SceI is more frequent in a *recA*$^-$ strain, this result implies that approximately 90 % of the recombination proficient cells had suffered at least one chromosomal DSB.

The genomes of strains DL3276 and BW27784 were sequenced using Solexa sequencing technology in order to screen DL3276 for all the desired chromosomal alterations as well as any mutations that potentially arose during the numerous stages of strain construction. This identified 15 SNPs in BW27784 that are not found in the wild-type *E. coli* K-12 sequenced strain MG1655. Four of these SNPs were located in intergenic regions and of the other 11 SNPs, only two were synonymous mutations. The 11 non-synonymous mutations included a premature stop codon in the *hsdR* gene (*hsdR514*) and a mutation in the *rhaD* gene that may have been introduced during the construction of BW27784 that included the creation of the Δ(*rhaBAD*)568 mutation (Khlebnikov *et al.*, 2001). It is not known what effect the other mutations have on the genes in which they are located. This sequencing also identified 4 SNPs present in DL3276 but not BW27784 or MG1655. These are from the transduction of the *lacI*^{q} allele and the *lacZ*(L8)$_\chi$- allele from strain DL1777 that

was used to make the strain *lacZ*$^{+}$ in order to integrate the 246 bp interrupted palindrome into the *lacZ* gene by PMGR. Although a useful technique, a combination of short read lengths and the bioinformatics analysis used meant that only insertions and deletions of up to 4 bp could be identified. As a result, this sequencing failed to identify the large insertions and deletions used to create strain DL3276.

The fluorescence microscopy used to image the TetR-eYFP and LacI-Cerulean was optimised and YFP and CFP foci shown only to form in cells expressing the fluorescent repressors and the two operator arrays. The imaged YFP and CFP foci therefore provide a robust method of identifying the position of the *tetO* and *lacO* arrays within individual cells. Surprisingly, despite being located only ~11 kb apart at their closest point (~30 kb apart at their most distant) the YFP and CFP foci representing a neighbouring *tetO* and *lacO* array were often only partially co-localised, with their centroids located on average ~210 nm apart. Since centroid analysis is limited by the resolution at which the images were acquired, this experiment could be improved by acquiring images at a resolution of 64.5 nm per pixel rather than 129 nm per pixel.

The average distance between neighbouring YFP and CFP foci was found not to differ when cells were grown in conditions where the intervening sequence was subject to an induced DSB. However, more in depth analyses would be required to ascertain whether or not a separation of broken DNA ends occurs following a two-ended DSB. In order to repair a DSB, a RecA nucleoprotein filament must search for homologous sequence to act as a template for homologous recombination. This process is assumed to be a passive process that is mediated by diffusion of the ends

of the DSB throughout the cell. If there is no change in the proximity of the *tetO* and *lacO* array then it would follow that either the two ends of the DSB are tethered and/or that the ends are not free to diffuse within the cell. It has been shown that DNA ends are tethered in *S. cerevisiae* by the Rad50/Mre11/Xrs2 complex following an I-SceI induced DSB (Lobachev *et al.*, 2004).

Finally, the gene encoding the RFP derivative mCherry was fused to *tetR* and cloned into an operon on plasmid pDL3195 that expresses LacI-CFP from the weak constitutive promoter P_{ftsKi}. The resulting TetR-mCherry fusion protein was shown to form fluorescent foci in cells harbouring a *tetO* array in the *cynX* gene and therefore provides an alternative to TetR-eYFP for imaging a *tetO* array. Since their excitation and emission spectra are distinguishable, TetR-mCherry can also be used in conjunction with LacI-Cerulean for the dual labelling of *tetO* and *lacO* arrays. The use of TetR-mCherry in the place of TetR-eYFP for the imaging of a *tetO* array would be of particular use when combining the fluorescence microscopy analysis of a GFP (or YFP) fused protein of interest with the dual labelling of a *tetO* and *lacO* array.

Chapter 5

Non-Random Segregation of Sister Chromosomes in *Escherichia coli*

5.1 Introduction

Although details of the mechanism of chromosome segregation in *E. coli* remain elusive, recent advancements in fluorescence microscopy have led to a number of interesting observations. For example, it was shown that when cells are cultured under slow growth conditions, not only is the genetic map of the *E. coli* chromosome recapitulated within the cell (Nielsen *et al.*, 2006b; Wang *et al.*, 2006), but chromosome segregation is progressive and results in translational symmetry of the left and right chromosome arms (Nielsen *et al.*, 2006a; Wang *et al.*, 2006). Notably, due to the 5' to 3' polarity of DNA synthesis, each sister chromosome possesses a replichore (chromosome arm) that was replicated by leading strand synthesis and a replichore that was replicated by lagging strand synthesis. Therefore, in order for there to be translational symmetry of the left and right replichores, there must be mirror symmetry in the segregation of the leading and lagging strands of the two replication forks (Figure 5.1).

The observation that chromosome segregation leads to translational symmetry of the chromosome arms can be accounted for by three different situations (White *et al.*, 2008). First the two leading strands of replication could always segregate to opposite cell poles, with the two lagging strands flanking mid-cell. Secondly, the opposite could be true and the two lagging strands of replication could always segregate to the cell poles and the leading strands to mid-cell. Lastly, a random combination of these two patterns could be found within a population of cells.

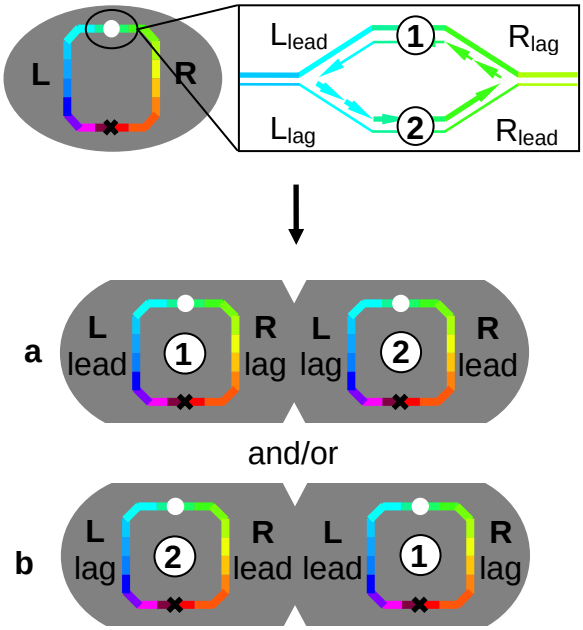

Figure 5.1 Chromosome segregation in *E. coli*. In *E. coli*, chromosome segregation results in translational symmetry of the left and right replichores (L and R respectively) of the sister chromosomes. Due to the polarity of DNA synthesis, the translational symmetry of the replichores means that there must be mirror symmetry in the leading (lead) and lagging (lag) strands of the two replication forks. Translational symmetry of replichores within a cell could be accounted for by either **a**, segregation of the lagging strands of replication to mid-cell and the leading strands of replication to the cell poles or **b**, segregation of the leading strands of replication to mid-cell and the lagging strands of replication to the cell poles. Figure taken from (White *et al.*, 2008).

The hypothesis that sister chromosomes are not segregated randomly in *E. coli* has been tested previously. In 1973, Pierucci and Zuchowski used tritiated thymidine to pulse label the chromosomes of *E. coli* B/r cells and inferred their pattern of segregation after 2 – 4 rounds of replication and cell division by incubating the cells on Methocel film, which caused them to grow in chains that allowed their lineage to be established. The distribution of radioactive cells within the chains was

not consistent with the radioactively labelled DNA strands being segregated randomly and the authors proposed that one of two daughter strands was segregated non-randomly as a result of being fixed to the cell membrane (Pierucci and Zuchowski, 1973). This work was furthered in 1978 by Cooper and collaborators who, by binding the tritiated thymidine labelled cells to a nitrocellulose membrane and eluting the newly divided cells, showed that the observed pattern of non-random chromosome segregation was not caused by a permanent attachment of one of the parental DNA strands to a cell pole (Cooper *et al.*, 1978). Finally, in 1984 5-Bromodeoxyuridine (BrdU) labelling of the chromosomal DNA was used by Canovas and collaborators in a detailed analysis of the pattern of chromosome segregation following two rounds of replication in *E. coli*. In agreement with the afore mentioned experiments, this study also showed that chromosome segregation is essentially, but not entirely, non-random. In addition, this study also revealed a significant bias (60 – 80%) towards the segregation of the parental DNA strands towards the opposite cell poles (Canovas *et al.*, 1984).

Although these investigations provide strong evidence to support the hypothesis that chromosome segregation in *E. coli* is not random, their work was controversial as several other authors had reported that chromosome segregation was entirely random (Chai and Lark, 1970; Lin *et al.*, 1971; Ryter *et al.*, 1968), a discrepancy that was at the time, put down to technical differences in their approaches. Also, due to the approach of pulse labelling the chromosomes, the results of these studies does not distinguish between the two models of non-random segregation where either the leading or lagging strand replicated DNA strands segregate to the cell poles. This chapter describes how cleavage of a DNA

palindrome by the hairpin endonuclease SbcCD was combined with fluorescence microscopy to further our understanding of chromosome segregation in *E. coli* by distinguishing sister chromosomes on the basis of whether they replicated the region surrounding the palindrome by leading or lagging strand DNA synthesis.

5.2 A System for Distinguishing Sister Chromosomes

In order to distinguish between the different models of leading and lagging strand replicated DNA segregation (Figure 5.1), a system was created that would permit the specific visualisation of a locus on the right replichore (*lacZ*) that was replicated by leading strand DNA synthesis (R_{lead}). This involved the construction of a strain that had the hairpin endonuclease SbcCD placed under control of the arabinose inducible promoter P_{BAD}, in addition to a 246 bp interrupted DNA palindrome that was integrated into the *lacZ* gene of the chromosome and flanked upstream by an array of *tetO* sites and downstream by an array of *lacO* sites (strain DL3276, see Chapter 4 for construction and characterisation). The *tetO* and *lacO* arrays are visualised by fluorescence microscopy upon the binding of TetR-eYFP and LacI-Cerulean respectively. This allows the cellular location of *lacZ* to be identified as a twin YFP/CFP focus and demonstrates the presence of DNA on both sides of the palindrome.

In the absence of SbcCD, the location of all copies of the palindrome can be followed as it is replicated and segregated during the cell cycle. Induction of SbcCD however, leads to the specific cleavage of the sister chromosome that replicated the palindrome in *lacZ* by lagging strand synthesis (Eykelenboom *et al.*, 2008). This is because SbcCD does not target the sequence of the palindrome, but rather a DNA

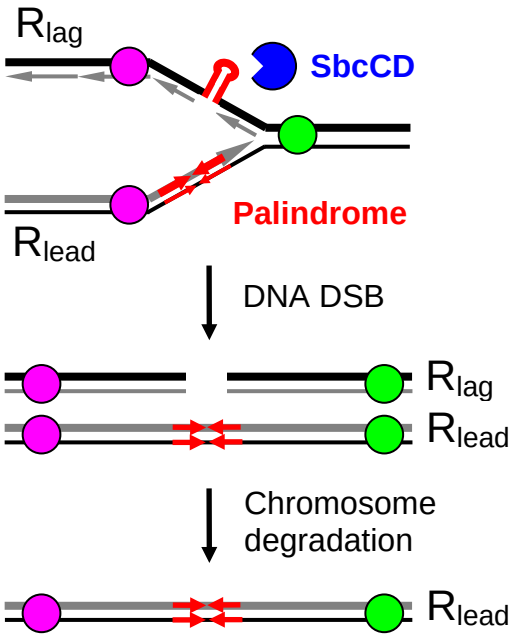

Figure 5.2 Distinguishing the leading and lagging strand of replication. SbcCD cleaves a DNA hairpin formed by a 246 bp interrupted DNA palindrome on the lagging strand template of replication. Induction of SbcCD in a *recA*$^-$ mutant harbouring the palindrome in the *lacZ* gene (situated on the right replichore, R), results in the selective degradation of the sister chromosome that replicated the right replichore by lagging strand synthesis (R_{lag}). Only the chromosome that replicated *lacZ* by leading strand synthesis (R_{lead}) remains intact. *lacZ* is flanked by a TetR-eYFP bound *tetO* array (magenta circle) and a LacI-Cerulean bound *lacO* array (green circle) allowing for visualisation of the location of this locus by fluorescence microscopy. Figure adapted from (White *et al.*, 2008).

hairpin that forms on the lagging strand template (Pinder *et al.*, 1998) because of the interrupted nature of DNA synthesis on this strand. In a recombination proficient cell, cleavage of the palindrome is followed by repair of the broken DNA by the RecBCD pathway of homologous recombination (Eykelenboom *et al.*, 2008). By making these cells *recA*$^-$ however, repair will be inhibited (Krasin and Hutchinson, 1977) and the broken chromosome will become degraded, primarily by the

exonuclease activity of the RecBCD complex (Zahradka *et al.*, 2009). Since the uncleaved chromosome will remain intact (Skarstad and Boye, 1993), the remaining twin YFP/CFP focus will represent the copy of *lacZ* that was replicated by leading strand synthesis, Figure 5.2.

5.3 Operator Arrays are Degraded Following DSB Induction

The prediction that cleavage of the palindrome by SbcCD will result in the selective degradation of one of a pair of sister chromosomes in a *recA*$^-$ mutant was tested. Cultures of *recA*$^-$ P_{BAD}-*sbcDC* strains either harbouring the 246 bp interrupted DNA palindrome in *lacZ* (DL3343) or not (DL3344) were first grown in M9-minimal medium supplemented with 100 ng ml^{-1} ATC and 0.2 % glucose to an OD_{600} of 1.0. These cultures were diluted to an OD_{600} of 0.2 in M9-minimal medium supplemented with 100 ng ml^{-1} ATC and either 0.001 % arabinose (SbcCD$^+$) or 0.2 % glucose (SbcCD$^-$) and incubated at 37 °C with agitation. To produce a timecourse, two independent cultures of strain DL3343 grown in SbcCD$^+$ conditions were sampled at 30 min intervals following SbcCD induction (growth in 0.001 % arabinose) for image acquisition. A third independent culture of strain DL3343 grown in SbcCD$^+$ conditions was sampled only after 90 min of SbcCD induction. All other cultures were sampled only after 90 min of growth in the indicated growth medium. Cells were imaged at a resolution of 0.129 μm per pixel and multiple *z*-sections (± 800 nm, 9 images at a 200 nm interval) of both CFP and YFP signals were captured. The stacks of *z*-planes were deconvolved using the software Autodeblur and Autovisualize v9.32 and subsequently combined to give a maximum projection

image using MetaMorph 6.3r2. Cell lengths were measured using the 'fiber length' measurement of the image analysis software MetaMorph v6.3r2 and the number of visible YFP and CFP foci were counted for each of the measured cells. At least 500 cells were analysed for each of the independent cultures to obtain sample averages and each experiment was repeated three times.

The majority of cell either had 0, 1, or 2 visible twin YFP/CFP foci, with the rest either having odd numbers of YFP and CFP foci or more than 2 pairs of twin YFP/CFP foci. The results of the experiment showed that induction of SbcCD in the strain harbouring the 246 bp palindrome (DL3343 arabinose) resulted in a sharp increase in the number of cells in the population with a single twin YFP/CFP focus. This was strongly associated with a reduction in the number of cells in the population with two visible twin YFP/CFP foci and was not observed under control conditions (Figure 5.3). These results therefore indicate that as predicted, SbcCD only cleaves one of a pair of replicating chromosomes and that cleavage of the palindrome in the *recA*$^{-}$ mutant results in the degradation of flanking DNA. However, a slight increase in the number of cells with no fluorescent foci was observed following SbcCD induction. These could either represent cells in which SbcCD has cleaved both sister chromosomes, or cells in which SbcCD has cleaved one sister chromosome and a spontaneous DSB has occurred on the second sister chromosome. Examples of cell types observed following SbcCD induction in strain DL3343 are shown in Figure 5.4.

a

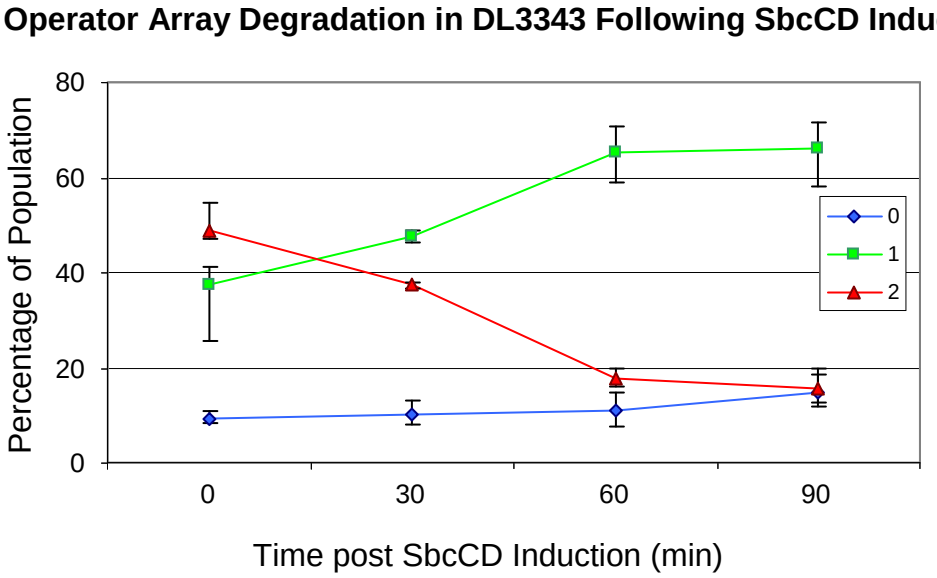

b

Strain	Genotype	SbcCD$^-$	SbcCD$^+$
DL3344	*lacZ*$^+$	27.6% ± 7.42	23.1% ± 3.02
DL3343	*lacZ*::pal	28.9% ± 6.46	64.3% ± 3.99

Errors indicate standard error of the mean

Figure 5.3 Operator array degradation following cleavage of the palindrome. **a**, the number of visibly segregated copies of *lacZ* (0, 1, 2) in *recA*$^-$ SbcCD inducible cells harbouring a 246 bp DNA palindrome in the *lacZ* gene (DL3343) as a function of time of SbcCD induction. Error bars indicate range, *n* = 2. **b**, The percentage of *recA*$^-$ SbcCD inducible cells either harbouring a 246 bp DNA palindrome in the *lacZ* gene (DL3343) or not (DL3344) that had a single visibly segregated copy of lacZ (twin YFP/CFP focus) following 90 min growth in M9-minimal media supplemented with either 0.2% glucose (SbcCD$^-$) or 0.001% arabinose (SbcCD$^+$), *n* = 3.

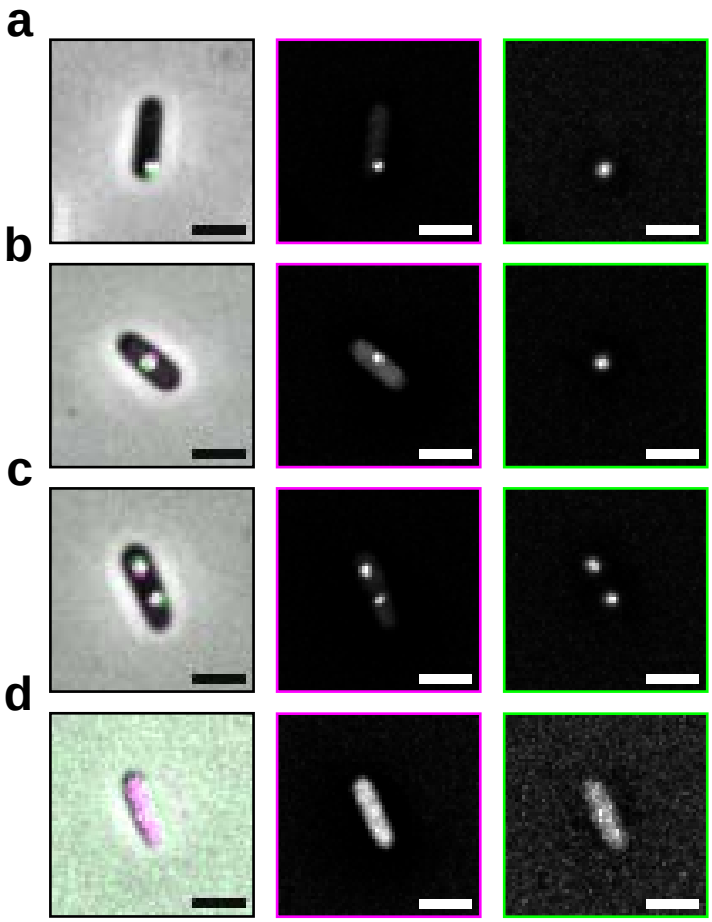

Figure 5.4 Four major classes of DL3343 cells following SbcCD induction. Following 90 min of growth in arabinose the majority of DL3343 (P_{BAD}-*sbcDC lacZ*::pal *recA*$^-$) cells had a single twin YFP/CFP focus that was located close to either the cell pole (**a**) or mid-cell (**b**). A similar number of cells were identified with two twin YFP/CFP foci (**c**) and no YFP or CFP foci (**d**). YFP is pseudocoloured magenta and CFP green, overlapping YFP and CFP foci appear white. Images were acquired at a resolution of 129 nm per pixel, calibration bar shows 2 μm.

5.4 Leading Strand Replicated *lacZ* Segregates to the Cell Pole

Section 5.3 showed how this system could be used to selectively degrade the sister chromosome that replicated *lacZ* by lagging strand synthesis. To determine the segregation pattern of leading and lagging strand replicated DNA, it was necessary to classify the location of the remaining twin YFP/CFP focus representing leading strand replicated *lacZ* (R_{lead}) as being closer to either mid-cell or the cell pole. However, cells with only a single twin YFP/CFP focus could represent cells that had yet to replicate and/or segregate *lacZ*, as well as cells that had one of the sister chromosomes broken and degraded. Since replication initiation is related to cell growth (Boye *et al.*, 1996), it was deemed necessary to exclude small cells with a single YFP/CFP focus from the analysis as these were most likely to represent cells that had not yet replicated or segregated *lacZ*. Specifically, cells smaller than 1.50 µm in length were exluded from analysis.

In the absence of an SbcCD induced DSB (DL3344 glucose), excluding cells with no visible fluorescent foci, 85 % of cells (± 4 %, s.e.m., n = 3) larger than 1.50 µm in length had more than one single YFP/CFP focus. The data described in section 5.3 was re-analysed for cells longer than 1.50 µm only. Similar to that observed for the entire population, an increase in the number of cells with only a single twin YFP/CFP focus was observed along with a decrease in the number of cells with two twin YFP/CFP foci. However, the increase in the number of cells with a single YFP/CFP focus and the decrease in the number of cells with two segregated YFP/CFP foci were more dramatic for the sub-population of cells longer than 1.50 µm (Figure 5.5) than to that observed for the entire population.

a

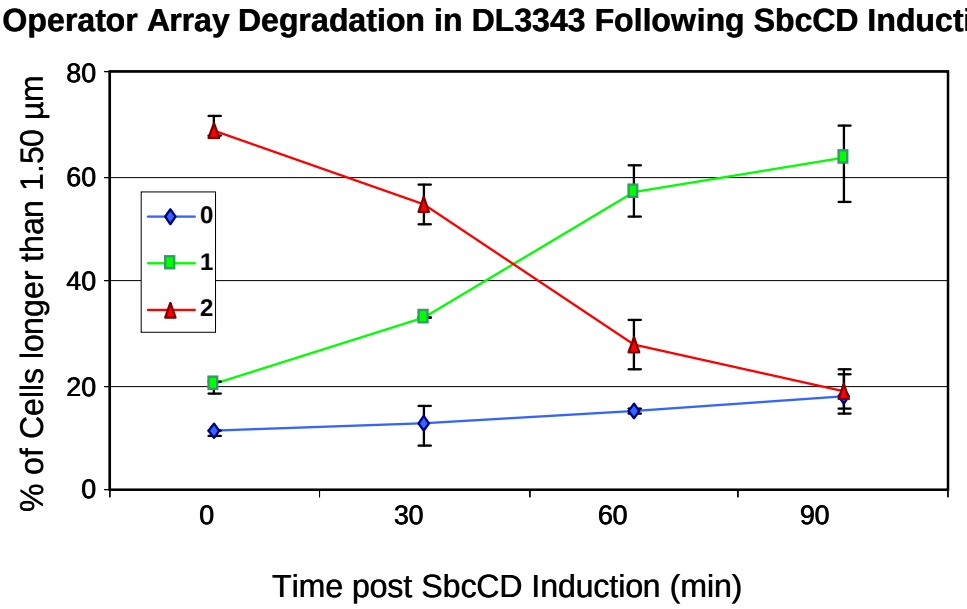

b

Strain	Genotype	SbcCD$^-$	SbcCD$^+$
DL3344	*lacZ*$^+$	13.6% ± 3.97	12.4% ± 2.03
DL3343	*lacZ*::pal	15.4% ± 0.56	61.9% ± 4.71

Errors indicate standard error of the mean

Figure 5.5 Operator array degradation in large cells following cleavage of the palindrome. **a**, the number of visibly segregated copies of *lacZ* (0, 1, 2) in *recA*$^-$ SbcCD inducible cells that harboured a 246 bp DNA palindrome in the *lacZ* gene (DL3343) and were longer than 1.50 µm, as a function of time of SbcCD induction. Error bars indicate range, *n* = 2. **b**, The percentage of *recA*$^-$ SbcCD inducible cells either harbouring a 246 bp DNA palindrome in the *lacZ* gene (DL3343) or not (DL3344) that were longer than 1.50 µm and had a single visibly segregated copy of *lacZ* (twin YFP/CFP focus) following 90 min growth in M9-minimal media supplemented with either 0.2% glucose (SbcCD$^-$) or 0.001% arabinose (SbcCD$^+$), *n* = 3. Figure **a** taken from (White *et al.*, 2008).

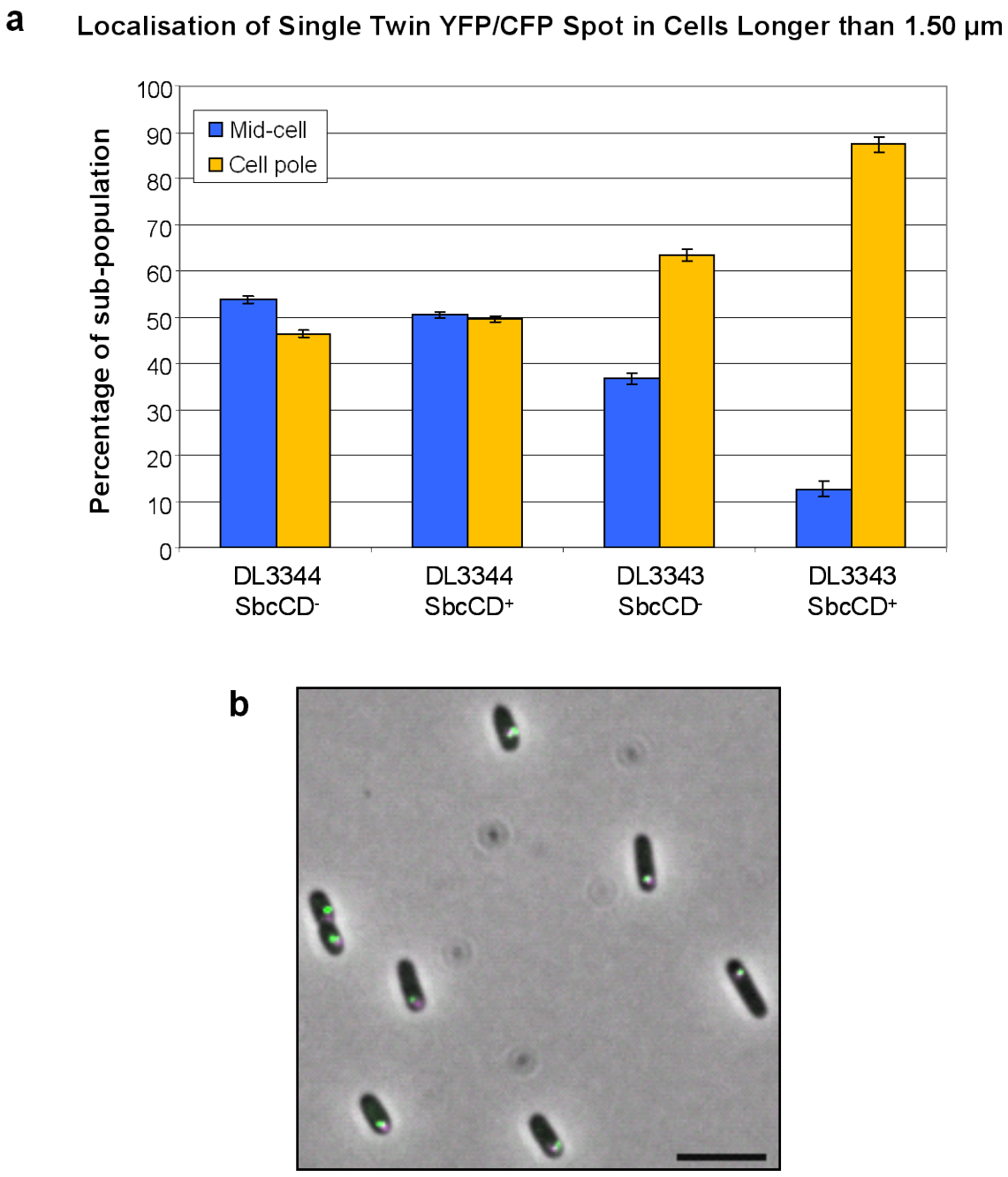

Figure 5.6 Localisation of *lacZ* in large P_{BAD}-*sbcDC* cells with a single twin YFP/CFP focus. **a**, Location of single twin YFP/CFP focus in cells longer than 1.50 µm, classified as either being closer to mid-cell or a cell pole. Error bars show standard error of the mean, *n* = 3. **b**, Representative field of view of DL3343 (P_{BAD}-*sbcDC lacZ*::pal *recA*$^-$) cells following 90 min of SbcCD induction (0.001% arabinose). YFP is pseudocoloured magenta and CFP green, overlapping YFP and CFP foci appear white; calibration bar shows 5 µm. Figure **a** adapted from (White *et al.*, 2008).

To quantify the location of the single YFP/CFP focus in cells larger than 1.50 µm, its location was classified as being closer to either a cell pole (*e.g.* Figure 5.4a) or mid-cell (*e.g.* Figure 5.4b). In the absence of an SbcCD-induced DSB, a similar number of cells longer than 1.50 µm had their YFP/CFP focus located at mid-cell as a cell pole (Figure 5.6a). Strikingly however, 90 min of SbcCD induction in a strain harbouring the 246 bp palindrome (DL3343) resulted in the YFP/CFP focus being located at a cell pole in 87 % (± 2 %, s.e.m, $n = 3$) of cells (for representative field of view see Figure 5.6b). A slight bias towards the single YFP/CFP focus being located at the cell pole was also observed in strain DL3343 in the absence of SbcCD induction (growth in 0.2 % glucose). This is potentially a result of leaky expression of SbcCD from the arabinose inducible promoter P_{BAD} in minimal growth medium (Khlebnikov *et al.*, 2001). This result is consistent with the hypothesis that chromosome segregation in *E. coli* is not random as a result of the segregation of leading strand replicated DNA to the cell poles.

5.5 Intact Sister Chromosomes Remain in One Cell Half

To investigate the effect of cleavage of the DNA palindrome by SbcCD on chromosome segregation, DNA was visualised by either DAPI staining or mounting cells on gelatine. DAPI is a fluorescent DNA stain, whereas gelatine allows *E. coli* nucleoids to be observed by phase-contrast microscopy (Mason and Powelson, 1956). To prevent cross-signal from plasmid DNA, strains isogenic to DL3343 and DL3344 but lacking plasmid pDL3196 (DL3339 and DL3340 respectively) were used. Importantly, because operator arrays were not being visualised, plasmid

pMW1 which expressed TetR-eYFP and LacI-Cerulean was not essential for this investigation. Cultures of *recA*$^-$ P_{BAD}-*sbcDC* strains either harbouring the 246 bp interrupted DNA palindrome in *lacZ* (DL3339) or not (DL3340) were first grown in M9-minimal medium supplemented with 0.2 % glucose (SbcCD$^-$) to an OD_{600} of 1.0. These cultures were diluted to an OD_{600} of 0.2 in M9-minimal medium supplemented with either 0.001 % arabinose (SbcCD$^+$) or 0.2 % glucose (SbcCD$^-$) and incubated at 37 °C with agitation. To visualise DNA, either 1 μg ml$^-$ DAPI was added to cultures for 15 min prior to mounting cells on a bed of 1 % agarose-H_20, or cells were directly mounted on a bed of 27 % bovine gelatine-M9 minimal medium. Importantly, nucleoids were not condensed by chloramphenicol treatment prior to DNA visualisation (DL3339 and DL3340 are chloramphenicol resistant). Cells were imaged at a resolution of 0.129 μm per pixel.

In the absence of an induced DSB, most cells had nucleoids that were diffuse within the cells with a few anucleate cells present. Figure 5.7a shows a representative field of view of *lacZ*::pal strain DL3339 that was grown in SbcCD$^-$ conditions with DAPI stained nucleoids. These cells are similar to those observed in the *lacZ*$^+$ strain DL3340 when grown in either SbcCD$^+$ or SbcCD$^-$ conditions, and similar results were obtained when using gelatine to visualise the nucleoids (data not shown). However, a distinct phenotype was observed in the *lacZ*::pal strain DL3339 when grown in SbcCD$^+$ conditions. These were elongated cells that appear to have had a chromosome degregated in one half of the cell. A gradient of such phenotypes were observed, ranging from cells that had less DNA in one half of the cell compared to the other, to cells that had recently divided to give one cell with DNA and another cell without. This phenotype was observed both when nucleoids were observed with

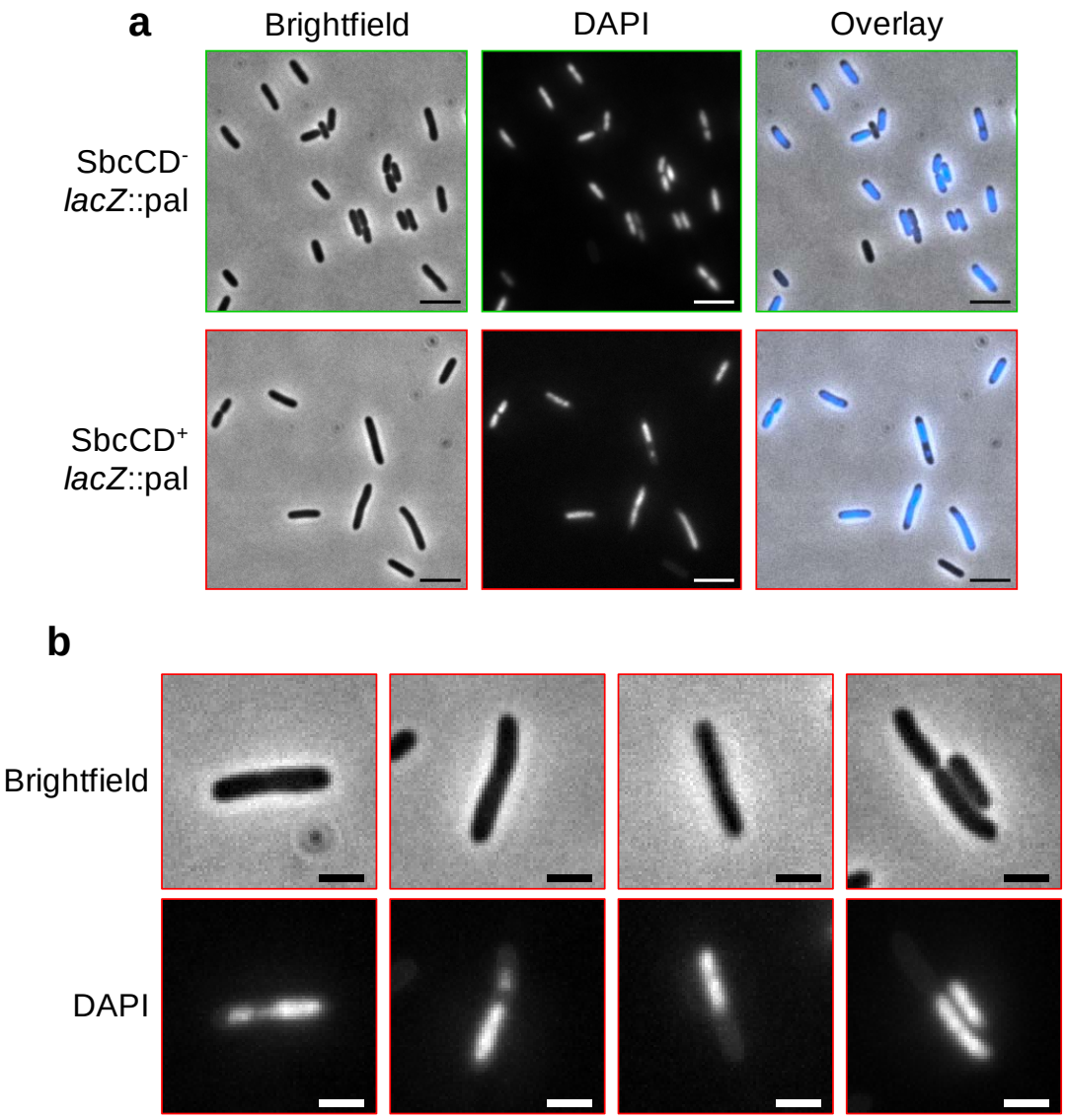

Figure 5.7 DAPI stained nucleoids of *recA*⁻ mutants harbouring a DNA palindrome in *lacZ*. **a**, DAPI staining of *recA*⁻ P_{BAD}-*sbcDC* cells harbouring a 246 bp palindrome in the *lacZ* gene (DL3339) following 90 min growth in M9-minimal medium supplemented with either 0.2% glucose (SbcCD⁻) or 0.001% arabinose (SbcCD⁺). Nucleoids were not condensed by chloramphenicol treatment prior to staining with DAPI. In the overlay images, DAPI signal is pseudo-coloured blue; calibration bar shows 10 μm. **b**, examples of DL3339 cells grown in DSB induced conditions (SbcCD⁺, 0.001% arabinose) that have phenotype indicative of degradation of a sister chromosome. Calibration bar shows 2 μm.

DAPI (Figure 5.7b) and gelatine (data not shown) and indicates that even following the extensive DNA degredation initiated by a DSB induced in one sister chromosome, the intact sister chromosome remains in one cell half.

5.6 Segregation of Leading Strand Replicated *lacZ* to the Cell Pole is not an Artefact of DSB Induction

To test the alternative hypothesis that leading strand replicated *lacZ* segregates to the cell poles in response to the induced DSB, a site-specific endonuclease (I-SceI) that does not discriminate between leading and lagging strand replicated DNA was used to induce a DSB in *lacZ*. Strains DL3345 and DL3346 are isogenic to strains DL3343 and DL3344 used in the previous experiment (section 5.4), except both are *sbcCD*$^{+}$ and contain an arabinose inducible I-SceI construct (P_{BAD}-*I-SceI*). Additionally, strain DL3345 harbours a unique I-SceI cleavage site (I-SceI_{cs}) in place of the DNA palindrome present in the *lacZ* gene of DL3343 (DL3346 is a *lacZ*$^{+}$ control strain). DL3345 and DL3346 are *recA*$^{-}$ derivatives of strains DL3285 and DL3286, for details of their construction see Chapter 4.

Cultures of the *recA*$^{-}$ P_{BAD}-*I-SceI* strains either harbouring a unique I-SceI cleavage site in the *lacZ* gene (DL3345) or not (DL3346) were first grown in M9-minimal medium supplemented with 100 ng ml^{-1} ATC and 0.2 % glucose to an OD_{600} of 1.0. These cultures were diluted to an OD_{600} of 0.2 in M9-minimal medium supplemented with 100 ng ml^{-1} ATC and either 0.001 % arabinose (I-SceI^{+}) or 0.2 % glucose (I-SceI^{-}), incubated at 37 °C with agitation, and then sampled after 90 min of further growth for microscopy. Cells were imaged at a resolution of 0.129 μm per pixel and multiple *z*-sections (± 800 nm, 9 images at a 200 nm interval) of both CFP

Strain	Genotype	I-SceI$^-$	I-SceI$^+$
DL3346	*lacZ*$^+$	11.9% ± 2.12	10.3% ± 3.04
DL3345	*lacZ*::I-SceI$_{cs}$	15.9% ± 1.82	30.2% ± 4.19

Errors indicate standard error of the mean

Table 5.1 Frequency of DSB induced on one sister chromosome by I-SceI. Percentage of *recA*$^-$ I-SceI inducible cells either harbouring a unique I-SceI cleavage site in the *lacZ* gene (DL3345) or not (DL3346), that were longer than 1.50 µm and had a single visibly segregated copy of *lacZ* (twin YFP/CFP focus) following 90 min growtin in M9-minimal media supplemented with either 0.2% glucose (I-SceI$^-$) or 0.001% arabinose (I-SceI$^+$), *n*= 3.

and YFP signals were captured. The stacks of *z*-planes were deconvolved using the software Autodeblur and Autovisualize v9.32 and subsequently combined to give a maximum projection image using MetaMorph 6.3r2. Cell lengths were measured using the 'fiber length' measurement of the image analysis software MetaMorph v6.3r2 and the number of visible YFP and CFP foci were counted for each of the measured cells. At least 500 cells were analysed in total for each of the independent cultures to obtain sample averages and each experiment was repeated three times.

The results showed that there was an approximate 3-fold increase in the number of large (longer than 1.50 µm) cells with a single copy of *lacZ* (visible twin YFP/CFP focus) when I-SceI was induced for 90 min in cells containing a unique I-SceI cleavage site (30.2%) compared to an isogenic strain lacking the I-SceI cleavage site (10.3%), Table 5.1. This result shows that the I-SceI endonuclease can be used to induce a DSB in one of a pair of sister chromosomes (see section 4.8), although less efficiently than with the use of inducible SbcCD and a 246 bp interrupted DNA palindrome.

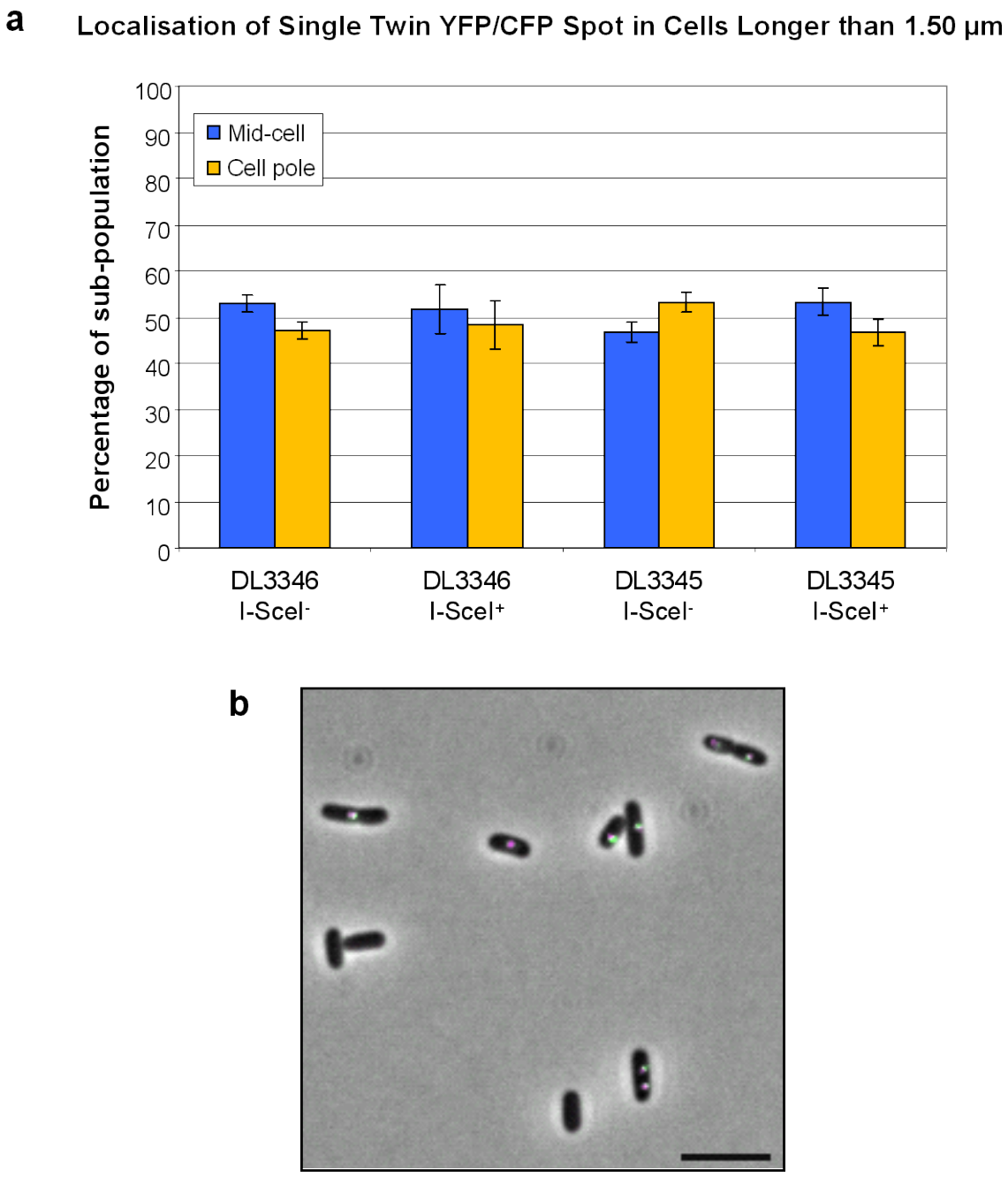

Figure 5.8 Localisation of *lacZ* in large P_{BAD}-*I-SceI* cells with a single twin YFP/CFP focus. **a**, Location of single twin YFP/CFP focus in cells longer than 1.50 µm, classified as either being closer to mid-cell or a cell pole. Error bars show standard error of the mean, *n* = 3. **b**, Representative field of view of DL3345 (P_{BAD}-*I-SceI lacZ*::I-SceI$_{cs}$ *recA*$^-$) cells following 90 min of I-SceI induction (0.001% arabinose). Cells were heterogeneous with respect to the number and position of YFP and CFP foci across fields of view. YFP is pseudocoloured magenta and CFP green, overlapping YFP and CFP foci appear white; calibration bar shows 5 µm. Figure **a** adapted from (White *et al.*, 2008).

As described for an SbcCD induced DSB in section 5.4, to quantify the location of *lacZ* following an I-SceI induced DSB on one of the sister chromosomes, only cells that were than longer 1.50 μm and contained a single visible twin YFP/CFP spot were included in the analysis and the location of the single twin YFP/CFP spot classed as being either closer to mid-cell or the cell pole. In the absence of an I-SceI induced DSB, a similar number of cells longer than 1.50 μm had their YFP/CFP focus located at mid-cell as a cell pole. Since this pattern of *lacZ* localisation was also observed in the culture subject to I-SceI induced DSBs (Figure 5.8), these results are inconsistent with the hypothesis that *lacZ* localises to the cell pole in response to an induced DSB in the chromosome.

5.7 SbcCD Does Not Selectively Cleave DNA Hairpins Located at Mid-Cell

It was shown in section 5.6 that segregation of leading strand replicated *lacZ* to the cell pole is not an artefact of DSB induction. A final hypothesis was that the observed segregation pattern of leading strand replicated *lacZ* (section 5.4) did not reflect the true segregation pattern of sister chromosomes, but was caused by the selective cleavage of DNA hairpins located at mid-cell by SbcCD. Consistent with this, SbcC-GFP has been shown to localise to mid-cell (Darmon *et al.*, 2007). However, in that study SbcC-GFP was expressed from the IPTG inducible promoter P_{trc} rather than the arabinose inducible promoter P_{BAD} used in this study. The localisation of SbcCD in *E. coli* following expression from P_{BAD} is as of yet unknown and could differ as a result of overexpression.

Also, it was shown in that study that only 54 % of cells had a focus of SbcC-GFP at mid-cell with the remainder possessing two SbcC-GFP foci, one at the one-quarter and the other at the three-quarter positions of the cell (Darmon *et al.*, 2007). This pattern of localisation is consistent with that observed for the *E. coli* replication factory (Lau *et al.*, 2003) and indeed SbcC-GFP was shown to co-localise with SeqA-RFP (Darmon *et al.*, 2007), a component of the replication factory (Molina and Skarstad, 2004). It is therefore unlikely that SbcCD distinguished the two copies of *lacZ* on the sister chromosomes on the basis of their cellular location, especially when considering the observation of sister chromosome cohesion following passage of the replisome (Wang *et al.*, 2008).

In order to test the hypothesis that SbcCD only cleaves a DNA hairpin on the lagging strand template when it is located at mid-cell and the segregation of leading and lagging strand replicated DNA is random, we set out to calculate the frequency of DNA hairpin cleavage by SbcCD. If this hypotheis is true, then there will be a maximum of 25 % of chromosomes cleaved per replication cycle. To calculate the frequency of chromosome cleavage by SbcCD we used the frequency of operator array degradation in *recA*$^-$ cephalexin-induced filaments following induction of SbcCD as an indirect measurement. Cephalexin is a β-lactam antibiotic that prevents septum formation in *E. coli* by inhibiting the divisome component FtsI (Hedge and Spratt, 1985; Pogliano *et al.*, 1997). This method of inhibiting cell division does not affect chromosome segregation so that the normal pattern of segregation is repeated in tandem along the length of these long filamentous cells (Wang *et al.*, 2006; Wang *et al.*, 2005).

Cultures of *recA*$^{-}$ P_{BAD}-*sbcDC* harbouring the 246 bp interrupted DNA palindrome in *lacZ* (DL3343) or not (DL3344) were first grown in M9-minimal medium supplemented with 100 ng ml^{-1} ATC and 0.2 % glucose to an OD_{600} of 1.0. These cultures were then diluted to an OD_{600} of 0.4 in M9-minimal medium supplemented with 0.2 % glucose, 100 ng ml^{-1} ATC and 10 µg ml^{-} cephalexin (to inhibit cell division). Following 90 min of growth at 37 °C with agitation, these cultures were diluted to an OD_{600} of 0.2 in M9-minimal medium supplemented with 0.001 % arabinose, 100 ng ml^{-1} ATC and 10 µg ml^{-} cephalexin in order to induce SbcCD. These cultures were grown for a further 120 min in SbcCD induced conditions prior to sampling for microscopy. Cells were imaged at a resolution of 0.129 µm per pixel and multiple *z*-sections (± 800 nm, 9 images at a 200 nm interval) of both CFP and YFP signals were captured. The stacks of *z*-planes were deconvolved using the software Autodeblur and Autovisualize v9.32 and subsequently combined to give a maximum projection image using MetaMorph 6.3r2. Cell lengths were measured using the 'fiber length' measurement of the image analysis software MetaMorph v6.3r2 and the number of visible YFP and CFP foci were counted for each of the measured cells.

The number of visible twin YFP/CFP foci was divided by the cell length to give a standardised value of the number of segregated copies of *lacZ* per cell length (µm). In the absence of the induced DSB (DL3344 SbcCD^{+}) this gave a value of 0.72. In the presence of SbcCD and the 246 bp palindrome (DL3343 SbcCD^{+}) however, the same calculation gave a value of 0.34. This shows that there are fewer segregated copies of the *lacZ* region in these cells (Figure 5.9), presumably due to degradation of chromosomes following cleavage of DNA hairpins by SbcCD. To

calculate the frequency of chromosome cleavage by SbcCD, the value obtained for the *lacZ*$^{+}$ strain (0.72; DL3344 SbcCD^{+}) was divided by that obtained for the *lacZ*::pal strain (0.34; DL3343 SbcCD^{+}). This calculation gave a value of 53 %, consistent with the hypothesis that SbcCD cleaves one of a pair of replicating sister chromosomes and inconsistent with the hypothesis that SbcCD only cleaves one of a pair of sister chromosomes when chromosome segregation occurs in a particular manner.

Although this estimate of the frequency of chromosome cleavage by SbcCD is consistent with genetic data that shows that almost every cell suffers a DSB as evidenced by the severe death phenotype of recombination mutants (Figure 3.1 and (Eykelenboom *et al.*, 2008)), a previous calculation of cleavage efficiency using quantitative Southern blotting gave a lower estimate of 36% of chromosomes being cleaved (Eykelenboom *et al.*, 2008). However, this value is still larger than the maximum 25 % of cleaved chromosomes predicted by the hypothesis and could be considered a lower estimate of the true value of chromosome cleavage due to inefficient transfer of either the large cleaved fragments or the small degradation products during the Southern blot procedure.

a

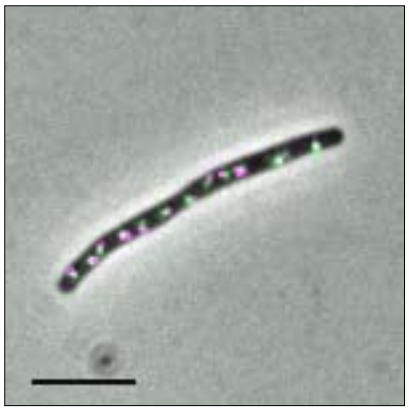

b

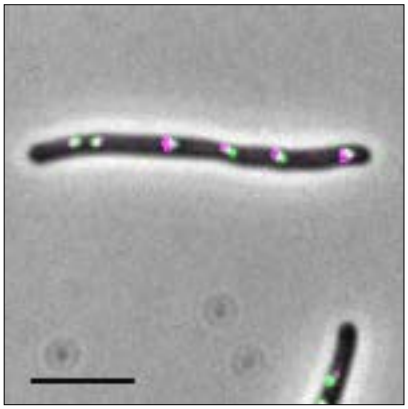

c

Strain	*n*	Mean Length (μm)	Mean number of YFP/CFP foci	YFP/CFP foci per micrometer
SbcCD$^+$ *lacZ*$^+$	333	8.92 ± 0.44	6.3 ± 0.3	0.72 ± 0.02 (X)
SbcCD$^+$ *lacZ*::pal	358	14.22 ± 0.57	4.5 ± 0.2	0.34 ± 0.01 (Y)

Errors indicate standard error of the mean

Figure 5.9 Induction of SbcCD in cephalexin induced filaments. SbcCD was induced for 120 min in the *recA*$^-$ P_{BAD}-*sbcDC* strains **a**, DL3344 (*lacZ*$^+$) and **b**, DL3343 (*lacZ*::pal) following 90 min of cephalexin treatment to inhibit cell division. YFP is pseudocoloured magenta and CFP green, overlapping YFP and CFP foci appear white. Images were acquired at a resolution of 129 nm per pixel, calibration bar shows 5 μm. **c**, mean cell lengths and the number of visible YFP/CFP twin foci (indicating the number of segregated copies of *lacZ*) per cell were counted. The frequency of chromosome cleavage by SbcCD (0.53) was calculated as 1 – Y/X. Figure adapted from (White *et al.*, 2008).

5.8 Conclusions

It was recently shown that under slow growth conditions, *E. coli* cells segregate their sister chromosomes in a manner that results in translational symmetry of their chromosome arms (Nielsen *et al.*, 2006b; Wang *et al.*, 2006). By selectively degrading the sister chromosome that replicated *lacZ* by lagging strand synthesis, we have confirmed earlier reports that chromosome segregation is not random in the majority of cell divisions (Canovas *et al.*, 1984; Cooper *et al.*, 1978; Pierucci and Zuchowski, 1973). In addition to this, we consolidate these two observations by showing that they result from mirror symmetry in the pattern of segregation of the leading and lagging strands of the two replication forks, where specifically it is the two leading strands of replication that segregate towards opposite cell poles and the two lagging strands of replication that segregate to mid-cell. Interestingly, this hypothesis that leading strand replicated DNA segregates toward the cell poles was previously proposed (Wang *et al.*, 2005; Woldringh and Nanninga, 2006) in order to explain the preponderance of highly expressed genes on the leading strands of the left and right replichores (Rocha *et al.*, 2003). However, no direct evidence to support this hypothesis was presented.

Non-random segregation of sister chromosomes has also been observed in mammalian stem cells, an observation that led to the immortal strand hypothesis (Cairns, 1975). This hypothesis states that the observed behaviour of non-random chromosome segregation is caused by stem cells preferentially retaining grandmother DNA template strands in an attempt to limit the accumulation of replication induced mutations. However, both the immortal strand hypothesis and the observation of non-random chromosome segregation on which it is based, is controversial (Kiel *et*

al., 2007; Rando, 2007; Waghmare *et al.*, 2008). Interestingly, during the course of this investigation it was proposed that in order to segregate chromosomes non-randomly, eukaryotic cells could distinguish genetically identical sister chromosomes on the basis of whether their centromeres had been replicated by leading or lagging strand synthesis (Lew *et al.*, 2008). Here we provide evidence that *E. coli* uses such a mechanism to segregate its sister chromosomes non-randomly.

It is however, difficult to relate the immortal strand hypothesis to *E. coli* biology since it divides symmetrically into two daughter cells. If *E. coli* were to grow in long chains then non-random segregation of sister chromosomes would result in the oldest DNA strands being segregated to the filament poles (Figure 5.10). Indeed this has been observed by pulse labelling *E. coli* chromosomes with BrdU and forcing cells to filament using a temperature sensitive allele of *ftsA* (Canovas *et al.*, 1984). However, in contrast to that expected for the immortal strand hypothesis, it was recently shown that *E. coli* cells that inherit 'old' cell poles have reduced reproductive capacity due to increased chance of inheriting toxic protein aggregates known as inclusion bodies (Lindner *et al.*, 2008; Maisonneuve *et al.*, 2008). This coupled with the fact that DNA DSBs are repaired by replication following extensive resection by RecBCD, makes it unlikely that *E. coli* cells segregate their chromosomes non-randomly in order to reduce the number of replication induced mutations in certain cells. It is possible that non-random chromosome segregation provides no selective advantage to *E. coli*. The phenomena of translational symmetry of chromosome arms, segregation of leading strand replicated DNA to cell poles, and non random segregation of sister chromosomes are tightly linked. Any

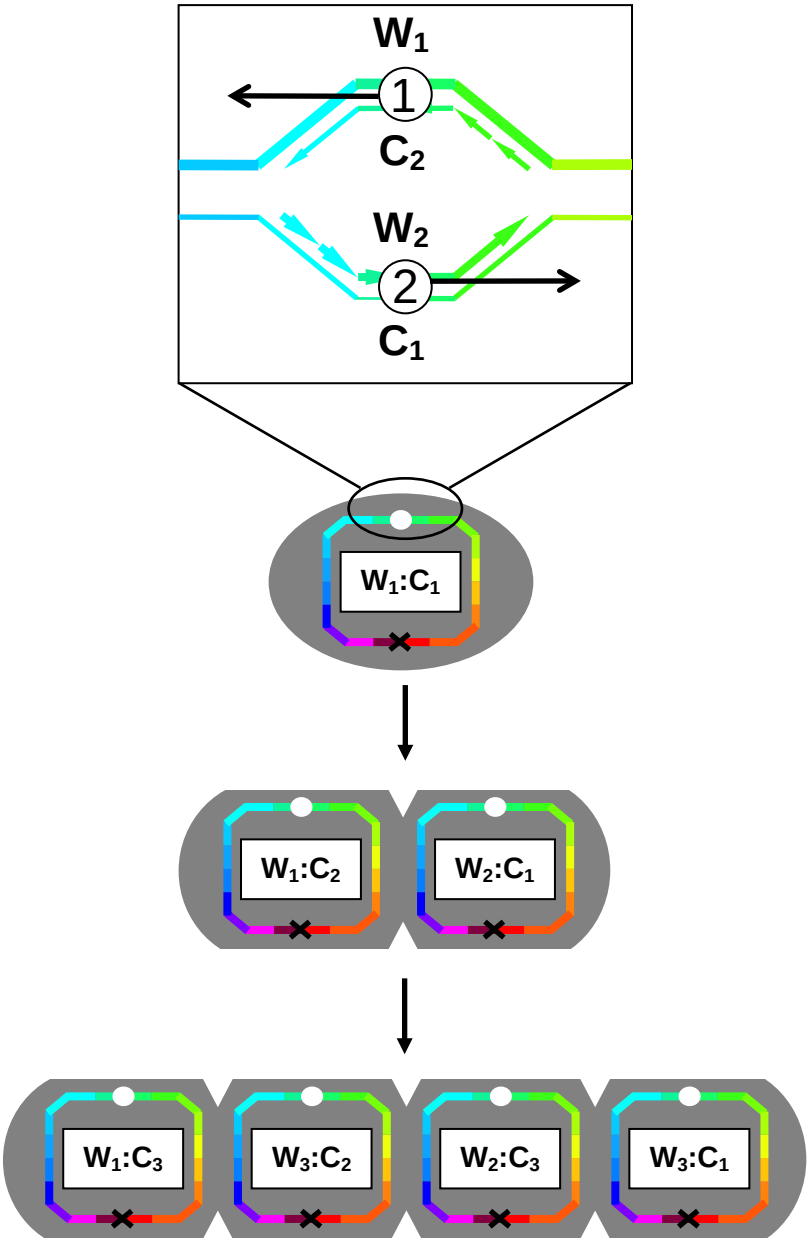

Figure 5.10 Segregation of 'Grandmother' DNA strands in *E. coli*. DNA is composed of two complementary strands known as Watson (W) and Crick (C). Due to non-random chromosome segregation, the oldest Watson and Crick strands will segregate to the oldest cell poles in chains of *E. coli* cells. Subscript numbers indicate the generation in which the Watson and Crick strands were synthesised.

one of these factors could provide a selective advantage to the cell with the other two being consequential. Alternatively, none of these phenomena may improve the fitness of *E. coli* cells and may simply all be downstream consequences of the mechanism of chromosome segregation.

An important observation to note when considering the biological implications of non-random chromosome segregation, is that although non-random chromosome segregation predominates, an element of random segregation has also been observed (Canovas *et al.*, 1984). This fits with the more recent observations that translational symmetry of chromosome arms is only observed in 80 % (Nielsen *et al.*, 2006b) to 85 % (Wang *et al.*, 2006) of cells, and may also explain why in this study, the leading strand replicated right replichore was only found to segregate to the cell pole in ~90 % of cells. These observations are summarised in Figure 5.11. The fact that cells can deviate from the norm of segregating leading strand replicated DNA to the cell poles makes it unclear whether or not this pattern of chromosome segregation confers a selective advantage to the cells.

The data from this study do not provide an insight into the potential mechanism underlying this aspect of chromosome segregation. Any attempts to address this would be greatly facilitated by a better understanding of the fundamental mechanism of chromosome segregation in *E. coli*. Recent advancements have been in understanding the mechanism of chromosome segregation in other prokaryotic model organisms. For example, it has been shown in *C. crescentus* that chromosome segregation is facilitated by anchoring the origins of replications to the cell poles *via* protein-protein interactions involving the protein ParB (Bowman *et al.*, 2008; Ebersbach *et al.*, 2008a). Likewise, chromosome segregation in *B. subtilis* has also

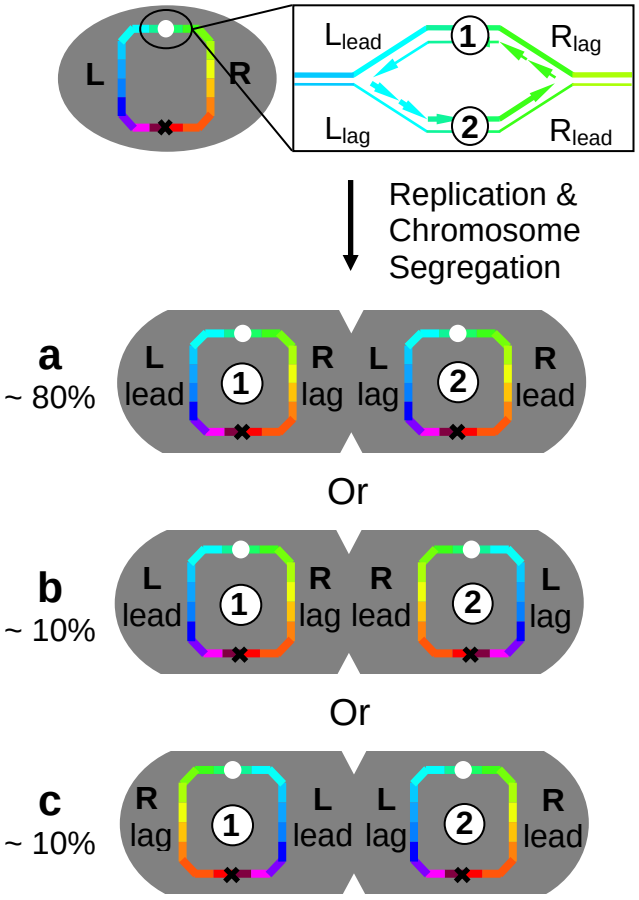

Figure 5.11 Non-random segregation of sister chromosomes in *E. coli*. Figure is adapted from (White *et al.*, 2008). In approximately 80% of cells, *E. coli* segregates its leading strand replicated DNA to the cell poles resulting in translational symmetry of the chromosome arms, **a**. In the rest of cells, mirror symmetry in the segregation of the chromosome arms is observed resulting in translational symmetry of the leading and lagging strand replicated DNA, **b** and **c**. Figure adapted from (White *et al.*, 2008).

been shown to be facilitated by binding of the same protein (ParB/SpoOJ) to the origins of replication (Gruber and Errington, 2009). However, *E. coli* lacks a ParB homologue and its origins of replication do not migrate to the cell poles. The *E. coli* origins of replication have been shown to migrate rapidly following segregation indicating that chromosome segregation may be an active process (Niki *et al.*, 2000),

and a centromere-like sequence (*migS*) has been identified (Yamaichi and Niki, 2004). Although there is currently no evidence to suggest that a protein binds to *migS,* the structural maintenance of chromosome protein MukB has been implicated in having a role in the cellular localisation of *E. coli* origins of replication (Danilova *et al.*, 2007). The actin-like cytoskeletal protein MreB (Gitai *et al.*, 2005; Kruse *et al.*, 2006) has been implicated in playing a force generating role in chromosome segregation, although this has been disputed (Karczmarek *et al.*, 2007) and recent evidence suggests that if MreB does play a role in chromosome segregation, it is likely to be in the regulation of catenation (Madabhushi and Marians, 2009).

The fact that a significant proportion of cells do not segregate their leading strand replicated DNA to the cell poles, suggests that a stringent mechanism of ensuring this pattern of chromosome segregation does not exist. In support of this, it has recently been shown that fewer cells specifically segregate their leading strand replicated DNA to the cell poles following a period of induced replication blockage (Liu *et al.*, 2009). This pattern of chromosome segregation may therefore be a result of the biomechanics of DNA replication and chromosome segregation causing a bias towards the leading strand replicated DNA to the cell poles. For example, in *E. coli* the individual polymerases responsible for leading and lagging strand synthesis are physically linked in a structure known as a replisome (O'Donnell, 2006). Within the replisome the lagging strand template is looped to allow the two polymerases to translocate in the same direction. Although this loop is small, it may physically constrain the lagging strand replicated DNA while allowing the leading strand replicated DNA to segregate outwards towards the cell poles (Figure 5.12). However, such structural models fail to take into account the observation of

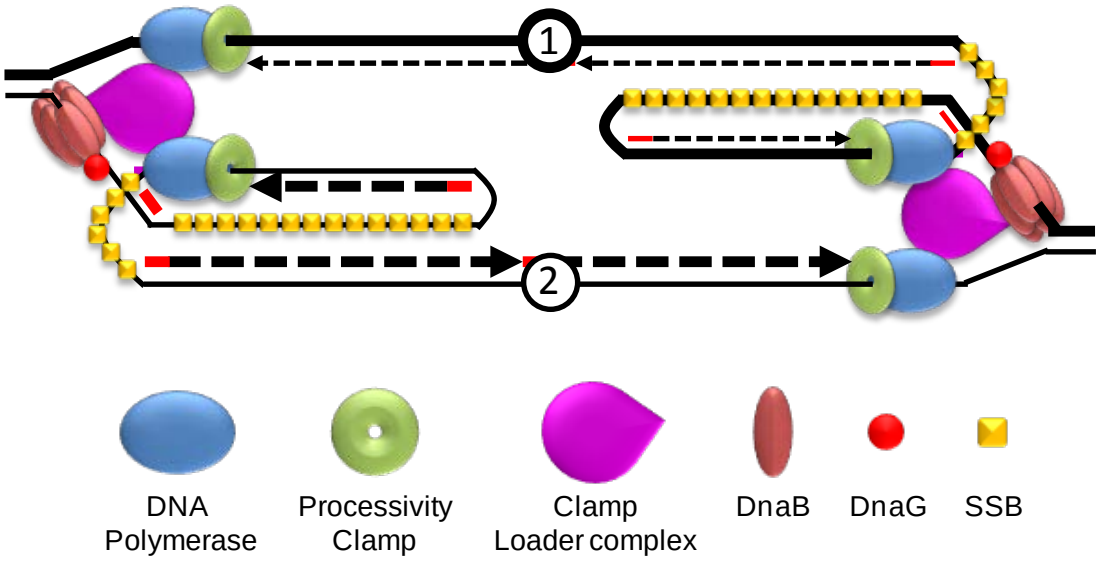

Figure 5.12 Replication fork structure and segregation of leading and lagging strand replicated DNA. The strong bias towards segregation of leading strand replicated DNA to the cell poles, and lagging strand replicated DNA to mid-cell, may be a biomechanical consequence of the structure of the two replisomes, where the two lagging strand templates are looped to allow the two replisome associated polymerases to translocate in the same direction in space. This could constrain the lagging strand replicated DNA while allowing the leading strand replicated DNA to segregate out towards the cell poles. However, this model does not take into account post-replicative sister chromosome cohesion.

post-replicative sister chromosome cohesion (Wang *et al.*, 2008). It is also currently unclear how replication forks established during DNA DSB repair, which introduce stretches of both leading and lagging strand replicated DNA into the broken sister chromosome, impact upon chromosome segregation.

Chapter 6

Plasmid Instability and the Expression of TetR-eYFP and LacI-Cerulean from the Chromosome

6.1 Introduction

Chapter four described in detail, how strains were constructed that would allow the dsDNA ends of a DSB induced in the *lacZ* gene of the *E. coli* chromosome to be followed by fluorescence microscopy. Briefly, this involved the integration of an array of *tetO* sites upstream, and an array of *lacO* sites downstream of a site-specific cleavage site in the *lacZ* gene, which allowed the cellular locations of these two operator arrays to be visualised indirectly when bound by variants of their DNA binding repressor proteins that had been fused to derivatives of GFP. Chapters four and five showed how the locations of the *tetO* and *lacO* arrays could be determined following the expression of TetR-eYFP and LacI-Cerulean from a weak constitutive promoter on a high copy number plasmid (pDL3196).

Although this system of expressing the fluorescent repressors provided good imaging for both the recombination proficient strains (DL3283, DL3284, DL3285 and DL3286) and their *recA*$^-$ derivatives (DL3343, DL3344, DL3345 and DL3346), it was not suitable for other mutant backgrounds. Of particular interest was the study of chromosome dynamics following DSB induction in a Δ*recB* mutant. This would allow the hypothesis that DNA ends are free to diffuse following cleavage of the chromosome to be tested by preventing repair while limiting resection of the broken DNA. Although Δ*recB* derivatives of P_{BAD}-*sbcDC* strains harbouring the operator arrays and either the DNA palindrome in *lacZ* (DL3543) or not (DL3544) were constructed, they were unable to stably maintain plasmid pDL3196, thereby preventing the operator arrays from being imaged. This was not surprising since plasmid pDL3196 has an origin of replication derived from pBR322 and these ColE1-type plasmids have been shown to be unstable in *recB*$^-$ mutants (Cohen and

Clark, 1986). This therefore made it necessary to establish an alternative system for the expression of TetR-eYFP and LacI-Cerulean that could be stably maintained in a Δ*recB* background.

6.2 Cloning *tetR-eyfp* and *lacI-cerulean* into pGB2

Although ColE1-type plasmids are unstable in *recB*$^-$ mutants, plasmids with a pSC101 origin of replication can be stably maintained (Biek and Cohen, 1986). pGB2 is a low copy number plasmid harbouring a pSC101 origin of replication as well as a multiple cloning site and a spectinomycin resistance cassette (Churchward *et al.*, 1984). The operon of *tetR-eyfp* and *lacI-cerulean* under control of the weak constitutive promoter P_{ftsKi} was amplified from plasmid pDL3196 by PCR using primers pGB2F and pGB2R. This PCR product was then digested with SalI and HindIII and cloned into the SalI/HindIII restriction sites in the MCS of pGB2 to give plasmid pDL3718. Finally, pDL3718 was used to transform Δ*recB* strains DL3543 and DL3544 to give strains DL3726 and DL3727 respectively.

It was shown in section 4.5.3 that strains harbouring the *tetO* array in the *cynX* gene required the inducer anhydrotetracycline for viability when TetR-eYFP was expressed from a weak constitutive promoter on the high copy number plasmid pDL3196. This was not the case when TetR-eYFP was expressed from the same promoter on the low copy number plasmid pDL3718, suggesting that insufficient TetR-eYFP was expressed to act as an efficient roadblock to replication at the *tetO* array. To check whether enough TetR-eYFP and LacI-Cerulean was binding the *tetO* and *lacO* array for fluorescence imaging, strain DL3726 was grown in minimal medium supplemented with 0.2 % glucose (SbcCD repressed) to an OD_{600} of 0.2 and

sampled for microscopy. Cells were imaged at a resolution of 0.129 μm per pixel and multiple *z*-sections (± 800 nm, 9 images at a 200 nm interval) were acquired for both CFP and YFP images. Both CFP and YFP fluorescence images were captured with an exposure time of 1500 ms (strains harbouring pDL3196 were typically imaged using exposure times of 500 ms and 300 ms for CFP and YFP fluorescence respectively). Post-acquisition, the stacks of *z*-planes were deconvolved using the software Autodeblur and Autovisualize v9.32 and subsequently combined to give a maximum projection image using MetaMorph 6.3r2. Representative images are shown in Figure 6.1.

This experiment showed that TetR-eYFP and LacI-Cerulean were unable to consistently form bright fluorescent foci in cells harbouring a *tetO* and *lacO* array

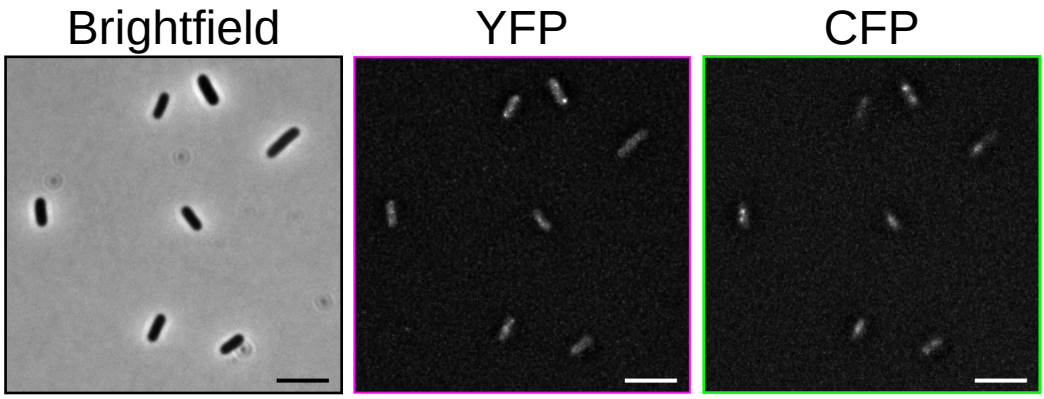

Figure 6.1 Expression of TetR-eYFP and LacI-Cerulean from pDL3718. A Δ*recB* mutant harbouring the superconstruct and expressing TetR-eYFP and LacI-Cerulean from the low copy number plasmid pDL3718 (DL3726) was grown to an OD_{600} of 0.2 and sampled for microscopy. Images were acquired at a resolution of 0.129 μm per pixel with long (1.5 s) exposure times for YFP and CFP fluorescence. Shown are maximum projections of deconvolved images; calibration bar shows 5 μm

when expressed from P_{ftsKi} on the low copy number plasmid pDL3718. Similar results were obtained whether the strain harbouring the *tetO* and *lacO* array was Δ*recB or recB*$^{+}$ (data not shown) suggesting that the poor imaging was a result of expressing the proteins from a weak promoter on a low copy number plasmid, as opposed to plasmid instability in the Δ*recB* mutant. The use of plasmid pDL3718 was therefore deemed inadequate for use as a vector for imaging the *tetO* and *lacO* arrays in a Δ*recB* mutant of *E. coli*.

6.3 Creating a Strong Constitutive Synthetic Promoter

During this investigation it was shown that RecD was essential for viability following cleavage of a 246 bp palindrome by SbcCD (Rachael Stobbs, unpublished). This result was surprising because unlike RecB and RecC, RecD is not essential for viability following UV-light induced DSBs (Lovett *et al.*, 1988). It would therefore be interesting to investigate the cellular localisation of DNA ends in a Δ*recD* mutant and compare and contrast the results to those obtained for both a Δ*recB* mutant and a recombination proficient strain. However, as with *recB*$^{-}$ strains, *recD*$^{-}$ mutants display high levels of plasmid instability, but unlike *recB*$^{-}$ mutants these cells have difficulties in maintaining both ColE1-type plasmids and plasmids with a pSC101 origin of replication (Biek and Cohen, 1986). This therefore prevented both pDL3196 (section 4.4.3) and pDL3718 (section 6.2) from being used as a vector for the expression of TetR-eYFP and LacI-Cerulean in a Δ*recD* strain.

To negate any problems associated with plasmid instability in these mutants (and other potentially interesting mutants such as Δ*recG*) altogether, it was desirable to establish a system for expressing TetR-eYFP and LacI-Cerulean from the

chromosome. Section 6.2 described how the constitutive promoter P_{ftsKi} did not drive high enough expression of TetR-eYFP and LacI-Cerulean when present on the low copy number plasmid pDL3718 to consistently produce bright fluorescent foci in strains harbouring a *tetO* and *lacO* array (Figure 6.1). It was therefore likely that the same problem would be encountered if the same operon was integrated into the chromosome as a single copy. To solve this problem, site-directed mutagenesis (SDM) was used to mutate P_{ftsKi} from a weak constitutive promoter to a strong constitutive promoter by altering its -10 and -35 elements.

E. coli has well defined promoter regions consisting of four important DNA sequences known as the -10, -35, extended -10 and UP elements that have been shown to interact directly with RNA polymerase (Browning and Busby, 2004). The -10 and -35 elements (named after their approximate distances from the transcription initiation site) are both well conserved, hexameric sequences whose consensus (-10 element: TATAAT; -35 element: TTGACA) have long been defined (McClure, 1985). Since these two elements interact directly with RNA polymerase, the distance between the two elements is also important although the actual sequence of this spacer is not (Campbell *et al.*, 2002; Murakami *et al.*, 2002). The extended -10 element is located immediately upstream of the -10 element and composed of the sequence motif TGn (Sanderson *et al.*, 2003). Finally, the UP element is an AT rich motif of ~20 bp that is located upstream of the -35 element (Gourse *et al.*, 2000).

P_{ftsKi} is a constitutive promoter located in the C-terminal 1074 bp of *ftsK* gene of *E. coli* that was cloned into a pBR322 derivative for the expression of TetR-eYFP and LacI-eCFP. This resulted in the plasmid pWX6 (Wang *et al.*, 2005) from which plasmids pDL3195, pDL3195 and pDL3196 were derived (section 4.4.3). The 1074

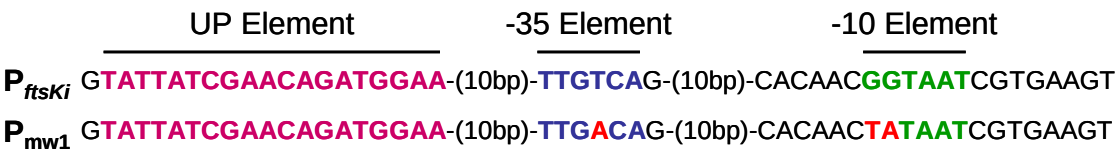

Figure 6.2 Mutagenesis of promoter P_{ftsKi}. Putative UP (purple), -35 (blue) and -10 (green) elements were identified for promoter P_{ftsKi}. To increase transcription from this promoter, two sequential rounds of SDM were performed on pDL3718 to change the hexameric sequences of the -35 and -10 elements to consensus (mutated bases are indicated in red). This new synthetic promoter was named P_{mw1}.

bp of DNA containing the promoter was also cloned along with *lacI-cerulean* and *tetR-eyfp* into pGB2 to give plasmid pDL3718 (section 6.2). To better define this promoter, its sequence was examined and putative UP, -35, and -10 elements defined (Figure 6.2). Strikingly, this analysis failed to identify an extended -10 element for P_{ftsKi} due to the lack of a TGn motif directly upstream of its -10 element.

As well as lacking an extended -10 element, this promoter also differs from consensus at two positions for its -10 element and a single position for its -35 element. It is difficult to predict which of these factors is likely to be most responsible for the weak promoter strength of P_{ftsKi} since the contribution of each element to promoter strength varies between different promoters (Browning and Busby, 2004). Therefore, the strategy used to increase transcription from this promoter involved changing the -10 and -35 elements of P_{ftsKi} to consensus by site-directed mutagenesis (SDM) since the consensus sequences for these elements are very well defined. Figure 6.2 shows the sequence of P_{ftsKi} along with the sequence of the promoter following SDM (named P_{mw1}).

The -10 and -35 elements of P_{ftsKi} located on pDL3718 were first altered independently by SDM using primer pairs Minus10_F/R (to give pDL4003) and Minus35_F/R (to give pDL4004) respectively. Subsequently these two alterations were combined by SDM of pDL4004 using primer pair Minus35_F/R to give plasmid pDL4005. Successful mutagenesis was confirmed by sequencing using primers pMW2seqF and pMW2seqR. To test the effect that these mutations had on the levels of TetR-eYFP and LacI-Cerulean expression, these three plasmids (pDL4003, pDL4004, and pDL4005) and plasmid pDL3718 from which they were derived, were used to transform a strain that harboured an array of *tetO* sites in *cynX* and an array of *lacO* sites in *mhpC* (DL3277).

Whereas DL3277 could be transformed with plasmids pDL3718, pDL4003 and pDL4004 in the absence of the inducers ATC and IPTG, both were required for successful transformation using plasmid pDL4005. Since these inducers were not required for transformation of a strain lacking both the *tetO* and *lacO* array (DL2006), it is likely that only expression of TetR-eYFP and LacI-Cerulean from P_{mw1} (located on pDL4005) was high enough to block replication at one or both of these operator arrays (see section 4.5). Although the YFP and CFP fluorescence intensities were not measured for these transformants, it was visible by eye that the plasmids expressing TetR-eYFP and LacI-Cerulean from P_{ftsKi} with either a consensus -10 element (pDL4003) or a consensus -35 element (pD4004) resulted in YFP and CFP foci that were not significantly different to one another and only slightly brighter than the strain expressing TetR-eYFP and LacI-Cerulean from P_{ftsKi} (pDL3718). On the other hand, bright CFP and YFP foci were consistently imaged

from strain DL3277 harbouring pDL4005 (P_{mw1}-*lacI-cerulean,tetR-eyfp*) even when cultured in the presence of 100 ng ml^{-1} ATC and 0.1 mM IPTG (data not shown).

6.4 Expression of TetR-eYFP and LacI-Cerulean from the Chromosome

The P_{mw1}-*lacI-cerulean,tetR-eyfp* operon from pDL4005 was cloned into the PMGR vector pDL2802 in order to integrate it into the chromosome. Plasmid pDL2802 is a PMGR vector (cloned by Ewa Okely, unpublished) that was designed to facilitate the integration of any DNA sequence of interest into the *ykgC* gene of *E. coli* by harbouring a unique NotI restriction site in between its two homology arms. *ykgC* is a non-essential gene of unknown function that has been annotated as a putative oxidoreductase. To construct pDL2903, two homology arms were amplified from the chromosome of MG1655 using primer pairs YkgC-F1/YkgC-R1 and YkgC-F2/YkgC-R2 and subsequently fused by crossover PCR using primers YkgC-F1 and YkgC-R2. Finally, this PCR fragment was cloned into PstI and SalI restriction sites of pTOF24.

The P_{mw1}-*lacI-cerulean,tetR-eyfp* operon from pDL4005 was amplified using primers FP_NotI_F and FP_NotI_R that were designed to flank the PCR fragment with NotI restriction sites. This PCR fragment was then cloned into the NotI restriction site of pDL2802 to give plasmid pDL4068. Unlike plasmid pDL4005, the 983 bp of *ftsK* upstream of P_{mw1} is not present in pDL4068 in order to reduce the probability of pDL4068 recombining with *ftsK* rather than *ykgC*. Plasmid pDL4048 was used to integrate the P_{mw1}-*lacI-cerulean,tetR-eyfp* operon into strains DL3276 and DL3277, DL3278 and DL3279 to give strains DL4069 and DL4070, DL4072,

and DL4073. Finally, plasmid pDL2698 was used to make strains DL4069 and DL4070 Δ*recB* by PMGR, resulting in strains DL4096 and DL4097. Plasmid pDL2698 is a vector (cloned by Ewa Okely, unpublished) for the deletion of *recB* by PMGR. To construct pDL2698, two homology arms were amplified from the chromosome of MG1655 using primer pair recB-KO-F1/R1 and recB-KO-F2/R2 and subsequently fused by crossover PCR using primers recB-KO-F1 and recB-KO-R2. Finally, this PCR fragment was cloned into the PstI and SalI restriction sites of pTOF24.

Strain DL4070 and its Δ*recB* derivative DL4097 were grown to an OD_{600} of ~ 0.2 in M9-minimal media supplemented with 0.2 % glucose (SbcCD repressed) and either 100 ng ml^{-1} of ATC or not prior to sampling for microscopy. Cells were imaged at a resolution of 0.129 μm per pixel and multiple *z*-sections (± 800 nm, 9 images at a 200 nm interval) of both CFP and YFP signals were captured. Post-acquisition, the stacks of *z*-planes were deconvolved using the software Autodeblur and Autovisualize v9.32 and subsequently combined to give a maximum projection image using MetaMorph 6.3r2. Representative images are shown in Figure 6.3. This result showed that expression of LacI-Cerulean and TetR-eYFP from P_{mw1} on the chromosome is a good alternative to the use of pDL3196 for the fluorescence imaging of the *tetO* and *lacO* arrays that can be used in mutant backgrounds that show high levels of plasmid instability.

Although DL4070 could be grown in the absence of the inducer ATC, the majority of cells were elongated and contained only a single visible twin CFP/YFP spot located at mid-cell. This is likely to be caused by a replication fork being blocked at the *tetO* array as a result of tightly bound TetR-eYFP protein (see section

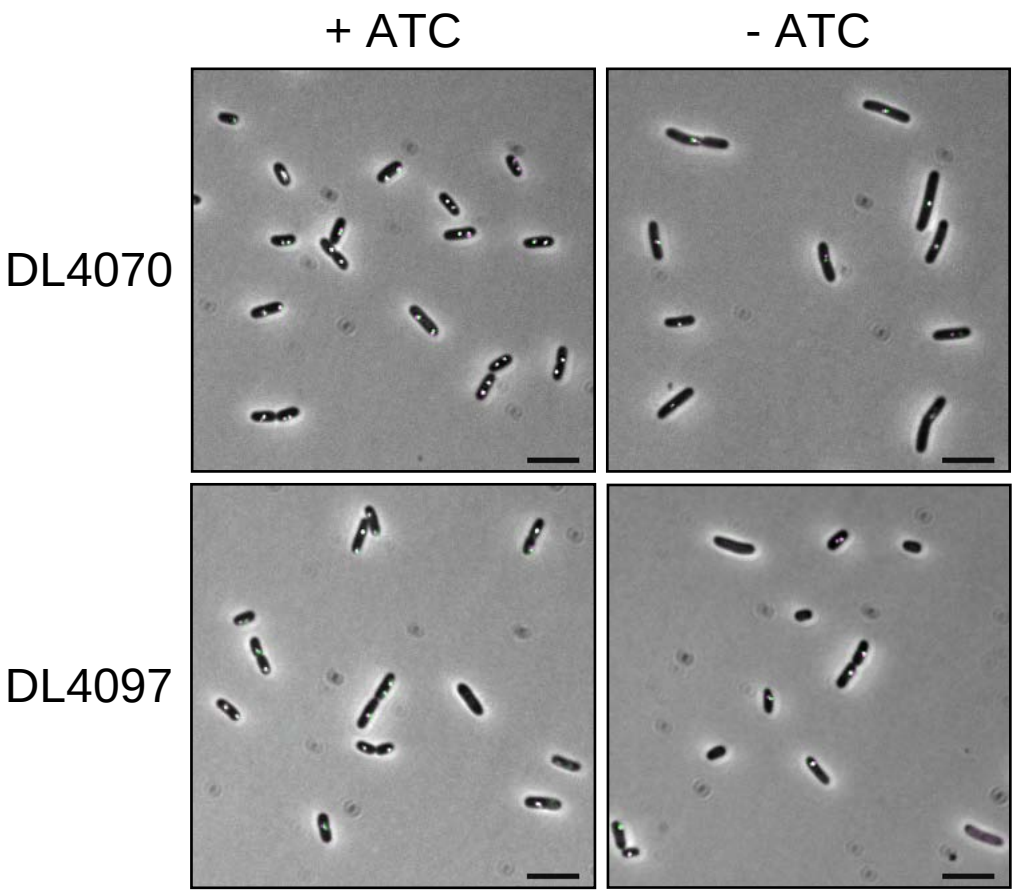

Figure 6.3 Expressing TetR-eYFP and LacI-Cerulean from the chromosome. Strain DL4070 and its Δ*recB* derivative DL4097, both of which express LacI-Cerulean and TetR-eYFP from the chromosome, were grown to mid-exponential phase of growth in M9-minimal medium supplemented with 0.2 % glucose (SbcCD repressed) and 100 ng ml^{-1} ATC (+ ATC) or not (- ATC). CFP signal is pseudocoloured green and YFP magenta. Overlapping CFP and YFP signals appears white. Calibration bar shows 5 μm.

4.5.3). Replication did not appear to be blocked in strain DL4070 when grown in the presence of 100 ng ml^{-1} of ATC (Figure 6.3). Further to this study, the lengths of Δ*recB* cells harbouring a *tetO* and *lacO* array and either expressing TetR-eYFP and LacI-Cerulean from the chromosome (DL4096 and DL4097) or not (DL3543 and DL3544) were compared, (Mark Strebel, unpublished). This showed that there was

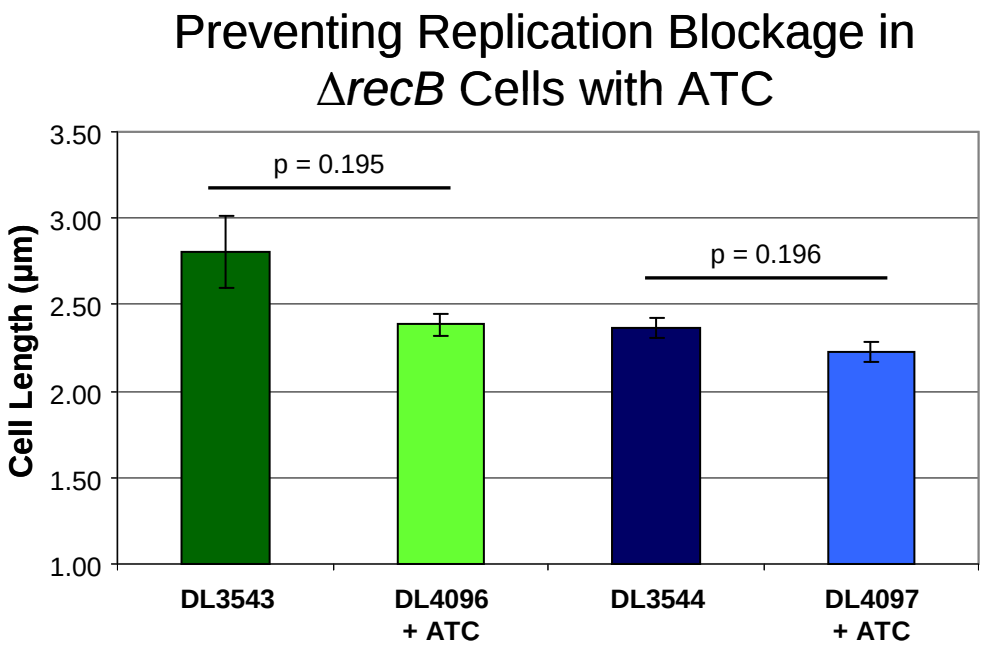

Figure 6.4 Preventing replication blockage in *recB* cells with ATC. Mean cell lengths of Δ*recB* P_{BAD}-*sbcDC* strains harbouring a 246 bp interrupted DNA palindrome at *lacZ* (DL3543 & DL4096) or not (DL3544 & DL4097). All four strains harbour a *tetO* in *cynX* and *lacO* array in *mhpC*, but only DL4096 and DL4097 express TetR-eYFP and LacI-Cerulean (from the chromosome). Strains were grown to mid-exponential phase of growth in M9-minimal medium supplemented with 0.2 % glucose (SbcCD repressed) and either 100 ng ml^{-1} ATC (for DL4096 and DL4097) or not (for DL3543 and DL3544) prior to sampling for microscopy. Cells were imaged at a resolution of 0.129 m per pixel. At least 300 cells were measured in each of 3 independent experiments. 2 sample t-tests were performed using the means of the three independent experiments to obtain p values. These experiments were carried out by Mark Strebel, unpublished.

no significant difference between the cell lengths of strains not expressing TetR-eYFP and isogenic strains expressing TetR-eYFP but grown in the presence of 100 ng ml^{-1} ATC (Figure 6.4). This result shows that 100 ng ml^{-1} of ATC is sufficient to allow replication to proceed through the *tetO* array while allowing a TetR-eYFP focus to form (Figure 6.3).

This experiment also showed that the Δ*recB* strain DL4097 as well as the *recB*$^{+}$ strain DL4070 could be grown in the absence of ATC. This was unexpected because it has been shown that along with RecA and UvrD, RecB is essential for survival if replication progression is blocked by the protein Tus at an ectopic *Ter* site (Bidnenko *et al.*, 2006). It has also been suggested that RecB may be essential for viability if replication is blocked at a *tetO* array by tightly bound TetR-YFP although this study was complicated by the instability of the vector expressing TetR-YFP (Possoz *et al.*, 2006). The requirement for RecB is believed to be caused by a second round of replication colliding with the original blocked fork. This is predicted to result in the collapse of the two new replication forks (Figure 6.5), which would then require homologous recombination to restart (Bidnenko *et al.*, 2002).

It is possible that in the slow growth conditions of the M9-minimal that the original blocked fork can manage to replicate through the *tetO* array before the next round of replication forks collide with it. To test this hypothesis, cells were cultured in nutrient rich L broth medium where the interval between successive rounds of replication are shorter (see section 3.3.4) to increase the likelihood of replication forks colliding following blockage at a TetR-eYFP bound *tetO* array. Strain DL4070 and its Δ*recB* derivative DL4097 which harbour a *tetO* array in the *cynX* gene were grown to an OD_{600} of ~ 0.5 in L broth supplemented with 0.2% glucose (SbcCD

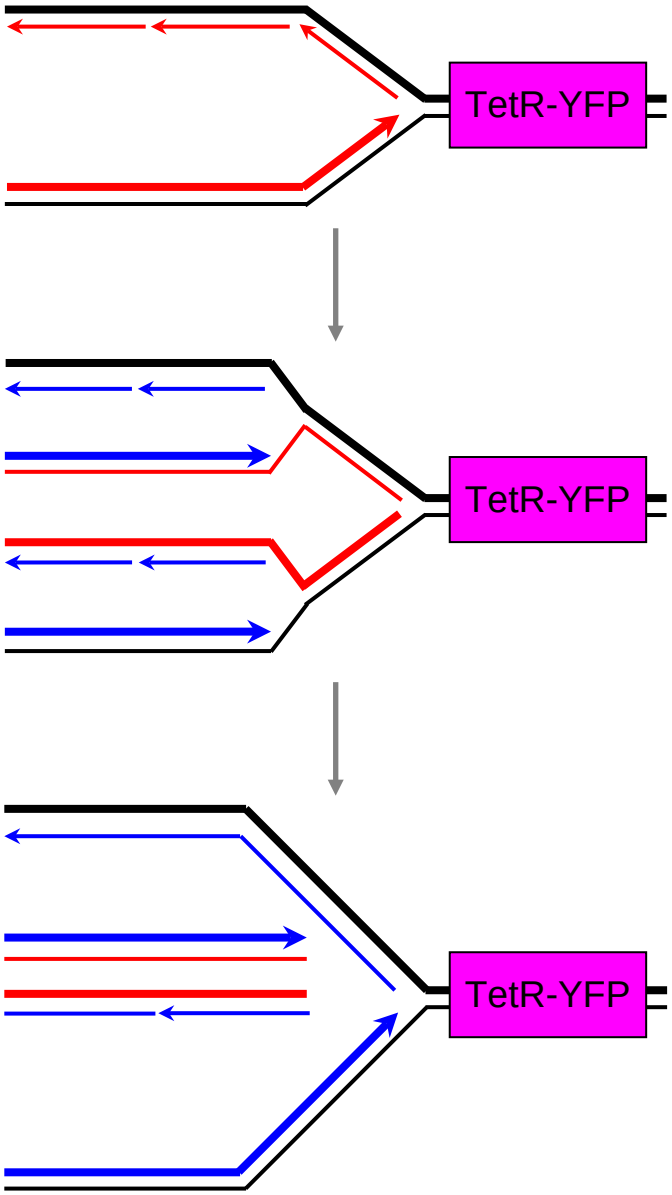

Figure 6.5 Replication fork collapse at a blocked fork. In the absence of the inducer ATC a replication fork will become blocked at the *tetO* array in the *cynX* gene as a result of tightly bound TetR-eYFP protein. Although blocked forks have been shown to be stable, if the block is not relieved then subsequent rounds of replication will collapse at the initial fork. This results in dsDNA ends that require the RecBCD pathway of homologous recombination for repair.

repressed) and either 100 ng ml^{-1} of ATC or not prior to sampling for microscopy. Cells were imaged at a resolution of 0.129 μm per pixel and multiple *z*-sections (± 800 nm, 9 images at a 200 nm interval) of both CFP and YFP signals were captured. Unlike with cells cultured in M9-minimal media, CFP and YFP images were captured with the longer exposure times of 750 ms and 500 ms respectively. Post-acquisition, the stacks of *z*-planes were deconvolved using the software Autodeblur and Autovisualize v9.32 and subsequently combined to give a maximum projection image using MetaMorph 6.3r2. Representative images are shown in Figure 6.6.

As for M9-minimal medium, the Δ*recB* strain DL4097 grew in L broth medium in the absence of any ATC. It is therefore possible that RecB is not essential for viability following replication blockage at a TetR-eYFP bound *tetO* array in these strains. However, unlike when grown in M9-minimal medium (Figure 6.3) the $recB^+$ strain DL4070 has no obvious phenotype suggestive of replication blockage when grown in L broth in the absence of ATC making it possible that TetR-eYFP bound *tetO* array in the *cynX* gene does not provide a proficient roadblock to DNA replication in L broth. It is unclear why ATC would be necessary for normal growth in M9-minimal medium but not L broth medium. The *tetR-eyfp* gene located in *ykgC* is located 46.3 kb upstream (origin proximal) to the *tetO* array in *cynX* and so this observation is not likely to be a result of an increase in the ratio of *tetO* to *tetR-eyfp* in the cell. However, it is possible that expression of TetR-eYFP from the synthetic promoter P_{mw1} is regulated in a cell growth dependent manner by some unknown mechanism.

As for the $recB^+$ strain DL4070, the $recB^-$ strain DL4097 also had a phenotype associated with growth in M9-minimal media in the absence of ATC

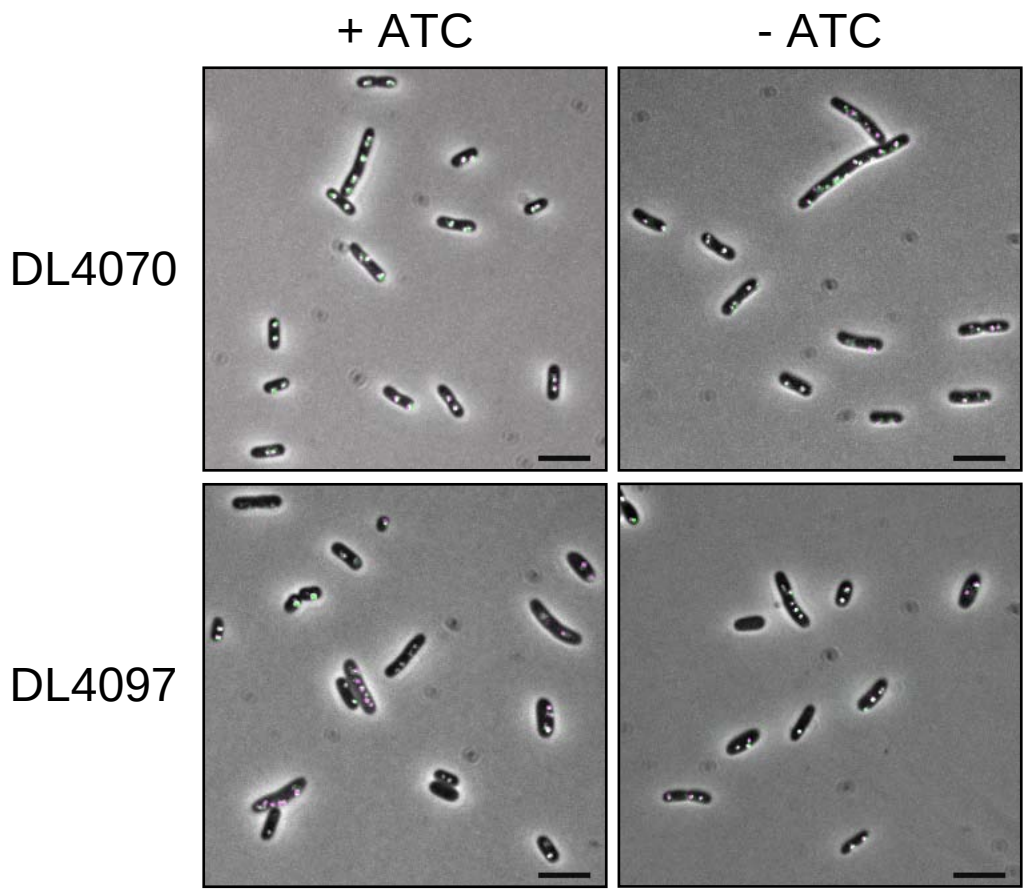

Figure 6.6 Localisation of *lacZ* in L broth in the presence and absence of ATC. Strain DL4070 and its Δ*recB* derivative DL4097, both of which express LacI-Cerulean and TetR-eYFP from the chromosome, were grown to mid-exponential phase of growth in L broth supplemented with 0.2 % glucose (SbcCD repressed) and 100 ng ml^{-1} ATC (+ ATC) or not (- ATC). CFP signal is pseudocoloured green and YFP magenta. Overlapping CFP and YFP signals appears white. Calibration bar shows 5 μm.

(Figure 6.3) making it likely that TetR-eYFP bound *tetO* array was also affecting DNA replication in this strain. However, the phenotype of these cells was clearly distinguishable from that observed for the *recB*$^{+}$ strain DL4070. When grown in M9-minimal medium lacking ATC, DL4070 cells are elongated with a single twin

YFP/CFP spot located at approximately mid-cell. While DL4097 also had many cells with only a single twin YFP/CFP focus, the position of this was not as biased towards being located at mid-cell. Also a significant proportion of the imaged cells had no visible YFP or CFP foci. It is therefore possible that when cultured in M9-minimal medium lacking ATC, DL4097 survives by picking up suppressor mutations that prevent replication from being blocked at the *tetO* array. Since these cells have neither YFP nor CFP foci and the selection should only be on the TetR-eYFP and *tetO* array, it is probable that any potential suppressor mutation is affecting transcription of the P_{mw1}-*lacI-cerulean,tetR-eyfp* operon rather than the *tetO* array.

6.5 Conclusions

Since a number of recombination mutations such as *recB*$^-$ and *recG*$^-$ show high levels of plasmid instability, it was necessary to develop a plasmid free system for visualising the DNA flanking an induced DSB by fluorescence microscopy. The strategy employed to do this was to integrate the *tetR-eyfp* and *lacI-cerulean* genes into the chromosome of strains harbouring the 'superconstruct' (Chapter 4). The promoter P_{ftsKi}, which had been successfully employed to express TetR-eYFP and LacI-Cerulean from a high copy number plasmid, was shown not to drive enough expression of the TetR-eYFP and LacI-Cerulean proteins for fluorescence imaging of the *tetO* and *lacO* array when present on a low copy number plasmid. It was therefore necessary to use an alternative promoter for expressing TetR-eYFP and LacI-Cerulean from the chromosome.

Although P_{ftsKi} was deemed unsuitable for controlling the expression of TetR-eYFP and LacI-Cerulean from the chromosome, it had the desirable quality of being

a constitutive promoter. To create a synthetic promoter that would constitutively express TetR-eYFP and LacI-Cerulean from the chromosome to a level that would allow bright YFP and CFP foci to be imaged in strains harbouring a *tetO* and *lacO* array, the -10 and -35 elements of P_{ftsKi} on plasmid pDL3718 were mutated to consensus by SDM to generate the promoter P_{mw1}. Following the observation that this promoter expressed high levels of the fluorescent repressor proteins when present on the low copy number plasmid pDL3718, the operon P_{mw1}-*lacI-cerulean,tetR-eyfp* was cloned into a PMGR vector and subsequently integrated into the *ykgC* gene of strains harbouring the superconstruct.

Expression of TetR-eYFP and LacI-Cerulean from the chromosome was shown to produce bright YFP and CFP foci in both *recB*$^+$ and Δ*recB* strains harbouring a *tetO* array in *cynX* and a *lacO* array in *mhpC* when grown in either M9-minimal or L broth media. In the recombination proficient strain DL4070, TetR-eYFP was shown to be present at a high enough concentration to block replication at the *tetO* array in *cynX* if cultured in M9-minimal medium in the absence of the inducer ATC. Interestingly, no phenotype was observed when DL4070 was cultured in L broth in the absence of ATC that would indicate that TetR-YFP bound *tetO* was blocking replication. It is unclear why this protein would block replication in the slow growth conditions of M9-minimal media but not the fast growth conditions of L broth.

Finally, despite clear indications that replication was blocked in DL4070 when cultured in M9-minimal medium lacking ATC, a Δ*recB* derivative (DL4097) was viable in the same growth conditions. RecB has previously been shown to be essential for cellular viability when a second round of replication collides with a

blocked fork to produce dsDNA ends (Bidnenko *et al.*, 2002; Possoz *et al.*, 2006). Although it is possible that replication forks did not collide in this situation, or that replication fork progression was not blocked in the first place, there was a phenotype associated with the growth of DL4097 in M9-minimal medium lacking ATC. Unlike the *recB*$^{+}$ strain DL4070, the most striking consequence of growth in M9-minimal medium lacking ATC was the appearance of a large subpopulation of cells with no visible YFP or CFP foci. It is possible that these cells have picked up suppressor mutations that inhibit expression of TetR-eYFP and LacI-Cerulean.

Chapter 7

Conclusions and Further Work

7.1 Conclusions

The combination of an inducible system for the expression of the hairpin endonuclease SbcCD with the chromosomal insertion of a 246 bp interrupted DNA palindrome has proved to be a unique and powerful tool for the study of DNA DSB repair in *E. coli*. This is because induction of SbcCD expression results in the cleavage of a DNA hairpin formed by the palindrome on the lagging strand template of replication to form a DSB as opposed to cleaving all copies of the palindrome (Eykelenboom *et al.*, 2008). The aim of this thesis was to exploit this system to investigate the effect of a single chromosomal DSB on the dynamics of the *E. coli* cell cycle, primarily through the use of genetics and cell biology techniques.

Cleavage of the palindrome by SbcCD was shown to result in the induction of the SOS response and that this induction was essential, specifically in order to increase expression of the recombinase RecA (John Eykelenboom, unpublished). This requirement for increased RecA expression was investigated in more detail and shown only to occur when cells were cultured in chronic DSB induced conditions and to be less extreme in slow growth conditions. This suggests that a single DSB can be efficiently repaired in the absence of SOS induction.

The observation that exponential growth in DSB induced conditions had no detectable effect on the generation time and viability of a recombination proficient strain (John Eykelenboom, unpublished) was investigated in more detail by microscopy. Analysis of cell lengths showed that DSB induction resulted in mild inhibition of cell division, with cells grown in DSB induced conditions ~11 % longer than controls. Since the SOS response had been shown to be induced in these growth conditions, it was hypothesised that the SOS inducible inhibitor of cell division SfiA

may be responsible for this increase in cell length. Δ*sfiA* mutants were constructed and used to show that SfiA is not essential for cellular viability following cleavage of a 246 bp palindrome by SbcCD in either fast or slow growth conditions. Following this investigation, induction of SfiA was shown to be the main factor responsible for the delay in cell division caused by cleavage of the palindrome by SbcCD (Elise Darmon, unpublished).

DAPI staining of condensed nucleoids was then used to test the effect of DSB induction on chromosome segregation. This revealed that as well as causing a delay in cell division, cleavage of the palindrome by SbcCD also caused a delay in chromosome segregation as revealed by the significant increase in the number of cells with only a single visible nucleoid. Although the two phenomena may not be linked, it is possible that in the absence of SfiA nucleoid occlusion is responsible for the remaining delay in cell division.

The effect of continual growth in DSB induced conditions on the cell cycle of *E. coli* was modelled in an attempt to explain the observation that despite causing an increase in average cell length, no effect of DSB induction was detected on generation time. This model predicted that by keeping the frequency of replication initiation constant, generation time would only increase in the first generation of DSB induction. Not only this, but because growth rate increases exponentially, this extra cell mass would be maintained through subsequent generations despite the generation time returning to that observed prior to DSB induction. This model therefore helps to consolidate these two apparently conflicting observations, as well as explain how cell mass and generation time can equilibrate in chronic DSB induced growth conditions.

To better investigate the effect of DSB repair on the dynamics of chromosome segregation in *E. coli*, a construct was designed and build into the chromosome that would allow the cellular locations of the DNA flanking a site-specific DSB to be followed by fluorescence microscopy. Briefly this involved flanking a 246 bp interrupted DNA palindrome (located in *lacZ*) with an array of *tetO* and an array of *lacO* sites in a P_{BAD}-*sbcDC* strain that expressed the fluorescent repressor proteins TetR-YFP and LacI-CFP.

TetR-YFP and LacI-CFP bind the *tetO* and *lacO* array respectively resulting in an increased local concentration of the proteins and hence formation of fluorescent foci. It was shown that cells lacking the operator arrays but expressing TetR-YFP and LacI-CFP did not have YFP or CFP foci indicating that the presence of fluorescent foci provides a robust method for identifying the location of the operator arrays. Also, a functional TetR-mCherry fusion protein was created for use as an alternative to TetR-YFP in the dual labelling of *tetO* and *lacO* arrays with LacI-CFP. Although not used in this study, the combination of TetR-mCherry and LacI-CFP for the dual labelling of *tetO* and *lacO* arrays would allow this system to be used in conjunction with either a GFP or YFP fusion protein of interest.

Two approaches were used to improve the imaging of the *lacO* array. First *lacI* was deleted from the chromosome to prevent competitive binding of LacI with LacI-CFP and prevent spurious recombination with the plasmid harbouring *lacI-cfp*. Second, the CFP fused to LacI was changed from enhanced CFP to a brighter and more photostable mutant of CFP known as Cerulean (Rizzo *et al.*, 2004). Finally, an array of three Chi sites was integrated into the chromosome either side of the palindrome to prevent resection of the operator arrays by RecBCD following

cleavage of the palindrome by SbcCD. This genome of this strain (DL3276) was then sequenced using Solexa technology which showed that no single base pair mutations or small (less than 3 bp) insertions or deletions were introduced during the construction process. Unfortunately this approach lacked the ability to detect insertion or deletions larger than 3 bp.

To complement this system, a similar strain was constructed that had an alternative, replication independent, method of inducing a site-specific DSB in the *lacZ* gene. Briefly, this involved placing expression of the homing endonuclease I-SceI under the control of the arabinose inducible promoter P_{BAD} and integrating this construct in a strain with an endogenous *sbcDC* operon and a unique I-$SceI_{cs}$ in place of the palindrome in the *lacZ* gene. The functionality of this system was tested genetically by comparing the viabilities of a recombination proficient and a *recA*$^-$ strain under conditions of an I-SceI induced DSB. I-SceI induced DSBs have the capacity to either prevent repair by cleaving all sister chromosomes or preventing exit from SOS by continually cleaving repaired DNA. Therefore the cellular concentration of I-SceI was optimised by titration of inducer (arabinose) concentration to an extent where a recombination proficient strain was fully viable, but a recombination deficient (*recA*) strain had at least 90 % reduction in viability.

In agreement with published data (Possoz *et al.*, 2006), operator bound TetR-YFP was shown to block replication in the absence of its cognate inducer ATC. However, a combination of growth curves, viability and cytological analysis showed that no block to replication could be detected at the *tetO* array when TetR-YFP was expressed in the presence of 100 ng ml^{-1} ATC. Following deletion of *lacI*, no

replication block at the *lacO* array by operator bound LacI-CFP could be detected, even in the absence of its cognate inducer IPTG.

YFP and CFP foci representing *tetO* and *lacO* arrays separated by ~ 11 kb on the same sister chromosome were shown to often overlap, but to not completely co-localise. The distance between the centroids of these foci was measured and found to be ~ 210 nm on average. The accuracy of this measurement could be improved by using images acquired at a higher resolution (*e.g.* 64.5 nm per pixel as opposed to 129 nm per pixel) because by identifying the centroids, this technique overcomes the limitations imposed by the optical resolution of light microscopes. Also, the use of shorter exposure times between the acquisition of YFP and CFP images would be beneficial in order to reduce the possibility that the position of both the *tetO* and *lacO* array has moved between the sequential image acquisitions.

Although average distance between neighbouring YFP and CFP foci centroids was not affected by either the presence of the 246 bp interrupted palindrome or expression of SbcCD, more cells with foci located > 500 nm apart were observed when SbcCD was expressed in cells harbouring the palindrome compared to the three controls. It is possible that some of these cells represent instances where the palindrome has been cleaved by SbcCD causing the two DNA ends of the break to separate during the process of repair.

Since SbcCD specifically cleaves a DNA hairpin formed on the lagging but not the leading strand template of replication, it has the ability to distinguish two genetically identical sister chromosomes. This ability was exploited to distinguish three possibilities for the establishment of translational symmetry of sister chromosomes during chromosome segregation in slow growth conditions (Nielsen *et*

al., 2006b; Wang *et al.*, 2006). This resulted in evidence for the non-random segregation of sister chromosomes in *E. coli* (White *et al.*, 2008).

Finally, it became apparent that the use of a plasmid vector for the expression of TetR-YFP and LacI-CFP was less than ideal due to the fact that some recombination mutants (*e.g. recB*$^-$, *recD*$^-$, and *recG*$^-$) show high levels of plasmid instability. It was therefore desirable to integrate the genes encoding TetR-YFP and LacI-CFP into the chromosome. By first cloning these genes into the low copy number plasmid pGB2 it was clear that the constitutive promoter P_{ftsKi} would not result in the transcription of enough of the fluorescent repressor proteins to form bright foci at the operator arrays if present as a single copy in the chromosome. To overcome this problem, a synthetic promoter based on P_{ftsKi} was created that would keep the attractive quality that P_{ftsKi} had of being a constitutive promoter, but would drive expression of the genes under its control to a higher level.

The DNA sequence known to contain P_{ftsKi} was studied in detail, and putative UP, -35 and -10 elements identified. Strikingly P_{ftsKi} lacked an identifiable extended -10 element. Although the lack of an extended -10 element may the primary factor responsible for P_{ftsKi} being a weak promoter, the strategy employed for increasing the strength of P_{ftsKi} was to mutate its -35 and -10 elements to consensus. This strategy was successful and a cassette with *tetR-yfp* and *lacI-cfp* under the control of the new promoter (named P_{mw1}) was integrated in the *ykgC* gene of the chromosome of *E. coli*. Expression of TetR-YFP and LacI-CFP from this cassette was shown to be high enough to form bright fluorescent foci at the *tetO* and *lacO* arrays in cells cultured in both M9-minimal medium and L broth. This system should provide a useful tool in

the study of chromosome dynamics following an induced DSB in the chromosome of *E. coli*.

7.2 Future Work

Strains of *E. coli* were constructed that have the potential to allow DSB repair by homologous recombination to followed in single cells and in real time by fluorescence microscopy. By investigating the cellular events that follow DSB induction in recombination proficient cells in real time by time-lapse microscopy and observing the 'recombination intermediates' that should accumulate in recombination mutants (*e.g.* Δ*recB* and Δ*ruvABC*), it should be possible to build up a picture of how the events of DSB repair are co-ordinated within the cell. Of particular interest is the question of whether or not RecA-mediated homology search is random or directed.

Also, this system of cytological analysis of DSBs provides another method of assigning phenotypes to recombination mutants. As well as having the potential to better understand why certain proteins are essential following an induced DSB; this may help elucidate the role of proteins whose functions remain unclear. A good example of this would be a comparison of the phenotypes of Δ*ruvABC* and Δ*recG* mutants since both RuvABC and RecG are essential following cleavage of a DNA hairpin by SbcCD, even though RecG is often believed to act as an alternative mechanism of Holliday junction resolution (Meddows *et al.*, 2004).

Finally, as well as studying the co-ordination of DNA within cells following an induced DSB via the use of fluorescent repressor bound operator arrays, it would also be interesting to investigate the dynamics of repair proteins at the site of the

DSB. The use of TetR-YFP and LacI-CFP in the dual labelling of the DNA flanking the DSB site could be used in conjunction with RFP based fusion proteins. Alternatively, the TetR-mCherry fusion protein constructed in this study could be used along with LacI-CFP for the dual labelling of the operator arrays allowing the dynamics of either GFP or YFP based fusion proteins to be investigated at the site of an induced DSB.

References

Alberts, B.M., Barry, J., Bedinger, P., Formosa, T., Jongeneel, C.V., and Kreuzer, K.N. (1983). Studies on DNA replication in the bacteriophage T4 in vitro system. Cold Spring Harbor symposia on quantitative biology *47 Pt 2*, 655-668.

Allard, J.F., and Cytrynbaum, E.N. (2009). Force generation by a dynamic Z-ring in *Escherichia coli* cell division. Proc Natl Acad Sci U S A *106*, 145-150.

Anderson, D.G., and Kowalczykowski, S.C. (1998). Reconstitution of an SOS response pathway: derepression of transcription in response to DNA breaks. Cell *95*, 975-979.

Aussel, L., Barre, F.X., Aroyo, M., Stasiak, A., Stasiak, A.Z., and Sherratt, D. (2002). FtsK Is a DNA motor protein that activates chromosome dimer resolution by switching the catalytic state of the XerC and XerD recombinases. Cell *108*, 195-205.

Bach, T., Krekling, M.A., and Skarstad, K. (2003). Excess SeqA prolongs sequestration of *oriC* and delays nucleoid segregation and cell division. EMBO J *22*, 315-323.

Bach, T., and Skarstad, K. (2004). Re-replication from non-sequesterable origins generates three-nucleoid cells which divide asymmetrically. Mol Microbiol *51*, 1589-1600.

Bailey, S., Eliason, W.K., and Steitz, T.A. (2007). Structure of hexameric DnaB helicase and its complex with a domain of DnaG primase. Science (New York, NY *318*, 459-463.

Barzel, A., and Kupiec, M. (2008). Finding a match: how do homologous sequences get together for recombination? Nat Rev Genet *9*, 27-37.

Bates, D., and Kleckner, N. (2005). Chromosome and replisome dynamics in *E. coli*: loss of sister cohesion triggers global chromosome movement and mediates chromosome segregation. Cell *121*, 899-911.

Beam, C.E., Saveson, C.J., and Lovett, S.T. (2002). Role for *radA/sms* in recombination intermediate processing in *Escherichia coli*. J Bacteriol *184*, 6836-6844.

Bell, C.E. (2005). Structure and mechanism of *Escherichia coli* RecA ATPase. Mol Microbiol *58*, 358-366.

Ben-Yehuda, S., Rudner, D.Z., and Losick, R. (2003). Assembly of the SpoIIIE DNA translocase depends on chromosome trapping in *Bacillus subtilis*. Curr Biol *13*, 2196-2200.

Berkmen, M.B., and Grossman, A.D. (2006). Spatial and temporal organization of the *Bacillus subtilis* replication cycle. Mol Microbiol *62*, 57-71.

Bernander, R., and Nordstrom, K. (1990). Chromosome replication does not trigger cell division in *E. coli*. Cell *60*, 365-374.

Bernhardt, T.G., and de Boer, P.A. (2005). SlmA, a nucleoid-associated, FtsZ binding protein required for blocking septal ring assembly over chromosomes in *E. coli*. Molecular cell *18*, 555-564.

Bettencourt-Dias, M., and Glover, D.M. (2007). Centrosome biogenesis and function: centrosomics brings new understanding. Nature reviews *8*, 451-463.

Bidnenko, V., Ehrlich, S.D., and Michel, B. (2002). Replication fork collapse at replication terminator sequences. Embo J *21*, 3898-3907.

Bidnenko, V., Lestini, R., and Michel, B. (2006). The *Escherichia coli* UvrD helicase is essential for Tus removal during recombination-dependent replication restart from *Ter* sites. Mol Microbiol *62*, 382-396.

Biek, D.P., and Cohen, S.N. (1986). Identification and characterization of *recD*, a gene affecting plasmid maintenance and recombination in *Escherichia coli*. J Bacteriol *167*, 594-603.

Bigot, S., Saleh, O.A., Lesterlin, C., Pages, C., El Karoui, M., Dennis, C., Grigoriev, M., Allemand, J.F., Barre, F.X., and Cornet, F. (2005). KOPS: DNA motifs that control *E. coli* chromosome segregation by orienting the FtsK translocase. EMBO J *24*, 3770-3780.

Bigot, S., Sivanathan, V., Possoz, C., Barre, F.X., and Cornet, F. (2007). FtsK, a literate chromosome segregation machine. Mol Microbiol *64*, 1434-1441.

Blakely, G., May, G., McCulloch, R., Arciszewska, L.K., Burke, M., Lovett, S.T., and Sherratt, D.J. (1993). Two related recombinases are required for site-specific recombination at *dif* and *cer* in *E. coli* K12. Cell *75*, 351-361.

Blakely, G.W., Davidson, A.O., and Sherratt, D.J. (2000). Sequential strand exchange by XerC and XerD during site-specific recombination at *dif*. The Journal of biological chemistry *275*, 9930-9936.

Blattner, F.R., Plunkett, G., 3rd, Bloch, C.A., Perna, N.T., Burland, V., Riley, M., Collado-Vides, J., Glasner, J.D., Rode, C.K., Mayhew, G.F., *et al.* (1997). The complete genome sequence of *Escherichia coli* K-12. Science (New York, NY *277*, 1453-1474.

Boeneman, K., Fossum, S., Yang, Y., Fingland, N., Skarstad, K., and Crooke, E. (2009). *Escherichia coli* DnaA forms helical structures along the longitudinal cell axis distinct from MreB filaments. Mol Microbiol.

Borde, V. (2007). The multiple roles of the Mre11 complex for meiotic recombination. Chromosome Res *15*, 551-563.

Bowman, G.R., Comolli, L.R., Zhu, J., Eckart, M., Koenig, M., Downing, K.H., Moerner, W.E., Earnest, T., and Shapiro, L. (2008). A polymeric protein anchors the chromosomal origin/ParB complex at a bacterial cell pole. Cell *134*, 945-955.

Boye, E., Stokke, T., Kleckner, N., and Skarstad, K. (1996). Coordinating DNA replication initiation with cell growth: differential roles for DnaA and SeqA proteins. Proc Natl Acad Sci U S A *93*, 12206-12211.

Breier, A.M., Weier, H.U., and Cozzarelli, N.R. (2005). Independence of replisomes in *Escherichia coli* chromosomal replication. Proc Natl Acad Sci U S A *102*, 3942-3947.

Brent, R., and Ptashne, M. (1981). Mechanism of action of the *lexA* gene product. Proc Natl Acad Sci U S A *78*, 4204-4208.

Browning, D.F., and Busby, S.J. (2004). The regulation of bacterial transcription initiation. Nat Rev Microbiol *2*, 57-65.

Cadman, C.J., and McGlynn, P. (2004). PriA helicase and SSB interact physically and functionally. Nucleic acids research *32*, 6378-6387.

Cairns, J. (1975). Mutation selection and the natural history of cancer. Nature *255*, 197-200.

Camara, J.E., Breier, A.M., Brendler, T., Austin, S., Cozzarelli, N.R., and Crooke, E. (2005). Hda inactivation of DnaA is the predominant mechanism preventing hyperinitiation of *Escherichia coli* DNA replication. EMBO Rep *6*, 736-741.

Campbell, E.A., Muzzin, O., Chlenov, M., Sun, J.L., Olson, C.A., Weinman, O., Trester-Zedlitz, M.L., and Darst, S.A. (2002). Structure of the bacterial RNA polymerase promoter specificity sigma subunit. Molecular cell *9*, 527-539.

Canovas, J.L., Tresguerres, E.F., Yousif, A.M., Lopez-Saez, J.F., and Navarrete, M.H. (1984). DNA segregation in *Escherichia coli* cells with 5-bromodeoxyuridine-substituted nucleoids. J Bacteriol *158*, 128-133.

Carlson, J.G. (1956). On the mitotic movements of chromosomes. Science (New York, NY *124*, 203-206.

Chai, N.C., and Lark, K.G. (1970). Cytological studies of deoxyribonucleic acid replication in *Escherichia coli* 15T-: replication at slow growth rates and after a shift-up into rich medium. J Bacteriol *104*, 401-409.

Champoux, J.J. (2001). DNA topoisomerases: structure, function, and mechanism. Annual review of biochemistry *70*, 369-413.

Chen, J.C., and Beckwith, J. (2001). FtsQ, FtsL and FtsI require FtsK, but not FtsN, for co-localization with FtsZ during *Escherichia coli* cell division. Mol Microbiol *42*, 395-413.

Chen, Z., Yang, H., and Pavletich, N.P. (2008). Mechanism of homologous recombination from the RecA-ssDNA/dsDNA structures. Nature *453*, 489-484.

Chodavarapu, S., Felczak, M.M., Yaniv, J.R., and Kaguni, J.M. (2008). *Escherichia col*i DnaA interacts with HU in initiation at the *E. coli* replication origin. Mol Microbiol *67*, 781-792.

Churchward, G., Belin, D., and Nagamine, Y. (1984). A pSC101-derived plasmid which shows no sequence homology to other commonly used cloning vectors. Gene *31*, 165-171.

Cohen, A., and Clark, A.J. (1986). Synthesis of linear plasmid multimers in *Escherichia coli* K-12. J Bacteriol *167*, 327-335.

Colloms, S.D., McCulloch, R., Grant, K., Neilson, L., and Sherratt, D.J. (1996). Xer-mediated site-specific recombination in vitro. Embo J *15*, 1172-1181.

Connelly, J.C., de Leau, E.S., and Leach, D.R. (1999). DNA cleavage and degradation by the SbcCD protein complex from *Escherichia coli*. Nucleic acids research *27*, 1039-1046.

Connelly, J.C., de Leau, E.S., Okely, E.A., and Leach, D.R. (1997). Overexpression, purification, and characterization of the SbcCD protein from *Escherichia coli*. The Journal of biological chemistry *272*, 19819-19826.

Connelly, J.C., Kirkham, L.A., and Leach, D.R. (1998). The SbcCD nuclease of *Escherichia coli* is a structural maintenance of chromosomes (SMC) family protein that cleaves hairpin DNA. Proc Natl Acad Sci U S A *95*, 7969-7974.

Connelly, J.C., and Leach, D.R. (2002). Tethering on the brink: the evolutionarily conserved Mre11-Rad50 complex. Trends Biochem Sci *27*, 410-418.

Cooper, S. (2006). Regulation of DNA synthesis in bacteria: Analysis of the Bates/Kleckner licensing/initiation-mass model for cell cycle control. Mol Microbiol *62*, 303-307.

Cooper, S., Schwimmer, M., and Scanlon, S. (1978). Probabilistic behavior of DNA segregation in *Escherichia coli*. J Bacteriol *134*, 60-65.

Cordell, S.C., Robinson, E.J., and Lowe, J. (2003). Crystal structure of the SOS cell division inhibitor SulA and in complex with FtsZ. Proc Natl Acad Sci U S A *100*, 7889-7894.

Corn, J.E., and Berger, J.M. (2006). Regulation of bacterial priming and daughter strand synthesis through helicase-primase interactions. Nucleic acids research *34*, 4082-4088.

Corn, J.E., Pelton, J.G., and Berger, J.M. (2008). Identification of a DNA primase template tracking site redefines the geometry of primer synthesis. Nat Struct Mol Biol *15*, 163-169.

Courcelle, J., Khodursky, A., Peter, B., Brown, P.O., and Hanawalt, P.C. (2001). Comparative gene expression profiles following UV exposure in wild-type and SOS-deficient *Escherichia coli*. Genetics *158*, 41-64.

Cox, J.M., Li, H., Wood, E.A., Chitteni-Pattu, S., Inman, R.B., and Cox, M.M. (2008). Defective dissociation of a "slow" RecA mutant protein imparts an *Escherichia coli* growth defect. The Journal of biological chemistry *283*, 24909-24921.

Cromie, G.A., Connelly, J.C., and Leach, D.R. (2001). Recombination at double-strand breaks and DNA ends: conserved mechanisms from phage to humans. Molecular cell *8*, 1163-1174.

Cromie, G.A., Hyppa, R.W., Taylor, A.F., Zakharyevich, K., Hunter, N., and Smith, G.R. (2006). Single Holliday junctions are intermediates of meiotic recombination. Cell *127*, 1167-1178.

Cromie, G.A., Millar, C.B., Schmidt, K.H., and Leach, D.R. (2000). Palindromes as substrates for multiple pathways of recombination in *Escherichia coli*. Genetics *154*, 513-522.

Cui, Y., Petrushenko, Z.M., and Rybenkov, V.V. (2008). MukB acts as a macromolecular clamp in DNA condensation. Nat Struct Mol Biol *15*, 411-418.

Dajkovic, A., Lan, G., Sun, S.X., Wirtz, D., and Lutkenhaus, J. (2008). MinC spatially controls bacterial cytokinesis by antagonizing the scaffolding function of FtsZ. Curr Biol *18*, 235-244.

Danilova, O., Reyes-Lamothe, R., Pinskaya, M., Sherratt, D., and Possoz, C. (2007). MukB colocalizes with the *oriC* region and is required for organization of the two *Escherichia coli* chromosome arms into separate cell halves. Mol Microbiol *65*, 1485-1492.

Darmon, E., Lopez-Vernaza, M.A., Helness, A.C., Borking, A., Wilson, E., Thacker, Z., Wardrope, L., and Leach, D.R. (2007). SbcCD regulation and localization in *Escherichia coli*. J Bacteriol *189*, 6686-6694.

Della, M., Palmbos, P.L., Tseng, H.M., Tonkin, L.M., Daley, J.M., Topper, L.M., Pitcher, R.S., Tomkinson, A.E., Wilson, T.E., and Doherty, A.J. (2004). Mycobacterial Ku and ligase proteins constitute a two-component NHEJ repair machine. Science (New York, NY *306*, 683-685.

DeLuca, J.G. (2007). Spindle microtubules: getting attached at both ends. Curr Biol *17*, R966-969.

Dillingham, M.S., and Kowalczykowski, S.C. (2008). RecBCD enzyme and the repair of double-stranded DNA breaks. Microbiol Mol Biol Rev *72*, 642-671, Table of Contents.

Dillingham, M.S., Spies, M., and Kowalczykowski, S.C. (2003). RecBCD enzyme is a bipolar DNA helicase. Nature *423*, 893-897.

Donachie, W.D. (1968). Relationship between cell size and time of initiation of DNA replication. Nature *219*, 1077-1079.

Duggin, I.G., and Bell, S.D. (2009). Termination structures in the *Escherichia coli* chromosome replication fork trap. Journal of molecular biology *387*, 532-539.

Duggin, I.G., Wake, R.G., Bell, S.D., and Hill, T.M. (2008). The replication fork trap and termination of chromosome replication. Mol Microbiol *70*, 1323-1333.

Dworkin, J., and Losick, R. (2002). Does RNA polymerase help drive chromosome segregation in bacteria? Proc Natl Acad Sci U S A *99*, 14089-14094.

Ebersbach, G., Briegel, A., Jensen, G.J., and Jacobs-Wagner, C. (2008a). A self-associating protein critical for chromosome attachment, division, and polar organization in *Caulobacter*. Cell *134*, 956-968.

Ebersbach, G., Galli, E., Moller-Jensen, J., Lowe, J., and Gerdes, K. (2008b). Novel coiled-coil cell division factor ZapB stimulates Z ring assembly and cell division. Mol Microbiol *68*, 720-735.

Eggleston, A.K., and West, S.C. (2000). Cleavage of holliday junctions by the *Escherichia coli* RuvABC complex. The Journal of biological chemistry *275*, 26467-26476.

Elmore, S., Muller, M., Vischer, N., Odijk, T., and Woldringh, C.L. (2005). Single-particle tracking of *oriC*-GFP fluorescent spots during chromosome segregation in *Escherichia coli*. Journal of structural biology *151*, 275-287.

Erill, I., Campoy, S., and Barbe, J. (2007). Aeons of distress: an evolutionary perspective on the bacterial SOS response. FEMS Microbiol Rev *31*, 637-656.

Errington, J., Daniel, R.A., and Scheffers, D.J. (2003). Cytokinesis in bacteria. Microbiol Mol Biol Rev *67*, 52-65, table of contents.

Esnault, E., Valens, M., Espeli, O., and Boccard, F. (2007). Chromosome structuring limits genome plasticity in *Escherichia coli*. PLoS Genet *3*, e226.

Espeli, O., Nurse, P., Levine, C., Lee, C., and Marians, K.J. (2003). SetB: an integral membrane protein that affects chromosome segregation in *Escherichia coli*. Mol Microbiol *50*, 495-509.

Eykelenboom, J.K., Blackwood, J.K., Okely, E., and Leach, D.R. (2008). SbcCD causes a double-strand break at a DNA palindrome in the *Escherichia coli* chromosome. Molecular cell *29*, 644-651.

Farah, J.A., Cromie, G., Steiner, W.W., and Smith, G.R. (2005). A novel recombination pathway initiated by the Mre11/Rad50/Nbs1 complex eliminates palindromes during meiosis in *Schizosaccharomyces pombe*. Genetics *169*, 1261-1274.

Fekete, R.A., and Chattoraj, D.K. (2005). A cis-acting sequence involved in chromosome segregation in *Escherichia coli*. Mol Microbiol *55*, 175-183.

Fossum, S., Crooke, E., and Skarstad, K. (2007). Organization of sister origins and replisomes during multifork DNA replication in *Escherichia coli*. Embo J *26*, 4514-4522.

Foti, J.J., Schienda, J., Sutera, V.A., Jr., and Lovett, S.T. (2005). A bacterial G protein-mediated response to replication arrest. Molecular cell *17*, 549-560.

Franke, G.C., Dobinsky, S., Mack, D., Wang, C.J., Sobottka, I., Christner, M., Knobloch, J.K., Horstkotte, M.A., Aepfelbacher, M., and Rohde, H. (2007). Expression and functional characterization of *gfpmut3.1* and its unstable variants in *Staphylococcus epidermidis*. Journal of microbiological methods *71*, 123-132.

Fujimitsu, K., Senriuchi, T., and Katayama, T. (2009). Specific genomic sequences of *E. coli* promote replicational initiation by directly reactivating ADP-DnaA. Genes Dev *23*, 1221-1233.

Gao, D., and McHenry, C.S. (2001a). tau binds and organizes *Escherichia coli* replication proteins through distinct domains. Domain IV, located within the unique C terminus of tau, binds the replication fork, helicase, DnaB. The Journal of biological chemistry *276*, 4441-4446.

Gao, D., and McHenry, C.S. (2001b). tau binds and organizes *Escherichia coli* replication through distinct domains. Partial proteolysis of terminally tagged tau to determine candidate domains and to assign domain V as the alpha binding domain. The Journal of biological chemistry *276*, 4433-4440.

Gao, G., Bi, X., Chen, J., Srikanta, D., and Rong, Y.S. (2009). Mre11-Rad50-Nbs complex is required to cap telomeres during *Drosophila* embryogenesis. Proc Natl Acad Sci U S A *106*, 10728-10733.

Gerton, J.L., and Hawley, R.S. (2005). Homologous chromosome interactions in meiosis: diversity amidst conservation. Nat Rev Genet *6*, 477-487.

Gitai, Z., Dye, N.A., Reisenauer, A., Wachi, M., and Shapiro, L. (2005). MreB actin-mediated segregation of a specific region of a bacterial chromosome. Cell *120*, 329-341.

Goehring, N.W., and Beckwith, J. (2005). Diverse paths to midcell: assembly of the bacterial cell division machinery. Curr Biol *15*, R514-526.

Goehring, N.W., Gonzalez, M.D., and Beckwith, J. (2006). Premature targeting of cell division proteins to midcell reveals hierarchies of protein interactions involved in divisome assembly. Mol Microbiol *61*, 33-45.

Goehring, N.W., Robichon, C., and Beckwith, J. (2007). Role for the nonessential N terminus of FtsN in divisome assembly. J Bacteriol *189*, 646-649.

Gonzalez, M.D., and Beckwith, J. (2009). Divisome under construction: distinct domains of the small membrane protein FtsB are necessary for interaction with multiple cell division proteins. J Bacteriol *191*, 2815-2825.

Gottesman, S., Halpern, E., and Trisler, P. (1981). Role of *sulA* and *sulB* in filamentation by *lon* mutants of *Escherichia coli* K-12. J Bacteriol *148*, 265-273.

Gourse, R.L., Ross, W., and Gaal, T. (2000). UPs and downs in bacterial transcription initiation: the role of the alpha subunit of RNA polymerase in promoter recognition. Mol Microbiol *37*, 687-695.

Grenga, L., Luzi, G., Paolozzi, L., and Ghelardini, P. (2008). The *Escherichia coli* FtsK functional domains involved in its interaction with its divisome protein partners. FEMS Microbiol Lett *287*, 163-167.

Grimwade, J.E., Torgue, J.J., McGarry, K.C., Rozgaja, T., Enloe, S.T., and Leonard, A.C. (2007). Mutational analysis reveals *Escherichia coli oriC* interacts with both DnaA-ATP and DnaA-ADP during pre-RC assembly. Mol Microbiol *66*, 428-439.

Gruber, S., and Errington, J. (2009). Recruitment of condensin to replication origin regions by ParB/SpoOJ promotes chromosome segregation in *B. subtilis*. Cell *137*, 685-696.

Gruenig, M.C., Renzette, N., Long, E., Chitteni-Pattu, S., Inman, R.B., Cox, M.M., and Sandler, S.J. (2008). RecA-mediated SOS induction requires an extended filament conformation but no ATP hydrolysis. Mol Microbiol *69*, 1165-1179.

Gur, E., and Sauer, R.T. (2008). Recognition of misfolded proteins by Lon, a AAA(+) protease. Genes Dev *22*, 2267-2277.

Guzman, L.M., Belin, D., Carson, M.J., and Beckwith, J. (1995). Tight regulation, modulation, and high-level expression by vectors containing the arabinose P_{BAD} promoter. J Bacteriol *177*, 4121-4130.

Haber, J.E., Ira, G., Malkova, A., and Sugawara, N. (2004). Repairing a double-strand chromosome break by homologous recombination: revisiting Robin Holliday's model. Philos Trans R Soc Lond B Biol Sci *359*, 79-86.

Haering, C.H., Farcas, A.M., Arumugam, P., Metson, J., and Nasmyth, K. (2008). The cohesin ring concatenates sister DNA molecules. Nature *454*, 297-301.

Haeusser, D.P., and Levin, P.A. (2008). The great divide: coordinating cell cycle events during bacterial growth and division. Current opinion in microbiology *11*, 94-99.

Hamdan, S.M., Loparo, J.J., Takahashi, M., Richardson, C.C., and van Oijen, A.M. (2009). Dynamics of DNA replication loops reveal temporal control of lagging-strand synthesis. Nature *457*, 336-339.

Hanawalt, P.C. (2007). Paradigms for the three Rs: DNA replication, recombination, and repair. Molecular cell *28*, 702-707.

Harper, J.W., and Elledge, S.J. (2007). The DNA damage response: ten years after. Molecular cell *28*, 739-745.

Harris, D.R., Pollock, S.V., Wood, E.A., Goiffon, R.J., Klingele, A.J., Cabot, E.L., Schackwitz, W., Martin, J., Eggington, J., Durfee, T.J., *et al.* (2009). Directed Evolution of Ionizing Radiation Resistance in *Escherichia coli*. J Bacteriol.

Hasty, P. (2008). Is NHEJ a tumor suppressor or an aging suppressor? Cell Cycle *7*, 1139-1145.

Hauf, S., Waizenegger, I.C., and Peters, J.M. (2001). Cohesin cleavage by Separase required for anaphase and cytokinesis in human cells. Science (New York, NY *293*, 1320-1323.

Hedge, P.J., and Spratt, B.G. (1985). Resistance to beta-lactam antibiotics by re-modelling the active site of an *E. coli* penicillin-binding protein. Nature *318*, 478-480.

Heller, R.C., and Marians, K.J. (2006). Replisome assembly and the direct restart of stalled replication forks. Nature reviews *7*, 932-943.

Hendrickson, H., and Lawrence, J.G. (2007). Mutational bias suggests that replication termination occurs near the *dif* site, not at *Ter* sites. Mol Microbiol *64*, 42-56.

Hill, T.M., Sharma, B., Valjavec-Gratian, M., and Smith, J. (1997). *sfi*-independent filamentation in *Escherichia coli* Is *lexA* dependent and requires DNA damage for induction. J Bacteriol *179*, 1931-1939.

Horton, R.M., Hunt, H.D., Ho, S.N., Pullen, J.K., and Pease, L.R. (1989). Engineering hybrid genes without the use of restriction enzymes: gene splicing by overlap extension. Gene *77*, 61-68.

Hudson, D.F., Marshall, K.M., and Earnshaw, W.C. (2009). Condensin: Architect of mitotic chromosomes. Chromosome Res *17*, 131-144.

Hunter, N., and Kleckner, N. (2001). The single-end invasion: an asymmetric intermediate at the double-strand break to double-Holliday junction transition of meiotic recombination. Cell *106*, 59-70.

Inoue, S. (1981). Cell division and the mitotic spindle. J Cell Biol *91*, 131s-147s.

Iwasaki, H., Nakata, A., Walker, G.C., and Shinagawa, H. (1990). The *Escherichia coli polB* gene, which encodes DNA polymerase II, is regulated by the SOS system. J Bacteriol *172*, 6268-6273.

Jacob, F., Brenner, S., and Cuzin, F. (1963). On the Regulation of DNA Replication in Bacteria. Cold Spring Harbor symposia on quantitative biology *28*, 329-348.

Jiang, Q., Karata, K., Woodgate, R., Cox, M.M., and Goodman, M.F. (2009). The active form of DNA polymerase V is UmuD'(2)C-RecA-ATP. Nature *460*, 359-363.

Johnson, A., and O'Donnell, M. (2005). Cellular DNA replicases: components and dynamics at the replication fork. Annual review of biochemistry *74*, 283-315.

Johnson, B.F., and Greenberg, J. (1975). Mapping of *sul*, the suppressor of *lon* in *Escherichia coli*. J Bacteriol *122*, 570-574.

Jun, S., and Mulder, B. (2006). Entropy-driven spatial organization of highly confined polymers: lessons for the bacterial chromosome. Proc Natl Acad Sci U S A *103*, 12388-12393.

Kadyk, L.C., and Hartwell, L.H. (1992). Sister chromatids are preferred over homologs as substrates for recombinational repair in *Saccharomyces cerevisiae*. Genetics *132*, 387-402.

Kaplan, D.L., and Bastia, D. (2009). Mechanisms of polar arrest of a replication fork. Mol Microbiol *72*, 279-285.

Kaplan, D.L., and O'Donnell, M. (2006). RuvA is a sliding collar that protects Holliday junctions from unwinding while promoting branch migration. Journal of molecular biology *355*, 473-490.

Karczmarek, A., Martinez-Arteaga, R., Alexeeva, S., Hansen, F.G., Vicente, M., Nanninga, N., and den Blaauwen, T. (2007). DNA and origin region segregation are not affected by the transition from rod to sphere after inhibition of *Escherichia coli* MreB by A22. Mol Microbiol *65*, 51-63.

Karu, A.E., and Belk, E.D. (1982). Induction of *E. coli* RecA protein via RecBC and alternate pathways: quantitation by enzyme-linked immunosorbent assay (ELISA). Mol Gen Genet *185*, 275-282.

Kastan, M.B., and Bartek, J. (2004). Cell-cycle checkpoints and cancer. Nature *432*, 316-323.

Kato, J., and Katayama, T. (2001). Hda, a novel DnaA-related protein, regulates the replication cycle in *Escherichia coli*. EMBO J *20*, 4253-4262.

Kelley, W.L. (2006). Lex marks the spot: the virulent side of SOS and a closer look at the LexA regulon. Mol Microbiol *62*, 1228-1238.

Kennedy, S.P., Chevalier, F., and Barre, F.X. (2008). Delayed activation of Xer recombination at *dif* by FtsK during septum assembly in *Escherichia coli*. Mol Microbiol *68*, 1018-1028.

Khanna, K.K., and Jackson, S.P. (2001). DNA double-strand breaks: signalling, repair and the cancer connection. Nat Genet *27*, 247-254.

Khlebnikov, A., Datsenko, K.A., Skaug, T., Wanner, B.L., and Keasling, J.D. (2001). Homogeneous expression of the P(BAD) promoter in *Escherichia coli* by constitutive expression of the low-affinity high-capacity AraE transporter. Microbiology *147*, 3241-3247.

Kiel, M.J., He, S., Ashkenazi, R., Gentry, S.N., Teta, M., Kushner, J.A., Jackson, T.L., and Morrison, S.J. (2007). Haematopoietic stem cells do not asymmetrically segregate chromosomes or retain BrdU. Nature *449*, 238-242.

Kinoshita, E., van der Linden, E., Sanchez, H., and Wyman, C. (2009). RAD50, an SMC family member with multiple roles in DNA break repair: how does ATP affect function? Chromosome Res *17*, 277-288.

Kogo, H., Inagaki, H., Ohye, T., Kato, T., Emanuel, B.S., and Kurahashi, H. (2007). Cruciform extrusion propensity of human translocation-mediating palindromic AT-rich repeats. Nucleic acids research *35*, 1198-1208.

Kogoma, T. (1997). Stable DNA replication: interplay between DNA replication, homologous recombination, and transcription. Microbiol Mol Biol Rev *61*, 212-238.

Koonin, E.V. (1992). DnaC protein contains a modified ATP-binding motif and belongs to a novel family of ATPases including also DnaA. Nucleic acids research *20*, 1997.

Kosa, J.L., Zdraveski, Z.Z., Currier, S., Marinus, M.G., and Essigmann, J.M. (2004). RecN and RecG are required for *Escherichia coli* survival of Bleomycin-induced damage. Mutat Res *554*, 149-157.

Kowalczykowski, S.C. (2000). Initiation of genetic recombination and recombination-dependent replication. Trends Biochem Sci *25*, 156-165.

Krasin, F., and Hutchinson, F. (1977). Repair of DNA double-strand breaks in *Escherichia coli*, which requires *recA* function and the presence of a duplicate genome. Journal of molecular biology *116*, 81-98.

Kruse, T., Blagoev, B., Lobner-Olesen, A., Wachi, M., Sasaki, K., Iwai, N., Mann, M., and Gerdes, K. (2006). Actin homolog MreB and RNA polymerase interact and are both required for chromosome segregation in *Escherichia coli*. Genes Dev *20*, 113-124.

Kruse, T., Bork-Jensen, J., and Gerdes, K. (2005). The morphogenetic MreBCD proteins of *Escherichia coli* form an essential membrane-bound complex. Mol Microbiol *55*, 78-89.

Kurokawa, K., Nishida, S., Emoto, A., Sekimizu, K., and Katayama, T. (1999). Replication cycle-coordinated change of the adenine nucleotide-bound forms of DnaA protein in *Escherichia coli*. EMBO J *18*, 6642-6652.

Kuzminov, A. (1995). Collapse and repair of replication forks in *Escherichia coli*. Mol Microbiol *16*, 373-384.

Lan, G., Daniels, B.R., Dobrowsky, T.M., Wirtz, D., and Sun, S.X. (2009). Condensation of FtsZ filaments can drive bacterial cell division. Proc Natl Acad Sci U S A *106*, 121-126.

Langston, L.D., and O'Donnell, M. (2006). DNA replication: keep moving and don't mind the gap. Molecular cell *23*, 155-160.

Lau, I.F., Filipe, S.R., Soballe, B., Okstad, O.A., Barre, F.X., and Sherratt, D.J. (2003). Spatial and temporal organization of replicating *Escherichia coli* chromosomes. Mol Microbiol *49*, 731-743.

Lawler, M.L., and Brun, Y.V. (2007). Advantages and mechanisms of polarity and cell shape determination in *Caulobacter crescentus*. Current opinion in microbiology *10*, 630-637.

Lecointe, F., Serena, C., Velten, M., Costes, A., McGovern, S., Meile, J.C., Errington, J., Ehrlich, S.D., Noirot, P., and Polard, P. (2007). Anticipating chromosomal replication fork arrest: SSB targets repair DNA helicases to active forks. Embo J *26*, 4239-4251.

Lemon, K.P., and Grossman, A.D. (2000). Movement of replicating DNA through a stationary replisome. Molecular cell *6*, 1321-1330.

Lenarcic, R., Halbedel, S., Visser, L., Shaw, M., Wu, L.J., Errington, J., Marenduzzo, D., and Hamoen, L.W. (2009). Localisation of DivIVA by targeting to negatively curved membranes. EMBO J.

Lesterlin, C., Barre, F.X., and Cornet, F. (2004). Genetic recombination and the cell cycle: what we have learned from chromosome dimers. Mol Microbiol *54*, 1151-1160.

Lesterlin, C., Pages, C., Dubarry, N., Dasgupta, S., and Cornet, F. (2008). Asymmetry of chromosome Replichores renders the DNA translocase activity of FtsK essential for cell division and cell shape maintenance in *Escherichia coli*. PLoS Genet *4*, e1000288.

Lew, D.J., Burke, D.J., and Dutta, A. (2008). The immortal strand hypothesis: how could it work? Cell *133*, 21-23.

Lieber, M.R., Ma, Y., Pannicke, U., and Schwarz, K. (2003). Mechanism and regulation of human non-homologous DNA end-joining. Nature reviews *4*, 712-720.

Lin, E.C., Hirota, Y., and Jacob, F. (1971). On the process of cellular division in *Escherichia coli*. VI. Use of a methocel-autoradiographic method for the study of cellular division in *Escherichia coli*. J Bacteriol *108*, 375-385.

Lindner, A.B., Madden, R., Demarez, A., Stewart, E.J., and Taddei, F. (2008). Asymmetric segregation of protein aggregates is associated with cellular aging and rejuvenation. Proc Natl Acad Sci U S A *105*, 3076-3081.

Link, A.J., Phillips, D., and Church, G.M. (1997). Methods for generating precise deletions and insertions in the genome of wild-type *Escherichia coli*: application to open reading frame characterization. J Bacteriol *179*, 6228-6237.

Little, J.W., Edmiston, S.H., Pacelli, L.Z., and Mount, D.W. (1980). Cleavage of the *Escherichia coli* LexA protein by the RecA protease. Proc Natl Acad Sci U S A *77*, 3225-3229.

Liu, X., Wang, X., Reyes-Lamothe, R., and Sherratt, D. (2009). Replication-directed sister chromosome alignment in *Escherichia coli*. Mol Microbiol *advanced online publication*, doi: 10.1111/j.1365-2958.2009.06791.x.

Liu, J., Xu, L., Sandler, S.J., and Marians, K.J. (1999). Replication fork assembly at recombination intermediates is required for bacterial growth. Proc Natl Acad Sci U S A *96*, 3552-3555.

Livny, J., Yamaichi, Y., and Waldor, M.K. (2007). Distribution of centromere-like *parS* sites in bacteria: insights from comparative genomics. J Bacteriol *189*, 8693-8703.

Lloyd, R.G., Buckman, C., and Benson, F.E. (1987). Genetic analysis of conjugational recombination in *Escherichia coli* K12 strains deficient in RecBCD enzyme. Journal of general microbiology *133*, 2531-2538.

Lobachev, K., Vitriol, E., Stemple, J., Resnick, M.A., and Bloom, K. (2004). Chromosome fragmentation after induction of a double-strand break is an active process prevented by the RMX repair complex. Curr Biol *14*, 2107-2112.

Lobner-Olesen, A., Skovgaard, O., and Marinus, M.G. (2005). Dam methylation: coordinating cellular processes. Current opinion in microbiology *8*, 154-160.

Lovett, S.T., Luisi-DeLuca, C., and Kolodner, R.D. (1988). The genetic dependence of recombination in *recD* mutants of *Escherichia coli*. Genetics *120*, 37-45.

Lowe, J., Ellonen, A., Allen, M.D., Atkinson, C., Sherratt, D.J., and Grainge, I. (2008). Molecular mechanism of sequence-directed DNA loading and translocation by FtsK. Molecular cell *31*, 498-509.

Lutkenhaus, J. (2002). Dynamic proteins in bacteria. Current opinion in microbiology *5*, 548-552.

Madabhushi, R., and Marians, K.J. (2009). Actin homolog MreB affects chromosome segregation by regulating Topoisomerase IV in *Escherichia coli*. Molecular cell *33*, 171-180.

Maisnier-Patin, S., Nordstrom, K., and Dasgupta, S. (2001). Replication arrests during a single round of replication of the *Escherichia col*i chromosome in the absence of DnaC activity. Mol Microbiol *42*, 1371-1382.

Maisonneuve, E., Ezraty, B., and Dukan, S. (2008). Protein aggregates: an aging factor involved in cell death. J Bacteriol *190*, 6070-6075.

Malan, T.P., and McClure, W.R. (1984). Dual promoter control of the *Escherichia coli* lactose operon. Cell *39*, 173-180.

Malone, R.E., Chattoraj, D.K., Faulds, D.H., Stahl, M.M., and Stahl, F.W. (1978). Hotspots for generalized recombination in the *Escherichia coli* chromosome. Journal of molecular biology *121*, 473-491.

Mason, D.J., and Powelson, D.M. (1956). Nuclear division as observed in live bacteria by a new technique. J Bacteriol *71*, 474-479.

Massey, T.H., Mercogliano, C.P., Yates, J., Sherratt, D.J., and Lowe, J. (2006). Double-stranded DNA translocation: structure and mechanism of hexameric FtsK. Molecular cell *23*, 457-469.

McClure, W.R. (1985). Mechanism and control of transcription initiation in prokaryotes. Annual review of biochemistry *54*, 171-204.

McGlynn, P., and Guy, C.P. (2008). Replication forks blocked by protein-DNA complexes have limited stability in vitro. Journal of molecular biology *381*, 249-255.

McGlynn, P., and Lloyd, R.G. (2002). Recombinational repair and restart of damaged replication forks. Nature reviews *3*, 859-870.

McInerney, P., Johnson, A., Katz, F., and O'Donnell, M. (2007). Characterization of a triple DNA polymerase replisome. Molecular cell *27*, 527-538.

Meddows, T.R., Savory, A.P., Grove, J.I., Moore, T., and Lloyd, R.G. (2005). RecN protein and transcription factor DksA combine to promote faithful recombinational repair of DNA double-strand breaks. Mol Microbiol *57*, 97-110.

Meddows, T.R., Savory, A.P., and Lloyd, R.G. (2004). RecG helicase promotes DNA double-strand break repair. Mol Microbiol *52*, 119-132.

Merlin, C., McAteer, S., and Masters, M. (2002). Tools for characterization of *Escherichia coli* genes of unknown function. J Bacteriol *184*, 4573-4581.

Michel, B., Grompone, G., Flores, M.J., and Bidnenko, V. (2004). Multiple pathways process stalled replication forks. Proc Natl Acad Sci U S A *101*, 12783-12788.

Michie, K.A., and Lowe, J. (2006). Dynamic filaments of the bacterial cytoskeleton. Annual review of biochemistry *75*, 467-492.

Minsky, A. (2003). Structural aspects of DNA repair: the role of restricted diffusion. Mol Microbiol *50*, 367-376.

Mitkova, A.V., Khopde, S.M., and Biswas, S.B. (2003). Mechanism and stoichiometry of interaction of DnaG primase with DnaB helicase of Escherichia coli in RNA primer synthesis. The Journal of biological chemistry *278*, 52253-52261.

Mizusawa, S., and Gottesman, S. (1983). Protein degradation in *Escherichia coli*: the *lon* gene controls the stability of SulA protein. Proc Natl Acad Sci U S A *80*, 358-362.

Molina, F., and Skarstad, K. (2004). Replication fork and SeqA focus distributions in Escherichia coli suggest a replication hyperstructure dependent on nucleotide metabolism. Mol Microbiol *52*, 1597-1612.

Monteilhet, C., Perrin, A., Thierry, A., Colleaux, L., and Dujon, B. (1990). Purification and characterization of the in vitro activity of I-Sce I, a novel and highly specific endonuclease encoded by a group I intron. Nucleic acids research *18*, 1407-1413.

Morigen, Odsbu, I., and Skarstad, K. (2009). Growth rate dependent numbers of SeqA structures organize the multiple replication forks in rapidly growing *Escherichia coli*. Genes Cells.

Mott, M.L., and Berger, J.M. (2007). DNA replication initiation: mechanisms and regulation in bacteria. Nat Rev Microbiol *5*, 343-354.

Mott, M.L., Erzberger, J.P., Coons, M.M., and Berger, J.M. (2008). Structural synergy and molecular crosstalk between bacterial helicase loaders and replication initiators. Cell *135*, 623-634.

Moure, C.M., Gimble, F.S., and Quiocho, F.A. (2008). Crystal structures of I-SceI complexed to nicked DNA substrates: snapshots of intermediates along the DNA cleavage reaction pathway. Nucleic acids research *36*, 3287-3296.

Moynahan, M.E., Pierce, A.J., and Jasin, M. (2001). BRCA2 is required for homology-directed repair of chromosomal breaks. Molecular cell *7*, 263-272.

Muller-Hill, B., Crapo, L., and Gilbert, W. (1968). Mutants that make more Lac Repressor. Proc Natl Acad Sci U S A *59*, 1259-1264.

Murakami, K.S., Masuda, S., Campbell, E.A., Muzzin, O., and Darst, S.A. (2002). Structural basis of transcription initiation: an RNA polymerase holoenzyme-DNA complex. Science (New York, NY *296*, 1285-1290.

Musacchio, A., and Salmon, E.D. (2007). The spindle-assembly checkpoint in space and time. Nature reviews *8*, 379-393.

Nielsen, H.J., Li, Y., Youngren, B., Hansen, F.G., and Austin, S. (2006a). Progressive segregation of the *Escherichia coli* chromosome. Mol Microbiol *61*, 383-393.

Nielsen, H.J., Ottesen, J.R., Youngren, B., Austin, S.J., and Hansen, F.G. (2006b). The *Escherichia coli* chromosome is organized with the left and right chromosome arms in separate cell halves. Mol Microbiol *62*, 331-338.

Nievera, C., Torgue, J.J., Grimwade, J.E., and Leonard, A.C. (2006). SeqA blocking of DnaA-*oriC* interactions ensures staged assembly of the *E. coli* pre-RC. Molecular cell *24*, 581-592.

Niki, H., Yamaichi, Y., and Hiraga, S. (2000). Dynamic organization of chromosomal DNA in *Escherichia coli*. Genes Dev *14*, 212-223.

Nogales, E. (2000). Structural insights into microtubule function. Annual review of biochemistry *69*, 277-302.

Nollmann, M., Crisona, N.J., and Arimondo, P.B. (2007). Thirty years of *Escherichia coli* DNA gyrase: from in vivo function to single-molecule mechanism. Biochimie *89*, 490-499.

Nozaki, S., Niki, H., and Ogawa, T. (2009a). Replication initiator DnaA of *Escherichia coli* changes its assembly form on the replication origin during the cell cycle. J Bacteriol *191*, 4807-4814.

Nozaki, S., Yamada, Y., and Ogawa, T. (2009b). Initiator titration complex formed at *datA* with the aid of IHF regulates replication timing in *Escherichia coli*. Genes Cells *14*, 329-341.

O'Donnell, M. (2006). Replisome architecture and dynamics in *Escherichia coli*. The Journal of biological chemistry *281*, 10653-10656.

Ohsumi, K., Yamazoe, M., and Hiraga, S. (2001). Different localization of SeqA-bound nascent DNA clusters and MukF-MukE-MukB complex in *Escherichia coli* cells. Mol Microbiol *40*, 835-845.

Osman, F., Gaskell, L., and Whitby, M.C. (2009). Efficient second strand cleavage during Holliday junction resolution by RuvC requires both increased junction flexibility and an exposed 5' phosphate. PLoS One *4*, e5347.

Patel, P.H., Suzuki, M., Adman, E., Shinkai, A., and Loeb, L.A. (2001). Prokaryotic DNA polymerase I: evolution, structure, and "base flipping" mechanism for nucleotide selection. Journal of molecular biology *308*, 823-837.

Paull, T.T., and Gellert, M. (1998). The 3' to 5' exonuclease activity of Mre 11 facilitates repair of DNA double-strand breaks. Molecular cell *1*, 969-979.

Payne, B.T., van Knippenberg, I.C., Bell, H., Filipe, S.R., Sherratt, D.J., and McGlynn, P. (2006). Replication fork blockage by transcription factor-DNA complexes in *Escherichia coli*. Nucleic acids research *34*, 5194-5202.

Pennington, J.M., and Rosenberg, S.M. (2007). Spontaneous DNA breakage in single living *Escherichia coli* cells. Nat Genet *39*, 797-802.

Peter, B.J., Ullsperger, C., Hiasa, H., Marians, K.J., and Cozzarelli, N.R. (1998). The structure of supercoiled intermediates in DNA replication. Cell *94*, 819-827.

Peters, J.M., Tedeschi, A., and Schmitz, J. (2008). The cohesin complex and its roles in chromosome biology. Genes Dev *22*, 3089-3114.

Phillips, R.J., Hickleton, D.C., Boehmer, P.E., and Emmerson, P.T. (1997). The RecB protein of *Escherichia coli* translocates along single-stranded DNA in the 3' to 5' direction: a proposed ratchet mechanism. Mol Gen Genet *254*, 319-329.

Pickett-Heaps, J.D., Tippit, D.H., and Porter, K.R. (1982). Rethinking mitosis. Cell *29*, 729-744.

Pierucci, O., and Zuchowski, C. (1973). Non-random segregation of DNA strands in *Escherichia coli* B-r. Journal of molecular biology *80*, 477-503.

Piggot, P.J., and Hilbert, D.W. (2004). Sporulation of *Bacillus subtilis*. Current opinion in microbiology *7*, 579-586.

Pinder, D.J., Blake, C.E., Lindsey, J.C., and Leach, D.R. (1998). Replication strand preference for deletions associated with DNA palindromes. Mol Microbiol *28*, 719-727.

Pitcher, R.S., Brissett, N.C., and Doherty, A.J. (2007). Nonhomologous end-joining in bacteria: a microbial perspective. Annu Rev Microbiol *61*, 259-282.

Pogliano, J., Pogliano, K., Weiss, D.S., Losick, R., and Beckwith, J. (1997). Inactivation of FtsI inhibits constriction of the FtsZ cytokinetic ring and delays the assembly of FtsZ rings at potential division sites. Proc Natl Acad Sci U S A *94*, 559-564.

Pomerantz, R.T., and O'Donnell, M. (2008). The replisome uses mRNA as a primer after colliding with RNA polymerase. Nature *456*, 762-766.

Possoz, C., Filipe, S.R., Grainge, I., and Sherratt, D.J. (2006). Tracking of controlled *Escherichia coli* replication fork stalling and restart at repressor-bound DNA in vivo. EMBO J *25*, 2596-2604.

Rafferty, J.B., Sedelnikova, S.E., Hargreaves, D., Artymiuk, P.J., Baker, P.J., Sharples, G.J., Mahdi, A.A., Lloyd, R.G., and Rice, D.W. (1996). Crystal structure of DNA recombination protein RuvA and a model for its binding to the Holliday junction. Science (New York, NY *274*, 415-421.

Rando, T.A. (2007). The immortal strand hypothesis: segregation and reconstruction. Cell *129*, 1239-1243.

Raskin, D.M., and de Boer, P.A. (1999). Rapid pole-to-pole oscillation of a protein required for directing division to the middle of *Escherichia coli*. Proc Natl Acad Sci U S A *96*, 4971-4976.

Recchia, G.D., Aroyo, M., Wolf, D., Blakely, G., and Sherratt, D.J. (1999). FtsK-dependent and -independent pathways of Xer site-specific recombination. Embo J *18*, 5724-5734.

Renzette, N., Gumlaw, N., Nordman, J.T., Krieger, M., Yeh, S.P., Long, E., Centore, R., Boonsombat, R., and Sandler, S.J. (2005). Localization of RecA in *Escherichia coli* K-12 using RecA-GFP. Mol Microbiol *57*, 1074-1085.

Reyes-Lamothe, R., Possoz, C., Danilova, O., and Sherratt, D.J. (2008). Independent positioning and action of *Escherichia coli* replisomes in live cells. Cell *133*, 90-102.

Rhoades, M.M., and Vilkomerson, H. (1942). On the Anaphase Movement of Chromosomes. Proc Natl Acad Sci U S A *28*, 433-436.

Rizzo, M.A., Springer, G.H., Granada, B., and Piston, D.W. (2004). An improved Cyan Fluorescent Protein variant useful for FRET. Nat Biotechnol *22*, 445-449.

Rocha, E.P. (2004). The replication-related organization of bacterial genomes. Microbiology *150*, 1609-1627.

Rocha, E.P., Fralick, J., Vediyappan, G., Danchin, A., and Norris, V. (2003). A strand-specific model for chromosome segregation in bacteria. Mol Microbiol *49*, 895-903.

Rodrigue, A., Lafrance, M., Gauthier, M.C., McDonald, D., Hendzel, M., West, S.C., Jasin, M., and Masson, J.Y. (2006). Interplay between human DNA repair proteins at a unique double-strand break in vivo. EMBO J *25*, 222-231.

Rogers, G.C., Rogers, S.L., Schwimmer, T.A., Ems-McClung, S.C., Walczak, C.E., Vale, R.D., Scholey, J.M., and Sharp, D.J. (2004). Two mitotic kinesins cooperate to drive sister chromatid separation during anaphase. Nature *427*, 364-370.

Rowland, S.L., Fu, X., Sayed, M.A., Zhang, Y., Cook, W.R., and Rothfield, L.I. (2000). Membrane redistribution of the *Escherichia coli* MinD protein induced by MinE. J Bacteriol *182*, 613-619.

Rudolph, C.J., Upton, A.L., Harris, L., and Lloyd, R.G. (2009). Pathological replication in cells lacking RecG DNA translocase. Mol Microbiol.

Rudolph, C.J., Upton, A.L., and Lloyd, R.G. (2007). Replication fork stalling and cell cycle arrest in UV-irradiated *Escherichia coli*. Genes Dev *21*, 668-681.

Rudolph, C.J., Upton, A.L., and Lloyd, R.G. (2008). Maintaining replication fork integrity in UV-irradiated *Escherichia coli* cells. DNA Repair (Amst) *7*, 1589-1602.

Ryan, V.T., Grimwade, J.E., Nievera, C.J., and Leonard, A.C. (2002). IHF and HU stimulate assembly of pre-replication complexes at *Escherichia coli oriC* by two different mechanisms. Mol Microbiol *46*, 113-124.

Ryter, A., Hirota, Y., and Jacob, F. (1968). DNA-membrane complex and nuclear segregation in bacteria. Cold Spring Harbor symposia on quantitative biology *33*, 669-676.

Sanderson, A., Mitchell, J.E., Minchin, S.D., and Busby, S.J. (2003). Substitutions in the *Escherichia col*i RNA polymerase sigma70 factor that affect recognition of extended -10 elements at promoters. FEBS letters *544*, 199-205.

Schlacher, K., Cox, M.M., Woodgate, R., and Goodman, M.F. (2006). RecA acts in trans to allow replication of damaged DNA by DNA polymerase V. Nature *442*, 883-887.

Schlacher, K., and Goodman, M.F. (2007). Lessons from 50 years of SOS DNA-damage-induced mutagenesis. Nature reviews *8*, 587-594.

Seitz, H., Weigel, C., and Messer, W. (2000). The interaction domains of the DnaA and DnaB replication proteins of *Escherichia coli*. Mol Microbiol *37*, 1270-1279.

Sekimizu, K., Yung, B.Y., and Kornberg, A. (1988). The DnaA protein of *Escherichia coli*. Abundance, improved purification, and membrane binding. The Journal of biological chemistry *263*, 7136-7140.

Shaner, N.C., Campbell, R.E., Steinbach, P.A., Giepmans, B.N., Palmer, A.E., and Tsien, R.Y. (2004). Improved monomeric red, orange and yellow fluorescent proteins derived from *Discosoma sp*. red fluorescent protein. Nat Biotechnol *22*, 1567-1572.

Shaner, N.C., Lin, M.Z., McKeown, M.R., Steinbach, P.A., Hazelwood, K.L., Davidson, M.W., and Tsien, R.Y. (2008). Improving the photostability of bright monomeric orange and red fluorescent proteins. Nature methods *5*, 545-551.

Shaner, N.C., Steinbach, P.A., and Tsien, R.Y. (2005). A guide to choosing fluorescent proteins. Nature methods *2*, 905-909.

Sharan, S.K., Thomason, L.C., Kuznetsov, S.G., and Court, D.L. (2009). Recombineering: a homologous recombination-based method of genetic engineering. Nature protocols *4*, 206-223.

Shen, B., and Lutkenhaus, J. (2009). The conserved C-terminal tail of FtsZ is required for the septal localization and division inhibitory activity of $MinC^{C}$/MinD. Mol Microbiol *72*, 410-424.

Siegele, D.A., and Hu, J.C. (1997). Gene expression from plasmids containing the *araBAD* promoter at subsaturating inducer concentrations represents mixed populations. Proc Natl Acad Sci U S A *94*, 8168-8172.

Simmons, L.A., Felczak, M., and Kaguni, J.M. (2003). DnaA Protein of *Escherichia coli*: oligomerization at the *E. coli* chromosomal origin is required for initiation and involves specific N-terminal amino acids. Mol Microbiol *49*, 849-858.

Singleton, M.R., Dillingham, M.S., Gaudier, M., Kowalczykowski, S.C., and Wigley, D.B. (2004). Crystal structure of RecBCD enzyme reveals a machine for processing DNA breaks. Nature *432*, 187-193.

Skarstad, K., and Boye, E. (1993). Degradation of individual chromosomes in *recA* mutants of *Escherichia coli*. J Bacteriol *175*, 5505-5509.

Song, M.H., Miliaras, N.B., Peel, N., and O'Connell, K.F. (2008). Centrioles: some self-assembly required. Curr Opin Cell Biol *20*, 688-693.

Spies, M., Amitani, I., Baskin, R.J., and Kowalczykowski, S.C. (2007). RecBCD enzyme switches lead motor subunits in response to chi recognition. Cell *131*, 694-705.

Spies, M., Bianco, P.R., Dillingham, M.S., Handa, N., Baskin, R.J., and Kowalczykowski, S.C. (2003). A molecular throttle: the recombination hotspot chi controls DNA translocation by the RecBCD helicase. Cell *114*, 647-654.

Spies, M., and Kowalczykowski, S.C. (2006). The RecA binding locus of RecBCD is a general domain for recruitment of DNA strand exchange proteins. Molecular cell *21*, 573-580.

St-Pierre, J., Douziech, M., Bazile, F., Pascariu, M., Bonneil, E., Sauve, V., Ratsima, H., and D'Amours, D. (2009). Polo kinase regulates mitotic chromosome condensation by hyperactivation of condensin DNA supercoiling activity. Molecular cell *34*, 416-426.

Stohl, E.A., Brockman, J.P., Burkle, K.L., Morimatsu, K., Kowalczykowski, S.C., and Seifert, H.S. (2003). *Escherichia coli* RecX inhibits RecA recombinase and coprotease activities in vitro and in vivo. The Journal of biological chemistry *278*, 2278-2285.

Strom, L., Karlsson, C., Lindroos, H.B., Wedahl, S., Katou, Y., Shirahige, K., and Sjogren, C. (2007). Postreplicative formation of cohesion is required for repair and induced by a single DNA break. Science (New York, NY *317*, 242-245.

Sullivan, N.L., Marquis, K.A., and Rudner, D.Z. (2009). Recruitment of SMC by ParB-*parS* organizes the origin region and promotes efficient chromosome segregation. Cell *137*, 697-707.

Sun, Y., Kucej, M., Fan, H.Y., Yu, H., Sun, Q.Y., and Zou, H. (2009). Separase is recruited to mitotic chromosomes to dissolve sister chromatid cohesion in a DNA-dependent manner. Cell *137*, 123-132.

Suski, C., and Marians, K.J. (2008). Resolution of converging replication forks by RecQ and Topoisomerase III. Molecular cell *30*, 779-789.

Sutera, V.A., Jr., and Lovett, S.T. (2006). The role of replication initiation control in promoting survival of replication fork damage. Mol Microbiol *60*, 229-239.

Sutton, M.D., Smith, B.T., Godoy, V.G., and Walker, G.C. (2000). The SOS response: recent insights into *umuDC*-dependent mutagenesis and DNA damage tolerance. Annu Rev Genet *34*, 479-497.

Szostak, J.W., Orr-Weaver, T.L., Rothstein, R.J., and Stahl, F.W. (1983). The double-strand-break repair model for recombination. Cell *33*, 25-35.

Tanaka, T.U., Stark, M.J., and Tanaka, K. (2005). Kinetochore capture and bi-orientation on the mitotic spindle. Nature reviews *6*, 929-942.

Thanbichler, M., and Shapiro, L. (2006). Chromosome organization and segregation in bacteria. Journal of structural biology *156*, 292-303.

Thanbichler, M., and Shapiro, L. (2008). Getting organized--how bacterial cells move proteins and DNA. Nat Rev Microbiol *6*, 28-40.

Thierauf, A., Perez, G., and Maloy, A.S. (2009). Generalized transduction. Methods in molecular biology (Clifton, NJ *501*, 267-286.

Thompson, L.H., and Schild, D. (2002). Recombinational DNA repair and human disease. Mutat Res *509*, 49-78.

Tittel-Elmer, M., Alabert, C., Pasero, P., and Cobb, J.A. (2009). The MRX complex stabilizes the replisome independently of the S phase checkpoint during replication stress. EMBO J *28*, 1142-1156.

Toro, E., Hong, S.H., McAdams, H.H., and Shapiro, L. (2008). *Caulobacter* requires a dedicated mechanism to initiate chromosome segregation. Proc Natl Acad Sci U S A *105*, 15435-15440.

Tremblay, A., Jasin, M., and Chartrand, P. (2000). A double-strand break in a chromosomal LINE element can be repaired by gene conversion with various endogenous LINE elements in mouse cells. Molecular and cellular biology *20*, 54-60.

Trusca, D., Scott, S., Thompson, C., and Bramhill, D. (1998). Bacterial SOS checkpoint protein SulA inhibits polymerization of purified FtsZ cell division protein. J Bacteriol *180*, 3946-3953.

Uchida, K., Furukohri, A., Shinozaki, Y., Mori, T., Ogawara, D., Kanaya, S., Nohmi, T., Maki, H., and Akiyama, M. (2008). Overproduction of *Escherichia coli* DNA polymerase DinB (Pol IV) inhibits replication fork progression and is lethal. Mol Microbiol *70*, 608-622.

Unal, E., Heidinger-Pauli, J.M., and Koshland, D. (2007). DNA double-strand breaks trigger genome-wide sister-chromatid cohesion through Eco1 (Ctf7). Science (New York, NY *317*, 245-248.

van der Heijden, T., Modesti, M., Hage, S., Kanaar, R., Wyman, C., and Dekker, C. (2008). Homologous recombination in real time: DNA strand exchange by RecA. Molecular cell *30*, 530-538.

van Helvoort, J.M., Kool, J., and Woldringh, C.L. (1996). Chloramphenicol causes fusion of separated nucleoids in *Escherichia coli* K-12 cells and filaments. J Bacteriol *178*, 4289-4293.

Viollier, P.H., Thanbichler, M., McGrath, P.T., West, L., Meewan, M., McAdams, H.H., and Shapiro, L. (2004). Rapid and sequential movement of individual chromosomal loci to specific subcellular locations during bacterial DNA replication. Proc Natl Acad Sci U S A *101*, 9257-9262.

Waghmare, S.K., Bansal, R., Lee, J., Zhang, Y.V., McDermitt, D.J., and Tumbar, T. (2008). Quantitative proliferation dynamics and random chromosome segregation of hair follicle stem cells. EMBO J *27*, 1309-1320.

Wagner, J., Gruz, P., Kim, S.R., Yamada, M., Matsui, K., Fuchs, R.P., and Nohmi, T. (1999). The *dinB* gene encodes a novel *E. coli* DNA polymerase, DNA pol IV, involved in mutagenesis. Molecular cell *4*, 281-286.

Walker, G.C. (1984). Mutagenesis and inducible responses to deoxyribonucleic acid damage in *Escherichia coli*. Microbiol Rev *48*, 60-93.

Wang, X., Liu, X., Possoz, C., and Sherratt, D.J. (2006). The two *Escherichia coli* chromosome arms locate to separate cell halves. Genes Dev *20*, 1727-1731.

Wang, X., Possoz, C., and Sherratt, D.J. (2005). Dancing around the divisome: asymmetric chromosome segregation in *Escherichia coli*. Genes Dev *19*, 2367-2377.

Wang, X., Reyes-Lamothe, R., and Sherratt, D.J. (2008). Modulation of *Escherichia coli* sister chromosome cohesion by Topoisomerase IV. Genes Dev *22*, 2426-2433.

Watrin, E., and Peters, J.M. (2009). The cohesin complex is required for the DNA damage-induced G2/M checkpoint in mammalian cells. EMBO J.

Weart, R.B., Lee, A.H., Chien, A.C., Haeusser, D.P., Hill, N.S., and Levin, P.A. (2007). A metabolic sensor governing cell size in bacteria. Cell *130*, 335-347.

Weiss, D.S. (2004). Bacterial cell division and the septal ring. Mol Microbiol *54*, 588-597.

Wertman, K.F., Wyman, A.R., and Botstein, D. (1986). Host/vector interactions which affect the viability of recombinant phage lambda clones. Gene *49*, 253-262.

White, M.A., Eykelenboom, J.K., Lopez-Vernaza, M.A., Wilson, E., and Leach, D.R. (2008). Non-random segregation of sister chromosomes in *Escherichia coli*. Nature *455*, 1248-1250.

Witte, G., Urbanke, C., and Curth, U. (2003). DNA polymerase III chi subunit ties single-stranded DNA binding protein to the bacterial replication machinery. Nucleic acids research *31*, 4434-4440.

Wold, S., Crooke, E., and Skarstad, K. (1996). The *Escherichia coli* Fis protein prevents initiation of DNA replication from *oriC* in vitro. Nucleic acids research *24*, 3527-3532.

Wold, S., Skarstad, K., Steen, H.B., Stokke, T., and Boye, E. (1994). The initiation mass for DNA replication in *Escherichia coli* K-12 is dependent on growth rate. Embo J *13*, 2097-2102.

Woldringh, C.L., and Nanninga, N. (2006). Structural and physical aspects of bacterial chromosome segregation. Journal of structural biology *156*, 273-283.

Wu, L.J., and Errington, J. (2003). RacA and the Soj-Spo0J system combine to effect polar chromosome segregation in sporulating *Bacillus subtilis*. Mol Microbiol *49*, 1463-1475.

Yamaichi, Y., and Niki, H. (2004). *migS*, a cis-acting site that affects bipolar positioning of *oriC* on the *Escherichia coli* chromosome. EMBO J *23*, 221-233.

Yano, K., Morotomi-Yano, K., Adachi, N., and Akiyama, H. (2009). Molecular mechanism of protein assembly on DNA double-strand breaks in the non-homologous end-joining pathway. J Radiat Res (Tokyo) *50*, 97-108.

Yates, J., Zhekov, I., Baker, R., Eklund, B., Sherratt, D.J., and Arciszewska, L.K. (2006). Dissection of a functional interaction between the DNA translocase, FtsK, and the XerD recombinase. Mol Microbiol *59*, 1754-1766.

Yu, X.C., and Margolin, W. (1999). FtsZ ring clusters in min and partition mutants: role of both the Min system and the nucleoid in regulating FtsZ ring localization. Mol Microbiol *32*, 315-326.

Zahradka, K., Buljubasic, M., Petranovic, M., and Zahradka, D. (2009). Roles of ExoI and SbcCD nucleases in "reckless" DNA degradation in *recA* mutants of *Escherichia coli*. J Bacteriol *191*, 1677-1687.

Zaitsev, E.N., and Kowalczykowski, S.C. (1999). The simultaneous binding of two double-stranded DNA molecules by *Escherichia coli* RecA protein. Journal of molecular biology *287*, 21-31.

Zechiedrich, E.L., and Cozzarelli, N.R. (1995). Roles of Topoisomerase IV and DNA Gyrase in DNA unlinking during replication in *Escherichia coli*. Genes Dev *9*, 2859-2869.

Zechiedrich, E.L., Khodursky, A.B., and Cozzarelli, N.R. (1997). Topoisomerase IV, not Gyrase, decatenates products of site-specific recombination in *Escherichia coli*. Genes Dev *11*, 2580-2592.

Zimmerman, S.B. (2002). Toroidal nucleoids in *Escherichia coli* exposed to chloramphenicol. Journal of structural biology *138*, 199-206.

Appendix

Published Paper

White, M.A., Eykelenboom, J.K., Lopez-Vernaza, M.A., Wilson, E., and Leach, D.R. (2008). Non-random segregation of sister chromosomes in *Escherichia coli*. Nature *455*, 1248-1250.

http://www.nature.com/nature/journal/v455/n7217/full/nature07282.html
DOI: 10.1038/nature07282

Permission from Nature Publishing Group

"Ownership of copyright in the article remains with the Authors, and provided that, when reproducing the Contribution or extracts from it, the Authors acknowledge first and reference publication in the Journal, the Authors retain the following non-exclusive rights:

a) To reproduce the Contribution in whole or in part in any printed volume (book or thesis) of which they are the author(s)."

Vol 455|30 October 2008|doi:10.1038/nature07282

LETTERS

Non-random segregation of sister chromosomes in *Escherichia coli*

Martin A. White[1], John K. Eykelenboom[1], Manuel A. Lopez-Vernaza[1], Emily Wilson[1] & David R. F. Leach[1]

It has long been known that the 5′ to 3′ polarity of DNA synthesis results in both a leading and lagging strand at all replication forks[1]. Until now, however, there has been no evidence that leading or lagging strands are spatially organized in any way within a cell. Here we show that chromosome segregation in *Escherichia coli* is not random but is driven in a manner that results in the leading and lagging strands being addressed to particular cellular destinations. These destinations are consistent with the known patterns of chromosome segregation[2,3]. Our work demonstrates a new level of organization relating to the replication and segregation of the *E. coli* chromosome.

Prokaryotic cells were long considered to be featureless until recent advances in imaging revealed an array of internal structures and subcellular organizations[4]. One such example is the nuclear architecture of *E. coli*, where the domains of the left and right chromosome arms occupy distinct cellular locations[2]. During replication, these domains are progressively segregated by an unknown mechanism that results in translational symmetry of the chromosome arms (known as replichores)[2,3]. Counter-intuitively, to obtain this translational symmetry there must be mirror symmetry in the segregation of the leading and lagging strands of the two replication forks (Fig. 1A). This leads to three possible situations. Either the two lagging strands of replication are positioned at mid-cell while the leading strands migrate to the cell poles; the two lagging strands migrate to the cell poles while the leading strands are positioned at mid-cell; or a random combination of these two segregation patterns occurs within the population. The specific hypothesis that leading strands segregate to cell poles has been proposed[5,6] to explain the preponderance of highly expressed genes on the leading strands of the left (L) and right (R) replichores[7]. However, no evidence for or against this has yet been presented.

To distinguish these three possibilities, we designed a construct (Supplementary Fig. 1) that would allow us specifically to visualize a locus on the right replichore (*lacZ*) that was replicated on the leading strand of the replication fork (R_{lead}). This is accomplished by inducing SbcCD-mediated palindrome cleavage[8] in a *recA*$^-$ mutant that has the palindrome flanked upstream by an array of *tetO* sites and downstream by an array of *lacO* sites. These arrays are visualized by fluorescence microscopy upon the binding of TetR–yellow fluorescent protein (YFP) and LacI–cyan fluorescent protein (CFP), respectively, and allow us to follow the cellular position of the chromosomal region containing the palindrome as it is replicated and segregated. This is visible as a twin YFP–CFP spot, demonstrating the presence of DNA on both sides of the palindrome. Induction of SbcCD results in the specific cleavage of the palindrome that was replicated on the lagging strand[8] (R_{lag}) by formation of a DNA hairpin[9]. In a *recA*$^-$ mutant the broken chromosome is degraded[10] leaving behind the intact copy of the construct located on R_{lead} (Fig. 1B). As long as the labelling method does not disrupt the known pattern of chromosome segregation, then the location of only one of the chromosome arms needs to be known for the rest to be inferred (Fig. 1A).

The cellular position of this construct was followed during growth, and the number of segregated copies related to cell length. In the absence of induced double-strand breaks, 68.8% of exponentially growing cells longer than 1.50 μm had two visibly segregated copies of the construct. In these cells, the loci were segregated such that one was located at mid-cell and the other at a cell pole (Fig. 2a). This

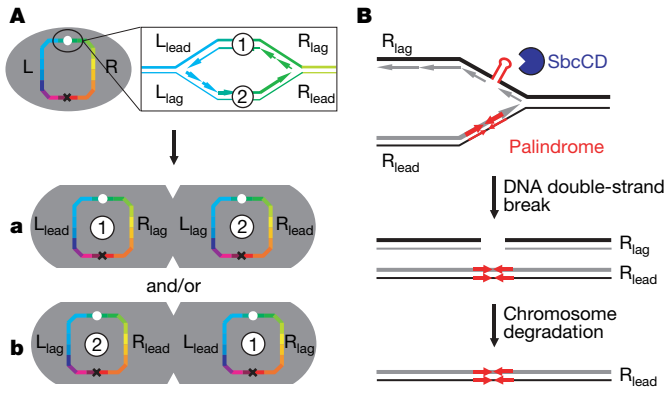

Figure 1 | Distinguishing leading and lagging strands. **A**, Cartoon demonstrating how mirror symmetry of leading and lagging strands accounts for translational symmetry of sister chromosomes. **Aa**, Segregation of leading strands towards the cell poles and of lagging strands towards mid-cell. **Ab**, Segregation of lagging strands towards the cell poles and of leading strands towards mid-cell. **B**, SbcCD cleaves a DNA hairpin formed by the palindrome on the lagging strand of replication, and the broken chromosome is degraded in a *recA*$^-$ mutant.

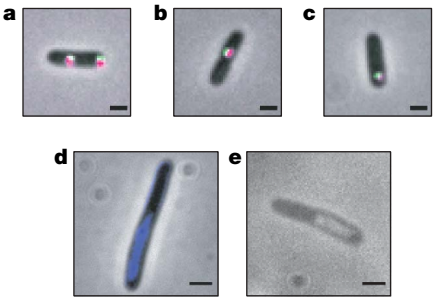

Figure 2 | Visualization of construct. *E. coli* cell containing: **a**, two segregated copies of the construct; **b**, one located at mid-cell; and **c**, one located at a cell pole. The CFP signal is pseudocoloured green, YFP magenta. Overlapping CFP and YFP signals appear white. Visualization of the nucleoid in cells subjected to SbcCD-mediated palindrome cleavage for 120 min by DAPI staining (DNA, blue) (**d**) and mounting on gelatin (DNA, white) (**e**). Scale bars, 1 μm (**a**–**c**) and 2 μm (**d**, **e**).

[1]Institute of Cell Biology, School of Biological Sciences, University of Edinburgh, King's Buildings, Edinburgh EH9 3JR, UK.

localization pattern is consistent with published data on the pattern of chromosome segregation and localization in *E. coli*[2,3] and was indistinguishable from the *recA*$^+$ parental strains. Localization was also not independently affected by either induction of SbcCD or the presence of the palindrome. The induction of SbcCD expression in a palindrome-containing strain, however, caused a decrease in the number of cells longer than 1.50 μm with two visibly segregated copies of the construct over time (Fig. 3a). This decrease was strongly associated with an increase in the number of cells with only one visible copy of the construct, suggesting that cleavage and degradation of one of the replicated chromosomes had occurred. This was not observed in the control strain lacking the palindrome whereby 80.2% ± 3.1 (range, $n = 574$) of cells had two visibly segregated copies of the construct at T_0 and 81.2% ± 1.8 (range, $n = 796$) after 90 min of SbcCD induction. Interestingly, visualization of the nucleoid by either DAPI staining or mounting cells on gelatin[11] revealed that even after extensive cleavage and degradation, the intact chromosome remains in one cell half (Fig. 2d, e).

For cells longer than 1.50 μm with only a single visible copy of the construct, the cellular position was classified as being closer to either the mid-cell (Fig. 2b) or the cell pole (Fig. 2c). In the absence of SbcCD-induced DNA double-strand breaks, the construct was found to be located in the two positions in approximately equal proportions (Fig. 3b). Notably, inducing SbcCD expression for 90 min in a strain containing a DNA palindrome resulted in the construct being located at the cell pole in most cells (89.2%). The slight bias towards being located at the cell pole (63.5%) at T_0 is probably caused by leaky expression of SbcCD from the inducible promoter (P_{BAD})[12] in minimal growth medium. The simplest explanation of this is that SbcCD is specifically cleaving the palindrome located at mid-cell because it possessed a DNA hairpin that formed on the lagging strand of replication. However, other formal possibilities must be considered.

Time-lapse microscopy suggests that the chromosome is cleaved before visible segregation of the sister loci in most cells (data not shown). Therefore, to test the alternative hypothesis that the remaining copy of the palindrome migrated to the cell pole in response to the induced double-strand break as opposed to the normal process of chromosome segregation, strains were constructed that allowed expression of I-SceI from an inducible promoter with a unique I-SceI cleavage site in place of the palindrome. I-SceI is a site-specific endonuclease and therefore cannot distinguish between the cleavage sites located on the two sister chromosomes. Induction of cleavage by I-SceI for 90 min also resulted in an increase in the number of cells longer than 1.50 μm with a single pair of foci (39.5% after 90 min of induction compared with 8.1% in a control strain lacking a cleavage site), again suggesting degradation of one of the sister chromosomes. The frequency was less than that observed with SbcCD-induced cleavage owing to a more dramatic increase in the cells with no visible foci, presumably because of instances of cleavage and degradation of all chromosomes. Unlike SbcCD-mediated palindrome cleavage, however, the position of the remaining copy of the construct was evenly distributed between mid-cell and cell pole positions (51.6% and 48.4%, respectively; Fig. 3b). This result argues against the possibility of the intact copy of the construct migrating to the cell pole in response to a DNA double-strand break. Furthermore, if cell division was inhibited by treatment with cephalexin to allow multiple rounds of replication and segregation within cells, induction of cleavage by SbcCD did not necessarily result in segregation to a cell pole (Fig. 4a, b).

A final possibility is that SbcCD can only cleave a hairpin when it is located at mid-cell. Consistent with this argument, SbcCD–green-fluorescent protein (GFP) localizes at mid-cell in 54% of the population, with the remainder possessing two foci at the one-quarter and three-quarter positions of the cell[13]. However, its co-localization with the replisomes makes it improbable that SbcCD is able to distinguish the two copies of the palindrome on the basis of their cellular location, considering that segregation of the two replicated sister loci is itself progressive from the replisomes. Also, the frequency of cleavage (more than 36% total DNA as measured on gels[8] and 52.8% of chromosomes as measured here by the frequency of chromosome degradation in cephalexin-induced filaments; Fig. 4c) is inconsistent with this possibility, which predicts a maximum of 25% cleavage per cell cycle if segregation of the leading and lagging strands is random.

Our data therefore provide strong evidence that segregation of the two sister chromosomes in *E. coli* is not random and results in the placement of the two lagging strands at the cell quarters flanking the mid-cell (Fig. 1Aa). Non-random segregation of sister chromosomes has been observed previously, most notably in mammalian stem cells. This led to the proposal of the immortal strand hypothesis[14], which suggests that stem cells preferentially retain the grandmother DNA template strands to limit the accumulation of replication-induced

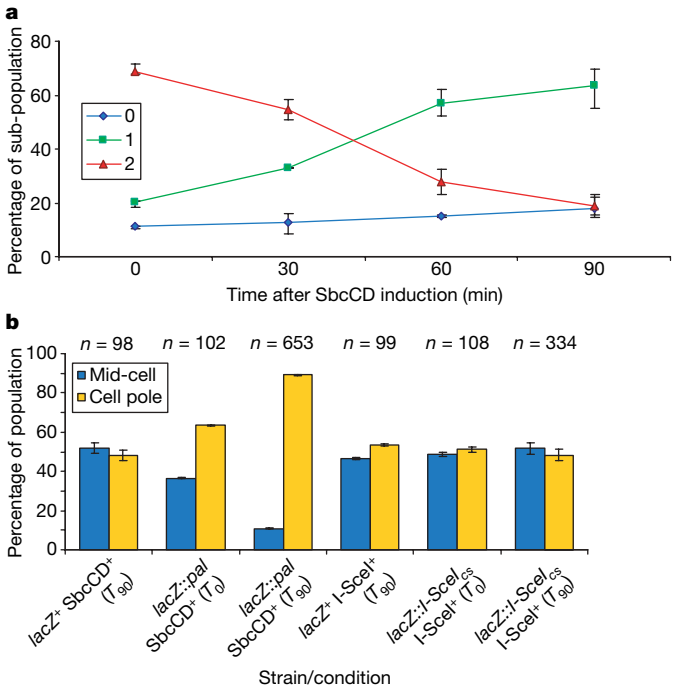

Figure 3 | Construct degradation and localization. **a**, Number of visibly segregated copies of the construct (0, 1, 2) in a *recA*$^-$-palindrome-containing strain as a function of time of SbcCD induction (error bars, range; $n \geq 500$ for all time points). **b**, Location of construct in cells longer than 1.50 μm with a single segregated copy of the construct; error bars, range; pal, palindrome.

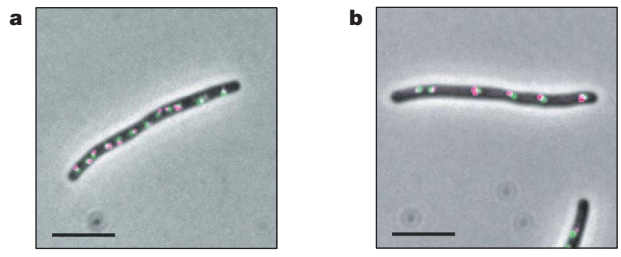

c

Strain	*n*	Mean length (μm)	Mean copies of construct	Copies per micrometre
lacZ$^+$ SbcCD$^+$ (T_{120})	333	8.92 ± 0.44	6.3 ± 0.3	0.72 ± 0.02 (*x*)
pal SbcCD$^+$ (T_{120})	358	14.22 ± 0.57	4.5 ± 0.2	0.34 ± 0.01 (*y*)

Errors indicate s.e.m.

Figure 4 | Induction of SbcCD in cephalexin-induced filaments. Cephalexin-treated cell without (**a**) and with (**b**) the palindrome after 120 min of SbcCD induction. The CFP signal is pseudocoloured green, YFP is magenta. Overlapping CFP and YFP signals appear white. Scale bars, 5 μm. **c**, Analysis of the consequences of SbcCD expression in cephalexin-treated cells. Frequency of cleavage was calculated as $1 - y/x$.

mutations. The immortal strand hypothesis is controversial[15–17], however, and other explanations for the observed asymmetric segregation, such as epigenetic markers, have been proposed[18]. These hypotheses require a mechanism of distinguishing sister chromatids. It has recently been postulated that such a discrimination could be made on the basis of whether the centromeric region of the chromosomes were replicated on the leading or lagging strand[19]. Here we have shown that a similar distinction is made by *E. coli*.

Our data do not provide a mechanistic understanding of this aspect of chromosome segregation. This is not surprising considering that the mechanism underlying chromosome segregation in *E. coli* is still unknown. The velocity at which the newly replicated origin regions are segregated indicates that chromosome segregation is an active process[20], and a centromere-like sequence (*migS*) has been identified[21]. Because later replicated regions of the chromosome do not migrate as rapidly, it has been proposed that segregation is a two-step process instigated by the active positioning of the origins[22]. Recent evidence suggests a role for the structural maintenance of chromosome protein MukB[23] in this initial step. It has also been suggested that the actin-like cytoskeleton protein MreB has a role in chromosome segregation[24,25], although this remains controversial[26].

One possibility is that the pattern of segregation that we have observed is a consequence of the structure of the two replisomes at the replication factory[27]. In *E. coli* the leading and lagging strand polymerases are physically linked in a structure known as the replisome. In the replisome, the lagging strand template is looped to allow the two polymerases to translocate in the same direction[1]. Although this loop is small, it may be enough to constrain the lagging strands physically to the replisome while allowing the leading strands to segregate to the cell poles. This would fit with the replication factory model, where the two replisomes are located at mid-cell. It is also plausible that it is advantageous for the cell to keep newly replicated lagging strands at mid-cell for further processing[28], and that this local requirement is reflected in global organization. Recent evidence, however, argues against the existence of a replication factory in *E. coli* and implies that the replisomes simply track along the DNA[29]. If this is indeed the case, then it would suggest that newly replicated DNA follows a nucleoid organization that is established at the initial stages of the segregation process.

METHODS SUMMARY

Strains and plasmids. Strains were BW27784 derivatives allowing homogeneous expression from P_{BAD}[12]. Mutations were introduced by either P1 transduction or plasmid-mediated gene replacement[8]. Insertions and deletions were confirmed by PCR. *recA*$^-$ mutants were confirmed as ultraviolet light sensitive. Full details of strains and plasmids used can be found in Supplementary Information.

Microscopy. Strains were grown at 37 °C in M9 minimal medium (with 0.2% glycerol) supplemented with 100 ng ml^{-1} anhydrotetracycline to prevent operator-bound TetR–YFP from blocking replication[30]. Unless otherwise stated, live cells were mounted on a bed of 1% agarose–H_2O for viewing under the microscope. To induce expression from P_{BAD}, cells were grown until the optical density at 600 nm ($OD_{600\,nm}$) = 1.0 in minimal medium supplemented with 0.2% glucose, before diluting to $OD_{600\,nm}$ = 0.2 in minimal medium supplemented with 0.001% arabinose (T_0). To inhibit cell division, cells were grown for 90 min in the presence of 10 μg ml^{-1} cephalexin before inducing SbcCD expression by diluting to OD_{600} = 0.2 in minimal medium (with 0.001% arabinose) supplemented with cephalexin. SbcCD was induced for 120 min before image acquisition. To prevent cross-signal from the plasmid, nucleoids were visualized in strains DL3339 and DL3340. Nucleoids were visualized either by staining with DAPI (1 μg ml^{-1}) or mounting live cells on 27% bovine gelatine–M9 minimal medium.

Images were acquired at a resolution of 0.129 μm per pixel using a Zeiss Axiovert 200 fluorescence microscope equipped with a Photometrics coolSNAP HQ CCD (charge-coupled device) camera and the acquisition software MetaMorph 6.3r2. CFP and YFP images were subject to three-dimensional adaptive point-spread function (blind) deconvolution using Autodeblur and Autovisualize v9.3 before analysis. Cell lengths were measured using the 'fibre length' measurement of MetaMorph 6.3r2. Images were pseudocoloured using MetaMorph 6.3r2. The range indicates the result of two independent experiments.

Received 16 May; accepted 23 July 2008.

1. McInerney, P., Johnson, A., Katz, F. & O'Donnell, M. Characterization of a triple DNA polymerase replisome. *Mol. Cell* **27,** 527–538 (2007).
2. Wang, X., Liu, X., Possoz, C. & Sherratt, D. J. The two *Escherichia coli* chromosome arms locate to separate cell halves. *Genes Dev.* **20,** 1727–1731 (2006).
3. Nielsen, H. J. *et al.* The *Escherichia coli* chromosome is organized with the left and right chromosome arms in separate cell halves. *Mol. Microbiol.* **62,** 331–338 (2006).
4. Thanbichler, M. & Shapiro, L. Getting organized—how bacterial cells move proteins and DNA. *Nature Rev. Microbiol.* **6,** 28–40 (2008).
5. Wang, X., Possoz, C. & Sherratt, D. J. Dancing around the divisome: asymmetric chromosome segregation in *Escherichia coli. Genes Dev.* **19,** 2367–2377 (2005).
6. Woldringh, C. L. & Nanninga, N. Structural and physical aspects of bacterial chromosome segregation. *J. Struct. Biol.* **156,** 273–283 (2006).
7. Rocha, E. P. *et al.* A strand-specific model for chromosome segregation in bacteria. *Mol. Microbiol.* **49,** 895–903 (2003).
8. Eykelenboom, J. K., Blackwood, J. K., Okely, E. & Leach, D. R. SbcCD causes a double-strand break at a DNA palindrome in the *Escherichia coli* chromosome. *Mol. Cell* **29,** 644–651 (2008).
9. Pinder, D. J., Blake, C. E., Lindsey, J. C. & Leach, D. R. Replication strand preference for deletions associated with DNA palindromes. *Mol. Microbiol.* **28,** 719–727 (1998).
10. Skarstad, K. & Boye, E. Degradation of individual chromosomes in *recA* mutants of *Escherichia coli. J. Bacteriol.* **175,** 5505–5509 (1993).
11. Mason, D. J. & Powelson, D. M. Nuclear division as observed in live bacteria by a new technique. *J. Bacteriol.* **71,** 474–479 (1956).
12. Khlebnikov, A. *et al.* Homogeneous expression of the P(BAD) promoter in *Escherichia coli* by constitutive expression of the low-affinity high-capacity AraE transporter. *Microbiology* **147,** 3241–3247 (2001).
13. Darmon, E. *et al.* SbcCD regulation and localization in *Escherichia coli. J. Bacteriol.* **189,** 6686–6694 (2007).
14. Cairns, J. Mutation selection and the natural history of cancer. *Nature* **255,** 197–200 (1975).
15. Rando, T. A. The immortal strand hypothesis: segregation and reconstruction. *Cell* **129,** 1239–1243 (2007).
16. Kiel, M. J. *et al.* Haematopoietic stem cells do not asymmetrically segregate chromosomes or retain BrdU. *Nature* **449,** 238–242 (2007).
17. Waghmare, S. K. *et al.* Quantitative proliferation dynamics and random chromosome segregation of hair follicle stem cells. *EMBO J.* **27,** 1309–1320 (2008).
18. Lansdorp, P. M. Immortal strands? Give me a break. *Cell* **129,** 1244–1247 (2007).
19. Lew, D. J., Burke, D. J. & Dutta, A. The immortal strand hypothesis: how could it work? *Cell* **133,** 21–23 (2008).
20. Niki, H., Yamaichi, Y. & Hiraga, S. Dynamic organization of chromosomal DNA in *Escherichia coli. Genes Dev.* **14,** 212–223 (2000).
21. Yamaichi, Y. & Niki, H. *migS*, a cis-acting site that affects bipolar positioning of *oriC* on the *Escherichia coli* chromosome. *EMBO J.* **23,** 221–233 (2004).
22. Thanbichler, M. & Shapiro, L. Chromosome organization and segregation in bacteria. *J. Struct. Biol.* **156,** 292–303 (2006).
23. Danilova, O. *et al.* MukB colocalizes with the *oriC* region and is required for organization of the two *Escherichia coli* chromosome arms into separate cell halves. *Mol. Microbiol.* **65,** 1485–1492 (2007).
24. Gitai, Z. *et al.* MreB actin-mediated segregation of a specific region of a bacterial chromosome. *Cell* **120,** 329–341 (2005).
25. Kruse, T. *et al.* Actin homolog MreB and RNA polymerase interact and are both required for chromosome segregation in *Escherichia coli. Genes Dev.* **20,** 113–124 (2006).
26. Karczmarek, A. *et al.* DNA and origin region segregation are not affected by the transition from rod to sphere after inhibition of *Escherichia coli* MreB by A22. *Mol. Microbiol.* **65,** 51–63 (2007).
27. Lemon, K. P. & Grossman, A. D. Localization of bacterial DNA polymerase: evidence for a factory model of replication. *Science* **282,** 1516–1519 (1998).
28. Rossi, M. L., Purohit, V., Brandt, P. D. & Bambara, R. A. Lagging strand replication proteins in genome stability and DNA repair. *Chem. Rev.* **106,** 453–473 (2006).
29. Reyes-Lamothe, R., Possoz, C., Danilova, O. & Sherratt, D. J. Independent positioning and action of *Escherichia coli* replisomes in live cells. *Cell* **133,** 90–102 (2008).
30. Possoz, C., Filipe, S. R., Grainge, I. & Sherratt, D. J. Tracking of controlled *Escherichia coli* replication fork stalling and restart at repressor-bound DNA *in vivo*. *EMBO J.* **25,** 2596–2604 (2006).

Supplementary Information is linked to the online version of the paper at www.nature.com/nature.

Acknowledgements We thank D. Sherratt for the gifts of plasmids pWX6, pLau43 and pLau44. We also thank E. Darmon and J. Blackwood for reading the manuscript. This work was supported by the Medical Research Council.

Author Contributions M.A.W. and D.R.F.L. conceived and designed the experiments; M.A.W. constructed all strains and plasmids apart from pDL1625, pDL1709 and pDL2542, which were constructed by J.K.E., E.W. and M.A.L.-V., respectively; M.A.W. performed the experiments; M.A.W. and D.R.F.L. analysed the data and wrote the paper.

Author Information Reprints and permissions information is available at www.nature.com/reprints. Correspondence and requests for materials should be addressed to D.R.F.L. (D.Leach@ed.ac.uk).